OVERLAP OF CYTOKINE AND TRANSCRIPTION FACTOR EXPRESSION IN T HELPER CELL SUBSETS

BY

SIOBHAN MARGARET RESTORICK

A thesis submitted to
The University of Birmingham
for the degree of
DOCTOR OF PHILOSOPHY

School of Immunity and Infection

College of Medical and Dental Sciences

The University of Birmingham

September 2013

ABSTRACT

Until recently, $CD4^+$ T Helper (T_H) cells were thought to be permanently committed to a single lineage (e.g. T_H1, T_H17, T_H2 etc.). However there is now increasing evidence that T_H cells are plastic in nature and can gain phenotypic features of other T_H subsets. Within this study I have investigated the overlap and plasticity of T_H1 cells and their presence in health and in the inflammatory setting of multiple sclerosis.

It has been recently shown that T_H17 cells stimulated in an IL-12 rich environment can become $CCR6^+IFN\gamma^+IL\text{-}17^+$ cells[1]. The expression of the T_H1 and T_H17 transcription factors, T-bet and RORC respectively, was initially investigated in different cytokine secreting subsets using multicolour flow cytometry. $IFN\gamma^+IL\text{-}17^+$ cells expressed both T-bet and RORC at a protein level.

Although CCR6 is considered a T_H17 marker there are other T_H cell subsets that express CCR6[2]. Using peripheral blood T cells isolated from healthy volunteer donors a novel subset of T_H1 cells has been identified that express functional CCR6. Using multicolour flow cytometry it was shown that $CCR6^+T_H1$ cells did not secrete any other T_H17 related cytokines (i.e. IL-22, IL-17F and IL-21) but expressed the T_H1 associated chemokine receptor CXCR3. These cells share phenotypic features of a T_H1 cell but transcriptionally express 'T_H17'-related genes. Optimisation of a cytokine capture technique allowed the isolation of viable $CCR6^+IFN\gamma^+$, $CCR6^+IL\text{-}17^+$ and $CCR6^+IFN\gamma^+IL\text{-}17^+$ cells as well as $CCR6^-IFN\gamma^+$ cells. Comparisons were made between the different subsets at a transcriptional level using qRT-PCR. $CCR6^+T_H1$

cells expressed 'T_H17'-related genes (e.g. RORC, IL-23R and IL4I1) similar to IL-17A secreting cells but also expressed T-bet and IL-12Rβ2 and no IL-1R1, similar to $CCR6^-T_H1$ cells. At a protein and transcriptional level $CCR6^+T_H1$ cells were distinct from $CCR6^+IFN\gamma^+IL\text{-}17^+$ cells. In addition, using a microarray screening method, candidate miRNAs that may play a role in controlling phenotypic features of these cells have been identified.

T_H17 cells have been implicated in the pathogenesis of multiple sclerosis and enter the cerebrospinal fluid through CCR6-dependent migration. $CCR6^+IFN\gamma^+$ cells were increased within the cerebrospinal fluid of patients with multiple sclerosis compared to the peripheral blood. Upon stimulation the $CCR6^+T_H1$ and $CCR6^-T_H1$ cells were a source of GM-CSF, a cytokine know to be important for the pathogenesis of the mouse model of MS, experimental autoimmune encephalomyelitis. Further research is needed to confirm if $CCR6^+T_H1$ play a role in the pathogenesis of the disease.

DEDICATIONS

To My Family

Mum, Dad, Jamie and Will

Thank You

x

ACKNOWLEDGEMENTS

I would like to thank my supervisors, Dr John Curnow for his excellent supervision. He has helped enormously with my personal and professional development over the last 4 years. He has been instrumental in developing my skills as a scientist, and was always there to help and discuss. For all this I am very grateful.

I would like to thank Dr Michael Douglas, Dr Ghaniah Hassan-Smith, and Dr Semma Kalra for collecting CSF and blood from multiple sclerosis patients for this study. I would also like to thanks all the healthy blood donors who have made contributions to my project.

I would also like to thank all of the members of the Curnow lab who I have worked with, both past and present. I would like to especially mention Lindsay Durant, Matt Edmunds, Emma Yates, Marie Voice, Robert Barry, Paul Thomlins, Alistair Denniston, Geraint Williams, Celia Menckeberg, Sherine Kottoor, and Steven Kissane. You have been a joy to work with! This is also the case with everyone that was the '3rd Floor' IBR, and the new CITR crew. Thank you for making work so enjoyable.

A special thank you to my family and my life-long friends Lydia, Charlie and Charl, who have always been there to reminded me I can do this. I would especially like to thank Jennifer Cowen, my term time bestie. She has made my time in Birmingham unforgettable and I am certain I could not have had as much fun doing this PhD without her.

I would finally like to thank Robert Richardson for being there for me through everything.

Nothing's going to stop us now!

TABLE OF CONTENTS

LIST OF FIGURES

LIST OF TABLES

ABBREVIATIONS

AhR	Aryl Hydrocarbon Receptor
APC	Antigen Presenting Cell
CCR	Chemokine receptor
CD	Cluster of Differentiation
CNS	Central Nervous System
CSF	Cerebral Spinal Fluid
Cp	Cycle Value
DC	Dendritic Cell
EAE	Experimental Autoimmune Encephalomyelitis
GAPDH	Glyceraldehyde 3-phosphate Dehydrogenase
G-CSF	Granulocyte Colony Stimulating Factor
GM-CSF	Granulocyte -Macrophage Colony Stimulating Factor
ICOS	Inducible Co-stimulator
IFNγ	Interferon Gamma
IL-	Interleukin
IL4I1	Interleukin-4–induced gene 1
JAK	Janus Kinase
MFI	Median Fluorescence Intensity

miR-	MicroRNA-
MHC	Major Histocompatibility
MMP	Matrix Metalloproteinase
MS	Multiple Sclerosis
NF-AT	Nuclear Factor of Activated T cell
NK	Natural Killer Cells
PAMP	Pathogen Associated Molecular Pattern
PBMC	Peripheral Blood Mononuclear Cells
PRR	Pattern Recognition Receptor
JIA	Juvenile idiopathic arthritis
RAR	Retinoic Acid Receptor
RF	Rheumatoid Factor
ROR	Retinoic Acid Receptor Related Orphan
SOCS	Suppressor of Cytokine Signalling
STAT	Signal Transducer and Activator of Transcription
TCR	T Cell Receptor
TGF	Transforming Growth Factor
T_H	T Helper
TNF	Tumour Necrosis Factor
T_{REG}	Regulatory T Cell

CHAPTER 1

INTRODUCTION

1.1 The Immune System

There are an extensive variety of pathogens that can infect the body and cause damage. They come in all shapes and sizes; tiny viruses (20-200nm), bacteria (~0.2-2µm), fungal infections (~100-1000 µm) and helminths such as tapeworms that can grow to a few meters in length. These different pathogens not only vary in size but also how they enter the body and their ideal site of infection. To protect the body from this diverse group of pathogens the immune system has evolved in to a complex multidimensional system.

There is a fine line that the immune system must walk. Protection against the pathogens to prevent infection is vital; however, this must be done without causing significant damage to the body. This is never clearer than in autoimmune diseases. Self-antigens are not tolerated by their own immune system and this can cause irrevocable and long lasting damage to the body. To truly understand why and how autoimmunity occurs we must first understand the cellular and molecular foundation of an immune response. Increasing our understanding of the immune system will help lead to effective treatments for not just autoimmunity but also other immune related diseases.

1.2 The Components of the Immune System

The human immune system works on three levels. The initial level is a physical defence against invading pathogens. The skin and mucosal tissue, which is open to the external environment, forms a physical barrier to prevent entry of the large majority of pathogens. Secondly, if the pathogen gets past the first physical barrier, there is the innate immune system. The first line of defence against infection made up of rapidly reacting cells. These innate cells use the same mechanisms to protect the body irrelevant of the type of infection. The complement system makes up the molecular arm to the innate system and also has similar feature to the innate cells, in that it is rapid in reacting and is non-specific. Thirdly, there are the adaptive immune systems; made up of specialized cells that react in a more directed manner, releasing molecules such as antibodies and cytokines in a more focussed way, and retaining memory of infection that can lead the fight against future re-infections.

All immune cells originate from a common precursor in the bone marrow, the pluripotent hematopoietic stem cell. These cells mature within the bone marrow and differentiate into either a common lymphoid progenitor[3] or a common myeloid progenitor[4]. It is at this stage the difference between the innate and adaptive immune cells starts to develop. Common myeloid progenitors will differentiate to become one of several different innate cell types; a granulocyte, mast cell, monocyte or dendritic cell[4]. Common lymphoid progenitor will become adaptive immune cells; T, B or natural killer (NK) cells[3].

1.2.1 Innate Immunity

The innate immune system consists of molecular elements, such as the complement system, and cellular components, such as macrophages and neutrophils. As mentioned, innate immune cells are the first cells to recognise the infectious agent, they all express pattern-recognition receptors (PRR). At least 5 classes of PRRs have been identified including Toll-like receptors (TLRs), C-type lectin receptors (CLRs) and cytosolic DNA receptors (CDRs). The PRR recognise pathogen associated molecular patterns (PAMP) which are conserved molecular structures that are vital for the survival of the infectious agent but are not found in mammalian biology. Examples of PAMP are;

- lipopolysaccharides (LPS), a major component of Gram-negative bacterial cell wall,
- lypoteichoic acid, a vital component of Gram-positive bacterial cell wall,
- mannans, part of the fungal cell wall,
- DNA motifs,
- dsRNA, involved in some virus's transcription.

PAMP will activate PRR to initiate a cascade of signals within the cell and induce activation. There is heterogeneous expression of these receptors on the different innate cell types[5].

The innate granulocytes (neutrophils, eosinophils, basophils) express granules containing enzymes and inflammatory proteins. Neutrophils are present in abundance in the human blood and are the first effector cells to appear at the site of an infection. As well as being important antimicrobial effector cells they also secrete cytokines and chemokines to orchestrate the immune response[6]. As they release lytic granules eosinophils and basophils

make up part of the immune response against multi-cellular parasites, although both cell types also play a role in allergic responses. Mast cells are also associated with allergic responses, as upon activation these cells release granules containing chemicals such as histamine and heparin that effect vascular permeability. Mast cells can become activated via the complement system or through crosslinking of IgE on their cell surface. Mast cells are resident in most tissues surrounding blood vessels and nerves, as well as at mucosal surfaces such as the gut and lungs.

Although NK cells are a type of cytotoxic lymphocytes and differentiate from a common lymphoid progenitor they are classically seen as an innate cell as they provide a rapid response to infections. These cells provide surveillance against virally infected cells and tumour cells. Their mechanisms of action are slightly different to other innate cells as instead of being activated by PAMP or binding to a major histocompatibility complex (MHC)/peptide complex, NK cells recognises 'stressed' body cells which have down regulated MHC. NK cells secrete interferon gamma (IFNγ) and release lytic granules to direct the killing of 'stressed' targeted cells. Alongside this method of activation NK cells also express activator and inhibitory receptors, such as NKG2D (activator) or killer-cell immunoglobulin-like receptors (KIRs - inhibitor). CD161 (cluster of differentiation 161) is an inhibitory NK cell receptor (also known as killer cell lectin-like receptor, B1) which when activated by its ligand, lectin like transcript 1 (LLT1), inhibits NK cell cytotoxicity and IFNγ secretion[7]. CD161 can also be expressed on a subset of lymphocytes[8].

In addition to the release of immune-stimulating molecules, such as cytokines or lytic granules, phagocytosis is another important function of innate immune cells. Phagocytosis involves the recognition and internalisation of a recognised pathogen or harmful substance. Upon internalisation of the pathogen the vesicle will fuse to a lysosome. The digestive enzymes in the lysosome will break down the pathogen within the vesicle. The process of recognition of pathogens for phagocytosis is aided in part by the complement system and antibodies, both of which assist in the process of opsonising the pathogen. Neutrophils, macrophages and dendritic cells (DC) are all phagocytic cells.

Macrophages and DC use phagocytosis as a way of obtaining peptide sequences from the pathogen to present to the adaptive immune system with the aim of activating it. These innate cells are considered antigen presenting cells (APC) and alert adaptive immune cells to the presence of an infection. Once an APC has encountered an invading organism it will mature. A monocyte matures in to either an inflammatory DC[9] or a macrophage, and a DC in to a mature DC. DC will migrate through tissues and the blood stream until it encounters an antigen[10]. Once mature the DC will migrate to draining lymphoid organs to present a peptide (antigen) in a MHC on their cell surface to an adaptive immune cell. Macrophages in general will stay within the tissue to present antigens to T cells to re-activate them. MHC molecules are specific to individuals, giving a mechanism that the body can identify non-self-cells as well as a way to present antigens to the immune system[11].

1.2.2 Adaptive Immunity

Adaptive cells produce a specific, directed attack on infectious agents and are able to develop memory so that any re-infection will be recognised and dealt with efficiently. Although innate cells such as macrophages and neutrophils are efficient at removing microorganisms from the body, there are instances in which these cells just cannot provide the response needed to remove the infection. In cases like this the adaptive immune cells will become involved and provide additional mechanisms to remove the threat.

T and B cells make up the adaptive immune cells. Unlike innate cells, which carrying several different receptors to recognise various pathogens, the adaptive cells emerge into the blood carrying only one receptor. The cells express an antigen receptor with a single specificity. This receptor was produced through a process of rearrangement of a variety of different gene segments that code for different parts of the receptor. This process has the potential to code for millions of different combinations of the same receptor, giving the adaptive cells the ability to recognise different pathogens and a large repertoire of antigens. Only cells that meet an antigen that their receptor recognises with sufficient affinity will start to proliferate and gain an effector function.

The B cells carry a similar receptor to T cells but once activated the (B cell receptor) BcR has a very different function. Activation induces proliferation and differentiation of the B cell into plasma cells, which produce high quantities of the soluble form of the BcR, known as an antibody. Also, unlike a T cell, a B cell can sample antigens that have not being processed or presented by an APC. The antibodies made by B cells make up an important part of the

humoral immune response which will bind the antigen and act as a neutralising agent or will opsonise any pathogen in part with the innate complement system.

There are different subsets of B cells aside from the plasma cell. Memory B cells are activated cells that are long lived, and upon reencounter of the antigen are very quickly reactivated, similar to memory T cells. There are different B cells depending on which part of the secondary lymphoid structure the cell resides; differentiated based on surface receptor expression. CD21 and CD1 are used to detect marginal B cells, while Immunoglobulin M (IgM), IgD and CD23 denote follicular B cells. B-1 cells express IgM to a greater extent than IgG and are found predominantly in the peritoneal and pleural cavities[12]. There are also B regulatory cells (B_{REGS}) that are involved in immune regulation[13] via mechanisms such as release of immunosuppressive cytokine like TGF-β and IL-10[14].

Within an immune response T cells have a broader function compared to B cells. T cells can be grouped based on the surface expression of either CD8 or CD4, and in general are defined by the cytokines they secrete once they have been activated. Cytokines are small, soluble, signalling molecules that can directly affect the function of the cells in the vicinity.

1.3 T Cells

1.3.1 Thymic T Cell Production

T cells develop in the thymus, after migrating from the bone marrow as lymphoid progenitors. Once a T cell has migrated to the thymus it undergoes a process of gene

segment rearrangement to produce an antigen specific T cell receptor (TcR). The TcR consists of a linked hetro-dimer of αβ (~95% peripheral T cell) or γδ chains. The hetro-dimer will complex with an invariant CD3 complex (made up of a γ, δ, two ε chains and two ζ chains). The TcR's specific conformation allows it to recognise a specific peptide sequence. Within the thymus the cells will undergo a process that will check the proficiency of the TcR construction, evaluating if the TcR will recognise self MHC molecules but not recognise self-peptides (positive and negative selection respectively). This process is not as binary as suggested and there is more of a sliding scale of affinities of the TcR for MHC molecules. Any cells that do not recognise MHC enough or recognise self-peptide too strongly will be removed by apoptosis. This is a tolerance mechanism which the body uses to protect against autoimmune disease[15].

Within the thymus thymocytes will express both CD4 and CD8[16]. However before leaving the thymus a T cell will down-regulate expression of one to become either single $CD8^+$, or single $CD4^+$ T cell. After the T cell has undergone these processes it will exit the thymus a naïve T cell and circulate between the blood and the secondary lymphoid organs of the body.

1.3.2 T Cell Activation and Memory

A naïve T cell ($CD45RA^+CCR7^+$) circulates through the peripheral lymphoid tissues sampling antigens:MHC complexes on dendritic cells at the T cell zone[17]. The T cell will continue to do this until it encounters an antigen that it recognises. Dendritic cells are thought to initiate

most, if not all, of the T cell activation *in vivo*[18,19]. The mature DC will increase MHC expression and display the pathogen derived peptides[20] (Signal 1), along with co-stimulatory molecules (Signal 2)[21–23]. The types of inflammatory cytokines (Signal 3) that are released by the mature DC depend on the type of pathogen that the DC has encountered. It is vital for a T cell to receive all three signals to effectively differentiate(reviewed in [24]). There is a further signal the cells need to enter the site of infection, sometimes called signal 4. Chemokine receptors can be markers of polarized T cell subsets and flexible programs of chemokine receptor gene expression can control tissue-specific migration of effector T cells[25]. Signal 4 is the interaction between the chemokines and their respective chemokine receptors on the surface of the T cell. Chemokines are secreted by the stromal cells and inflammatory cells at the site of an inflammatory reaction.

CD3 associates with the TcR and CD4 or CD8 within a lipid raft on the surface of a T cell. This association is important for initiation of the signalling cascade involving molecules such as mitogen activation protein kinase (MAPK) and phospholipase Cγ (PLCγ). The activation of these signalling molecules induce intracellular Ca^{2+} release, activation of the protein kinase C (PKC) pathway, activation of transcription factors such as AP-1, NFAT, and NFκB. The downstream effects of all of this is changes in gene expression[26].

For effective activation of the T cells co-stimulatory molecules need to associate with their respective receptors on APC. CD28[22], ICOS (Inducible co-stimulator)[23], LFA-1 (lymphocyte function-associated molecule-1) and VLA-4 (very late antigen-4) are all co-stimulatory molecules expressed on T cells. Respective receptors to these co-stimulatory molecules are

unregulated on APC due to signalling from PRR. This is a mechanism to prevent unnecessary activation of T cells where there is no 'danger' signals. If the secondary signals are not provided alongside TcR activation the cell either undergoes apoptosis or becomes unable to respond to subsequent activating signals (anergic)[27]. Upon activation cell surface marker such as CD69, CD71 and CD40L are up-regulated on the T cell, which are often used as a marker for recently activated cells.

A $CD8^+$ T cell can identify antigen presented on a MHC class I molecule. MHC I is expressed on all nucleated cells of the body. If an infection occurs antigens are presented on the surface of an APC in a MHC:peptide complex and co-stimulator molecules will be up regulated. $CD8^+$ T cells recognize cytosolic proteins from intracellular infections such as viruses or tumour antigens. Being able to identify infected cell allows the $CD8^+$ T cells to effectively kill them though apoptosis, $CD4^+$ T cell are unable to directly kill infected cells.

$CD4^+$ T cells recognize MHC class II molecules and the antigen presented in them. The expression of MHC II is restricted to APC, such as dendritic cells, macrophages and B cells which can present both internally and externally sourced antigen. $CD4^+$ T cells can respond to a wide range of pathogens and secrete cytokine to modulate the immune system to guide a more specific immune response.

Once a T cell has been sufficiently activated it will burst in to action by proliferating and acquiring a number of effector functions, such as expression of cytokines or cytotoxic ability. The cell will switch expression of the lymphocyte common antigen CD45, from the long glycosylated isoform CD45RA to the shorter isoform, CD45RO. CD45 contains an

intracellular protein tyrosine phosphatase domain that under rest conditions dephosphorylated $P56^{lck}$, upon TcR engagement CD45 disassociates with P56lck and this means it can be phosphorylated and aids effective TcR signalling[28]. The shortening of the isoform to CD45RO may allow for easier binding the TcR:MHC complex[29].

The combined intracellular signalling cascades that are induced from the TcR engagement, co-stimulatory molecules and cytokines are diverse, but all lead to effects on transcriptional regulation. Signal transducer and activator of transcription (STAT) proteins bridge the gap between the cytokine receptors at the cell surface and the nucleus. STAT proteins are phosphorylated and activated by stimulated cytokine receptors[30] at which point they translocate to the nucleus. Once in the nucleus, STAT proteins alongside other transcription factors orchestrate the differentiation of T cells[24]. Transcription factors are proteins that bind to specific genes and alter DNA transcription. Through suppression and transcription of lineage specific genes a phenotype is carved out for the cell.

Once activated, as well as shortening CD45, the naïve T cell may lose CCR7 expression. This chemokine receptor allows T cells to enter high endothelial vessels and migrate into secondary lymphoid tissue. Thus the expression of CCR7 on memory T cells can be used to further divide the $CD45R0^{+}$ cells based on their broad function as a memory cell. Central memory T cells (T_{CM}) are $CD45RO^{+}$ and express CCR7. T_{CM} cells do not produce much effector cytokines, such as IFNγ and Interleukin 4 (IL-4), but produces a lot of IL-2. Only once the T_{CM} cell has experienced antigen again will it start to proliferate and produce effector cytokines. Although T_{CM} cells do not initially produce effector cytokines, they have been

shown to be primed to differentiate into specific T_H subsets. $CD45RO^+CCR7^-$ effector Memory (T_{EM}) T cells have the capacity to express large quantities of effector cytokines. These two subsets of cells form our antigenic memory and are vital to provide the quick response to a second infection[31]. $CD8^+$ T cells can further re-express CD45RA to become revertant memory T cells (T_{EMRA}) but are still $CCR7^-$. Under resting conditions CD8 T_{EMRA} proliferate at a slow rate in response to γ–chain cytokines (e.g. IL-2, IL-7, IL-15 etc.) and maintains $CD8^+$ T cell memory [32].

1.3.3 T Cell Migration to the Site of Infection

There are many other chemokine receptors, along with CCR7, expressed on T cells that are critical mediators of cell migration in immune surveillance and inflammation. Chemokines are able to bind to several different receptors and as most chemokine receptors are able to bind to multiple chemokines. Chemokine receptor signalling results in cell chemotaxis.

All chemokine receptors are 7-transmembrane proteins coupled to G-protein signalling molecule[33,34]. They are classified into 4 groups based on the positioning of highly conserved cysteine of the amino acid sequence (CXC, CX3C, CC, and C). Binding of the chemokine leads to activation of a cascade of signalling proteins, including G protein coupled receptor kinases (GRKs), phospholipase C-β (PLC-β) and phosphatidylinositol 4,5-bisphosphate (PIP_2) leading to mobilization of calcium and activation of various protein kinase C (PKC). These signals will ultimately lead to actin polarisation, shape changes, and directed cell movement. Once the chemokine receptor has become appropriately activated it will become partially or totally

desensitised to repetitive stimulation by chemokines. In some cases the receptors will internalise, a vital mechanism to maintain the ability to detect a chemokine gradient [35].

Within $CD4^+$ T cells there is differential expression of chemokine receptors on different T helper subsets. For example T_H1 cells preferentially express CXCR3 and CCR5, T_H2 cells express CCR4[25,36] and T_H17 cells express CCR6[37]. Chemokine receptor expression on T helper subsets will be covered in more detail later when each T helper subset is individually discussed.

1.4 $CD8^+$ T Cells

$CD8^+$ T cells have cytotoxic components that allow them to efficiently destroy infected cells. Recognition of an antigen presented in the MHC will lead to activation, proliferation and differentiation of the $CD8^+$ T cell and the production and release of lytic granules. These granules contain perforin and granzyme[38]; enzymes that will induce controlled cell death (apoptosis) in the infected cell. Also Fas ligand on the $CD8^+$ T cell binds to Fas on the target cell to initiate intra-cellular caspase signalling pathways to kill the cell[39]. $CD8^+$ T cells also release IFNγ, TNF-α and TGF-β which contribute to the defence in several ways. IFNγ can initiate anti-viral responses in infected cells and activate macrophages. TNF-α and TGF-β also aid in the killing of infected cells via their receptors and in the activation of macrophages.

Interestingly, there is also a small but detectible population of $CD8^+$ T cells that secrete the inflammatory protein IL-17 (Tc17). These cells express, alongside IL-17, fewer lytic granules

than their IFNγ secreting counterparts[40]. There are also dual, IL-17/IFNγ secreting $CD8^+$ T cells suggesting a level of plasticity comparable to the $CD4^+$ counterparts. STAT-3 and other T_H17 polarising cytokines (IL-6, IL-23, IL-1β[40]) are important to the induction of Tc17 cells[41]. Tc17 cells have been shown *in vivo* to be important part of the immunity in influenza challenged mice[42] and are found in the murine model of multiple sclerosis, experimental autoimmune encephalomyelitis (EAE)[40].

1.5 $CD4^+$ T Helper Cell Subsets

Once the T cell migrates into the site of infection it will be the APC that re-activates the T cell. The cytokines secreted by the APC will drive any changes in T cell differentiation. Innate cells produce cytokine tailored to deal with the different infection. The initial innate response leads to the differentiation of a T helper cell which will complement the innate response. For example, in response to intracellular bacteria, such as mycobacteria, this will induce IFNγ expression in NK cells and IL-12 expression in macrophages. These cytokines specifically induce a T Helper 1 Cell (T_H1) phenotype in an activated T cell. The production of IFNγ by the T_H1 cell will further activate and optimise the response of macrophages to destroy the bacterial insult. More details of the induction, differentiation and maintenance of the different T helper subsets are given below (**Figure 1.1**).

1.5.1 T Helper 1 Cell

It was initially thought that there were two differentiation inflammatory paths a $CD4^+$ T cell could take in response to a pathogenic insult. In 1986 Mossman and Coffman described these as T_H1 and T_H2 $CD4^+$ T cells[43]. These cells were identified based on the cytokines they produced. A T_H1 cell expresses IFNγ while a T_H2 cell secretes IL-4.

As mentioned above, T_H1 cells develop in response to intracellular pathogens such as *Mycobacterium tuberculosis* and *Mycobacterium leprae*. In healthy humans when *ex-vivo* PBMC are stimulated with PMA and ionomycin approximately 30% of the memory $CD4^+$ T cells secrete IFNγ. T_H1 cells are heavily involved in mounting cellular immunity through the release of IFNγ and are crucial for activation of macrophages[44] and optimising the $CD8^+$ cytotoxic attack. IFNγ is a type II interferon cytokine originally discovered for its anti-viral activities[45]. IFNγ exists as a homo-dimer and although is part of a larger family of interferon cytokine has little homology with the Type I interferons, IFN-β or the other various IFN-α cytokines. T_H1 cells selectively migrate towards the ligands CXCL9, 10 and 11 due to their expression of the chemokine receptor CXCR3[36].

T_H1 cells are induced in an IFNγ and IL-12 rich environment, in both humans[46] and mice. The binding of IFNγ to its receptor (IFNγR), along with TcR stimulation, will lead to phosphorylation of Jak proteins associated with the IFNGR, resulting in activation of STAT-1. STAT-1 in turn will induce the expression of the T_H1 lineage defining T-box transcription factor, T-bet. T-bet was discovered by Laurie Glimcher *et al*. by using yeast one-hybrid screening, a method of assessing protein-DNA interactions in a simplified model[47]. STAT-$1^{-/-}$

and T-bet$^{-/-}$ mice cannot respond to IFNγ and die due to excessive mycobacterial and viral infections, highlighting the dependency of T_H1 cells on T-bet and STAT-1 signalling[48–51]. Interestingly $CD8^+$ T cells do not rely on T-bet for their IFNγ production, though NK cells do[52].

T-bet directly induces *Ifng* gene expression and IFNγ secretion in $CD4^+$ T cells, which acts as a feedback mechanism for the T_H1 phenotype and is the main functional cytokine produced by T_H1 cells. T-bet can induce H2.0-like homeobox protein, a transcription factor from the Hlx gene which will also stabilise the T_H1 phenotype[53].

IL-12 is well documented to enhance T_H1 development. IFNγ activation of T-bet up-regulates IL-12Rβ2 expression[54] which is not expressed on naïve $CD4^+$ T cells[55,56]. Binding of IL-12 to its receptor activates STAT-4 which reinforces T-bet expression and therefore the T_H1 phenotype.

T_H1 cells have long been associated with autoimmunity, though the discovery of T_H17 cells (covered in **Section 1.5.3**) has led to the idea that they may not be as important as initially thought[57].

1.5.2 T Helper 2 Cell (T_H2)

T_H2 cells provide humoral immunity against protozoa infections such as *Leishmania major*[58] and intestinal nematodes. Cytokines released by T_H2 cells favour the production and activation of mast cells and eosinophils. The cytokines also stimulate B cell growth,

differentiation, and isotype switching to IgE and IgG[59]. T_H2 cells express CCR3 and CCR4, giving them the ability to migrate towards chemokines including RANTES (CCL5) and CCL11.

GATA-3 is the transcription factor that is necessary for a T_H2 phenotype. Discovered in 1997, GATA-3 was shown to be expressed in naïve T cells, with decreased expression in T_H1 committed cells and transgenic expression of GATA-3 induces a T_H2 cytokine profile. Flavell *et al.* showed that GATA-3 controlled IL-4 expression by using an IL-4 promoter luciferase reporter gene[60] and later others showed GATA-3 directly activates IL-5 and IL-13 promoter regions as well[61].

There are two pathways able to induce a T_H2 phenotype. Firstly IL-4 is a cytokine that can activate STAT-6 which leads to GATA-3 activation[62]. The second induction pathway for T_H2 lineage commitment is via an IL-4 independent pathway. This can occur in the absence of STAT-6, through the Notch signalling system and can induce GATA-3, although at a reduced level[63]. IL-2 signalling via STAT-5 is an important factor in T_H2 induction by allowing the IL-4 gene to be more stably expressed[64]. Ikaros is another transcription factor which although has other roles in lymphocyte development acts to promote T_H2 lineage and repress T_H1 factors such as T-bet[65].

Germ line deletion of *GATA-3* results in embryonic lethality, demonstrating GATA-3 non-redundant role in foetal development. The only viable way to remove GATA-3 transcription is to selectively knock-out the gene in the cell of interest. T cell-specific GATA-$3^{-/-}$ mice, produced by inserting a Cre-loxP system between exon 4 and 5 of GATA-3 gene of the mouse and crossing it with a Cre-CD4 transgenic mouse, cannot polarise to a T_H2 phenotype and

even in T_H2 polarising conditions produce IFNγ. IL-5 and IL-13 production is abolished in the GATA-$3^{-/-}$, however IL-4 is not[66]. This might suggest that the default phenotype of a $CD4^+$ T cells is that of a T_H1 cell.

Upon publishing their discovery Coffman and Mossman expressed the opinion that there were probably other phenotypes of a $CD4^+$ T cell that were undiscovered[43]. We now know that there are several other subsets based on cytokine production and transcription factor expression. The T_H17 cell is defined by secreting IL-17A and expressing the transcription factor RORC in humans. Several other lineage such as T_H22, T follicular helper cells, T_H9 and regulatory cells (T_{REG}) also exist and further research is on-going to understanding these cells.

1.5.3 T Helper 17 Cell (T_H17)

Since the discovery of T_H17 cells there has been a scramble to understand these cells because of their presence and potential role in many autoimmune diseases. T_H17 cells were discovered, not by looking for IL-17 expressing T_H cells, but after researching a murine model of the autoimmune disease multiple sclerosis (MS); experimental autoimmune encephalomyelitis (EAE). The model was thought to be controlled by an IFNγ dominated T_H1 response, induced by IL-12. Contrary to this initial hypothesis mice that lacked IFNγ were not only still susceptible to EAE, but their morbidity was significantly poorer and more mice died[67].

IL-12 is a heterodimer protein composed of a p35 and a p40 subunit. IL-12 was found to have a common p40 subunit with the cytokine IL-23 (**Figure 1.2**) [68,69], a cytokine shown to play a role in IL-17 production by T cells. A comparison of EAE induction in mice genetically engineered to not express p35 or p40 identified that IL-12 was redundant in the induction of EAE as $p35^{-/-}$ mice were still susceptible to EAE[70]. Mice with a $p40^{-/-}$ were resistant to the induction of EAE identifying IL-23 as the critical factor [57,71]. After initial experiments it was thought IL-23 was an inducer of IL-17 expression, due to the association of IL-23 and T_H17 cells in EAE. Contrary to this the IL-23R is not expressed on naïve T cells. This demonstrates that although IL-23 plays a role in T_H17 cells maintenance it is not involved in the initial induction of the T_H17 cell phenotype[72,73].

1.5.3.1 IL-17 Cytokine

IL-17 was first cloned in 1993 and it was discovered to have 6 different isoforms (IL-17A-F)[74]. The two isoforms produced by $CD4^+$ T cells are IL-17A and IL-17F as well as a heterodimer of the two (IL-17A-IL-17F)[75]. T_H17 cells always express IL-17A and co-secrete IL-17F in about 20% of the cells.

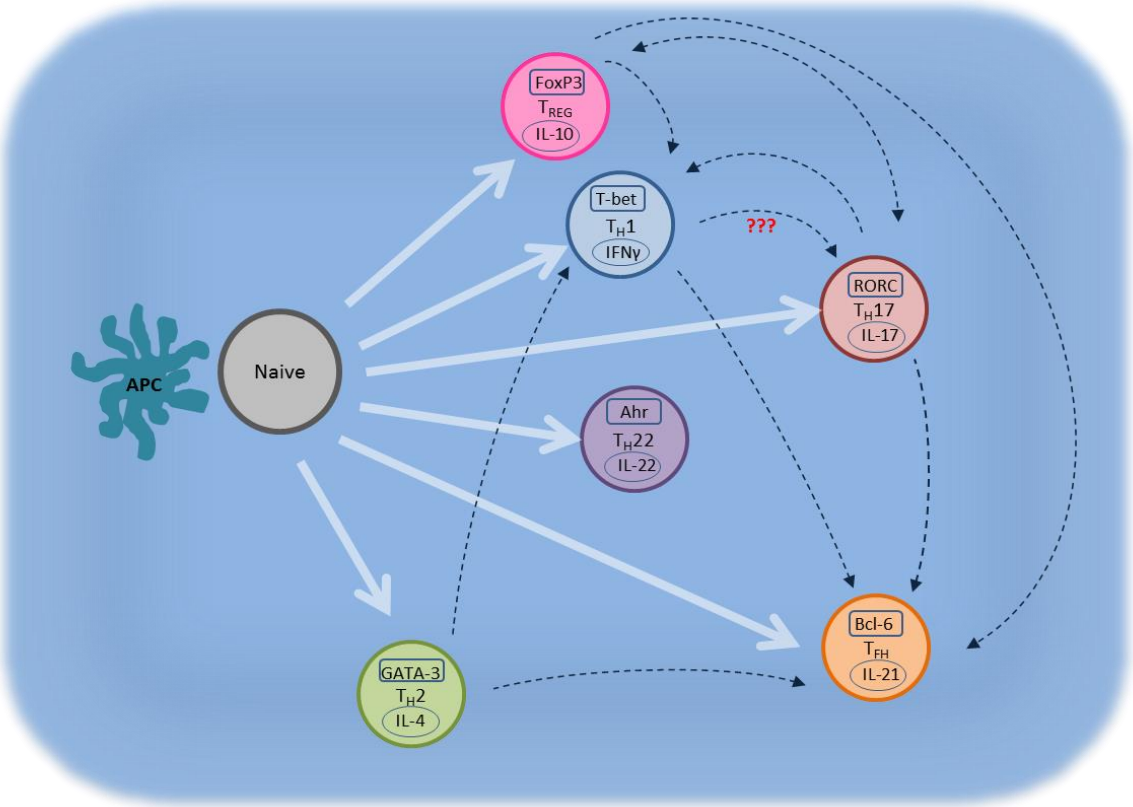

Figure 1.1: CD4$^+$ T Helper Cell Differentiation and Plasticity. APC present antigen and activate naïve CD4$^+$ T cells which leads to their differentiation down one of several different T_H phenotypes. It is the cytokine within the immediate environment that is the driving force behind which phenotype the T cell acquires. The T_H phenotype is defined by the cytokines expressed by the cells (key cytokine highlighted within the cell) and the lineage defining transcription factor. Until recently these were thought to be a stable phenotype. However, there has been evidence of T_H cells expressing two different lineage defining cytokine, and the associated transcription factors. Significant work has been done to understand if these changes in phenotype are transient or permanent. IFNγ$^+$$T_H1$ cells have been found to express RORC, the T_H17 transcription factor. It is unknown if these cells are ex-T_H17 cells or T_H1 cells gaining T_H17 functions. Dotted arrows show the direction in which plasticity is through to occur.

IL-17A and IL-17F and their heterodimer bind on T cells through a heteromeric receptor complex of IL-17RA and IL-17RC. These trans-membrane protein receptors are expressed by a variety of human cells including epithelial cells, fibroblasts. IL-17RA can be bound by IL-17A and IL-17F, but with 10-fold more affinity for IL-17A. Although these two isoforms of IL-17 bind to the same receptor they have different biological effects[76]. Only IL-17A$^{-/-}$ mice are susceptible to *C.albicans* infections even though the mice have normal levels of IL-17F [77]. Only IL-17A is capable of inducing cytokine production by macrophages while both IL-17A and IL-17F can both activate epithelial innate immune responses[78]. This suggests that although similar, IL-17A has a non-redundant role in immunity that IL-17F cannot replicate.

IL-17A acts on fibroblasts, endothelial cells, macrophages, epithelial cells and astrocytes. This cytokine induces anti-microbial peptides and neutrophil activating peptides[79]. IL-17A is also produced by a variety of innate cells such as NKT cells, macrophages and lymphoid tissue-inducer cell (LTi).

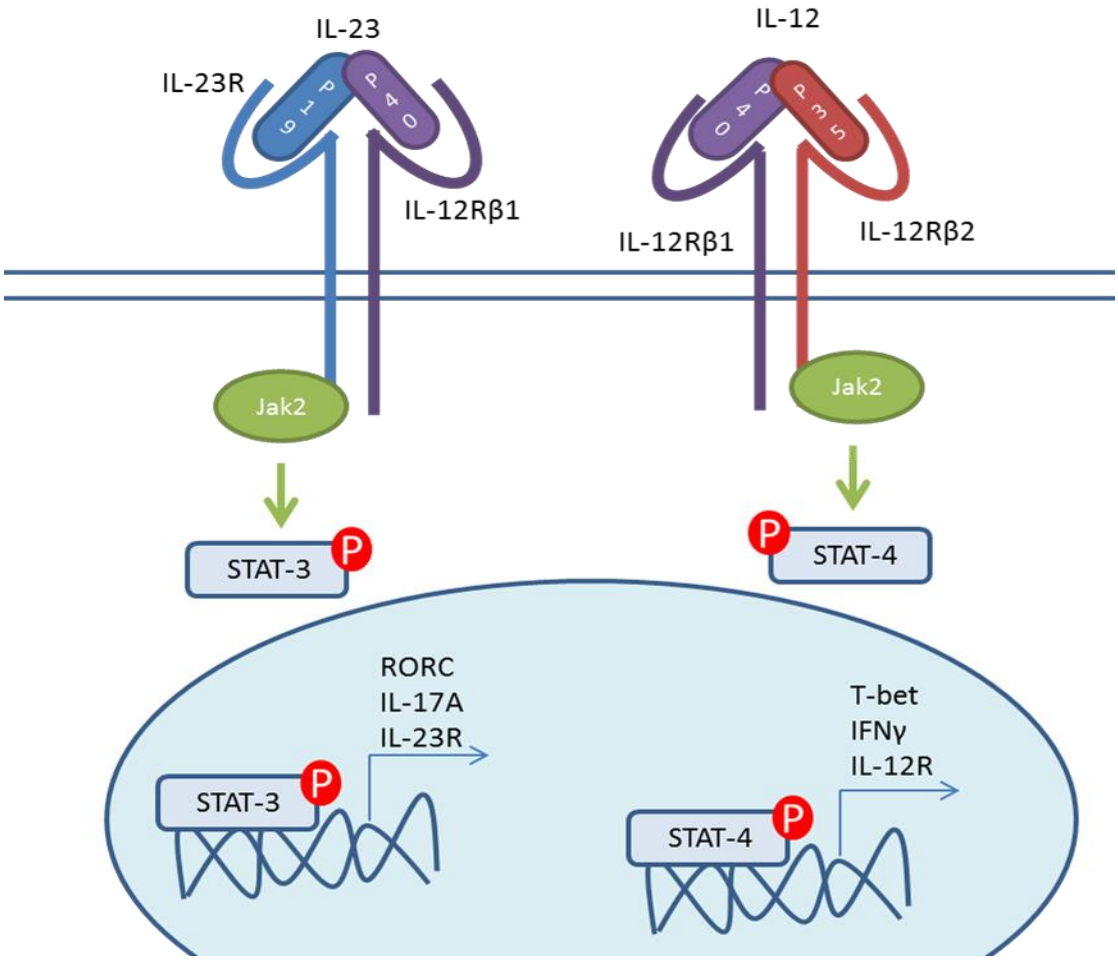

Figure 1.2: IL-23R and IL-12R structure and signalling. IL-23 is a heterodimer cytokine composed of p40 and p19 subunits. The p40 subunit is also shared with IL-12 and is paired with p35. The two receptors have a common IL-12Rβ1 subunit. The IL-12Rβ1 is paired with IL-12Rβ2 to make a functional IL-12R. The activated Jak2 phosphorylates STAT-4 allowing it to translocate to the nucleus where it aids in the transcription of genes associated with T_H1 phenotype. When IL-23 binds to its receptor, the Jak2 phosphorylates STAT-3 which translocate to the nucleus where it aids in the transcription of genes associated with T_H17 phenotype.

Although IL-17 has been labelled a 'pathogenic' cytokine due to its presence in many autoimmune diseases it plays a vital role in protecting the body against fungal and bacterial infections. Its actions are mainly through the recruitment and activation of neutrophils. The production of IL-17 by $CD4^+$ T cells in response to an infectious agent was first discovered in response to *Borrelia burgdorferi,* identifying IL-6 as a possible factor for the induction of this effector cytokine[80]. The need for IL-17 dependent induction of chemokines in the lung, responsible for neutrophil recruitment, was demonstrated using a murine model of *Klebsiella pneumoniae* lung infection. Human IL-17 also induces the expression of GM-CSF in cells such as fibroblasts, which promotes neutrophil maturation from $CD34^+$ hematopoietic progenitor in the bone marrow[81]. Adequate numbers of neutrophils are required for protection against fungal infections[82]. This is why T_H17 and the cytokine IL-17A play an important role , through neutrophil recruitment, in the removal of fungal infections, such as *Candida albicans,* from the body[83].

The lineage defining transcription factor for T_H17 cells is the steroid orphan nuclear receptor, RAR-related orphan receptor C (RORC)[84]. A slice variant of RORC, RORγt, is expressed in mice. RORC has been shown to directly bind to an *il17* gene promoter and also control the expression of CD161 [85], IL-23R and IL-1R, although it is not known if this is through direct effects on the genes. RORα is another variation of the orphan nuclear receptor and has been shown to be expressed in T_H17 cells. RORα can enhance IL-17 production but has been shown not to be necessary for T_H17 induction[86]. Aryl hydrocarbon receptor (Ahr) is a transcription factor associated with IL-22 production in T_H17 cells[87].

The T_H17 transcription factor RORγt is also expressed in immature $CD4^+/CD8^+$ T cells in the thymus and promotes thymocyte survival[88]. Lymphoid tissue inducer (LTi) cells are involved in the formation of secondary lymphoid organs and during lymph node and Peyes patch development it is vital for LTi cells to express RORγt [89].

1.5.3.2 Induction of T_H17 Cell Phenotype

A substantial amount of work has been done to identify the factors that induce T_H17 cells. Very early on it was noted that the T_H1 programme, and IFNγ, acted as a potent inhibitor of the T_H17 differentiation programme, instead of it being a shared developmental pathway[90]. At this point it is important to distinguish the difference in mice and human T_H17 cells differentiation. Although this study considers human T_H17 differentiation, a lot of the work done in this area is in murine models of disease and T_H differentiation so it is important to understand the workings of both systems.

Murine naïve cells require a combination of inflammatory cytokines to induce a T_H17 phenotype. Transforming growth factor (TGF)-β is key for the induction of T_H17 in mice along with IL-6[91,92]. IL-6 up-regulates IL-23R and IL-21 production. IL-21 is involved in a feedback loop which also itself up-regulates IL-23R[93]. This responsiveness is dependent on RORγt expression. The sensitivity of these cells to IL-23 is important for the survival and maintenance of a T_H17 phenotype[73]. IL-1 and TNF-α are also important co-factors for the induction of a T_H17 phenotype[94].

In mice it has been suggested that the cytokines required for effective T_H17 differentiation is dependent on the anatomical location that the T cells are activated in. IL-1β was shown to be vital at all sites of the body, whereas IL-6 was needed for skin and mucosal T_H17 priming but not needed in the spleen[95]. Whether this finding of difference in induction at different anatomical locations translates to the human system is unknown.

TGF-β plays a role not just in the induction of T_H17 cells in mice but also T_{REG}. In the presence of pro-inflammatory cytokines, such as IL-6 and IL-21, TGF-β at low concentrations induces RORC and T_H17 phenotype[92]. At high concentrations TGF-β has an antagonistic relationship and favours the induction of FoxP3 and a regulatory phenotype[96]. TGF-β in mice does not directly promote T_H17 phenotype or RORγt. TGF-β in this setting suppresses STAT-4 and GATA-3, preventing competition from the T_H1 and T_H2 lineage. In STAT-$6^{-/-}$, T-$bet^{-/-}$ mice only required IL-6 to differentiate naïve $CD4^+$ T cells to express IL-17 and RORγt[97].

Human T_H17 cell differentiation appears to be more elusive, especially when compared to the relatively easy differentiation of murine naïve cells to a T_H17 phenotype. IL-6, which signals through STAT-3, and IL-1β are strong inducers of IL-17 expression in naive T cells and are important for the initial expression of RORC in human T cells[98]. TGF-β and IL-21 were suggested to convert peripheral naïve cells into T_H17 cells. The effects of TGF-β on naïve T cells in culture were hotly debated as conflicting papers were published[98,99]. It was decided that the effect of TGF-β is a balancing act between the inductions of T_{REG} or T_H17 phenotype. Low concentrations of TGF-β and other inflammatory cytokines can induce T_H17 cells. Conversely, high levels of TGF-β will induce FoxP3 and a suppressive phenotype[99], similar to

mice. Large doses of IL-2 can suppress the induction of IL-17 in naive T cells[98]. IL-23 maintains the human memory T_H17 phenotype, signalling through STAT-3. Hyper IgE syndrome, in which there is a genetic defect in STAT-3, results in the absence of T_H17 cells and recurrent fungal infections[100]. STAT-3 directly binds to the IL-17 promoter and can induce IL-23R expression.

The level of TcR activation by either anti-CD3/anti-CD28 beads or antigen pulsed DC changes the number of IL-17 secreting cells in $CD4^+$ T cells. After culture with T_H17 polarising cytokines low TcR activation of T cells favoured T_H17 cell induction. High TcR activation led to the induction of FoxP3 expression and β–latency-associated peptide (LAP) expression. Nuclear translocation of nuclear factor of activated T cells (NFATc1) is induced with both low and high TcR activation. However, it will only bind to the IL-17 promoter with low TcR activation[101]. Furthermore, *in vivo* activated monocytes from inflamed joints of RA patients[102] or TLR activated DC[98], but not monocyte derived DC were potent T_H17 polarising cells. Naïve cells expressing IL-1R are more susceptible to conversion to T_H17 phenotype, due to their responsiveness to IL-1[103].

There have been some remarkable papers identifying cells that are more susceptible at acquiring a T_H17 phenotype. In umbilical cord blood and in the thymus a small percentage of naïve T cells, identified by the surface expression of CD161 (NKR-P1A), can convert to IL-17 producing cells in response to IL-1β and IL-23. The $CD161^+$ population in peripheral blood was enriched for IL-17A, IL-23R, CCR6 and RORC gene expression compared to the $CD161^-$

$CD4^+$ population. Lenti-viral transduction of RORC in $CD161^-CD4^+$ cells from UCB induced CD161 expression as well as IL-23R, CCR6 and IL-17 expression[8].

Leading on from the idea that there are pre-committed T_H17 cells, naturally occurring T_H17 (nT_H17) cells have been discovered. In mice nT_H17 cells acquire effector function in the thymus before they have encountered peripheral antigen. Their development is independent of STAT3 and IL-6, though still partially dependent on IL-23, and nT_H17 still expresses the lineage defining transcription factor RORγt. It is unclear whether these nT_H17 cells are as plastic as inducible T_H17 cells and if nT_H17 can convert to T_{REG} phenotype like its peripheral counterpart.

1.5.3.3 Molecular Signatures of T_H17 cells

In humans by definition an IL-17 secreting cell that expresses the transcription factor RORC is a T_H17 cell. However, due to the need to isolate viable cells and the emergence of plasticity in T_H differentiation the expression of these two molecules may not be enough to identify T_H17 cells. A surface marker that can define a discrete population of T_H17 cells or cells with T_H17 phenotypes is necessary, although unfortunately not identified yet.

As mentioned in the section above, IL-23 plays an important role in the maintenance of T_H17 cells. RORC can induce the expression of IL-23R in a positive feed-back loop. IL-23R is significantly up-regulated on T_H17 cells. Using an antibody to stain for IL-23R is rarely used in the literature and regularly people use an up-regulation of IL-23R at gene expression level as a sign of T_H17 differentiation.

IL4I1 is the gene for a secreted phenylalanine oxidase that is expressed in T_H17 cells but thought not to be expressed by T_H1 cells. This protein is associated with reduced expression of parts of the TcR CD3 chains. This effectively leads to reduced activation of the IL-2 promoter and reduced proliferation of T_H17 cells compared to other T_H subsets[104]. IL4I1 expression is identified through increased relative expression via qRT-PCR in the literature[105]. This molecule can also be secreted by DC to affect T cells directly[106].

As outlined above there are cells found in the thymus and naïve cord blood that are $CD161^+$ and are already RORC positive[8]. In humans $CD161^+$ cells are highly enriched with IL-17 secreting cells, though not all $IL\text{-}17^+$ cells express CD161. Curiously, adding to the argument that human T_H17 cells are different to murine T_H17 cells, murine T_H17 cells do not express the equivalent receptor (NK1.1) on IL-17 producing cells. A member of the C-type lectin superfamily, whose ligand is LLT-1, CD161 is not exclusively expressed on $CD4^+$ T cells. NK cells express CD161, and binding of LLT-1 to this receptor leads to inhibition of NK cell mediated cytotoxicity. Engagement of CD161 can inhibit TNF-α production by TCR activated CD8 T cells. T_C17 are $CD8^+$ T cells that express IL-17 and are contained within the $CD161^{++}$ population[107]. CD161 expression on B cells and DC is thought to be involved in NK cell-APC interactions[108]. The functional consequences of CD161 binding to its ligand in T cells is not known[8], though CD161 expression might have something to do with migration of these cells through the endothelium[109], increased IFNγ production and possibly a role in co-stimulation of T cells[7].

The chemokine receptor CCR6 is strongly associated with T_H17 cells[1,37]. All IL-17 secreting cells express CCR6, though not all CCR6 expressing cells make IL-17. Other chemokine receptors are more promiscuous, binding to several different chemokines, whereas $CCR6^+$ cells, as far as we know, only migrate towards one chemokine - CCL20 (MIP1α)[110]. In humans CCR6 has been used to identify cells that have characteristic of T_H17 cells in other populations. Within peripheral blood there are $CCR6^+T_{REG}$ cells that are $RORC^+FoxP3^+$ and express IL-17 but have suppressive potential[111]. It is not known if these cells express CD161 as well. CCR6 is expressed on B cells and is important for B cell differentiation and maturation[86,89].

1.5.4 T Helper 22 Cell (T_H22)

Initial studies identified IL-22 as a T_H17 associated cytokine[113]. However, $CD4^+$ T cells have now been identified that only secrete IL-22 without it being co-secreted with IL-17A or IFNγ. IL-22 had potent effects on keratinocytes, hepatocytes and other mucosal sites but is mainly associated with immunity and disease in the skin. T_H22 cells express homing markers such as CCR10, CCR6 and CCR4[114]. IL-22 in the skin can induce production of antimicrobial peptides, and can induce anti-apoptotic and pro-proliferative effects in responding cells[115,116]. A transcriptome analysis of T_H22 compared to T_H1 and T_H17 cells to determine if they were a separate lineage identified several genes that were unique to T_H22 cells. Many of these unique genes encoded proteins involved in tissue remodelling, such as FGF's, and chemokines involved in fibrosis and angiogenesis, such as CCL7 and CCL15[116] .

From naïve T cells TGF-β and IL-6 will drive a T_H22 phenotype and the induction of the ligand activated transcription factor, Ahr, which drives the expression of IL-22[114]. IL-23 seems to be responsible for amplification of IL-22 but cannot restore IL-22 induction in Ahr deficient T_H17 cells. There are subsets of NK cells that express IL-22(Nk-22) and also express Ahr[117].

1.5.5 T Follicular Helper cell (T_{FH})

Within the lymphoid tissue there is a subset of antigen experienced T cells that play a role in aiding B cell activation. They express CXCR5 and are known as T follicular helper cells (T_{FH})[118]. CXCR5 is the chemokine receptor for CXCL13 which is highly expressed in the B cell zones of secondary lymphoid structures and attracts B cells as well as T_{FH} cells. These cells aid in the formation and maintenance of germinal centres (regions of secondary lymphoid tissue that help B cell immunity). The expression of IL-21, ICOS and CD40L by T_{FH} is important in this process and in aiding isotype switching in B cells. Bcl6 is a transcriptional repressor associated with T_{FH} cells but considered the master regulator of the subset. It represses the lineage defining transcription of other subsets such as T-bet and GATA-3. An interesting aspect of T_{FH} is that these cells can also express characteristic of other T_H cells types such as signature cytokines of T_H1 or T_H2 and T_H17 cells.

1.5.6 Regulatory T cells (T_{REG})

Regulatory T cells are a vital subset of $CD4^+$ T cells that induce both tolerance to self and control otherwise pathogenic immunity. The main function of T_{REG} is to use an arsenal of

mechanisms to suppress the immune response. They make up 5-10% of the $CD4^+$ T cell population and can be produced in the thymus (nT_{REG}) or induced in the periphery (iT_{REG}). They are primarily characterised by the expression of a gene known as Forkhead Box P3 (FoxP3)[119] and the IL-2 receptor α chain (CD25)[120]. Similar to other T cells, they have a TcR specific for a cognate antigen; although the antigen is frequently a self-peptide. The importance of the transcription factor FoxP3 within the T_{REG} is demonstrated in the genetic disease immunedysregulation polyendocrinopathy enteropathy X-linked syndrome (IPEX), in which the sufferers lack functional FoxP3[121]. The phenotype of this disorder is a severe and extensive auto-immune disease.

T_{REG} cells employ a variety of different mechanisms to suppress T effector cell activation and proliferation. T_{REG} secrete the anti-inflammatory cytokines IL-10, IL-35 and TGF-β. T_{REG} can release protease enzymes such as granzyme and perforin that leads to destruction of effector cells. T_{REG} can also cause metabolic disturbances such as cytokine depletion by the high affinity receptor CD25, adenosine generation via CD73 and CD39 receptors and cAMP mediated inhibition of proliferation. Finally, T_{REG} can target dendritic cells function through CTLA-4 binding and removal, via trans-endocytosis, of CD80/86[122] from the surface of the cell. This affects maturation of effector cells and reduces their proliferative ability[123].

Naturally occurring regulatory T cells (nT_{REG}) are differentiated within the thymic medullary region in a MHC class II dependent process[124]. The self-reactive TcR that T_{REG} frequently carry is activated and causes expression of FoxP3. A murine model using a transgenic TcR specific for a self-peptide generated large numbers of T_{REG} while mice that did not express

the antigen could not produce any. There are clearly other signals that control T_{REG} differentiation as not every cell that expressed the transgenic TcR became a T_{REG}[125].

iT_{REG} are induced in the periphery, with early evidence of adoptive transfer experiments showing conversion of naïve cells to a T_{REG} phenotype. Naïve $CD4^+CD25^-$ T cells injected into lymphopenic mice increase in number and a small proportion gain T_{REG} cell markers such as CD25, CTLA-4 and FoxP3 expression. iT_{REG} development has been defined as dependent on antigen stimulation, IL-2 and TGF-β *in vitro*[126,127]. However the *in vivo* environment for iT_{REG} induction has not been completely defined. TGF-β relies on SMAD3 and the nuclear factor of activated T-cells (NFAT) to induce FoxP3, while the IL-2 lifts the TGF-β anti-proliferative effect. TGF-β has been shown to be less important to nT_{REG} development. IL-2 in addition does not play a vital role in nT_{REG} development and is dispensable, and can be replaced by IL-15 in $IL\text{-}2^{-/-}$ mice.

Additional suppressive populations are the T_R1 and T_H3 cells. T_R1 cells express IL-10 and TGF-β, which they employ as their main mechanism of suppression, although they do not express stable FoxP3. They are induced from naïve T cells in an IL-10 rich environment[128]. T_H3 produce TGF-β and play an important role in mucosal immunity and tolerance to antigens within the gut. Although there are no specific markers for T_H3 to allow for analysis of these cells, it is thought they are induced in a TGF-β rich gut environment[129].

There are many cytokines that can antagonise iT_{REG} induction. Cytokines from other T helper subsets (IFN-γ, IL-4, IL-17 etc.) can all inhibit induction. However a small subset of $CD103^+$

DC found in the small intestine and mesenteric lymph nodes can overcome this inhibition, with the co-production of TGF-β with retinoic acid[130,131].

There are arguments about the functional differences of nT_{REG} and iT_{REG}. The iT_{REG} seem to be able to suppress T effector cells as well as nT_{REG}. However on re-stimulation in a TGF-β depleted environment the iT_{REG} loose FoxP3 expression whereas the nT_{REG} do not. This suggests differences in the epigenetics and stability of iT_{REG} phenotype[132,133]. Overall however, it is generally accepted that nT_{REG} play a role in general tolerance and protection against autoimmune disease, while iT_{REG} are important in mucosal tolerance including the gut.

1.6 Maintenance of T Helper Lineages

There are several levels at which a cell's phenotype can be controlled. T_H phenotype is induced by the cytokines and the type of stimulation that a cell receives upon activation. Additionally, there are internal pathways and transcriptional mechanisms in place to either maintain or alter the cells effector function once it has differentiated.

T_H1 and T_H17 have several feedback mechanisms that allow maintenance of their phenotype. T_H1 induced by IFNγ and IL-12 produce IFNγ themselves, which acts in a feed forward amplification loop with STAT-1 and T-bet. T-bet up-regulates IL-12Rβ2, making the cells more responsive to environmental IL-12[54]. T_H17 cells are induced through cytokines that signal through STAT-3, which induces RORC. RORC can activate the cell to express IL-23R and produce IL-21. Both IL-21 (autocrine)[93] and IL-23 (environmental)[72] maintain the T_H17

phenotype and RORC expression. IL-2 can actually promote T_H1 and T_H2 phenotypes and suppress T_H17, its signalling through STAT-5 leading to alterations in important gene expressions such as IL-4 receptor α and IL-12Rβ2 and suppression of IL-6 receptor[134].

To further maintain a phenotype cells also have transcriptional mechanisms to suppress other T_H phenotypes. T_H1 and T_H17 can repress the phenotype of the other T_H cell. IFNγ has been shown to suppress a T_H17 phenotype while IL-17 and RORC can suppress T-bet and a T_H1 phenotype[90]. Jenner *et. al.* showed that T-bet and GATA-3 can occupy many of the same gene targets. The group identified GATA-3 binding to target genes within T_H1 cells. For example, in a T_H1 cell, T-bet could bind to IFNG and activate the gene while binding to the IL4 gene and directly repressing its expression. GATA-3 could act to oppose that by activation of the IL4 gene and repressing IFNG gene[135]. GATA-3 has been shown to suppress IL-12Rβ2 expression to weaken T-bet expression[56]. As well as the lineage defining transcription factors (T-bet, GATA-3, RORC etc.) there are other transcription factors and mediators that are induced to aid in the suppression of other phenotype. Runx3 is activated by T-bet to suppress the IL4 gene and contribute to the stability of the T_H1 lineage[136]. Runx1 is needed for the transactivation of RORγt and if T-bet is present it will bind Runx1 and suppress RORγt expression[137].

1.7 Plasticity of T Helper Lineage

Maintenance of an appropriate immune response is vital to ensure that the pathogen is effectively removed. Until recently differentiated T_H cells were thought to be permanently

committed to a single lineage. However, there is now increasing evidence that $CD4^+$ T_H cells can be plastic in nature. Appropriate stimulation can switch a memory $CD4^+$ T cell's phenotype to a different T_H lineage. There are examples in the literature of different lineage defining cytokines being co-expressed in a single cell, both *in vitro* and *in vivo*. Lineage defining transcription factors can also be found to be co-expressed in certain situations[138] (**Figure 1.1**).

1.7.1 Populations of T_H Cells that Exhibit Plasticity

T_{REG} have been shown to be a particularly plastic population as mentioned in **Section 1.5.3.2**. There is a strong link in mice between the induction of T_{REG} and T_H17 cells. TGF-β at high concentrations induces FoxP3, yet TGF-β with other inflammatory cytokines such as IL-6 induces a T_H17 phenotype. This is confirmed by TGF-$\beta^{-/-}$ mice being unable to develop either T_{REG} or T_H17. This suggests a link in the differentiation of these two very different effector subsets[58,96].

FoxP3 can inhibit RORγt activity by direct binding. Despite this there is evidence that cells can co-express these lineage defining transcription factors with both having an effect on the phenotype of the cell. Voo *et. al* identified $CCR6^+$ cells that expressed RORγt and FoxP3. They maintained their suppressive ability but upon stimulation produced IL-17[111]. Using a ROR-GFP knock-in mouse Zhou et al. showed that a small proportion of cultured cells treated with TGF-β could express both transcription factors RORγt and FoxP3. These co-

expressing cells are also found *in vivo*. A small percentage of cells that expressed FoxP3 had differentiated into IL-17 expressing cells, suggesting a lineage change[139].

T_{REG} can express characteristics of other pro-inflammatory subsets. Koch et al. proposed that CXCR3, a chemokine receptor expressed on T_H1 cells, can be a marker in T_{REG} of T-bet expression. $FoxP3^+CXCR3^+$ cells were shown, in mice, to play a role in controlling infection in a T_H1 immune response. The $T\text{-}bet^+$ T_{REG} cells still possess regulatory phenotypic markers and suppressive capabilities. The expression of T-bet appears to improve the homeostatic capacity of the T_{REG} in T_H1 environmental conditions[140].

Conversely, there appears to be situations where T_H1 cells can produce IL-10, a regulatory cytokine normally attributed to a T_{REG} cell. In a murine model of *T.gondii* infection IL-10 producing $CD4^+$ T cells could co-produce IFNγ and expressed T-bet. $IL\text{-}10^+IFN\gamma^+$ cells can suppress *T. gondii* growth with high levels of nitric oxide produced by APC (induced by IFNγ), but suppress IL-12 production in APC (through IL-10 suppression). These cells were $FoxP3^-$ $CD25^-$ and could proliferate, suggesting they did not have a T_{REG}/T_R1 phenotype or background [141].

T_H2/T_H17 cells have also been detected at both a very low level in healthy controls, and at higher proportion in patients with asthma. High levels of T_H2/T_H17 cells in asthma patients makes sense as the T_H2/T_H17 cells have been shown to have a greater ability to induce IgE, which is involved in the pathology of this disease. T_H17 clones which were stimulated in a T_H2 polarising environment were induced to become T_H2/T_H17 cells. T_H2 cells could not become IL-17 producing under T_H17 stimulating environment.

Unexpectedly, during an infection of the T_H1 promoting- lymphocytic choriomeningitis virus (LCMV) T_H2 cells in mice can be reprogrammed to express both GATA-3 and T-bet along with IL-4 and IFNγ. Without this switch, brought on by IL-12 and interferon's, the mice succumbed to fatal immunopathology[142].

T_H17 cells that co-express IFNγ are easily detected in the peripheral blood of healthy controls. Surprisingly both T_H17 and T_H17/T_H1 clones have been shown to express both RORC and T-bet at mRNA level. When T_H17 clones were re-stimulated in the presence of IL-12 it induced IFNγ production. IL-23, IL-12 or IL-2 could not induce T_H1 clones to produce or up-regulate IL-17, at mRNA or protein level. This suggests again more plasticity in the T_H17 lineage than the T_H1. T_H17/T_H1 cells express the same phenotypic markers as T_H17 such as CCR6, and IL-23R. Interestingly, T_H17 cells isolated and cultured *ex vivo* with IL-12 could not switch on IFNγ production[143]. Only when IL-12R was up-regulated did these cells convert[144]. This suggests that memory cell's ability to respond to cytokines is a vital factor in their phenotype stability.

From many diseases it has been the suggested that the plasticity of T_H17 may play a role in the pathogenesis of the disease. $CD161^+IFN\gamma^+IL\text{-}17^+$ cells were found in the synovial fluid (SF) of juvenile idiopathic arthritis (JIA) patients, and the number of these cells correlated with disease activity [145]. These T_H1/T_H17 cells were also present in the gut of people with Crohn's disease[1].

Within the literature there is a debate as to whether cells with a dual phenotype have transiently been able to acquire the additional features or if they are being directed down a permanent path.

Experiments using reporter mice gives scientist the ability to follow a single cells through its differentiation path[146]. An IL-17-YFP reporter mouse was used to determine the fate of T_H17 cells in two inflammatory situations, a chronic EAE model and an acute cutaneous infection of *Candida albicans.* In cells that express or have expressed IL-17A, these cells would appear YFP^+. Interestingly, there was a switch of some of the T_H17 cells (YFP^+) in EAE to secrete IFNγ, while the resolving *Candida* infection only resulted in IL-17 for a short time, with no IFNγ production from these cells. The interesting thing about the T_H1 cells within the spinal cord in the EAE model was that they were almost all $YFP^+IFN\gamma^+$ but were IL-17^-. This suggests in a highly inflammatory situation T_H17 cells can convert to T_H1 cells. They suggest that the switch to secreting IFNγ in T_H17 cells was down to their responsiveness to IL-23[146].

In humans T_H1 cells with phenotypic feature of a T_H17 cell have been described as $CD161^+IFN\gamma^+$ cells. Francesco Annunziato's group suggests that the non-classical T_H1 cells are T_H17 derived, as they share expression of RORC, IL-23R, IL4I1 along-side T-bet and IL-12Rβ2. These cells however are no longer secreting IL-17. The non-classical cells were found to be present in the SF of JIA patients[105].

Using humans $CD4^+$ T cells Sallusto *et. al* investigated the type of T_H17 response that results from exposure to *C.albicans* and *Staphylococcus aureus.* Monocytes were pulsed with either

of these pathogens and cultured with naïve $CD4^+$ T cells. The resulting IL-17 secreting cells differed. In response to *C. albicans* T_H17 cells secreted IFNγ, whereas *S. aureus* induced a IL-10 secreting T_H17 cell.[147] This result suggests that different inflammatory situations will illicit different profiles in T_H17 cells. Although this experiment demonstrates the possibility to express more than one lineage defining cytokine at once it does not answer whether T_H cells are plastic or just transiently up regulate other cytokines.

Within human systems it is always going to be extremely hard to find out the true fate of a cell. The only method of assessing the phenotype is to extract the cell and manipulate them *ex vivo*. This is not ideal, especially for T_H17 cells as we are still unsure as to the true differentiation pathway *in vivo*. The best approach is to make sure that the population is as homogeneous as possible. Purity of the population has to be assured by vigorous cell sorting to avoid potential contaminants[147,148].

All the examples of cells co-secreting two lineage defining cytokines or transcription factors goes against the paradigm of repression of the different lineage. This demonstrates that there is a certain level of flexibility in the differentiation process. Whether this is flexibility in the initial differentiation or once the cell has already differentiated is still unknown. The next step is to understand when and where these cells come into play. Are they in transition or are they a stable phenotype? Han et al. recently tested if poly-functional T cells were a true reflection of an immune response over time. They added one cell to a nano-well and sampled the supernatant for IFNγ, TNF-α and IL-2 every hour after stimulation. They showed that cells only transiently secreted two cytokines. This was the intermediate stages between

switching off one cytokine and switching on another. The delayed response of some cells to the stimulus meant that the production of cytokine overall was poly-functional but individual cells were rarely a true dual secretor[149]. However, as the murine fate mapping model[146] showed plasticity of a T_H phenotype might be different in a situation of chronic inflammation.

1.7.2 Control of Plasticity in $CD4^+$ T Cells

There is no sufficient evidence to show that the expression of lineage-specific transcription factors does not have exclusive expression patterns to the different lineage. There is a scale of transcription factor expression rather than the binary on/off expression that was initially proposed.

It is important to understand what induces the transcription factors and repressors and the effects these molecules have on the cells. Therefore, although we look at transcription factor expression it might also be important to look at other factors such as the relative level of transcription factor expression, epigenetics such as methylation of genes and post transcriptional modifications like miRNAs. This will help understand to what extent the transcription factors are controlling the cell's phenotype.

1.7.3 Why it is Important to Understand Plasticity?

Within many autoimmune diseases, such as arthritis, MS and Graves disease, $CD4^+$ T cells are considered key in the pathogenesis of the disease. Initial understanding which $CD4^+$ T cells cause the disease is important. Understanding the plastic element of these cells will give the potential to 'reset the clock' on some of the disease causing subsets. So, for example, if T_H17 cells are vital to the onset of MS then understanding the factors that leads to these cells becoming T_{REG} can lead to therapeutic potential[150].

On the flip side there are therapies coming to trial now that use cells from the patient's own blood to treat diseases like cancer. If we do not understand the factors that will switch these cells to other subsets, then the beneficial T_{REG} that could be inserted to treat the cancer could differentiate into harmful T_H1. This could cause more damage than the disease it is trying to treat.

Finally, working on T cells offers a great system to model plasticity. Understanding how plasticity occurs within T cells may lead to us to further understand plasticity in other organs of the body that are less accessible.

1.8 Autoimmunity

Multiple sclerosis is an autoimmune disease of the central nervous system. The disease is thought to be caused by auto-reactive adaptive immune cells responding against a neuron antigen leading to demyelination of neurons and causing neurological dysfunction. T cells,

specifically T_H1 and T_H17 cells have been implicated in playing an important role in the pathology of MS.

1.8.1 Anatomy of Central Nervous System

The central nervous system (CNS) is made up of the brain, spinal cord, optic nerve and the retina, which are all encapsulated with the bony structures of the skull and spinal cord. The brain parenchyma and spinal cord is encapsulated within the meninges. This structure is made of three membranes; in contact with the brain is the Pia mater, then the Arachnoid and finally the Dura mater next to the skull. Between the Pia mater and the Arachnoid is the subarachnoid space; a fluid filled space containing cerebrospinal fluid (CSF).

CSF is an important fluid for the protection of the brain and spinal cord but also for the metabolism and homeostasis of the CNS. CSF is a fluid generated by a structure within the ventricles of the brain called the choroid plexus (**Figure 1.3**). The choroid plexus is made up of a web of capillaries with special endothelia and surrounded by stroma. These structures are covered by a monolayer of epithelial cells and these cells control the movement of solutes and fluid, through diffusion and active transport, from the blood into the arachnoid space to make up the CSF. Interstitial fluid from the brain parenchyma also makes up a small portion of the CSF.

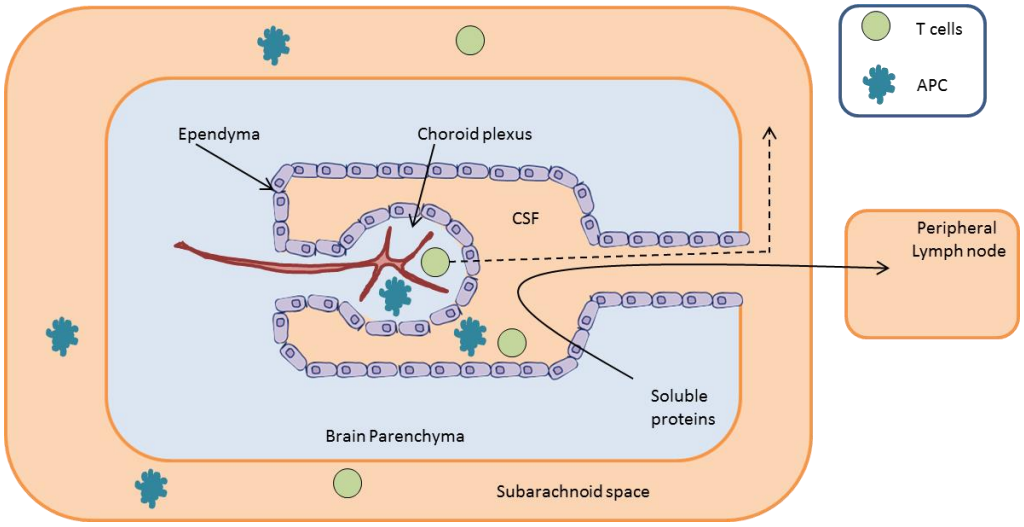

Figure 1.3: A Cartoon Version of the Central Nervous System. The brain parenchyma is surrounded by the fluid filled subarachnoid space. The choroid plexus within the cerebral ventricle is contains the ependymal cells that secrete the CSF fluid into the subarachnoid space. The T cells from the peripheral blood can enter the CNS through the choroid plexus, using CCR6 dependent migration. APC within the subarachnoid space will not leave the CNS, however soluble antigen from the brain parenchyma can be found in peripheral lymph nodes.

Within the brain parenchyma there is the white and grey matter of the brain. The white matter contains the glial cell and mylinated axons while the grey area of the brain consisting of neuronal cell bodies, neutrophil, glial cells and capillaries.

1.8.2 Immune System Within the CNS

The CNS has evolved as an immune privilege site, meaning there are mechanisms in place that will prevent inflammation to reduce the chance of damage to this vital organ. Immune privilege within the CNS can be verified by placing material such as tumour cells, viruses[151] or bacteria[152] in the brain parenchyma of mice. If done carefully there will be no cell mediated response to the material as antigen-carrying APC from the parenchyma will not reach peripheral lymph nodes to prime an immune response. This effectively means the brain is hidden from the peripherally immune system. However, when the antigen (in this case Bacillus Calmette–Guérin (BCG)) was injected peripherally in mice that had been exposed to BCG in the brain (with no response), there was a delayed type hypersensitivity response within the brain and demyelination of the nerves took place[153]. This suggests that it is the afferent arm of the immune response, the priming of antigen presenting cells that is prevented in the CNS. The efferent arm, primed antigen specific cells that have migrated into the site of infection, functions normally. It is the blood brain barrier (BBB) that keeps the fluid and cells of the brain parenchyma as a separate entity from the peripheral blood. The blood brain barrier is made up of special tight junctions in the capillaries in the brain, and surrounding these capillaries is a barrier of astrocyte foot processes (known as the glia limituns) (**Figure 1.4**). Soluble antigens are able to drain from the CNS in to the deep cervical lymph nodes [154](**Figure 1.3**) while APC are not to be able to migrate out of the CNS.

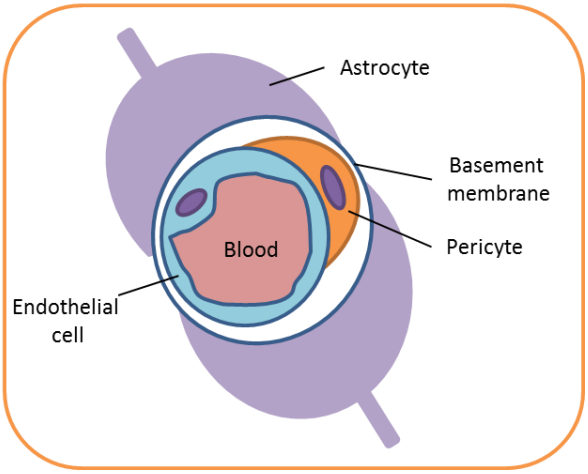

Figure 1.4: Components of the Blood Brain Barrier. The peripheral vascular system is kept separate from the brain parenchyma by the blood brain barrier (BBB). The capillaries in the brain have special tight junctions in there endothelium and surrounding these capillaries is a barrier of astrocyte foot processes (known as the glia limituns). Pericytes help sustain the blood–brain barrier.

Microglial cells, a resident macrophage within the brain, in healthy individuals are in a non-activated state due to the immunosuppressive environment of the parenchyma[155]. Neither CSF nor the CNS parenchyma contains naive T cells under physiological circumstances, and classical studies suggest that primary immune responses are not primed in the parenchyma[156]. In a healthy individual the CSF only contains T cells and a few B cells, with some monocytes, but no granulocytes.

1.8.3 Migration of T Cells into the CNS

The microglial cells within the brain parenchyma are a resident cell population which are replaced via proliferation of the resident cells. T cells within the blood however need to

somehow migrate into the CNS. T cells enter from the periphery into the CSF via the choroid plexus (**Figure 1.3**). This process is controlled through a few selective chemokine and migratory receptors. CCR6 has been shown to be very important for T cell migration, especially in the disease setting of EAE[157]. T_H17 and T_{REG} have been shown to express this chemokine receptor, though these are not the only cells to express it. P-selectin and α4 integrin is also important both in disease and in health of T cell migration into the brain[158,159].

Primed T cells need to be re-activated at the site of inflammation and using a Lewis rat model of EAE it was shown that only if APC are present in the subarachnoid space, to prime the T cells, can antigen specific T cells enter the brain parenchyma[160]. However once the BBB has been activated other T cells can migrate into the brain, highlighted by the presence of $CCR6^-$ cells found after the first initial wave of inflammation in murine EAE[157].

1.9 Multiple Sclerosis

MS is an autoimmune disease of the central nervous system. The first association of the appearance of demyelinated lesions in the brain to neurological dysfunction were in 1868[161].

The majority of patients have an initial clinically isolated syndrome, followed by a period of what is known as remission, where their symptoms abate. If a series of relapses of symptoms occur this would be diagnosed as relapsing remitting multiple sclerosis (RRMS). Throughout the relapses the sufferer's disability will return back to baseline level. However within remission the patient will gradually gain further disability. This is known as Secondary

Progressive MS (SPMS). 10-15% of patients will go through primary progressive disease in which there will be no remissions or relapses they will just gradual gain disability over time.

Diagnosis of MS is now undertaken through the visualisation of the lesions within the brain using magnetic resonance imaging (MRI). Samples of CSF can also be taken to look for the presence of oligo-clonal bands [162], highlighting the presence of antibodies in the CSF.

1.9.1 Disease Prevalence

Multiple sclerosis affects around 2.5 million people around the world, with the age of diagnosis being 20-40 years. MS is twice as likely to occur in women as men. The distribution of MS sufferers worldwide is not evenly spread, with more people being diagnosed the further from the equator. This has led to the hypothesis that Vitamin D, produced by the skin in response to sunlight and obtained through diet, may have a protective role[163]. There are certain ethnic groups that have lower incidents of MS, such as Inuit, Aborigines and Maoris. It is more common in Caucasians of northern European ancestry[164].

1.9.2 Risk Factors

1.9.2.1 Genetics

MS is not an inherited disease although there have been suggestions that there may be a genetic element. There is only about a 2% chance of a child developing MS if they have a parent with MS.

Genome wide association studies (GWAS) have become an important tool in understanding MS. GWAS analyses the whole genome of patients for small nuclear polymorphisms (SNP), changes in the nucleotide sequence of genes that are found in the patient cohort to a greater extent than in the general public.

HLADRB1*1501 (encode for a subunit of human leukocyte antigen) has repeatedly appeared in GWAS studies for MS. Other susceptibility loci are in the IL2RA and IL7RA genes[165]: both genes associated with T_{REG} function. The next step for GWAS studies is to link the SNP to a functional consequence for MS.

1.9.2.2 Environment

As mentioned above Vitamin D is thought to play a part in the prevalence of MS. A prospective study of a large cohort of women indicated that Vitamin D had a protective effect against MS[163]. The mechanism of action of Vitamin D is thought to be its ability to repress T_H1 cells and promote T_{REG}[166,167].

Many people have tried to associate infectious agents with onset of MS. Several different viruses have been suggested, including rabies, herpes simplex virus, measles, corona virus, Epstein-Barr virus and others, although none have been confirmed. To date the most promising candidate appears to be the Epstein-Barr virus as there is a greater risk of developing MS if the person has had late onset infectious mononucleosis (IM)[168].

1.9.3 Immunopathology

Multiple sclerosis is characterised by subcortical or periventricular white matter focal inflammatory demyelinating lesions. Within an active lesion there are $CD8^+$ T cells, with less $CD4^+$ T cells, monocytes and B cells although the major inflammatory cell type within a lesion are macrophages[169]. Once MS has become progressive the lesions gradually expand overtime with macrophage only at the periphery of the lesion.

B cells have been identified as playing an important role in MS with antibodies involved in the demyelination process[169]. Ectopic lymphoid follicles have been identified within the meninges of MS suffers[170], suggesting the presence of an antigen to maintain the follicle. Currently no antigen has been identified.

T cells and specifically $CD4^+$ T cells are thought to be the initiators of the inflammation. T cells migrating in to the brain across the BBB will initiate inflammation which is thought to affect the BBB effectiveness. The results in more inflammatory cells entering the parenchyma resulting in continued inflammation and demyelination of the nerves of the brain and spinal cord.

Experimental autoimmune encephalomyelitis (EAE) is a murine model of MS. Demyelination of the nerves is induced with an injection of a brain antigen (e.g. a myelin oligodendrocyte glycoprotein (MOG) or myelin basic protein (MBP) etc.) along with complete Freud adjuvant (CFA) and pertussis toxin (PT). The CFA induces an immune response to the antigen and the PT will act to break down the blood brain barrier (BBB) to allow immune cells into the CNS. Other methods of inducing a MS like responses include using a transgenic TcR model specific

for MOG protein and injecting MOG into the mice, or introducing MOG specific T cells into a $RAG^{-/-}$ mice.

The CNS is a site of immune privilege as the BBB tightly controls the entrance of cells in to the CNS. Because of this there has been a focus on understanding the mechanisms by which inflammatory cells enter the CNS in EAE and MS. The removal of CCR6, the T_H17 associated chemokine receptor, was protective against EAE induction. The CCR6 ligand CCL20 was expressed on the choroid plexus and was important for the first wave of auto-reactive T cells to enter the CNS. During the initial disease $CCR6^+T_H17$ and $CCR6^+T_H1$ cells were absent from the CNS[157]. VLA-4 (α4β1) is also involved in T cell migration into the brain parenchyma, and this finding in EAE[171] lead to the use of natalizumab a monoclonal antibody against VLA-4 intergrin[172].

IL-23 has a non-redundant function in EAE initiation[57] leading to the interest shifting from T_H1 cells to T_H17 cells. Stimulating T_H17 cells with IL-23 promotes GM-CSF which is also necessary for EAE induction[173]. GM-CSF acts on dendritic cells (DC) to enhance production of IL-23 and other inflammatory cytokines which in turn promotes further activation of T_H17 cells. Like T_H17 cells, T_H1 cells are dependent on GM-CSF production for initiating EAE[173], although the mechanisms that drive GM-CSF under T_H1 conditions remain unclear. Further data suggested that T_H17 cells cannot induce disease unless they have responded to IL-23, or TGF-β3. These 'pathogenic' T_H17 cells induced EAE and have a different transcriptional profile to 'conventional' T_H17. Pathogenic T_H17 cells contain both transcription factors RORγt and T-bet[174]. Removal of TIM-3, a negative regulator of T_H1 and T_H17 cytokine

secretion, leads to exacerbation of EAE. A defect in TIM-3 has been found in patients with MS[175,176].

CD39, an ectonucleotidase which hydrolyses ATP, is expressed by some T_{REG} and these are specifically able to suppress T_H17 cells. The mechanism of suppression is thought to be a contact dependent one[177]. ATP has been shown to increase IL-17 production[178] suggesting the CD39 mediated break down of ATP may play a role in the reduction of IL-17 production by T_H17 cell. Furthermore using a blocking antibody against LAP (Latency Associated Peptide), a protein that binds TGF-β and is expressed on $CD39^+T_{REG}$, reduces the suppressive effects of $CD39^+T_{REG}$ on T_H17 cells in culture[179]. Within RRMS patients these $CD39^+$ T_{REG} have been shown to have impaired function and a reduced ability to suppress T_H17 cells. Furthermore, RRMS patients had a high percentage of IFNγ secreting T_{REG} cells compared to controls. These $FoxP3^+IFN\gamma^+$ cells, induced through culture of T_{REG} with IL-12, had reduced suppressive function[180]. This identifies mechanisms in which inflammation in RRMS patients can go unchecked by peripheral tolerance.

1.10 MicroRNA

miRNA are small, endogenous, non-coding RNA molecules. They play a vital role in post transcriptional modification of gene transcription. miRNA are partially complementary to mRNA, and they function by down regulating the expression of the mRNA by either translational repression, mRNA degradation or deadenylation[181]. To date over 2000 human miRNA are known.

Large precursor miRNA are transcribed by RNase II enzyme[182]. miRNA start their life as pre-miRNA, a double stranded hairpin structure of ~70 nucleotide in length. A complex of several molecules process the pre-miRNA, in the nucleus, consisting of the RNase III enzyme Drosha[183], and the double-stranded-RNA-binding protein Pasha[184]. The pre-miRNA is then actively transported to the cytoplasm for further processing by the RNAse III enzyme Dicer. A double-stranded miRNA of approximately 22 nucleotides in length will be the end product. Dicer also initiates the formation of the RNA-induced silencing complex (RISC). RISC is the multicomponent nuclease, which the mRNA are directed to by the miRNA that destroys the mRNA[181].

MicroRNA molecules were only recently discovered [185]. However, their importance in the negative regulation of genes has become apparent in many different systems. Using a T cell specific Dicer or Dorsha deficient mice demonstrated the role of miRNA in proliferation, survival and differentiation in $CD4^+$ T cells[186,187]. Knockdowns of Dicer lead to extensive autoimmune disease which was shown to be due to the lack of stability of T_{REG} cells. Although the T_{REG} in the thymus developed normally they were unable to maintain their phenotype in the periphery [188]. The cluster of miRNA, miR-17 – 92, were overexpressed in human lymphomas, and shown to have anti-apoptotic effects through T cell proliferation and growth[189].

There has been a great interest in the role of miRNA in T helper cell differentiation, specifically in T_H cells in a disease setting due to their potential as a therapeutic target. T-bet, the T_H1 lineage defining transcription factor is vital of the stability and maintenance of

T_H1 phenotype. In mice miR-29 has been implicated in regulating T-bet and the downstream effector cytokine IFNγ. IFNγ was shown to regulate miR-29 expression in what seems a negative feedback loop in T_H1 cells, via effects on T-bet and Eomes[190], in direct competition with IFNγ/STAT-1/T-bet positive feedback loop. An increase in miR-29 was found in MS patients, and removal of miR-29 lead to exaggerated IFNγ production and EAE[191].

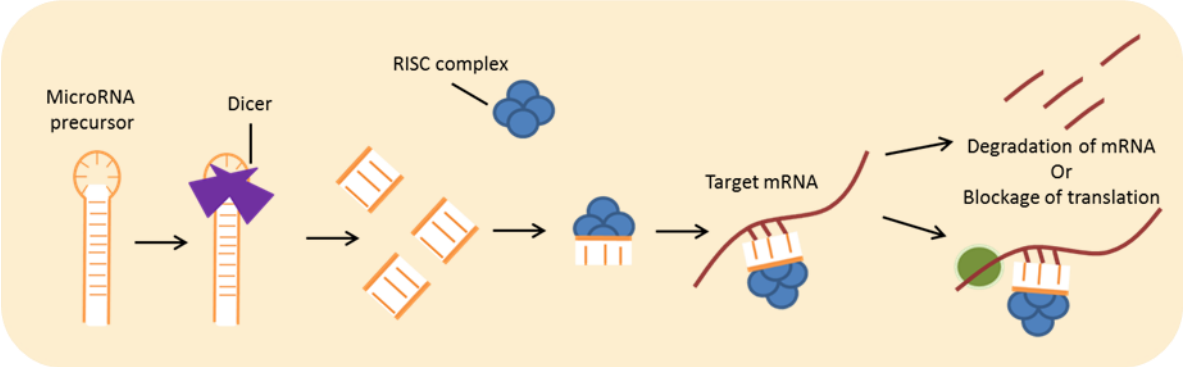

Figure 1.5 Processing and action of microRNAs. MicroRNA are transcribed as pre-miRNA that are activly spliced, by RNAse III enzyme Dicer in to double stranded miRNA. RNA-induced silencing complex (RISC), a nuclease will direct the miRNA to its target mRNA. The binding of the miRNA to it's target mRNA leads to reduced transcription, either due to its degredation or effects on the transcription of the mRNA.

The miR-29 has also been shown to be up-regulated in other T helper subsets, and is not exclusively expressed in T_H1 cells.

Due to the involvement of T_H17 cells in EAE there have been a few miRNA that are not only associated with T_H17 differentiation but also the pathogenesis of EAE. miR-155 expression in T cells is vital for the full development of EAE due to its involvement in induction of the T helper subsets T_H17 and T_H1[192]. Several genes vital for T_H17 differentiation were shown to be lacking in miR-$155^{-/-}$ mice, such as IL-23R. This makes T_H17 cells hypo-responsive to IL-23, which is an important cytokine for maintenance of T_H17 phenotype and RORγt maintenance. Ets, a negative regulator of the T_H17 phenotype, was also shown to be repressed by miR-155. miR-155 has been shown to also target IFNγ[193]. Ets-1 is also a target for miR-326[194]. The generation of miR-155 has also been shown to play a role in T_{REG} and T_H17 induction. This miRNA also targets SOCS1. SOCS1 can block IL-6 dependent STAT-3 activation, and complete removal of SOCS1 expression in mice resulted in more FoxP3 cells within the thymus of the animal.

In mice where T cells were stimulated with the myelin auto antigen, MOG, there was an up regulation of miR-301-a, miR-21 and miR-155. MicroRNA-301a is involved in the negative regulation of a STAT-3 inhibitor PIAS3, which was involved in Th17 cells induction in this EAE model[195].

THESIS AIMS

$CD4^+$ T helper cells are a vital part of the adaptive immune system. Initially it was thought that $CD4^+$ T cells were stable in their phenotype. However it is now clear that there is an element of plasticity in $CD4^+$ T cell differentiation. At the start of this study there was information about the cytokine and transcription factors expressed by individual T_H subsets. However, very little was known about T cell plasticity and the overlap of different T helper subsets. Therefore, the first aim of this study was to:

1) **Phenotype $CD4^+$ T cells that co-expressed two lineage defining cytokine, with a particular interest in cells that co-expressed IFNγ and IL-17.**

It has now been shown that T_H17 cells can switch on IFNγ production and express T-bet. It is still unknown if $IFN\gamma^+IL\text{-}17^+$ cells can develop in to 'ex-T_H17' cells that only secrete IFNγ. CCR6 and CD161 are surface markers used to enrich $CD4^+$ T cells for T_H17 cells. These markers are expressed by a subset of T_H1 cells. Therefore, this thesis also aims to:

2) **Identify if CCR6 or CD161 expression on T_H1 cells is a marker of a 'T_H17-related' phenotype.**
3) **Compare the phenotype and functional feature of $CCR6^+T_H1$ cells to $CCR6^-T_H1$ and T_H17 cells.**
4) **Identify novel miRNAs that could be involved in controlling T cell plasticity in T_H1 and T_H17 cells.**

Migration of CCR6^{+}T$_{H}$17 cells across the choroid plexus plays a role in initiating inflammation in multiple sclerosis. The fourth aim of this thesis is to:

5) **Identify if CCR6^{+}T$_{H}$1 cells are present in the blood and CSF of MS patients.**

CHAPTER 2

MATERIALS AND METHODS

2.1 List of Reagents

2.1.1 Media and Solutions

RPMI: RPMI (Roswell Park Memorial Institute) 1640 [Sigma-Aldrich Irvine, UK], 1% GPS (2mM l-glutamine, 100U/ml penicillin, 100ug/ml streptomycin) [HyClone, Northumberland, UK] 1% HEPES (4-(2-hydroxyethyl)-1-piperazineethanesulfonic acid) [Sigma-Aldrich]

RPMI/10% HIFCS: RPMI 1640 medium, 10% Heat Inactivated Fetal Calf Serum (HIFCS) [Biosera, Ringmer, UK]

RPMI/1% BSA: RPMI 1640 medium, 1% Bovine serum albumin (BSA) [Sigma-Aldrich]

X-VIVO: X-Vivo 15 [Lonza], 1% GPS (2mM l-glutamine, 100U/ml penicillin, 100ug/ml streptomycin) [HyClone, Northumberland, UK]

PBS: Phosphate buffered saline contains 8g/l NaCl, 0.26/l KCl, 1.15g/l NA_2HPO_4, 0.2g/ml KH_2PO_4 in distilled H_20; prepared as 1 PBS tablet per 100ml H_20 [Oxoid, Basinstoke,UK]

Macs buffer: PBS, 2mM ethylenediamine tetra-acetic acid (EDTA) [Sigma-Aldrich], 0.5% BSA

2.1.2 Antibodies

Target	Conjugate	Isotype	Clone	Company	Cat No	Dilution
CD3	APC-eFlour	IgG1κ	UCHT1	eBioscience	47-0038-42	1/100
CD4	PE/Cy7	IgG2a,κ	OKT4	Biolegend	317414	1/160
	APC	IgG2b,κ	OKT4	eBioscience	17-0048-42	1/40
CD8	Brilliant Violet	IgG1κ	RPA-T8	Biolegend	301047	1/80
CD14	APC-eFlour 780	IgG1κ	61D3	eBioscience	47-0149-42	1/20
CD25	PerCp/Cy5.5	IgG1κ	BC96	Biolegend	302626	1/20
CD45RA	PE CF594	IgG2a,κ	HI100	BD Horizon	562298	1/40
CD45RO	PE CF594	IgG2a,κ	UCHL1	BD Horizon	562299	1/40
CD69	APC Cy7	IgG1κ	FNSO	Biolegend	310914	1/80
CD127	FITC	IgG1κ	eBioRDR5	eBioscience	11-1278-42	1/40
CD161	PeCy7	IgG1	HP-3G10	eBioscience	25-1619-42	1/
CCR6	PE	IgG2b,κ	G034E3	Biolegend	353410	1/40
	AF 648	IgG2b,κ	G034E3	Biolegend	353404	1/40
CCR7	AF 488	IgG2a,κ	G043H7	Biolegend	353206	1/40
CXCR3	AF 647	IgG1κ	G025H7	Biolegend	353712	1/80

*Isotypes used at the concentration of the matched antibody

Table 2.1 Primary antibodies used for flow cytometry-against surface molecules. Abbreviations used Alexa Fluor (AF), Allophycocyanin (APC), Cyanine 5.5 (Cy5.5), Cyanine 7 (Cy7), Fluorescein isothiocyanate (FITC), Phycoerythrin (PE), Phycoerythrin Texas Red (PETR). All antibodies raised in mouse.

Target	Conjugate	Species	Isotype	Clone	Company	Cat No	Dilution
IFNγ	eFlour 450	Mouse	IgG1κ	45.B3	eBioscience	48-7319-42	1/80
	APC	Mouse	IgG1κ	45.B3	eBioscience	17-7319-82	1/40
TNFα	PE	Mouse	IgG_1	MAb11	R&D	IC210P	1/120
	PerCP-Cy5.5	Mouse	IgG1κ	MAb11	eBioscience	45-7349-42	1/80
IL-5	PE	Mouse	IgG2a,κ	JES1-39D10	Biolegend	500904	1/20
IL-10	PE	Rat	IgG1κ	JES3-9D7	eBioscience	12-7108-82	1/20
IL-17a		Mouse	IgG1κ	eBio64DEC17	eBioscience	53-7179-42	1/20
IL-22	eFlour 660	Mouse	IgG1κ	22URT1	eBioscience	50-7229-42	1/20
	PE	Mouse	IgG1κ	22URT1	eBioscience	12-7229-42	1/40
IL-21	PE	Mouse	IgG1κ	eBio3A3-N2	eBioscience	12-7219-42	1/40
GM-CSF	PE	Rat	IgG2a	BVD2-21C11	BD Pharmingen	554507	1/160
IL-2	PE	Rat	IgG2a,κ	MQ1-17H12	eBioscience	12-7029-82	1/120
IL-17f	PE	Rat	IgG1κ	SHLR17	eBioscience	12-7169-41	1/20

Table 2.2 Primary antibodies used for flow cytometry against intracellular cytokines. Abbreviations used Allophycocyanin (APC), Cyanine 5.5 (Cy5.5), Phycoerythrin (PE).

Target	Conjugate	Species	Isotype	Clone	Company	Cat No	Dilution
Tbet	AF 647	Mouse	IgG1κ	4B10	Biolegend	64480	1/80
	PE	Mouse	IgG1κ	eBio4B10	eBioscience	12-5825-82	1/80
GATA-3	AF 488	Mouse	IgG1κ	L50-823	BD Pharmingen	560163	1/20
	PE	Mouse	IgG1κ	L50-823	BD Pharmingen	560074	1/40
FoxP3	PE	Rat	IgG2a	PCH101	eBioscience	12-4776-73	1/20
RORγt/RORC	PE	Rat	IgG2a	AFKJS-9	eBioscience	12-6988-82	1/80

Table 2.3 Primary antibodies used for flow cytometry against intracellular transcription factors. Abbreviations used Alexa Fluor (AF), Phycoerythrin (PE).

2.2 Ethics

Blood from healthy controls were taken under the ethics, "T cell differentiation and function". Ethical review ERN_10-0728, approved by the Life and Health Sciences Ethical Review Committee, UoB.

Bloods and CSF from multiple sclerosis patients were taken the ethics, **"**Analysis of pathogenic and regulatory T cells in relapsing-remitting multiple sclerosis". Ethics reference: ERN_10-0762, collected through Human Biomaterials Resource Centre, UoB.

2.3 Multiple Sclerosis Patient and Control Samples

CSF/Blood	Diagnosis	Age
B	RRMS	59
B	SPMS/RRMS	48
B	RRMS	34
B	SPMS (With relapses)	59
B	RRMS	26
B	SPMS	43
B/CSF	Other Neurological Disease	38
B/CSF	MS	56
B/CSF	MS	31
B/CSF	Undiagnosed	52
B/CSF	Undiagnosed	45
B/CSF	Undiagnosed	50
B	SPMS (With relapses)	54
B	RRMS (no relapse 2yrs)	51
B/CSF	Small Vessel Disease	Unknown
B/CSF	Inter-cranial Hypertension	Unknown
B/CSF	Neuro-inflammation	Unknown
B	Undiagnosed	Unknown
B	Undiagnosed	Unknown

Table 2.4. Demographics of suspected MS patient. Information about age of patient and diagnosis of conditions were obtained after analysis due to lumber puncture being for diagnosis purpose. SPMS-Secondary progressive MS, RRMS – Relapsing remitting MS, CSF-cerebralspinal fluid, Blood- Peripheral Blood.

Blood/CSF	Sex	Age
B	F	21
B	F	31
B	F	26
B	F	25
B	F	25
B	F	23
B	F	24
B	M	55

Table 2.5 Healthy control demographics. Age and sex of healthy controls.

2.4 Purification of Cell Subsets

In this section, unless otherwise stated, where it is mentioned that the cells are washed it was at 300xg, for 8 minutes at 20°C and then the supernatant was removed. All work in this section was undertaken in a category II safety cabinet.

2.4.1 Peripheral Blood Mononuclear Cell (PBMC) Extraction from Whole Blood

Peripheral blood samples were obtained in Heparin Sodium [Wockhardt, Wrexham, UK] from healthy donors (recruited from amongst work colleagues). Informed consent was taken in accordance with the Human Tissue Act 2004. The blood was diluted at a ratio of 1:1 with RPMI medium. 18mls of the diluted blood was layered on top of 8mls of Ficol-Paque Plus [GE Healthcare Bioscience] in a 25ml tube. The tube was centrifuged at 300xg, 20°C for 30 minutes without brake. The mononuclear cell layer containing the PBMC was removed and was washed three times in RPMI/10% HIFCS. The cells were counted using an Improved Neubauer haemocytometer [Weber Scientific]. The yield of PBMC was calculated as

described by the manufacturer. The range of yield was 5 x 10^5 – 1.5 x 10^6 per ml of peripheral blood.

2.4.2 Positive Selection of CD4+ T cells from PBMC

PBMC were washed in filter-sterilized cold MACS buffer (2-8°C) and the supernatant was removed to leave a dry pellet. The cell pellet was resuspended in 80µL of MACS buffer/10^7 total cells and 20µL of CD4+ T Cell Microbeads [Miltenyi Biotech]/10^7 total cells. The cells were mixed well and incubated for 20 minutes in the refrigerator (2−8 °C).

The cell and bead mixture was washed in cold MACS buffer and resuspended in 500µL of MACS buffer. The cell suspension was added to a pre-rinsed MS column [Miltenyi Biotech] on a MiniMACS separator magnet [Miltenyi Biotech]. The unlabelled cell fraction (everything but CD4+ cells) in the effluent was collected and the column was washed with 1 mL of cold MACS buffer. The unlabelled cells were re-added to the column for a second selection process to improve the yield of CD4+ cells. The column was washed three times with 1ml of cold MACS buffer. Total effluent was collected. This was the unlabelled pre-enriched CD4- cell fraction. The column was then removed from the magnet and the CD4+ fraction eluted with 1ml MACS buffer and firm pressure on the column from a plunger.

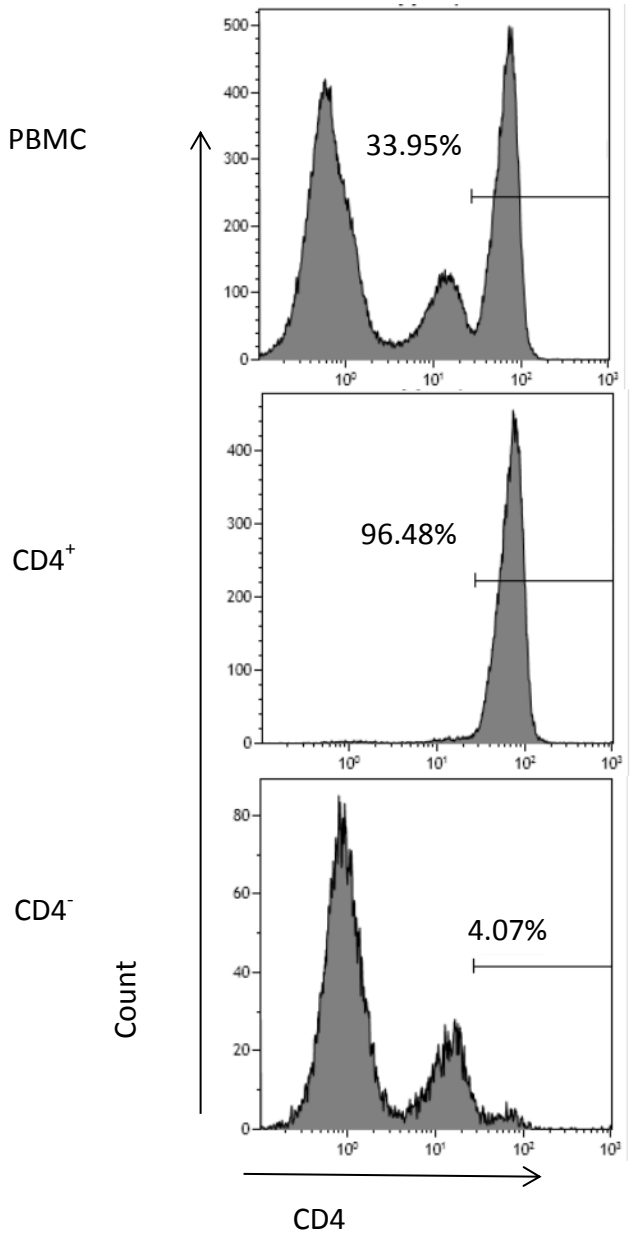

Figure 2.1 Representative purity check of CD4+ T cell isolation from PBMC. Gated on a mononuclear cell gate, plots show PBMC before CD4+ isolation and the positive and negative fractions after CD4 T cell isolation.

The range of yield was 2 x 10^5 – 5 x 10^5/10^6 of PBMC. These populations were highly enriched for CD4$^+$ cells, with a purity of >95 (**Figure 2.1**).The populations were analysed for the percentage of cells expressing CD4. Values shown represent the percentage of CD4$^+$ cells within the gate.

2.4.3 Purification of CD4$^+$CD25$^-$ cells

CD4$^+$CD25$^-$ T cell were isolated using a two-step separation (CD4+CD25+ Regulatory T Cell Isolation Kit, human [Miltenyi Biotech]). In the first step all cells not expressing CD4$^+$ were removed and in the second step the CD25$^+$ cells (T_{REG} enriched) were isolated from the CD4$^+$ fraction.

In the first negative selection step the PBMC cell pellet was re-suspended in 90µL of cold MACS buffer/10^7 total cells and 10µL of CD4$^+$ T Cell Biotin-Antibody Cocktail /10^7 total cells. This cocktail contained biotinylated antibodies against all the other cell types (CD8, CD14, CD15, CD16, CD19, CD36, CD56, CD123, TCRγ/δ and CD235a (glycophorin A)) within PBMC. The cell suspension was mixed well and incubated for 5 minutes in the refrigerator (2−8 °C). 20µL of Anti-Biotin MicroBeads per 10^7 cells was then added, which bound to the biotinylated antibodies attached to the cells from the last step. The cell suspension was mixed well and incubated for an additional 10 minutes in the refrigerator (2−8 °C). The volume of liquid was adjusted to a minimum of 500µL of buffer if needed.

The cell suspension was added to a pre-rinsed LD column [Miltenyi Biotech] placed on a QuadroMACS separator magnet [Miltenyi Biotech]. Unlabelled cells were collected in the

effluent and the column was washed with 1 mL of MACS buffer. The unlabelled cells were re-added to the column for a second selection process to improve purity. The column was washed three times with 1ml of cold MACS buffer. Total effluent was collected. This was the unlabelled pre-enriched CD4$^+$ cell fraction.

The unlabelled CD4$^+$ cells were positively labelled to isolate the CD25$^+$ T cells. The CD4$^+$ T cells were counted, washed and the cell pellet was resuspended in 90µL of buffer/10^7 total cells and 10µL of CD25 MicroBeads /10^7 cells. This mixture was incubated for 15 minutes in the refrigerator (2−8 °C). The cells were washed and the supernatant was aspirated off completely. The cell pellet was resuspended up to 10^8 cells in 500µL of buffer.

The cell suspension was applied onto the MACS column. The flow-through containing unlabelled cells was collected. The column was wash three times with 500µL of cold MACS buffer. The magnetically labelled CD25$^+$ cells were flush out by the addition of 1 mL of cold MACS buffer added to the column and immediately forced through using the plunger provided.

The yield was $2x10^5 – 5x10^5$ /10^6 of PBMC. These populations were highly enriched for CD4 with a purity of >95% (**Figure 2.2**). The yield of CD25$^+$ cells was between $1x10^4$-$5x10^4$ per 10^6 PBMC with a purity of between 40-60%., with the CD4$^+$CD25$^-$ fraction >90% pure.

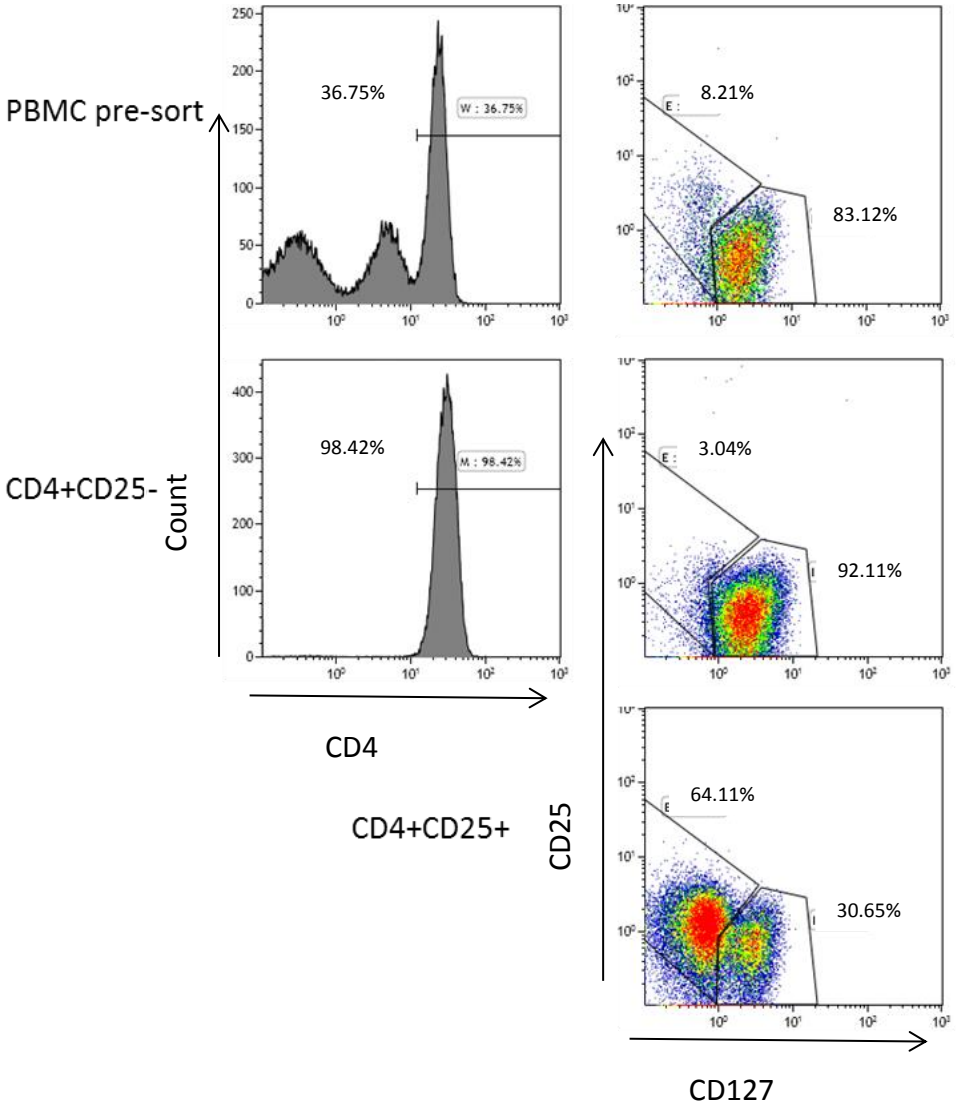

Figure 2.2 Representative purity check of a $CD4^+CD25^-$ T cell isolation from PBMC. Gated on a mononuclear cell gate, plots show PBMC before $CD4^+$ isolation, the $CD4^+CD25^-$ fraction and the $CD4^+CD25^+$ fraction. The populations were analysed for the percentage of cells expressing CD4, CD25 and CD127. Values shown represent the percentage of cells within the gate.

2.4.4 Purification of cytokine secreting cells

For all the cytokine capture experiments $CD4^+CD25^-$ T cells were isolated and left overnight in the fridge. On day two once the $CD4^+CD25^-$ T cells had been washed they were stimulated for 3 hours with Phorbol 12-myristate 13-acetate (PMA) [Sigma] and Ionomycin [Sigma] (50ng/ml and 500ng/ml respectively). At this stage if CCR6 cells were being isolated the cells were pre-stained for CCR6 as in **section 2.4.1.1**. PBMC were used only when stimulating with Staphylococcal Enterotoxin B (SEB) and Cytostim and where indicated with PMA/ionomycin. PBMC were stimulated on the day of isolation and not left in the fridge overnight.

Cells were cultured in 6 well plate [Corning] at a density of $5x10^6$ cells/cm^2. The cells were stimulated with either Cytostim (20µl/ml) [Miltenyi Biotech] or SEB (500ng/ml) or PMA (50µl/ml) with ionomycin (500µl/ml) for 3 hours at 37°C, 5% CO_2. Cytostim is an antibody-based reagent that acts similarly to a super-antigen but independently of certain Vβ domains of the TcR. Cytostim cross-links the TcR of a T cell to an MHC molecule of an antigen-presenting cell. SEB is an enterotoxin produced by the bacterium *Staphylococcus aureus*.

The cells were collected from the plate by washing each well with cold MACS buffer (2-4°C) apart from if PMA/ionomycin was used in which case the cells were washed three times. A pipette was used to collect as many cells as possible from the bottom of each well of a 6 well plate. The cells were transferred to a 15ml tube and washed with 10ml of cold MACS buffer. The supernatant was carefully pipetted off to prevent cells loss. 80µl/10^7 cells of cold MACS buffer along with 20µl/10^7 of the cytokine catch reagent (Cytokine Secretion Assay-Cell

Enrichment and Detection Kit [Miltenyi Biotech, Surrey, UK]) were added to the tube. This combination was mixed well and incubated on ice for 5 minutes. If the protocol was for a double cytokine capture 10µl/10^7 was used of each capture reagent. RPMI/10% HIFCS, that had been warmed for 10 minutes in a water bath at 35°C, was added to dilute the cells at 1x10^5 cells/ml. These cells were incubated for 45 minutes in the incubator, (37°C, 5% CO_2) spinning on a MACS Rotator [Miltenyi Biotech].

Cells were kept on ice for 10 minutes then washed in cold MACS buffer, centrifuged (300xg, 10 minutes, 4°C) and re-suspended in cold buffer at a concentration of 80µl/10^7 cells with 20µl/10^7 cells of the cytokine detection antibody. Again, if it was a double cytokine secretion assay 10µl/10^7 cells of each antibody was used (conjugated to PE, APC or FITC). This was then incubated on ice for 10 minutes and a final wash step of 10mls of cold MACS buffer was carried out.

At this stage the cells could either be further stained for other cell markers (e.g. CCR6, CD45RO) and analysed using flow cytometry or the cytokine secreting cells could be isolated. The cells were sorted for the cytokine positive cells using either FACS (Fluorescent Activating Cell Sorting) or MACS cell sorter columns.

The stained cells were passed through a damp Pre-Separation Filter (30µm) [Miltenyi Biotech] in 1ml of MACS buffer and the filter was then washed with a further 1ml of MACS buffer. The cells were passed through a FACS Mo-Flo Cell sorter [Beckman Coulter]. Single colour compensation tubes were required to compensate for fluorescence overlap. The FACS uses a method of isolating individual cell into droplets and administering a charge to

the cells of interest depending on their fluorescent profile. The charged cells can then be separated from the rest of the cells.

2.4.5 Markers of Recent Activation

Total PBMC were stained for CD4, CD45RO and either CD69 or CD71 in sterile PBS/2% BSA. After being left for 15 minutes on ice the cells were washed and placed in 1ml of sterile PBS/2%BSA. The different populations of interest were isolated on the MoFlo Cell Sorter. Once sorted the cells were stimulated and stained as in Section below (**Section 2.4**).

2.5 Surface and Intracellular Lymphocyte Staining

2.5.1 Surface Marker Staining

$0.5x10^6$-$1.5x10^6$ cells were re-suspended in 50µl of RPMI/10% HIFCS in a single well of a 96 well plate. To stimulate the cells to produce cytokine PMA and Ionomycin were both added at a concentration of 50ng/ml and 500ng/ml, respectively. Only RPMI/10% HIFCS was added to any non-stimulated wells. To prevent cytokine release 2µg/ml of Brefeldin A was added to all the wells including the non-stimulated portion. The wells were made up to 200µl with RPMI/10% HIFCS or stimulation solution of PMA and ionomycin and left in the incubator at 37°C, 5% CO_2, for 3 hours.

The plate was centrifuged for 4 minutes at 4°C and 300xg and the supernatant was flicked off. Antibodies specific for surface molecules were made up to 50µl in PBS/2%BSA and

added to the relevant wells. The plate was left on ice at 0-2°C, in the dark for 15 minutes. The wells were washed with 100µl of PBS/2%BSA and centrifuged for 4 minutes at 300xg. The cells were then fixed and permeabalised as detailed below (**Section 2.4.2**). Compensation beads [BD Pharmingen] were used for fluorescence compensation purposes.

2.4.1.1 CCR6 Surface Staining

When cells were stimulated with PMA/ionomycin there was a down regulation of CCR6 expression on the surface of the cell. To correct for this surface staining of CCR6 was done before and after stimulation. PBMC were added to a plate and were centrifuge for 4 minutes at 4°C and 300 x g and the supernatant was flicked off. CCR6 antibody was made up to 50µl in PBS/2%BSA and added to the relevant wells. The plate was kept at room temperature in the dark for 15 minutes. The wells were washed with 100µl of PBS/2%BSA and centrifuged for 4 minutes at 300xg. The cells were then stimulated with PMA/Ionomycin in the presence of Brefeldin A for 3 hours, as described above. The cells were then further stained for extracellular antibodies as described above (**Section 2.4.1)**, with the addition of the CCR6 antibody. The only alteration made to the protocol was that the cells were incubated at room temperature, in the dark, instead of on ice. The protocol for fix and permeabilisation of the cells was kept the same.

2.5.2 Cell Permeabilisation

The supernatant was removed by flicking the plate and the cells were re-suspended in 50µl of Reaction Buffer A [FIX & PERM®, Invitrogen]. The plate was left at room temperature and kept in the dark for 15 minutes. The wells were washed with 100µl of PBS/2%BSA and centrifuged. The antibodies for intracellular staining were made up to 50µl using Reaction Buffer B [FIX & PERM®] and added to the wells. They were left for 15-20 minutes in the dark at room temperature. The wells were then washed with 100µl of PBS/2%BSA and centrifuged. Once the cells had been re-suspended in 300µl of PBS/2% BSA they were then analysed.

2.6 Flow Cytometry Analysis

Cells were analysed by a nine colour flow cytometry on a Dako-Cyan. Data analysis was carried out using Kaluza® Flow Cytometry Analysis Software from Beckman Coulter. The number of events analysed per sample was between 10,000 and 500,000. The gating strategy for identification of memory $CD4^+$ and $CD8^+$ T cells is shown in **Figure 2.3**. For the transcription factor staining a matched isotype on the same fluorochrome and from the same company was used to set the negative gate. The negative gates for the cytokine staining were set as shown in **Figure 2.4** using stained unstimulated control cells.

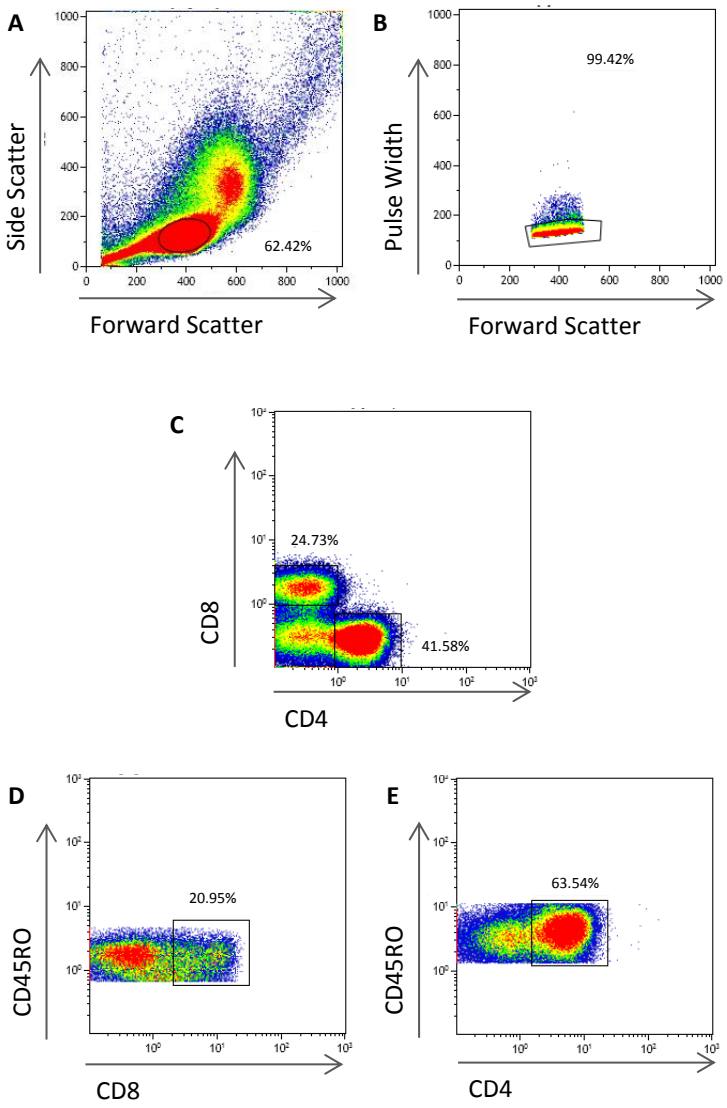

Figure 2.3 Gating strategies used to identify $CD8^+$ and $CD4^+$ memory T cells. (A) Live cells were gated by FSC vs SSC. (B) Single cells were selected by low pulse width. (C) $CD4^+CD8^-$ or $CD4^-CD8^+$ cells were gated for and based on the different populations either (D) $CD4^+CD45RO^+$ expression or (E) $CD8^+CD45RO^+$ cells were analysed.

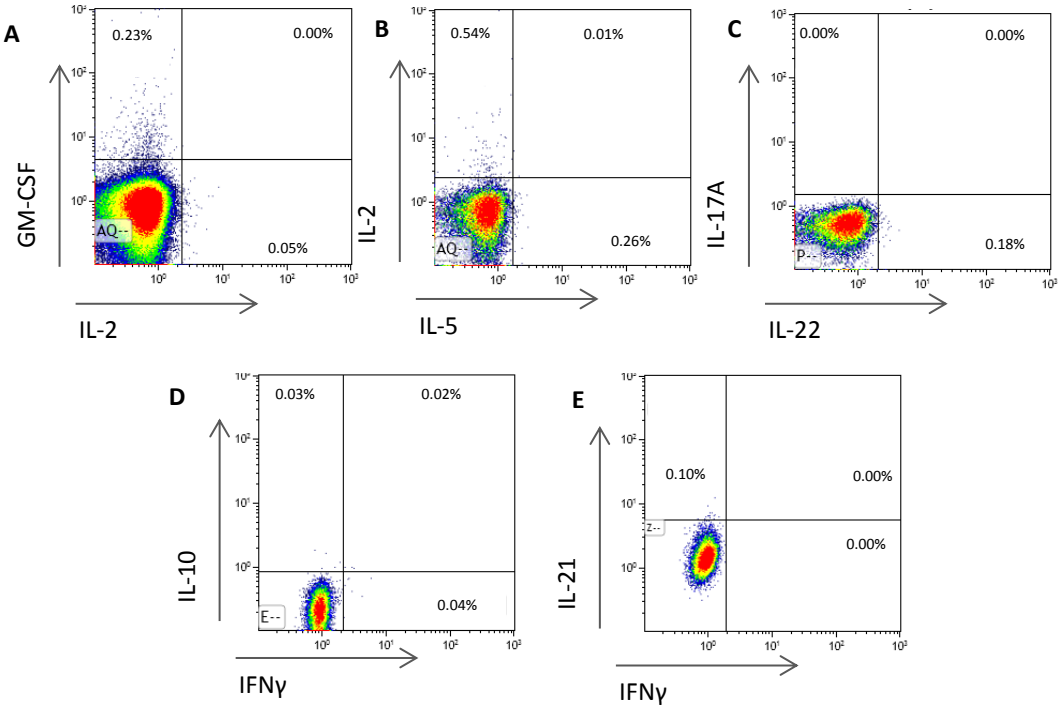

Figure 2.4 Cytokine unstimulated controls. PBMC were left unstimulated for 3 hours in the presence of Brefeldin A. All plots are gated on $CD4^+CD45RO^+$ cells. The cells were stained for the cytokines shown **(A)** GM-CSF and IL-2 **(B)** IL-2 and IL-5. **(C)** IL-17A and IL-22 **(D)** IL-10 and IFNγ and **(E)** IFNγ and IL-21. These plots were used to set the gates for the stimulated controls. Values represent percentage of cells in the gate.

2.7 Image Stream

PBMC were processed as described above as appropriate, apart from the addition of Po-pro 1 just before analysis (330nmol/500 µl - left on ice for 10 minutes). The cells were run on Image Stream^X [Amnis] with 10,000-100,000 cells analysed. Data analysis was carried out using IDEAS® software from Amnis.

2.8 Cell culture

2.8.1 Analysis of Proliferation

To analyse proliferation within a culture cells were pre-stained with Cell Proliferation Dye eFluor® 450 [eBioscience]. With every round of proliferation the cells passed on half the amount of dye to their daughter cells meaning the cells that have divided can be identified. Cells were stained following manufacturer's instructions. Briefly, the cells were washed three times in PBS to remove any serum to increase the efficiency of staining. The cells were then diluted in PBS (room temperature) at a concentration of $20x10^6$/ml. A 20µM solution of Cell Proliferation Dye eFluor® 450 in PBS was made up and was mixed 1:1 with the cell suspension. The suspension was vortexed and incubated in the dark at 37°C with 2% CO_2 for 10 minutes. To stop the labelling 20ml of cold RPMI/10% HIFCS was added to the cells and left on ice, in the dark, for 5 minutes. The cells were washed 3 times with RPMI/10% HIFCS and then transferred to culture conditions. The analysis of proliferation was undertaken on the Cyan in the V1 channel.

2.8.2 T_H17 Polarisation

Isolated cells were washed in X-vivo/1% GPS and placed into a round bottomed 96 well plate at a density of $5x10^4$ cells per well, where possible. Anti- CD3, anti-CD28 Dynal Beads [Invitrogen] were washed as recommended by the manufacture and placed in to the well at 1:3 or 1:32 bead to cell ratio. For neutral culturing conditions IL-2 at 50U/ml was added alongside the beads. For T_H17 polarising environment the Table 2.6 shows the cytokines added.

Cytokine	Concentration
IL-1β	10 ng/ml
IL-2	10 ng/ml
IL-6	20 ng/ml
IL-23	10 ng/ml
anti-IFNγ	100 ng/ml
anti-IL-4	100 ng/ml

Table 2.6. T_H17 polarising cytokines and the concentration within cultures. All cytokines [Peprotech] have been reconstituted in PBS 0.1% BSA. The concentrations shown are the final concentration required in the culture.

Cells were cultured for 5 days at 37°C, 5% CO_2. After 5 days the cells were washed, stimulated with PMA/Ionomycin and stained using the intracellular staining protocol. All T_H17 polarising cultures were in x-vivo media with 1% GPS.

2.9 Migration Assay

$CD4^+$ T cells were positively isolated from PBMC as stated above in section 2.3.2. The $CD4^+$ T cells were counted and then washed by centrifugation at 300xg for 10 minutes. The cells were resuspended in RPMI/2%BSA (with GPS) at 200,000 cells/75µl. The chemokines, CCL20 [Peprotech] and CXCL12 [Peprotech], were diluted to the desired concentration with RPMI/ 2% BSA.

To set up the plate 150µl of the chemokines were added to the bottom well of the MultiScreen Migration Invasion and Chemotaxis Filter Plate (5.0 µm) [Millipore]. To equilibrate the plate and the cells they were both placed in an incubator at 37°C, 2% CO_2, for 30 minutes. 75µl of the cell suspension was slowly dribbled down the side of the top well of the migration plate to prevent putting force on the cells and pushing them through the top well membrane. The complete plate was then placed back in the incubator at 37°C, 2% CO_2, for two hours.

The plate was taken apart and the liquid from the bottom and top compartments were carefully collected into separate tubes. The cells from the top and bottom wells were then washed and added to a 96 well plate. The collected cells were stimulated for 3 hours with PMA and Ionomycin in the presence of Brefeldin A, as stated above in **Section 2.4.1**. The

cells were then stained for intracellular IFNγ and IL-17 expression and analysed using flow cytometry. Counting beads were added to the flow cytometry tube to analyse the actual number of cells that had migrated from the top well towards the chemokine in the bottom well.

2.10 Gene Expression Analysis

2.10.1 RNA Extraction and Reverse Transcription

RNA isolation and cDNA synthesis were performed using the µMACS One-step cDNA Kit [Miltenyi Biotech]. The method was performed as manufacturer's instructions. MoFlo sorted cells were washed in cold PBS and then pelleted by centrifugation at 300xg for 8 minutes in a 1.5ml ependorff tube. 1 ml of Lysis/Binding buffer was added to the cells. To reduce viscosity of the lysate, mechanical shearing of DNA was performed by forcing the lysate 2-3 times with maximum pressure through a 21G needle attached to a 1-5ml syringe so no 'fuzzy' material or clumps remain in the lysate. The foam generated during lysate was removed by centrifuging the lysate for 1-3mins (13000xg). At this stage the lysate was pelleted and stored at -70°C until needed. The mechanical shearing was preformed again after the cells had been defrosted to be sure that all the cells had lysed. The lysate was applied to the top of a LysateClear column and centrifuged at 13,000xg for 3 mins. A µMACS column was placed in a magnetic field and rinsed with 100µl of Lysis/Binding buffer. Oligo(dT) Microbeads (50µl- pre 1ml lysate) were added to the lysate and mixed by pipetting up and down 2-3 times. These magnetic beads bind to the polyA tail of the mRNA. The lysate was added to the top of the LysateClear column resulting in the magnetically labelled mRNA being retained on column. To clear off any excess DNA or proteins left on the column

it was rinsed with 2x200µl Lysis/Binding buffer and then rinsed with 4x 100µl Wash Buffer to remove further rRNA and DNA.

2x100µl of Equilibration/Wash Buffer was added into the column matrix. The Lyophilised Enzyme Mix was then resuspended in 20µl Re-suspension Buffer (only pipette up and down twice) and added to the top of the column. To avoid evaporation 1µl of the sealing solution was added directly on top of the column matrix. The thermoMACS Separator was set to 42°C and incubated for 1 hour. Following from this 2x100µl of Equilibration/Wash buffer was added to the column before 20µl of the cDNA Release Solution is added. This was incubated for 10mins at 42°C and then the synthesized cDNA was eluted from the column and collected with 50µl cDNA Elution Buffer. The cDNA was then frozen at -70°C until it was used for qRT-PCR.

2.10.2 Real Time Quantitative Polymerase Chain Reaction (RT-qPCR)

All Gene Assays were from Applied Bioscience.

Gene	Code	Fluorochrome
GAPDH	Hs02758991_g1	VIC
T-bet	Hs00203436_m1	FAM
RORC	Hs01076122_m1	FAM
IFNγ	Hs00989291_m1	FAM
IL-17A	Hs00174383_m1	FAM
IL-23R	Hs00332759_m1	FAM
IL-12Rβ2	Hs01548202_m1	FAM
IL4I1	Hs00541746_m1	FAM
IL-1R1	Hs00991002_m1	FAM

Table 2.7 Human Gene Assays from Applied Bioscience

Reactions were performed in duplex, with both GAPDH and the target gene in one well, in a 384 well plate FastStart TaqMan® Probe Master (Rox) [Roche], a 2x concentrated master mix, in which 2.5µl was used. 0.35µl of the gene assay was added along with the desired quantity of cDNA, RNase free water was used to make the reaction volume to 5µl. All RT-PCR reactions were performed on the Light Cycler 480 [Roche] and analysed using the Light Cycler® 480 SW 1.5 software.

Stage/ Cycle	Temperature	Time	Ramp Rate
Pre-incubation	95°C	10 minute	4.4°C/s
Amplification /50 Cycles	95°C	15 sec	2.2 °C/s
	60°C	1 minutes	4.4°C/s
	72°C	1 sec	4.4°C/s
Melt Curve / 1 cycle	40°C	10 sec	2.5°C/s
	80°C	30 sec	0.6°C/s
	40°C	Hold	2 °C/s
	40°C	10sec	2 °C/s

Table 2.8 qRT-PCR programme on the Light Cycler 480

2.10.3 Gene expression analysis

Relative gene expression (R) was analysed using the equation below. Ct= Cycle Threshold, Sample=Target gene, Control= GAPDH,

$$R = 2^{-[\Delta Ct\ sample - \Delta Ct\ control]}$$

2.11 QuantiGene Plex 2.0 Assay, Luminex [BioPlex]

The QuantiGene Plex 2.0 Assay [Affemetrix, Panomics] system was used to directly analyse the expression levels of RNA of specific genes from cell lysates. This system allowed for the RNA levels of several genes to be measured in one sample without reverse transcription. The genes of interest were, RORC (SA-14729), Tbx21 (SA-98001), IL-17A (SA-12176), IL-17F (SA-23157) , IFNG (SA-10807), RUNX1 (SA-11783), IL-12Rβ2 (SA- 45601) and IL-23R (SA-50266). GAPDH (SA-10001) and HPRT1 (hypoxanthine phosporibosyltransferase 1-SA-10030) were used as controls.

The isolated cells were thawed and 400 cells/µl of Lysis Mixture was added directly to the cell pellet. This was mixed 10-15 times and vortexed for 1 minute. It was incubated at 50-55°C (water bath) for 30 minutes. After incubation the lysed cells were vortexed at max speed for 1 min and the viscosity was compared to the lysis mixture. The lysate was stored at -80°C for later use.

The working bead mixture for the Luminex was made up as stated in the table below.

Order of Addition	Reagent	1 well (µl)
1	Nuclease-free H20	5.2
2	Lysis Mix	6.6
3	Blocking reagent	2
4	Proteinase K	0.2
5	Capture beads (vortex before adding- 30sec)	1
6	2.0 Probe Set	5
Total		20

The working bead mixture was made up and vortexed for 10 seconds. 20µl was then pipetted into each well of the Hybridization Plate. 80µl lysate was added to each well of the Hybridization Plate that contained the working bead mix bringing the total volume of the well to 100ul. To add a negative control to the plate a well containing 80ul of diluent Lysis Mixture was added to 3 wells. The Hybridization plate was sealed using the pressure seal and incubated for 22 hours at 54°C at 600rpm.

Pre-Amplifier Hybridization

0.6ml of Wash Buffer Component 1 and 10ml of Wash Buffer Component 2 was mixed with 189ml of nuclease free water. Using a 15 ml tube, 36ul of 2.0 Pre-Amplifier was added to 12ml of Amplifier Diluent. This mixture was inverted several times to mix it, but it was not vortexed.

Wash Step

The hybridization plate was removed from incubator and the temperature of the incubator was adjusted to 50°C. The Hybridization Plate was centrifuged at 240xg for 1 minute at room temp and the plate seal was removed. The mixture in each well was disrupted by pipetting up and down 5 times and transferred from the Hybridization Plate to a Magnetic Separation Plate. The magnetic separation plate was used to wash the samples by inserting the plate into the hand held Magnetic plate washer. The plate was locked into place and the magnetic beads were allowed to settle on the bottom of well for 1 minute. The solution was removed from the wells by quickly inverting it over a sink and gently blotting onto a paper towel. 100µl of the 1xWash Buffer was added into each well and after 15 sec removed by quickly inverting the plate over the sink. Repeat this wash step twice more.

Pre Amp Hybridization

Using a 15 ml tube, 36µl of 2.0 Pre-Amplifier was added to 12mls of Amplifier Diluent to make up the 2.0 Pre-Amplifier Working Reagent. 100µl of this solution was added to each well of the Magnetic Separation Plate. The plate was sealed with a foil plate sealer and removed from the Hand Held Magnetic Plate Washer. The plate was vortexed at 800 rpm for 1 min at room temp to ensure beads were resuspended. The plate was incubated for 1 hour at 50°C with shaking at 600rpm.

After 1 hour the plate was removed from the incubator, the seal removed and it was inserted into the Hand Held Magnetic Plate Washer. The plate was washed as described above

Amplifier Hybridization

To make up the 2.0 Amplifier Working Reagent 36µl of 2.0 Amplifier was added to 12ml Amplifier Diluent and mixed several times and 100µl was added to each well. The plate was sealed with a foil plate sealer and removed from the Hand Held Magnetic Plate Washer. The plate was vortexed at 800 rpm for 1 min at room temp to ensure beads were resuspended. The plate was incubate for 1 hour at 50°C with shaking at 600rpm. After 1 hour the plate was removed from the incubator and the seal removed and inserted into the Hand Held Magnetic Plate Washer. The plate was washed as described above.

Hybridize Label Probe

To make up the Label Probe Working Reagent 36µl of Label Probe was added to 12ml of Label Probe Diluent and was mixed several times. 10µl of this mixture was added to each well of the Magnetic Separation plate. The plate was sealed with a foil plate sealer and removed from the Hand Held Magnetic Plate Washer. The plate was vortexed at 800 rpm for 1 min at room temperature to ensure the beads were resuspended. The plate was incubated for 1 hour at 50°C with shaking at 600rpm. The plate was then removed from the incubator, the seal removed and it was inserted into the Hand Held Magnetic Plate Washer. The plate was washed as described above.

To make up the SAPE Wash buffer in a 15ml tube 36µl of SAPE was added to 12ml of SAPE Diluent. It was mixed well and protected from the light. The wash steps from (A-B) were repeated but SAPE Wash Buffer was used instead of 1xWash Buffer.

Analysis

130µl of SAPE Wash buffer was added to each well. The plate was sealed with a foil plate sealer and removed from the Hand Held Magnetic Plate Washer. The plate was vortexed at 800 rpm for 1 min at room temp to ensure beads were resuspended. The plate was then analysed immediately on Luminex.

2.12 miRNA Screen

To isolate miRNA from different samples total RNA was initially isolated, including the miRNA. The miRNA was converted to cDNA using specific miRNA reverse transcription primers. Because of the small quantity of sample, the miRNA then had to be amplified to have enough sample to run on the Microfluidic cards.

2.12.1 RNA Isolation

To isolate the RNA the mirVana™ miRNA Isolation Kit [Invitrogen] was used. The starting material was cells isolated on the MoFlo cell sorter and then pelleted and frozen at -70°C. The cells were thawed and 500µl of the Lysis/Binding Buffer was added. A dilution of 10 part lysate to 1 part miRNA Homogenate Additive was mixed. The mixture was left on ice for 10 minutes and then a volume of Acid-Phenol:Chloroform that was equal to the lysate volume before addition of the miRNA Homogenate Additive (500µl) was added. This mixture was vortexed for 60 seconds and then centrifuged for 5 minutes at 10,000xg at room

temperature. The aqueous and organic phases were separated. The aqueous phase was kept while the organic phase was discarded. To isolate the total RNA 1.25 parts of 100% ethanol was added to 1 part aqueous phase. This mixture was added to a filter cartridge and centrifuged for approximately 15 sec at 10,000xg to pass the mixture through the filter. To wash the RNA bound to the filter 700µl of miRNA Wash Solution 1 was added to the Filter Cartridge and centrifuged for 5~10 seconds at 10,000xg. The effluent was discarded. 500µl of Wash Solution 2/3 was added to the filter and centrifuged for 15 sec at 10,000xg to pass the mixture through the filter. This was repeated once more and after discarding the flow-through from last wash the filter cartridge was placed back in the same collection tube and spun for 1 min at 10,000xg to remove any residual liquid from the filter. The filter cartridge was transferred into a fresh collection tube and 100µl of pre-heated Elution Solution was added to the centre of the filter. The filter was spun for 30 seconds at max speed to recover RNA. The RNA was store at -20°C.

To make it possible to use the maximum amount of RNA in the reverse transcription step a DNAclear™ Kit was used to reduce the volume the RNA was eluted in. To equilibrate a Micro Filter Cartridge 30µL of cDNA Binding Buffer was added to a Micro Filter. This was incubated for 5 minutes at room temperature. The sample volume was brought to 100µL with Nuclease-free Water. 250µL of cDNA Binding Buffer was added to each sample, and mixed thoroughly by gently vortexing. It was applied to the equilibrated Micro Filter Cartridge. The column was centrifuged for 1 min at 10,000xg after which the flow-through was discarded. The Micro Filter Cartridge was washed with 500µL of cDNA Wash Buffer and again centrifuged for 1 min at 10,000xg. The flow-through was discarded and the Micro Filter

Cartridge was spun for an additional minute to remove trace amounts of ethanol. The RNA was eluted with 2 aliquots of preheated (55°C) Nuclease-free Water (2 x 8µL) in a total volume of 16µL. The 8µL Nuclease-free Water was added to the filter and left for 2 min at room temperature and then centrifuged for 1 min at 10,000 x g. This was repeated a second time and the double-stranded RNA was collected in the Micro Elution Tube.

2.12.2 Reverse Transcription (RT)

For this reaction 1-350ng of RNA was needed. As I was unable to measure the RNA concentration I had to assume that the RNA isolation was efficient and that at least 1 ng/µL of RNA had been eluted. The RT mix was made up according to the table below in a PCR tube.

RT reaction Mix Components	**Volume for One Sample (µL)**
Megaplex RT primers (10x)	0.8
dNTPs with dTTP (100mM)	0.2
MultiScribe Reverse Transcriptase (50U/µl)	1.5
10x RT Buffer	0.8
MgCl2 (25mM)	0.9
RNase Inhibitor (20U/µl)	0.1
Nuclease-free water	0.2
Total	**4.5**

To the RT mixture 3µl of RNA was added bring the total volume for the reaction to 7µl. The mixture was mixed well and spun briefly to collect the mixture at the bottom of the tube. The tube was incubated on ice for 5 minutes before being added to the thermo-cycler. The conditions for the thermo-cycler are shown below. Ramp Rate: 1.5°C/s

Stage	Temp	Time
Cycle (40 cycles)	16°C	2 mins
	42°C	1 min
	50°C	1 sec
Hold	85°C	5min
Hold	4°C	hold

Once the reaction was finished the samples were then amplified straight away.

2.12.3 Pre-amplification Reaction

The pre-amplification reaction has a final volume of 25µL and contains 2.5µL RT product and 22.5µL PreAmp reaction mix.

PreAmp Reaction Mix Components	Volume for one sample (µl)
TaqMan PreAmp Master Mix (x2)	12.5
Megaplex PreAmp Primers (10x)	2.5
Nuclease-free water	7.5
Total	**22.5**

The reaction mixture was made up in a PCR tube and mixed by inverting six times. The tube was spun briefly and added to the thermo-cycler. The conditions for the pre-amplification reaction were as follows:

Ramp Rate: 1.5°C/s

Stage	Temp	Time
Hold	95 °C	10 min
Hold	55 °C	2 min
Hold	72 °C	2 min
Cycle (12 Cycles)	95 °C	15 sec
	60 °C	4 min
Hold (inactivate enzymes)	99.9°C	10 min
Hold	4°C	hold

Once the reaction was finished the tubes were briefly centrifuged and 75µl of 0.1XTE pH 8.0 was added to each sample. The Sample was kept at -70°C until the microfluidic cards were ready to be run.

2.12.4 TaqMan MicroRNA Microfluidic Cards

To run the samples on the array the PCR master mix was made up to which the amplified miRNA sample was added. The mixture was made up in a 1.5ml micro centrifuge tube.

Component	Volume for One Array (µl)
TaqMan Universal PCR Master Mix No AmpErase UNG 2x	450
Diluted PreAmp product	9
Nuclease Free water	441
Total	**900**

The tube was inverted six times to mix the reaction and briefly centrifuged. To each port on the TaqMan MicroRNA Array 100µl was added. The microfluidic card was centrifuged and then sealed.

The TaqMan® Array Human MicroRNA Card v3.0A contained a total of 384 TaqMan® MicroRNA Assays. The cards were run on the Applied Biosystems 7900HT Systems and analysed using the SDS software.

CHAPTER 3

EXPRESSION OF LINEAGE DEFINING CYTOKINES AND ASSOCIATED TRANSCRIPTION FACTORS IN CD4+ T CELLS

3.1 Introduction

T helper lineage are often defined by the cytokines they express upon stimulation. For example T_H1 cells secrete IFNγ, T_H2 cells secrete IL-5, IL-4 and IL-13, and T_H17 cells secrete IL-17A, while T_H22 cells express IL-22. At the start of this study there was emerging data demonstrating an element of plasticity in the cytokine a T_H lineage could secrete. $CD4^+$ cells in particular, but also $CD8^+$ T cells, have been shown in certain situations to co-express cytokines associated with a different lineage. Within memory T cells there are lineage defining transcription factors that control the expression of these cytokines as well as other features (e.g. chemokine receptors) of the different lineage.

The aims of this chapter are:

- to investigate the co-expression of effector cytokines within $CD4^+$ and $CD8^+$ T cells.
- to phenotype the expression of these transcription factors in $CD4^+$ T cells and specifically in situations in which two lineage defining effector cytokines are co-expressed.

T cell phenotypes were investigated using intracellular cytokine/transcription factor staining and flow cytometry. These methods allowed the analysis of cytokine(s) expressed, *ex vivo,* in single cells, and gave information about the co-expression of other elements such as transcription factors and surface markers.

Additionally, a method was required to isolate viable cytokine secreting cells to analyse the true expression of genes at a transcriptional level. Within the literature there were many who were isolating T_H populations based on surface markers, such as chemokine receptors, or were using cultured cells, both of which often gave heterogeneous populations[86,99,148,196]. In contrast this work has used cytokine capture, a method in which pure populations of *ex vivo* cytokine secreting cells were isolated.

3.2 Cytokine Production by CD4+ and CD8+ Peripheral Blood T Cells

T lymphocytes were identified using a FS and SS gate, shown in **Figure 2.3**. Single cells were identified using a FS and pulse width gate. To identify the proportion of T lymphocytes that had encountered antigen the cells were stained for a differentially spliced isoform of CD45, CD45RO. CD45 is a protein tyrosine phosphatase expressed on the surface of lymphocytes[197]. Naïve T cells express the isoform CD45RA. Upon antigen encounter the exon coding for the extracellular domain of CD45 is spliced to become the shorter CD45RO isoform. This shortening may allow the TcR to more readily associate with MHC[29]. Peripheral blood mononuclear cells (PBMC) were stimulated with PMA and ionomycin. These two reagents activate cells non-specifically and independently of TcR stimulation,

ensuring that all T cells are activated. PMA activates cells by utilising the intracellular signalling pathways protein kinase C, while ionomycin raises intracellular calcium (Ca^{2+}) levels[198]. This activation stimulates cells to produce cytokines as well as inducing proliferation. Brefeldin A is a naturally produced product from fungi that inhibits proteins transport from endoplasmic reticulum (ER) to Golgi and induces retrograde protein transport from the Golgi apparatus to the endoplasmic reticulum. Addition of Brefeldin A to the PMA and ionomycin treated cells leads to accumulation of cytokines inside the ER, instead of them being released, allowing their measurement by flow cytometry.

Within the stimulated PBMC approximately 50% of total lymphocytes expressed CD45RO, a marker of antigen experienced T cells (gated for $CD4^+$ **Figure 2.3** and **Figure 3.1**). Without stimulation $CD4^+$ T cells did not secrete detectable cytokine *ex vivo* (**Figure 3.1 A)**. The majority of effector cytokines were produced by the $CD45RO^+$ fraction except IL-2 which was also secreted by naïve T cells ($CD45RO^-$) **(Figure 3.1 C)**. IFNγ (median % of $CD4^+CD45RO^+$ secreting IFNγ =29.32%, range 18.74% - 40.43%), IL-5 (0.79%, 0.14%-1.32%), IL-10 (0.93%, 0.21%-1.37%) and IL-17A (2.27%, 1.12%-3.5%) are all effector cytokines associated with distinct T helper lineages **(Figure 3.1 A, B)**. The data shows that $CD4^+$ T cells also secreted IL2, IL-22, TNF-α, GM-CSF and IL-21 **(Figure 3.1 C)**.

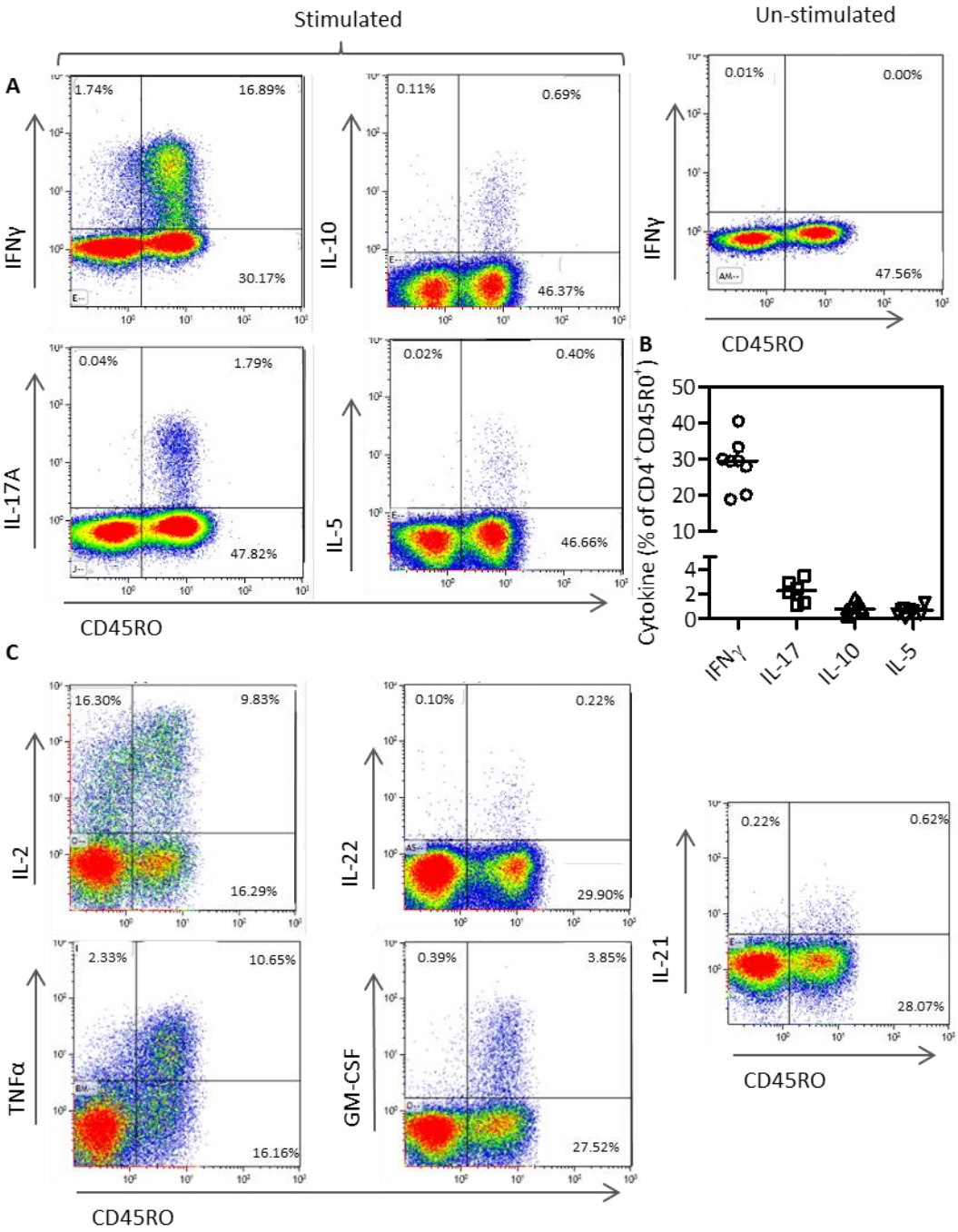

Figure 3.1. Cytokine expression of memory CD4⁺ T cells. PBMC were stimulated with PMA and Ionomycin for 3 hours in the presence of Brefeldin A. For the unstimulated control PBMC were left for three hours in the presence of just Brefeldin A. Cells were stained for surface markers and intracellular cytokine expression and analysed by flow cytometry. **(A)** Representative flow plots gated on CD4⁺ T cells, analysing expression of IFNγ, IL-10, IL-17A and IL-5 against CD45RO in stimulated cells, and IFNγ expression in un-stimulated sample. **(B)** Analysis of 6 independent experiment of cytokine expression, gated on CD4⁺CD45RO⁺ cells, line represents median. **(C)** Representative flow plots (n=2), using a different donor from **A**, gated on CD4⁺ T cells, analysing expression of IL-2, IL-22, TNF-α, GM-CSF and IL-21 expression against CD45RO (n=3). Values represent percentage of cells in the gate, negative gates were set based on a un-stimulated, stained control cells.

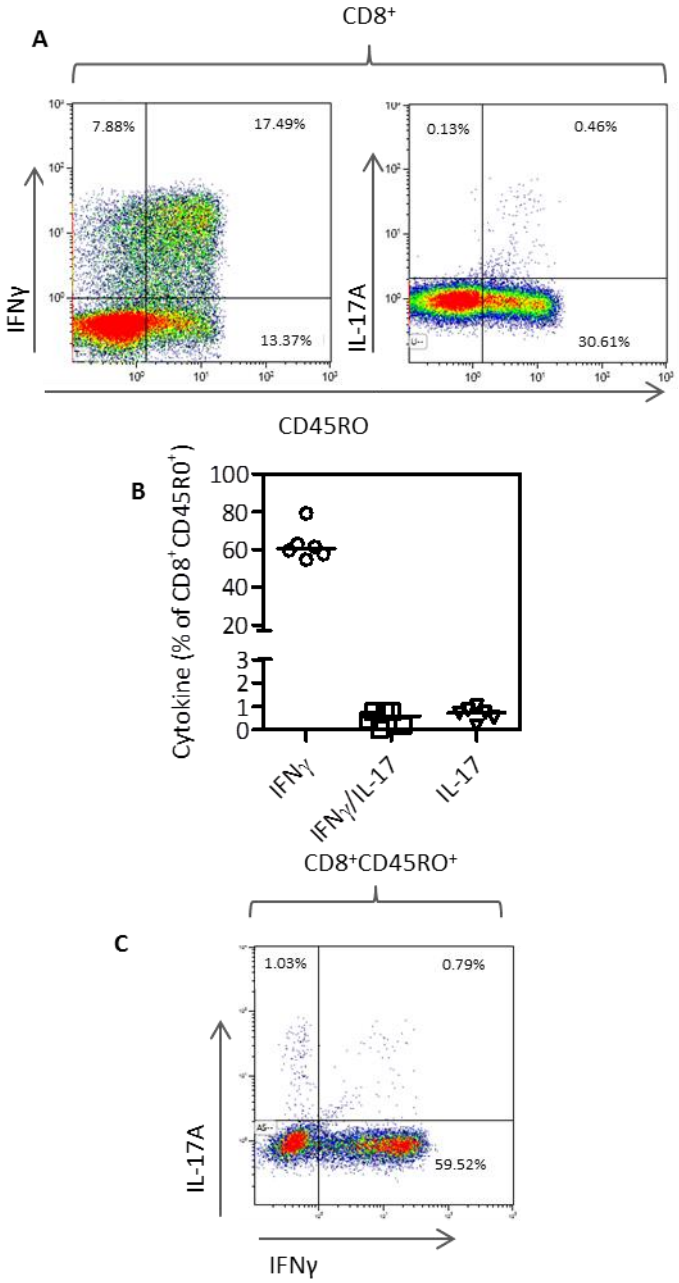

Figure 3.2. Cytokine expression by memory CD8+ T cells. Total PBMC were stimulated with PMA and Ionomycin for 3 hours in the presence of Brefeldin A. Cells were stained for surface markers and intracellular cytokine expression and analysed by flow cytometry. **(A)** gated on CD8+ T cells a representative flow plots of IFNγ and IL-17A expression against CD45RO,. **(B)** Analysing of 5 independent experiments measuring the percentage of IFNγ and IL-17 expression in CD8+CD45RO+ cells. Line represents median percentage. **(C)** Representative flow plots of IFNγ and IL-17A co-expression in CD8+CD45RO+ T cells (n=5). Values represent percentage of cells in the gate. Negative gates were set based on un-stimulated, stained control.

Within the CD8$^+$ T cell compartment IFNγ and IL-17A expression (median % of CD4$^+$CD45RO$^+$IFNγ$^+$ cells=61.62% Range=57.66%-79.14%, median IL-17$^+$= 0.72%, range= 0.19%-0.85%) was detected. IFNγ was the principal cytokine expressed by CD8$^+$ T cells, though it was not restricted to CD45RO$^+$ cells, 7.88% of CD45R0$^-$ cells expressed IFNγ. Co-staining for IFNγ and IL-17A identified an overlap in expression within the CD8$^+$CD45RO$^+$ cells (CD4$^+$CD45RO$^+$IFNγ$^+$IL-17$^+$=0.59% Range=0.19%-0.79%, **Figure 3.2 B,C).**

3.3 Co-staining of Transcription Factor and Cytokine Staining in CD4$^+$ T cells

The three human lineage defining transcription factors T-bet, GATA-3 and RORC relate to the lineage T_H1, T_H2 and T_H17, respectively [47,60,84]. Based on a matched isotype control there was a strong association of the T_H1 cytokine, IFNγ, and transcription factor T-bet in CD4$^+$ T cells **(Figure 3.3 A)**. Although some cells that were negative for IFNγ expressed T-bet, the highest expression of T-bet appeared to be in the cells that also expressed IFNγ (T-bet MFI IFNγ$^+$ =6.22, MFI IFNγ$^-$=2.52-**Figure 3.3**). Very few cells that expressed IL-5 expressed levels of T-bet at a detectable level based on the isotype (T-bet MFI IL-5$^+$=2.45, MFI IL-5$^-$= 2.88). When staining for T-bet in the IL-17A$^+$ population the cytokine positive cells appeared to have an intermediate level of expression of T-bet (T-bet MFI IL-17$^+$=3.99, IL-17$^-$MFI= 2.93). Approximately half of IL-17A$^+$ cells appeared to have levels of T-bet above detection of the isotype. Approximately $^2/_3$ of IL-10 secreting cells expressed T-bet to a detectable degree (T-bet MFI IL-10$^+$=2.73, IL-10$^-$=2.88 - **Figure 3.3 B**).

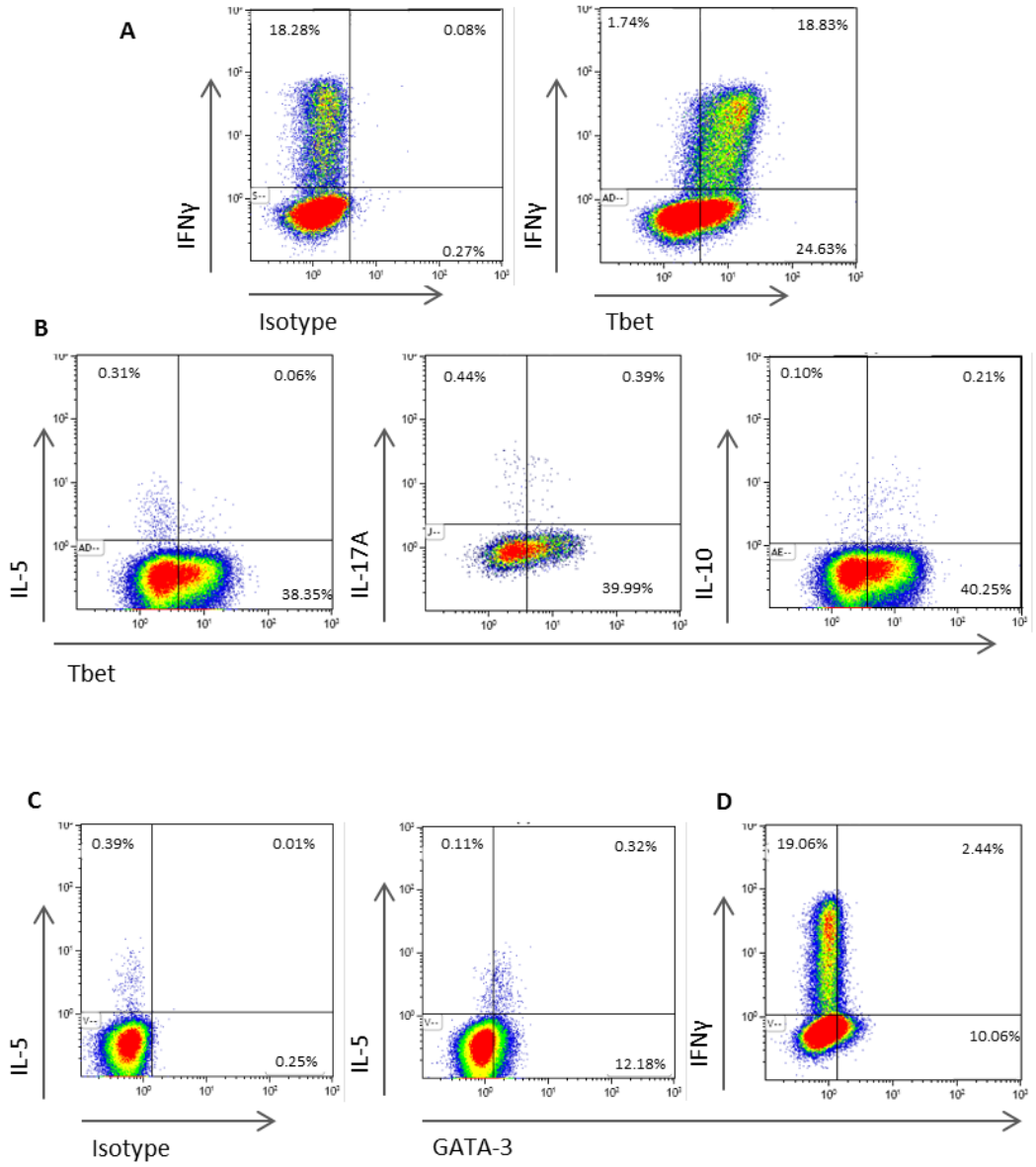

Figure 3.3. T-bet and GATA-3 expression in CD4⁺ memory T cells. PBMC were stimulated for 3 hours with PMA and Ionomycin in the presence of Brefeldin A to analyse their co-expression of intracellular cytokines and transcription factors by flow cytometry. All plots gated on CD4⁺ CD45RO⁺ cells **(A)** T-bet and IFNγ expression (n=15) and **(B)** Tbet expression in IL-5 (n=5), IL-17 (n=15) and IL-10 (n=12) expressing cells . Gates were set using matched isotype control (shown). **(C)** GATA-3 and IL-5 and **(D)** GATA-3 and IFNγ expression (n=6), base on matched isotype control (shown). Values represent percentage of cells within the gate. Negative gates for the cytokines staining were set based on a stained un-stimulated control.

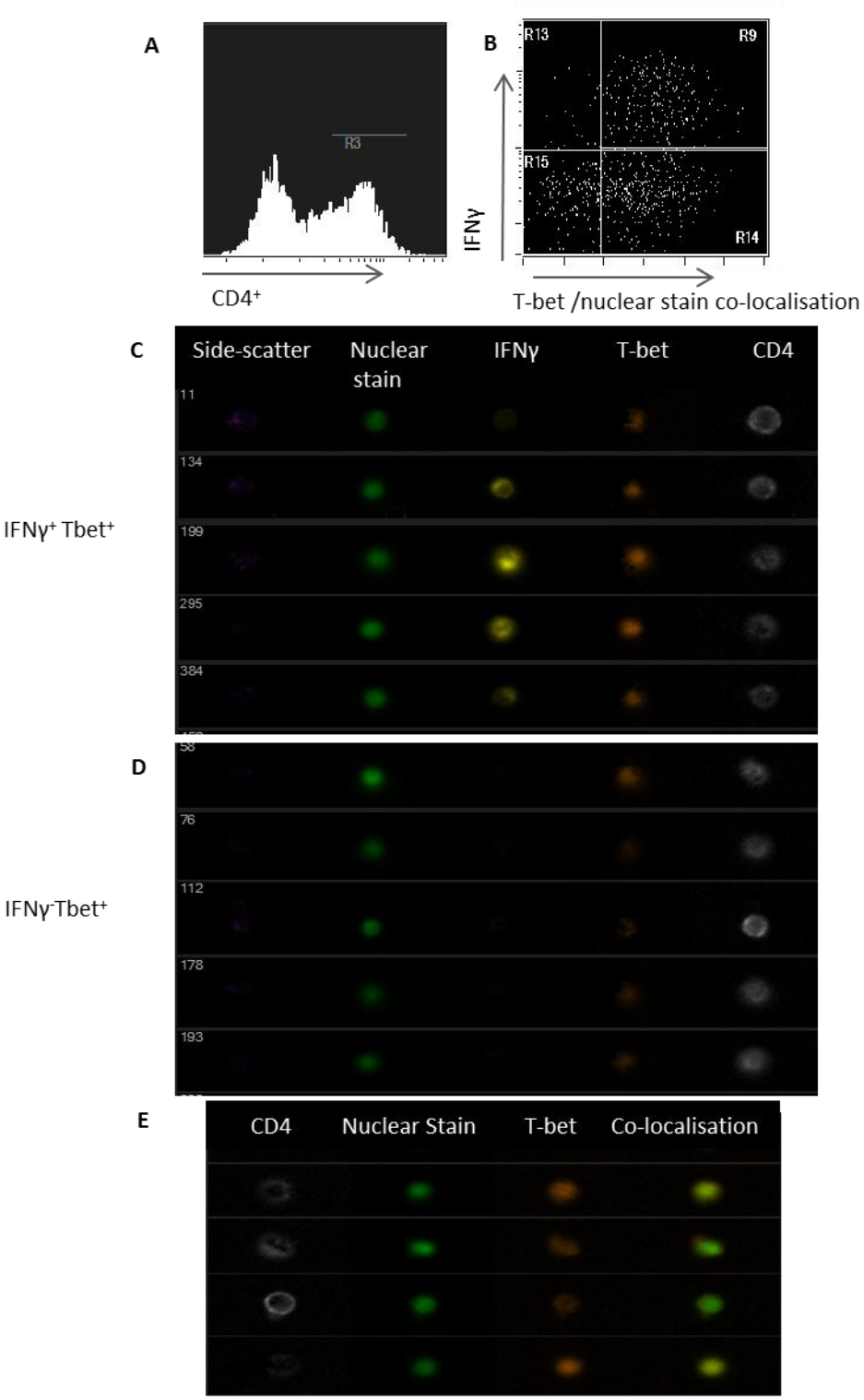

Figure 3.4: **Localisation of T-bet within the nucleus of CD4+ T cells.** PBMC were stimulated for 3 hours with PMA and Ionomycin in the presence of Brefeldin A to analyse their co-expression for CD4,T-bet and IFNγ using Image Stream technology. Po-Pro 1 was used to stain the nucleus **(A)** A CD4+ cell gate to analyse **(B)** the co-localisation of Po-Pro1 and T-bet in relation to IFNγ production. Representative images of **(C)** T-bet expression in IFNγ+ cells and **(D)** in IFNγ- cells in CD4+ cells. **(E)** Representative images of the co-localisation of T-bet and nuclear stain in CD4+ T cells. (n=2)

GATA-3 had a strong association with IL-5 in CD4$^+$ T cells **(Figure 3.3 C)**. There were low levels of GATA-3 in IFNγ$^+$ cells compared to IL-5$^+$ cells (GATA-3 MFI IL-5$^+$ =1.62, IFNγ$^+$= 1.01). **(Figure 3.3 D)**.

To confirm the T-bet expression within IFNγ secreting cells and that the T-bet staining was within the nucleus the Image Stream technology was used to visualise T-bet staining. Transcription factors work through interaction with DNA affecting the transcription of genes, so the co-staining of these cells with a nuclear stain will give us some confidence in the transcription factor antibody specificity. The Image Stream combines the fluorescence sensitivity of single cell analysis of the flow cytometer and the ability to produce images of every cell, similar to microscopy. The processing of the PBMC cells was similar to flow cytometry, apart from the addition of a nuclear stain (Po-Pro 1) to allow identification of the nucleus on the images. I gated on the CD4$^+$ population **(Figure 3.4 A)** and analysed the association of IFNγ and the co-localisation of T-bet and the nuclear stain. Analysis of T-bet expression using the Image Stream showed that T-bet associated with nuclear staining and with IFNγ **(Figure 3.4 B).** In **Figure 3.4 C** there are representative plots of IFNγ$^+$ cells and their T-bet expression. Within a CD4$^+$ T cell, the nucleus takes up a large percentage of the cell and there was only a small amount of visible cytoplasm. However, when you compare the CD4 surface staining to T-bet it was clear that the T-bet staining was not at the surface. This was confirmed in **Figure 3.4 E** as representative images of T-bet (orange) and the nuclear stain (green) were overlapping, indicating nuclear localisation of T-bet (yellow). In the IFNγ$^-$ population the T-bet staining appears to be less intense as compared to the IFNγ$^+$ cells, which supports the flow cytometry data **(Figure 3.4 D)**.

RORC is the transcription factor associated with T_H17 cells. Within the literature there was very little flow data on RORC expression, with the preference to analyse RORC expression by PCR or immunofluorescence analysis. In *ex vivo* PBMC, RORC expression was not detectable above the matched isotype control **(Figure 3.5 A).** There appeared to be a shift for the IL-17$^+$ cells to have higher MFI (MFI isotype IL-17$^+$= 0.81 MFI RORC IL-17$^+$=1.56) than the isotype control in the RORC channel. When IFNγ was co-stained with RORC there also appeared to be a shift of the IFNγ population compared to isotype, however this was still not to a level that exceeded the isotype control and the cytokine negative population also appeared to shift (MFI isotype IFNγ$^+$= 0.60 MFI RORC IFNγ$^+$=0.88).

Analysis of the co-localisation of RORC with nuclear stain in *ex vivo* cells using the Image Stream highlighted that there were very few cells in which there was a similarity in the positioning of the nuclear stain and RORC **(Figure 3.6 A)**. The localisation of RORC appeared to be more cytoplasmic, **(Figure 3.6 C)** especially when compared to localisation of CD4 surface staining. The IL-17 staining was also weak (**Figure 3.6 B).** This suggests that the RORC antibody staining, at least at this level of expression, was not specific for the nuclear transcription factor RORC.

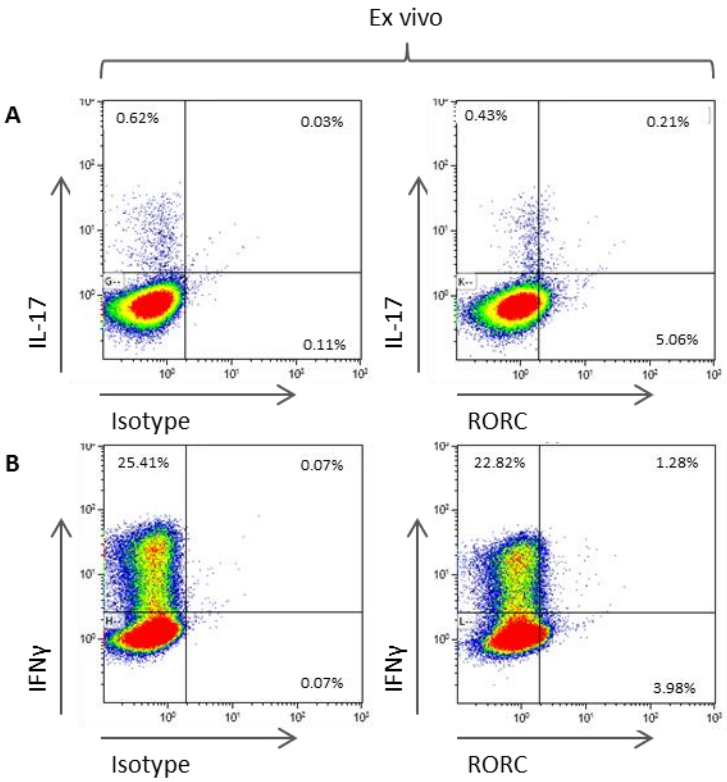

Figure 3.5 T_H17 lineage defining transcription factor, RORC, expression in *ex vivo* CD4+ T cells. PBMC were stimulated for 3 hours with PMA and Ionomycin in the presence of Brefeldin A. **(A)** Representative flow plots of the co-expression of RORC and IL-17, and **(B)** RORC and IFNγ in $CD4^+CD45RO^+$ cells. Gates base on matched isotype control (shown). Values represent percentage of cells in the gate. (n=2)

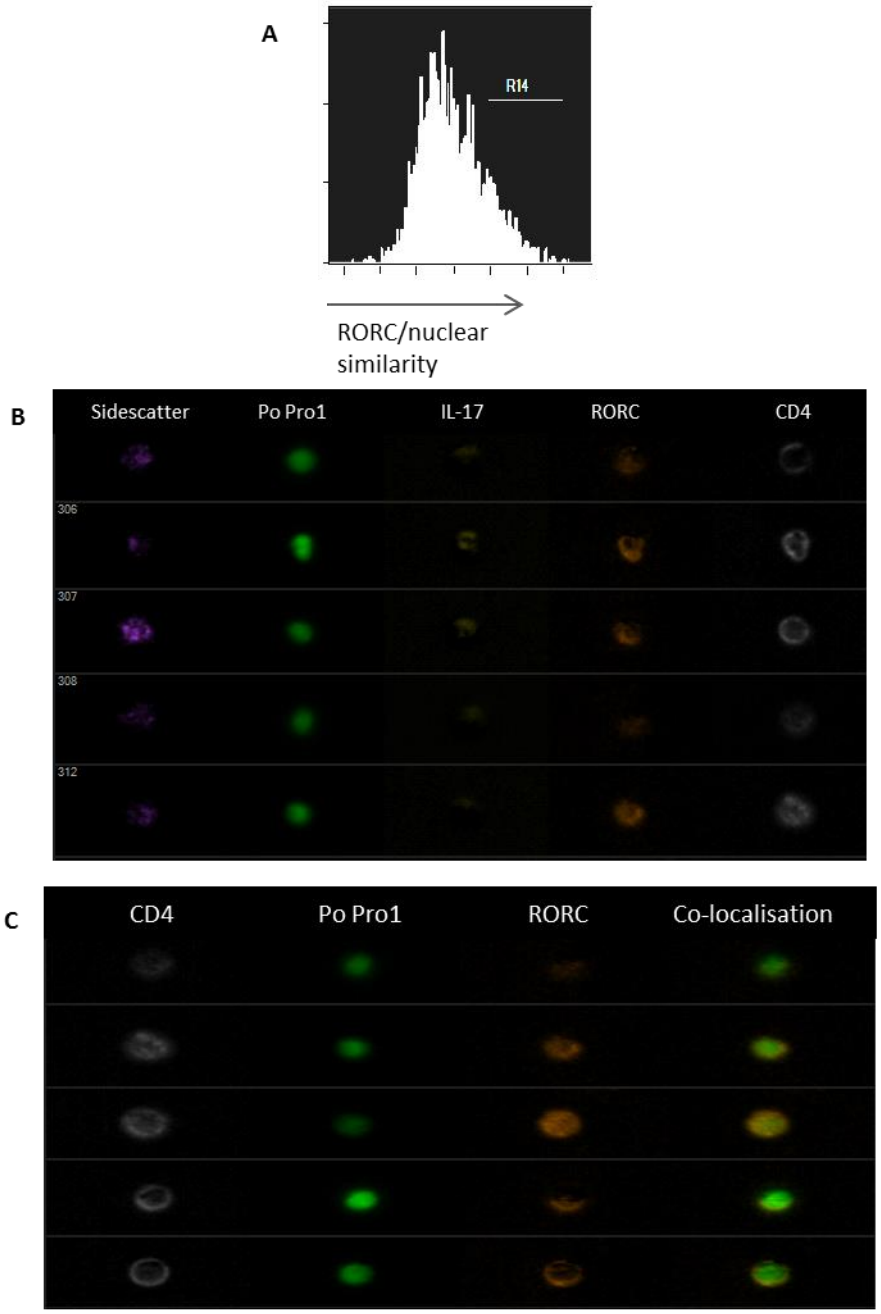

Figure 3.6: **Visualisation of the localisation of RORC staining in *ex vivo* CD4⁺ T cells** PBMC were stimulated for 3 hours with PMA and Ionomycin in the presence of Brefeldin A and were stained for CD4, RORC and IL-17 and analysed using Image Stream technology. Po-Pro1 was used to stain the nucleus. Gated on CD4⁺ cells the **(A)** similarity of Po-Pro1 and RORC, A high similarity score indicates that the Po-pro1 image and RORC image are highly similar (RORC is localised to the nucleus) R14 represents **(B)** Representative images of CD4⁺ cells that express **(B)** IL-17 and RORC. **(C)** and images of the co-localisation of RORC and Po-Pro1 nuclear stain. (n=1)

To further check if the antibody was specific, cells were cultured in T_H17 polarising conditions in an effort to up-regulate RORC expression in T_H17 cells. Initially, isolated total CD4$^+$ T cells were cultured with anti-CD3 and anti-CD28 stimulating antibodies for 3 days to induce proliferation. The stimulation was removed and the cells were allowed to rest for a further 4 days. The cytokines that induce T_H17 differentiation are IL-23, IL-1β and IL-6. Various combinations of these cytokines were added to the cell culture for the full 7 days of culture. A control of no cytokines and a T_H1 polarising culture (+IL-12) was used to compare the induction of IL-17 secreting cells. **Figure 3.7** demonstrates a representative example of a 7 day culture of CD4$^+$ T cells, after which they were stimulated and stained for IFNγ and IL-17 expression. The highest percentage of IL-17$^+$ cells occurred with IL-1β, IL-6 and IL-23 although it was only marginally higher than the no cytokine control. Furthermore the addition of IL-23 increased the percentage of IFNγ$^+$IL-17$^+$ cells compared to the control culture, whereas the addition of IL-1β, IL-6 and IL-23 reduced this percentage. Interestingly, in the cultures with IL-23 or IL-1β and IL-6 there were only approximately 14% IFNγ cells, whereas in the IL-1β, IL-6 and IL-23, the no cytokine control and the IL-12 culture there was approximately 20-25% IFNγ secreting cells. The culture of cells with IL-12 resulted in a reduction of IL-17 secreting cells compared to the control. This suggest that IL-23 is an inducer of IL-17 expression in total CD4$^+$ T cells, and the addition of IL-1β and IL-6 can increase the percentage of IL-17 secreting cells. IL-23 also affects the stimulation of IFNγ$^+$IL-17$^+$ cells, though conversely not IFNγ single secretors. As expected T_H1 polarising conditions was detrimental to the induction of IL-17.

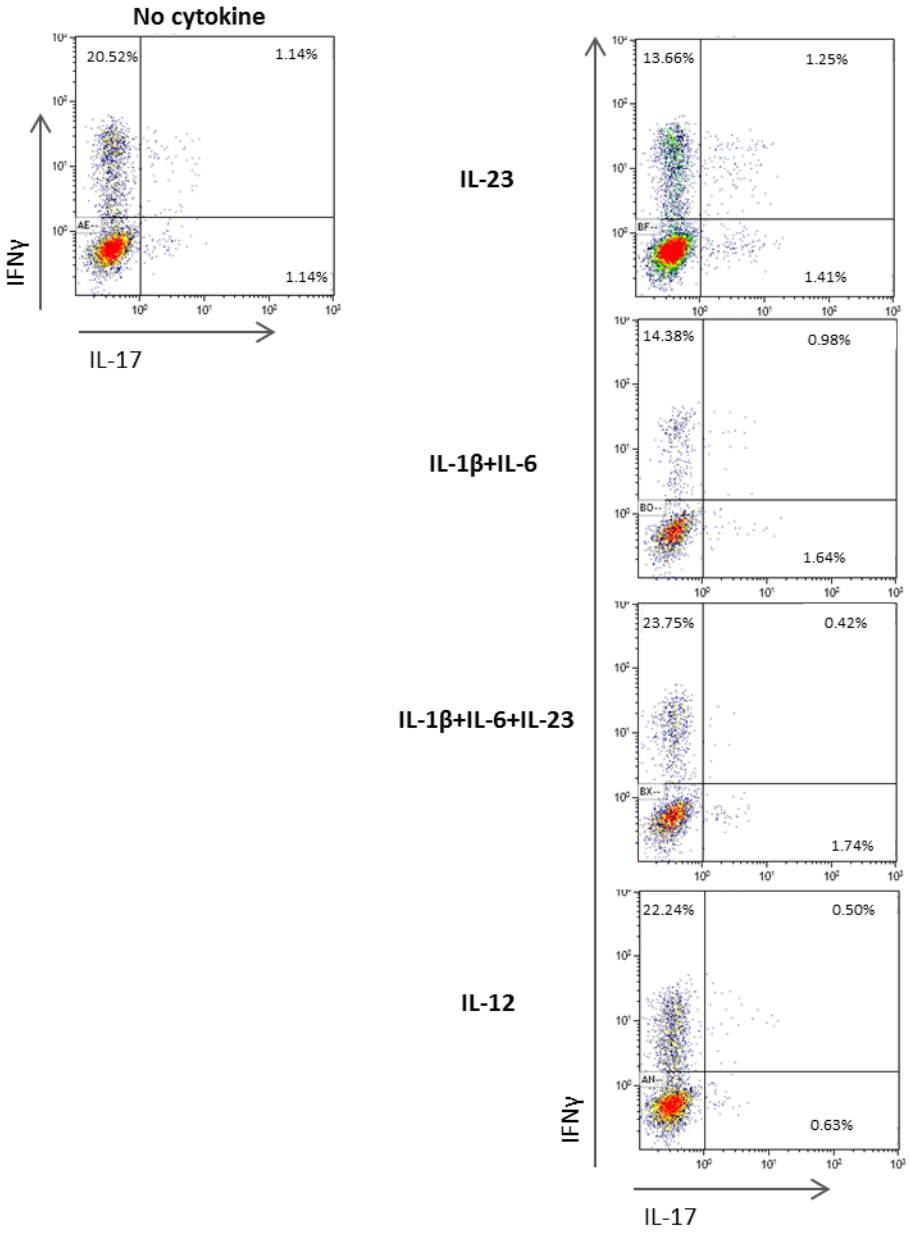

Figure 3.7. Analysis of different T_H17 polarising culture condition on IFNγ and IL-17 cytokine expression in CD4+ T cells. Bead isolated CD4+ T cells were culture at density of 1x10^{6}cells/ml, in presence of plate bound anti-CD3 soluble anti-CD28 stimulating antibodies. On day 3 the stimulation was removed. Cells were cultured in the presence of indicated cytokines for a total of 7 day. Cells were then stimulated for 3 hours with PMA and Ionomycin in the presence of Brefeldin A. The IFNγ and IL-17 expression was analysed gated on CD45RO+ cells. Values represent percentage of cells in the gate. (n=1)

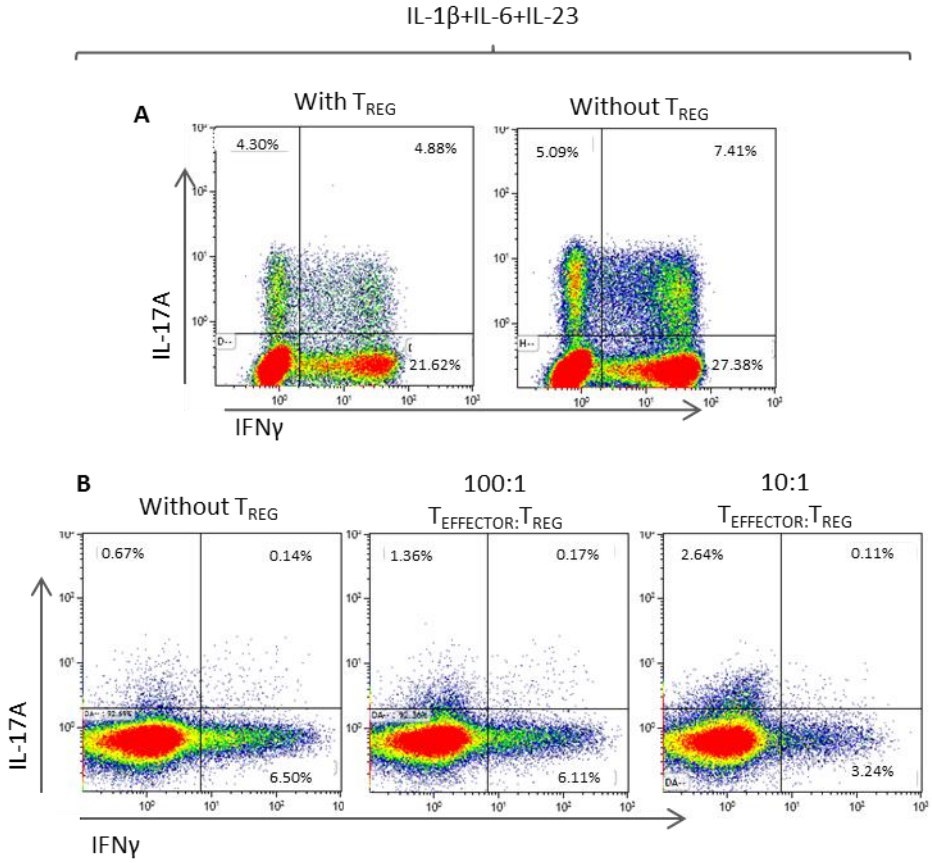

Figure 3.8. The effect of removing T_{REG} from a T_H17 polarising culture on the expression of IL-17 and IFNγ in CD4+ T cells. CD4+ T cells were isolated using negative bead selection and CD25+ cells were isolated from the CD4+ fraction using positive bead selection. **(A)** Total CD4+ and CD4+CD25- cells were culture at density of 1x10^{6}cells/ml, in presence of plate bound anti-CD3, soluble anti-CD28 stimulating antibodies, day 3 the stimulation was removed. Cells were cultured in the presence of IL-1β, IL-6 and IL-23 for total 7 day. Cells were then stimulated for 3 hours with PMA and Ionomycin in the presence of Brefeldin A, and the IFNγ and IL-17 expression was analysed in the CD45RO+ cells. (n=1). **(B)** Culture condition were repeated as in A but CD4+CD25+ cells were re-added to cultures at indicated ratio. Values represent percentage of cells in the gate. (n=1)

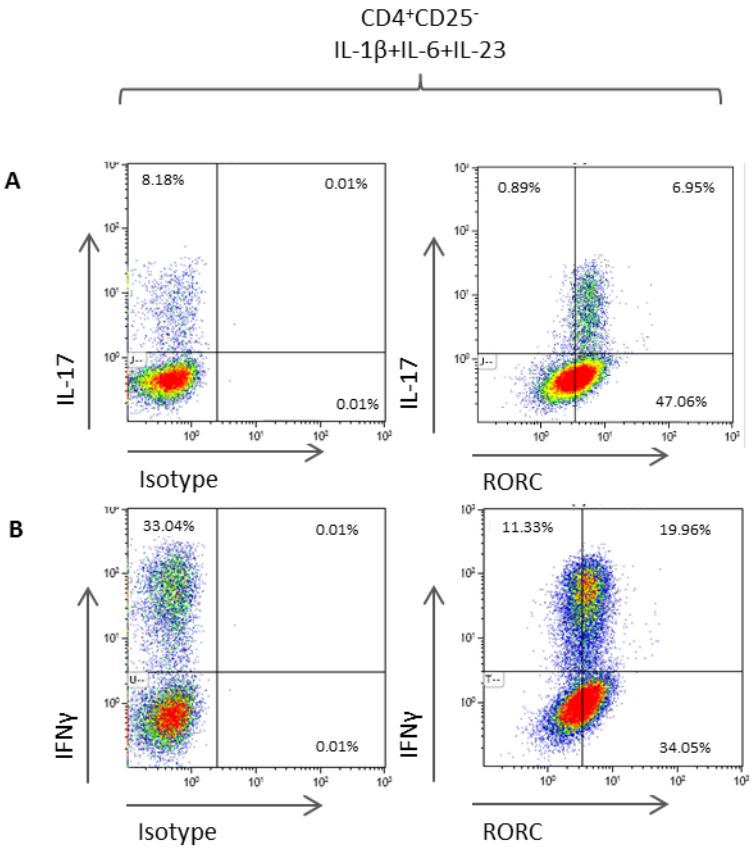

Figure 3.9. RORC staining in CD4+CD25- T cells cultured in T_H17 polarising conditions. CD4+ T cells were isolated using negative bead selection and CD25+ cells were isolated from the CD4+ fraction using positive bead selection. CD4+CD25- cells were culture at density of 1x10^{6}cells/ml, in presence of plate bound anti-CD3, soluble anti-CD28 stimulating antibodies, the stimulation was removed on day 3. Cells were cultured in the presence of IL-1β, IL-6 and IL-23 for total 7 day. Cells were then stimulated for 3 hours with PMA and Ionomycin in the presence of Brefeldin A. **(A)** RORC and IL-17 expression and **(B)** RORC and IFNγ expression was analysed in CD45RO+ cells. Gates based on matched isotype control (shown) Values represent percentage of cells in the gate. Images representative of RORC staining of 5 independent experiments.

There were variable results within the repeats of the T_H17 cultures. **Figure 3.8 A** was the IFNγ and IL-17 expression of cultured CD4$^+$ T cells with T_{REG} (CD4$^+$CD25$^+$) or with the T_{REG} removed (bead isolated). There was a significant increase in the percentage of IL-17 secreting cells within this particular culture. Approximately 9% of cells that expressed IL-17, approximately half of them also co-expressed IFNγ. This is an increase of approximately 7% on the previous culture using the same culture conditions, but different donor. Comparisons of the cultures with and without T_{REG} highlighted that more memory T cells expressed IL-17 when T_{REG} were removed from the culture, although this was not limited to the IL-17 population as the IFNγ$^+$ and the IFNγ$^+$IL-17$^+$ population had increased in percentage as well **(Figure 3.8 A).** Again, highlighting the variability obtained by using different donors, the cultures in **Figure 3.8 B** were the same culture conditions as in **Figure 3.8 A**. The culture without T_{REG} again showed poor IL-17 production, with only 0.81% of cells secreting IL-17. When T_{REG} were added to the culture at a ratio of 1:100 (T_{REG}:T effector cells), this increase IL-17 production. It also gave a slight reduction in the percentage of IFNγ$^+$ cells, although not of the percentage of IFNγ$^+$IL-17$^+$ cells. Following on from this when T_{REG} were added at a ratio of 1:10 (T_{REG}:T effector cells) there was again a reduction in the percentage of IFNγ$^+$ cells and an increase in the percentage of IL-17$^+$ cells, although this time the percentage of IL-17$^+$IFNγ$^+$ cells also were reduced.

After culturing CD4$^+$CD25$^-$ cells in T_H17 polarising conditions for 7 days (culture from **Figure 3.9 A)**, RORC expression was analysed. Over all, compared to the isotype staining, the MFI for RORC in IL-17 cells increased (MFI Isotype IL-17$^+$=0.51 MFI RORC IL-17 =5.45) **(Figure 3.9 A)**. However, this increase was also seen in the negative population and in the IFNγ$^+$ cells

(MFI Isotype IFNγ$^+$=0.50 MFI RORC IFNγ$^+$ =3.95). **(Figure 3.9 A, B)**. This suggests that although the staining for RORC was increased after culture the staining was no more specific after culture than before.

3.4 Optimisation of Cytokine Capture Protocol

To further analyse the phenotype of CD4$^+$ T helper subsets a method (Miltenyi Biotech) was optimised in which a bivalent antibody binds to CD45 on the surface of all lymphocytes. The second binding site of the antibody is for the cytokine of interest. In these experiments two bivalent antibodies were used either specific for IFNγ or IL-17. Any cytokine that is released from the cell will be captured on the cells surface by the antibody. A second, fluorescently labelled, antibody binds to the captured cytokine and identifies a cytokine secreting cell. This method is described in more detail in **Figure 3.10.**

Initially, to identify the stimulation agent that would provide a balance between the most accurate staining of the cytokine produced by each individual cell and providing a high yield of cells, three methods of stimulation were tested. These were Cytostim (Miltenyi Biotech), Staphylococcal Enterotoxin B and PMA/ionomycin. Cytostim is a super-antigen, which was used at 20µl/ml, the concentration recommended by the supplier. It stimulates a proportion of CD4$^+$ T cells by crosslinking the TcR and MHC molecules independently of certain Vβ domains. Miltenyi Biotech quote that approximately 75% of CD4$^+$ T cells unregulated CD69 after 3 hours of stimulation with Cytostim, which increases to 90% CD69$^+$ CD4 T cells after 6 hours. SEB is also a super-antigen which crosslinks MHC II and TcR. PMA and ionomycin

activate cells non-specifically and independently of TcR stimulation, ensuring that all T cells are activated.

The results of these experiments are as follows. Cytostim gave small percentage of IL-17 and IFNγ secreting cells **(Figure 3.11 A)** in proportion to intracellular staining **(Figure 3.14 D)**, and was variable between donors. Although the staining for IFNγ and IL-17 looked clean for SEB and the different populations were easily identifiable, the population of cells that were stimulated were small, meaning they did not give enough cells after sorting. **(Figure 3.8 B)**. Using either of these stimulation types would lead to an increased chance of the populations not being homogeneous, especially the IL-17$^+$. If only a small fraction of the IFNγ$^+$ cells are labelled there is more of a chance that cells expressing IL-17 and IFNγ will be labelled for only IL-17 and contaminate this populations. Due to the small percentage of IL-17 cells any cells contaminating this population will have a greater impact on any analysis than if IL-17 cells contaminated IFNγ population. Using a stimulation agent, such as PMA and ionomycin, which increases the labelling of IFNγ cells increases the chance of getting a pure IL-17$^+$ population.

PMA and ionomycin stimulation for cytokine capture stimulated all the cells and resulted in a detectable percentage of cells secreted IFNγ and IL-17 **(Figure 3.8 C)**. A time course was undertaken to optimise the time for stimulation with PMA and ionomycin. The longer the cells were left to stimulate the higher the percentage of IL-17 secreting cells that were positively labelled. After two hours there was very little increase in the percentage of positive cells for IFNγ. However, the shift of the IFNγ cytokine capture staining towards

higher MFI (MFI IFNγ capture 0.5hr=0.2, 1hr=0.4, 2hr=2.25, 3hr=3.98, 4hr=5.54) identifies false positive staining. The shift indicates that all the negative cells not secreting cytokine were picking up the excess IFNγ that was being secreted by the true T_H1 cells making it hard to identify the true T_H1 cells **(Figure 3.11 D)**.

The protocol was optimised to remove the negative cells picking up the IFNγ on their surface. After the surface cytokine staining the cells were left in Brefeldin A for 3 hours to prevent release of any excess cytokine. Then the cells could be intracellularly stained in an effort to identify true IFNγ positive cells.

Within the protocol there was a stage during which the cells are cultured in media to allow IFNγ to be captured on the cell surface **(Figure 3.10 C)**. To investigate if it was at this stage that excess IFNγ in the system was staining $IFN\gamma^-$ cells, the cells were cultured at different cell densities to identify if the false positive would dilute out **(Figure 3.12 A-D)**. The cells that were cultured at different densities did not seem to make that much difference to the overall capture staining sensitivity. Diluting the cells 10 fold only increased the percentage of true IFNγ positive cells by 1.66%, and decreased the IFNγ false positive cells by 0.35% **(Figure 3.12 B, D)**.

The surface bivalent antibody was added to the cells in suspension for 10 minutes in a small volume **(Figure 3.10 B)**. To investigate if it was at this stage the cells were picking up excess IFNγ the supernatant from the cells was either removed or added to un-stimulated cells to identify if the negative cells picked up any IFNγ. The data showed that adding the supernatant to un-stimulated cells did not result in any significant false positive staining

(Figure 3.13 C). Removing the IFNγ capture-antibody supernatant from the cells seemed to increase the true positive staining of IFNγ cells compared to the normal capture protocol **(Figure 3.13 A, B)**. There was no non-specific binding of IFNγ (e.g.to IFNγR) to the surface of the cells, as there was no staining of stimulated cell without the capture antibody **(Figure 3.13 D)**.

PMA and ionomycin is a strong stimulus for $CD4^+$ T cells, one of the reasons why it was so useful in cytokine capture. After stimulation the protocol from the supplier states to only wash the cells once before proceeding with the rest of the protocol **(Figure 3.10 between the stages of A and B)**. By washing the cells three times, to try to fully remove any excess PMA/ionomycin, the cells no longer produced more IFNγ after this step in the protocol. This was highlighted by the lack of any intracellular staining for IFNγ **(Figure 3.14 A, B)** but appeared to bring the IFNγ background staining back to the base line.

The final stage of optimisation of cytokine capture was to check whether the washing step had any effect on IL-17 staining, and also to test the effects of different fluorescence molecules on the intensity of the staining for IFNγ. Using an FITC conjugated secondary antibody led to cleaner staining than using APC as the background was reduced **(Figure 3.14 E,F)**. The washing step appeared to make no difference to IL-17 staining as there was still up to 1.5% IL-17 secreting cells.

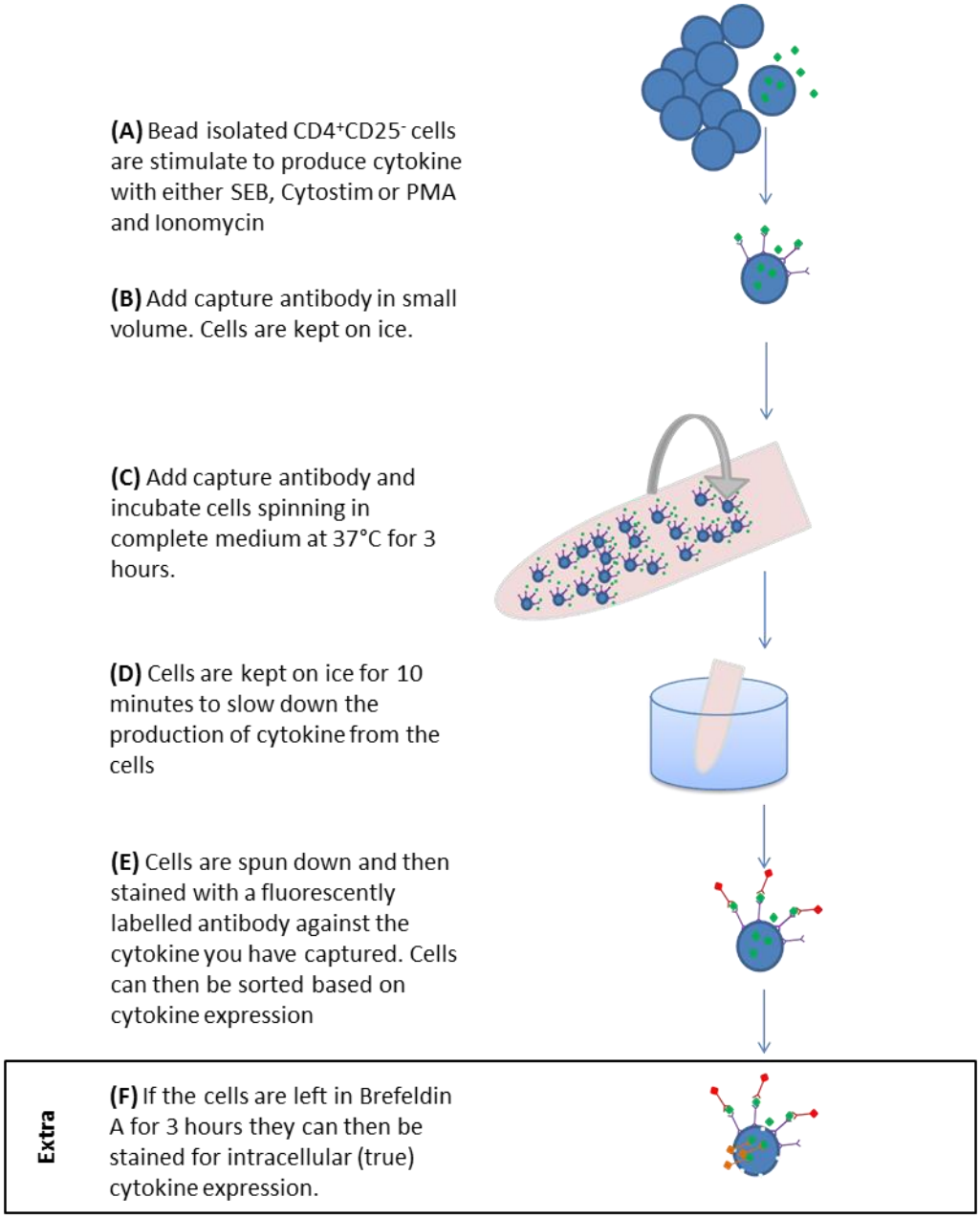

Figure 3.10 Schematic of the cytokine capture protocol to isolate viable cytokine secreting CD4+ T cells. (A-E) Step-wise description of the method used to identify and isolate viable IFNγ and IL-17 secreting cells. **(F)** For analysis of the accuracy of the surface cytokine capture the method was altered to allow for intra-cellular staining of cytokine production. This step was added to method where indicated in figure legend. Staphylococcal Enterotoxin B (SEB), Phorbol 12-myristate 13-acetate (PMA), RPMI+10% heat inactivated bovine serum albumin (complete media).

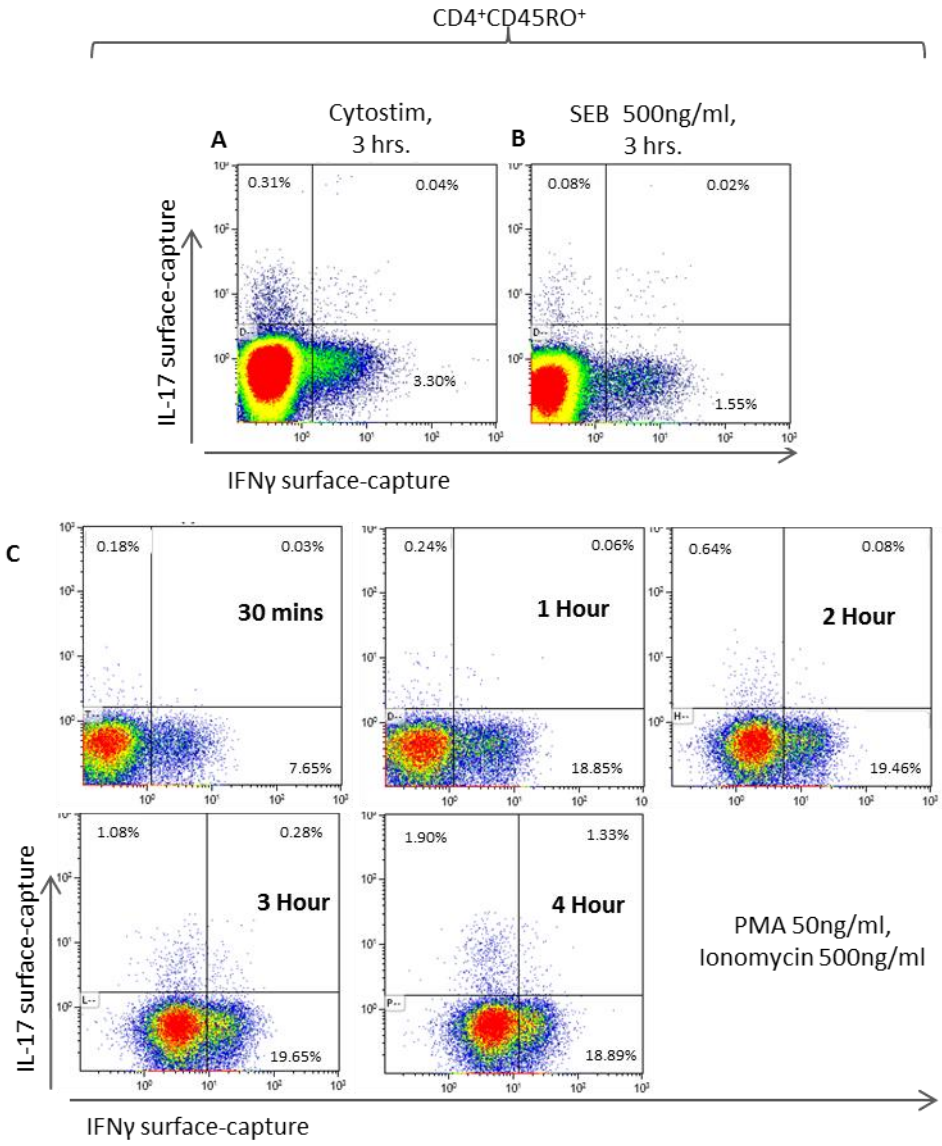

Figure 3.11. Optimisation of cytokine capture protocol: Testing different stimulation reagents to maximise cytokine secreting populations. Total PBMC were stimulated with either **(A)** 20µl/ml of CytoStim, **(B)** 500ng/ml SEB, both for 3 hours or **(C)** PMA/Ionomycin. For the time indicated. Cells were stained for CD4 and CD45RO along with surface-captured IFNγ and IL-17, using the protocol for cytokine capture. Values show the percentage of cells within the gate. (n=4) Staphylococcal Enterotoxin B (SEB), Phorbol 12-myristate 13-acetate (PMA).

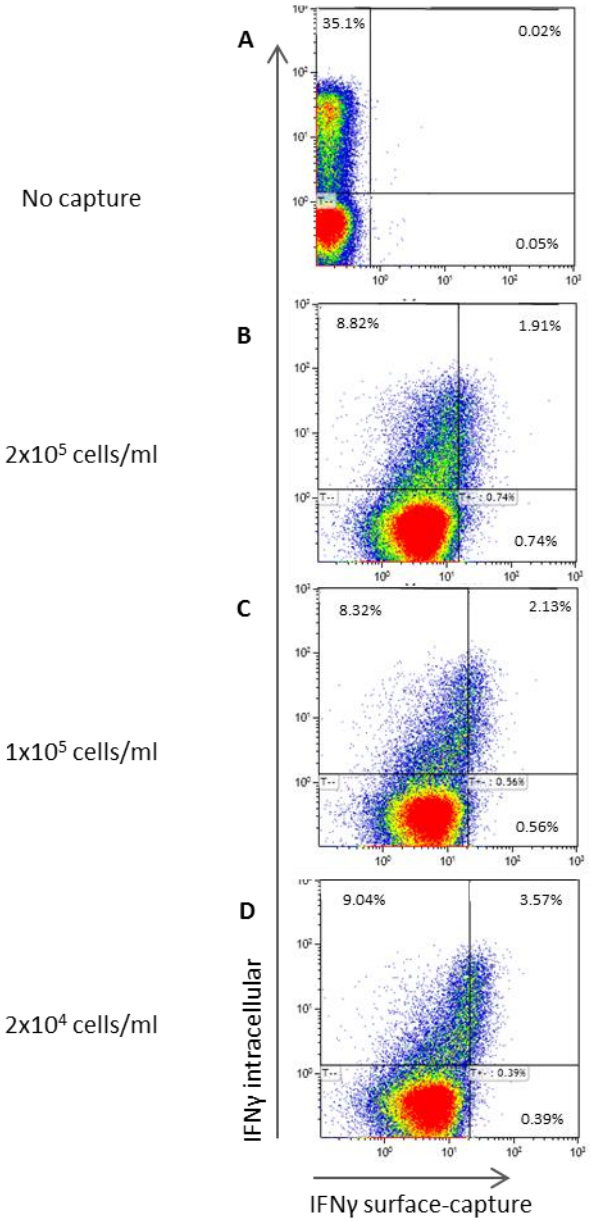

Figure 3.12. Optimisation of cytokine capture protocol: Testing cell density to optimise IFNγ secretion in PMA/Ionomycin stimulated T cells. PBMC were stimulated with 50ng/ml of PMA and 500ng/ml of Ionomycin for 3 hours. Cells were washed and mixed with **(B-D)** IFNγ capture antibody or **(A)** no capture antibody. The cells were gently rocked at 37°C, at 2% CO_2, in RPMI/10% HI-FCS for 45 minutes at a density of either **(B)** $2x10^5$, **(C)** $1x10^5$, or **(D)** $2x10^4$ cells/ml. The cells were put through the rest of the cytokine capture protocol staining for surface-captured IFNγ. Cells were then left in Brefeldin A for 3 hours and stained for CD4, CD45RO and intra-cellular IFNγ. Values represent percentage of cells within the gate. (n=1)

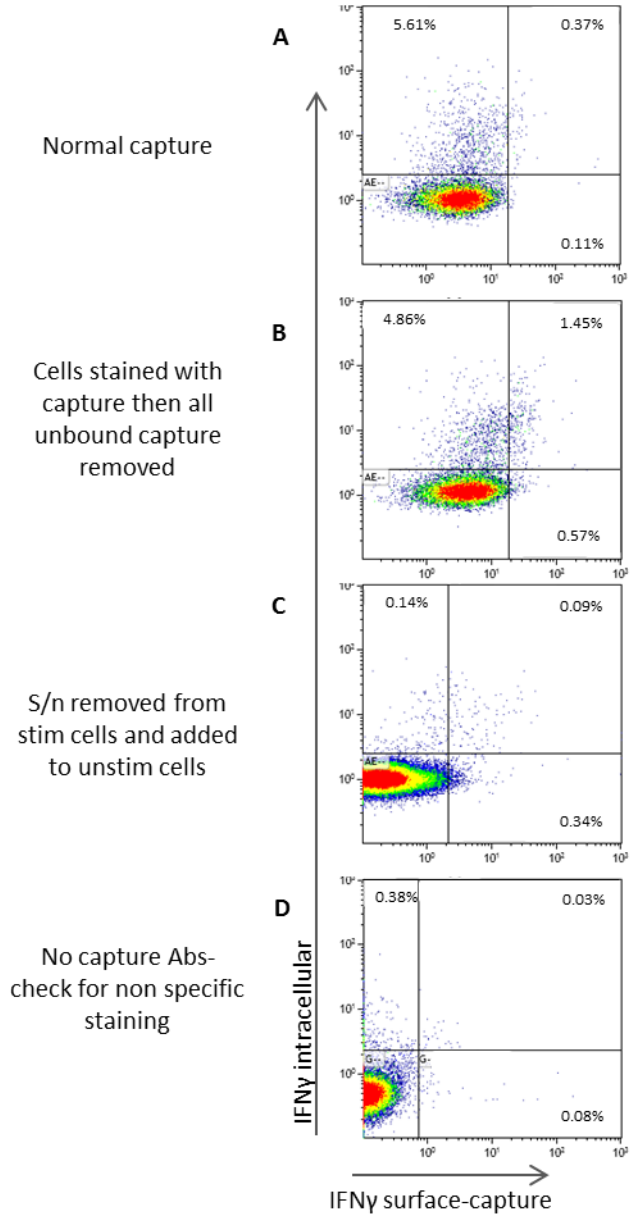

Figure 3.13. Optimisation of cytokine capture protocol: Identification of the stage at which false positive surface-capture of IFNγ occurs. PBMC were stimulated with 50ng/ml of PMA and 500ng/ml of Ionomycin for 3 hours or left un-stimulated. Cells were washed and either culture for 10 minutes on ice at density of $1x10^7$ cells/100µl **(A,B,C)** with or **(D)** without capture antibody. **(B)** The cells were spun down and the supernatant (s/n) removed and **(C)** added to un-stimulated cells. In **(A,D)** the cells were not spun down and were left in the s/n. **(A,B,C,D)** The cells were then put through the rest of the cytokine capture protocol for IFNγ staining. Cells were then left in Brefeldin A for 3 hours and stained for CD4, CD45RO and intracellular IFNγ production. Values represent percentage of cells within the gates. Abs – antibody (n=1).

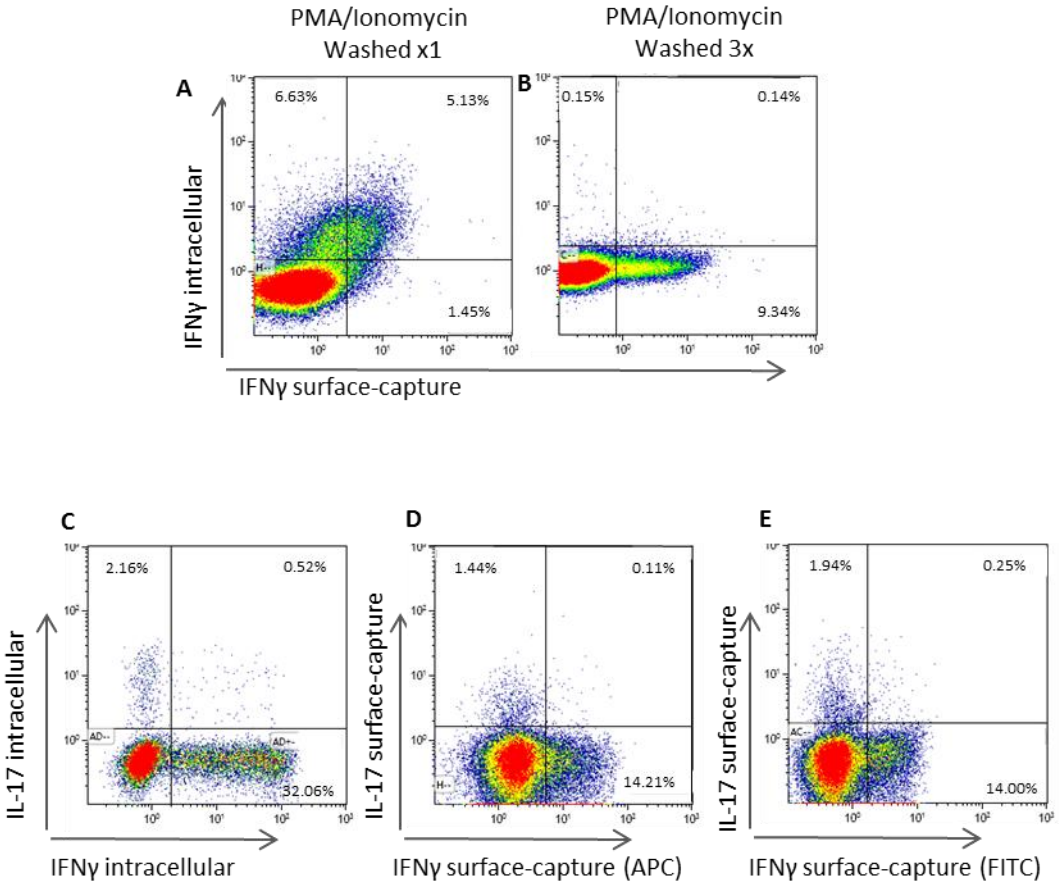

Figure 3.14. Optimisation of cytokine capture protocol: Proper removal of PMA + Ionomycin straight after stimulation improves true surface-captured cytokine staining. PBMC were stimulated with 50ng/ml of PMA and 500ng/ml of Ionomycin, for 3 hours. Cells were washed either **(A)** once or **(B,D,E)** three times and mixed with IFNγ and IL-17 capture antibody. The cells were then put through the rest of the cytokine capture protocol staining for surface-captured IFNγ and IL-17. Cells were then left in Brefeldin A for 3 hours and stained for CD4, CD45RO and intra-cellular IFNγ and IL-17. **(C)** A representative flow plot of intracellular staining of stimulated $CD4^+$ memory T cells for IFNγ and IL-17A. **(D)** Representative flow plot of surface-captured IFNγ (APC) and IL-17 (PE) and repeated with **(E)** IFNγ (FITC) and IL-17 (PE), using optimized protocol on bead isolated $CD4^+CD25^-$ T cells. Values represent percentage of cells within the gate. Allophycocyanin (APC), Phycoerythrin (PE). n=1

3.5 Analysis of Co-expression of Lineage Defining Cytokines

Multi-colour flow cytometry can stain stimulated PBMC for several different cytokines at once to analyse the co-expression of effector cytokines. Furthermore, the optimisation of the IFNγ and IL-17 cytokine capture method allowed me to analyse the gene expression within small homogeneous populations of IFNγ and IL-17 secreting cells and equate it with the flow cytometry data.

Using this technique there were several cytokines that were not detectably co-expressed. These were IL-10 and IL-17, IL-17 and IL-5 and IL-5 and IL-10 **(Figure 3.15)**. IFNγ appeared to be co-expressed with several different cytokines associated with other lineage, namely IL-5, IL-17A or IL-10 **(Figure 3.16, 3.17, 3.18)**. IFNγ and IL-5 were co-expressed by a small percentage of cells (IFNγ$^+$IL-5$^+$ median=0.09% Range= 0.1%-0.24%) **(Figure 3.16 B)**. The MFI of IFNγ was significantly reduced (p=0.006) in a cell that secretes both IFNγ and IL-5 (mean IFNγ MFI in IFNγ$^+$IL-5$^+$=66.06) compared to a single IFNγ secreting cell (mean IFNγ MFI IFNγ$^+$=128.79- **Figure 3.16 C**). This reduction was also found in the IL-5 MFI. The MFI of IL-5 was significantly reduced (p=0.015) in cells that co-expressed IFNγ and IL-5 (mean IL-5 MFI IL-5$^+$=26.78) compared to cells that just secreted IL-5 (mean IL-5 MFI IL-5$^+$=42.09-**Figure 3.16 B, C**).

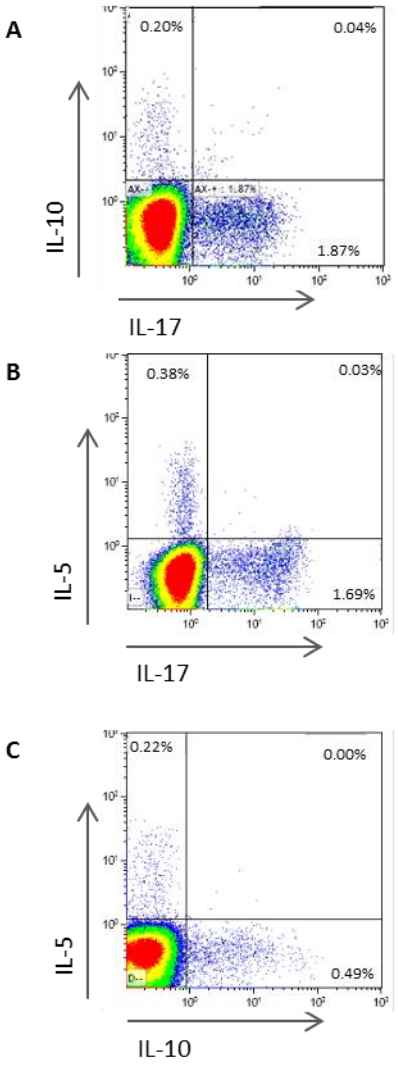

Figure 3.15. Memory CD4+ T cells that co-expressed IL-10 and IL-17, IL-5 and IL-17 or IL-10 and IL-5 could not be detected using flow cytometry. PBMC were stimulated for 3 hours with PMA and Ionomycin in the presence of Brefeldin A to analyse by flow cytometry the co-expression of intracellular cytokines. Cells were gated on CD4+ and CD45RO+. Representative flow plots of **(A)** IL-17A and IL-10, **(B)** IL-17A and IL-5 and **(C)** IL-10 and IL-5 secretion gated on CD4+CD45RO+ cells (n=10) Values shown are percentage of cells in each gate.

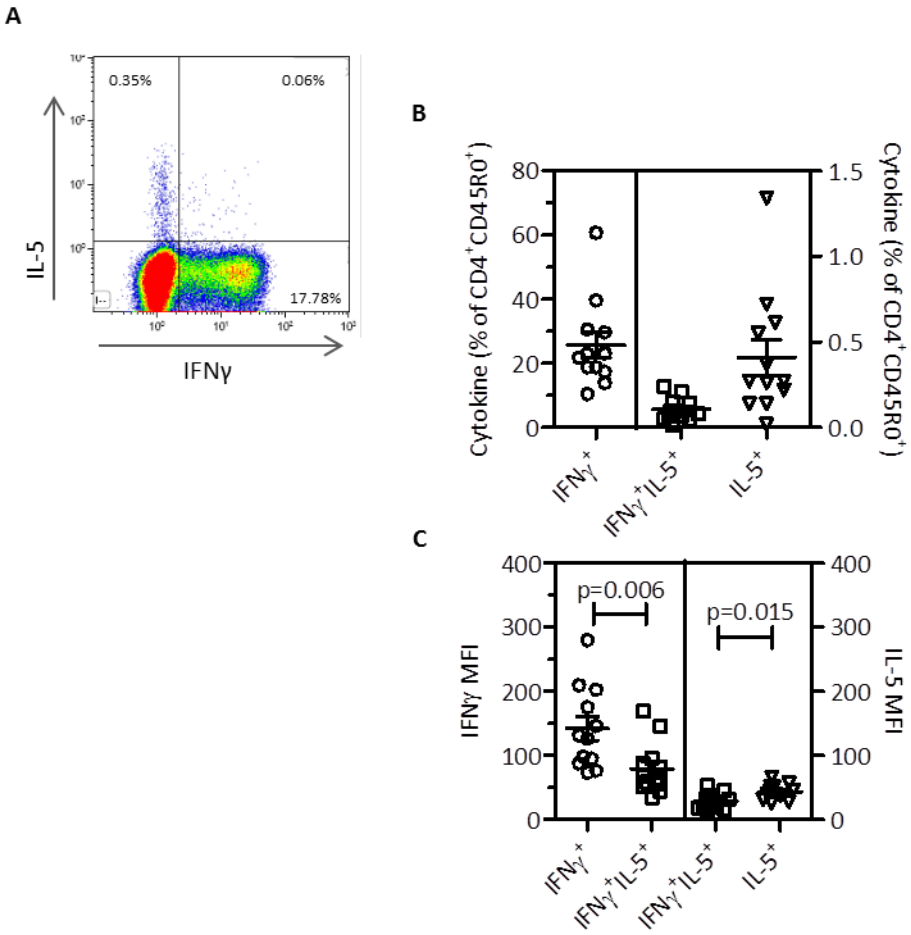

Figure 3.16. A small population of memory CD4+ T cells co-expressed IFNγ with IL-5. PBMC were stimulated for 3 hours with PMA and Ionomycin in the presence of Brefeldin A to analyse by flow cytometry the co-expression of intracellular cytokines. Cells were gated on CD4+ and CD45RO+. Representative FACS plots of secretion of **(A)** IL-17A and IFNγ **(B)** Percentage of CD4+CD45RO+ cells secreting IFNγ, IFNγ and IL-5 or IL-5 alone. (n=10) **(C)** Analysis of the median fluorescent intensity (MFI) of IFNγ and IL-5 (n=10) in single and co-expressing populations. **(C)** Bars represent mean and standard error of the mean (SEM). Significance was detected using a Student's T test, p values are shown where significance was reached.

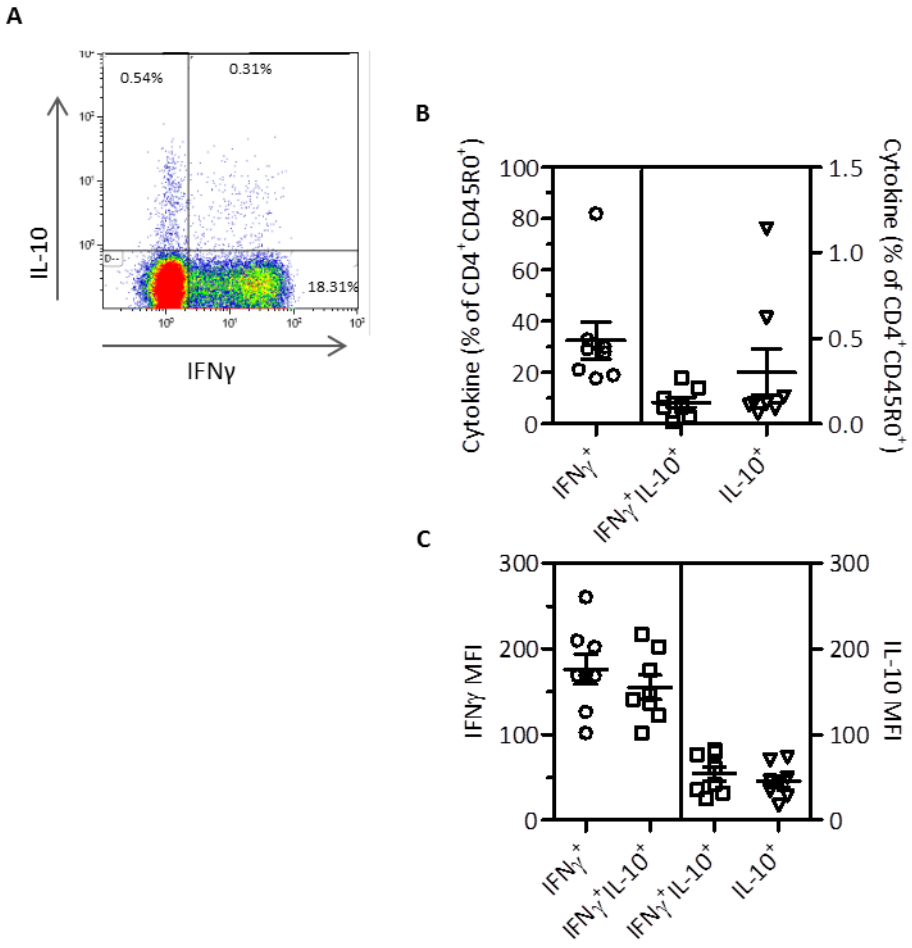

Figure 3.17. A small population of memory CD4+T cells co-expressed IFNγ with IL-10. PBMC were stimulated for 3 hours with PMA and Ionomycin in the presence of Brefeldin A to analyse by flow cytometry the co-expression of intracellular cytokines. Cells were gated on CD4+ and CD45RO+. Representative FACS plots of secretion of **(A)** IL-10 and IFNγ **(B)** Analysis of percentage of CD4+CD45RO+ cells secreting IFNγ, IFNγ and IL-10 or IL-10 alone. (n=8) **(C)** Analysis of the median fluorescent intensity (MFI) of IFNγ and IL-10 (n=8) in single and co-expressing populations. **(C)** A Student's T test was used to test for significance differences between subsets. Mean and standard error of the mean (SEM) are shown.

Following on from this, approximately half of the IL-10 secreting cells also co-secreted IFNγ (IFNγ$^+$IL-10$^+$ median= 0.11% range=0.01%-0.27% **Figure 3.17 A, B**). However in this case the co-expression of IFNγ and IL-10 made no significance difference to the MFI of either cytokines (p≤0.05) (mean MFI of IFNγ in IFNγ$^+$ =168.83, IFNγ$^+$IL-10$^+$=143.53, mean MFI of IL-10 in IL-10$^+$ =43.635, IFNγ$^+$IL-10$^+$=51.34-**Figure 3.17 C**).

Co-staining for IL-17A and IFNγ gave a small but easily identifiable population of IFNγ$^+$IL-17A$^+$ cells (median=0.24% range=0.05%-0.51%, **Figure 3.18 A, B**). There was a statistically significant decrease for IFNγ when IL-17A was co-expressed compared to single IFNγ$^+$ T cells (mean MFI of IFNγ in IFNγ$^+$ =143.72, IFNγ$^+$IL-17$^+$=72.36, mean MFI of IL-17 in IL-17$^+$ =77.68, IFNγ$^+$IL-17$^+$=59.23-**Figure 3.18 C)**. To identify if the reduction in IFNγ was at an mRNA level as well as at the protein level, cytokine secreting cells were isolated using the cytokine capture method. Once the cytokine secreting populations were isolated, mRNA was isolated from the cells and converted to cDNA. To analyse the amount of message of each cytokine, qRT-PCR was undertaken. The house keeping gene GAPDH was used to give a relative expression of the cytokine mRNA **(Figure 3.19 A)**. The lower IFNγ protein in the dual IFNγ$^+$IL-17$^+$ cells was replicated at the mRNA level **(Figure 3.19 B)**. This showed there was no significant difference in the IL-17 MFI in IFNγ$^+$IL-17$^+$ and IL-17$^+$ cells **(Figure 3.18 C)**, which was replicated at the mRNA level **(Figure 3.19 B)**.

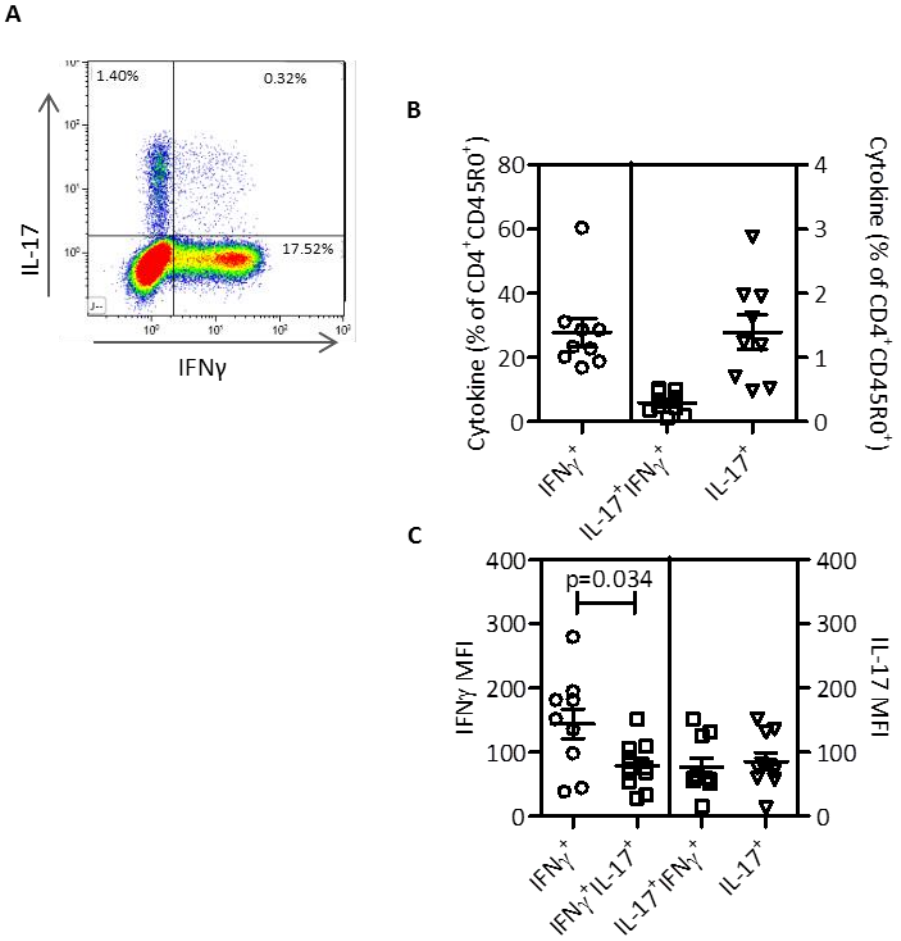

Figure 3.18. A small population of memory CD4+ T cells co-expressed IFNγ with IL-17A. PBMC were stimulated for 3 hours with PMA and Ionomycin in the presence of Brefeldin A to analyse by flow cytometry the co-expression of intracellular cytokines. Cells were gated on CD4+ and CD45RO+. Representative FACS plots of secretion of **(A)** IL-17A and IFNγ **(B)** Analysis of percentage of CD4+CD45RO+ cells secreting IFNγ, IFNγ and IL-17A or IL-17A alone. (n=9) **(C)** Analysis of the median fluorescent intensity (MFI) of IFNγ and IL-17A (n=9) in single and co-expressing populations. **(C)** Significance was detected using a Student's T test, p values are shown where significance was reached. Mean and standard error of the mean (SEM) are shown.

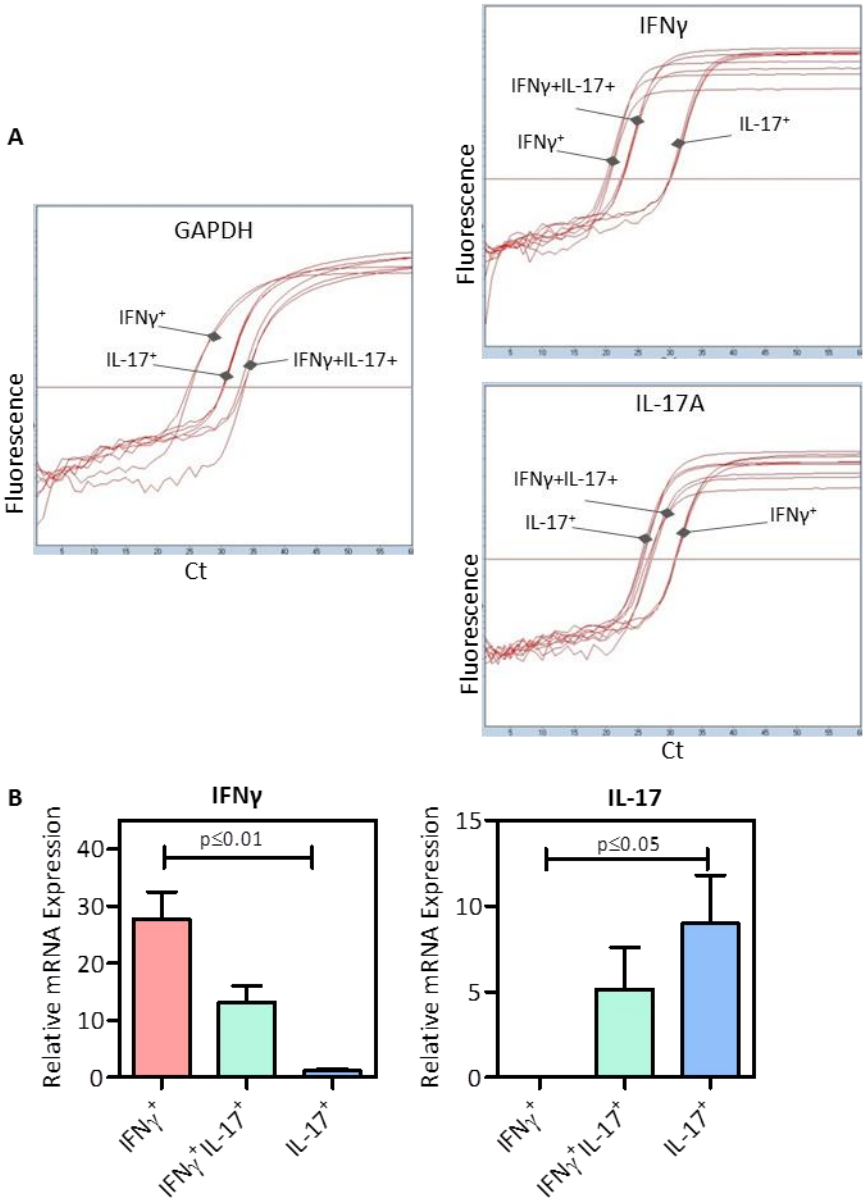

Figure 3.19. Protein expression of IL-17 and IFNγ results in lower IFNγ per cell than single IFNγ secretors at a mRNA level. Cytokine secreting populations (IFNγ+, IFNγ+IL-17+, IL-17+) were isolated from CD4+CD25- bead purified cells using cytokine capture and a MoFlo cell sorter. qRT-PCR was used to assess the expression of IFNγ and IL-17A genes relative to GAPDH. **(A)** Representative amplification curve for GAPDH, IL-17A and IFNγ (n=4). **(B)** Analysis of IFNγ ($p=0.0031$ for IFNγ+ vs IL-17+) and IL-17A ($p=0.021$ for IFNγ+ vs IL-17+) mRNA expression relative to GAPDH in IFNγ+, IFNγ+IL-17+, IL-17+ populations of CD4+ memory T cells. Mean and standard error of the mean (SEM) represented by bars. A Kruskal-Wallis with a Dunns multiple comparison post test was used to identify significance.

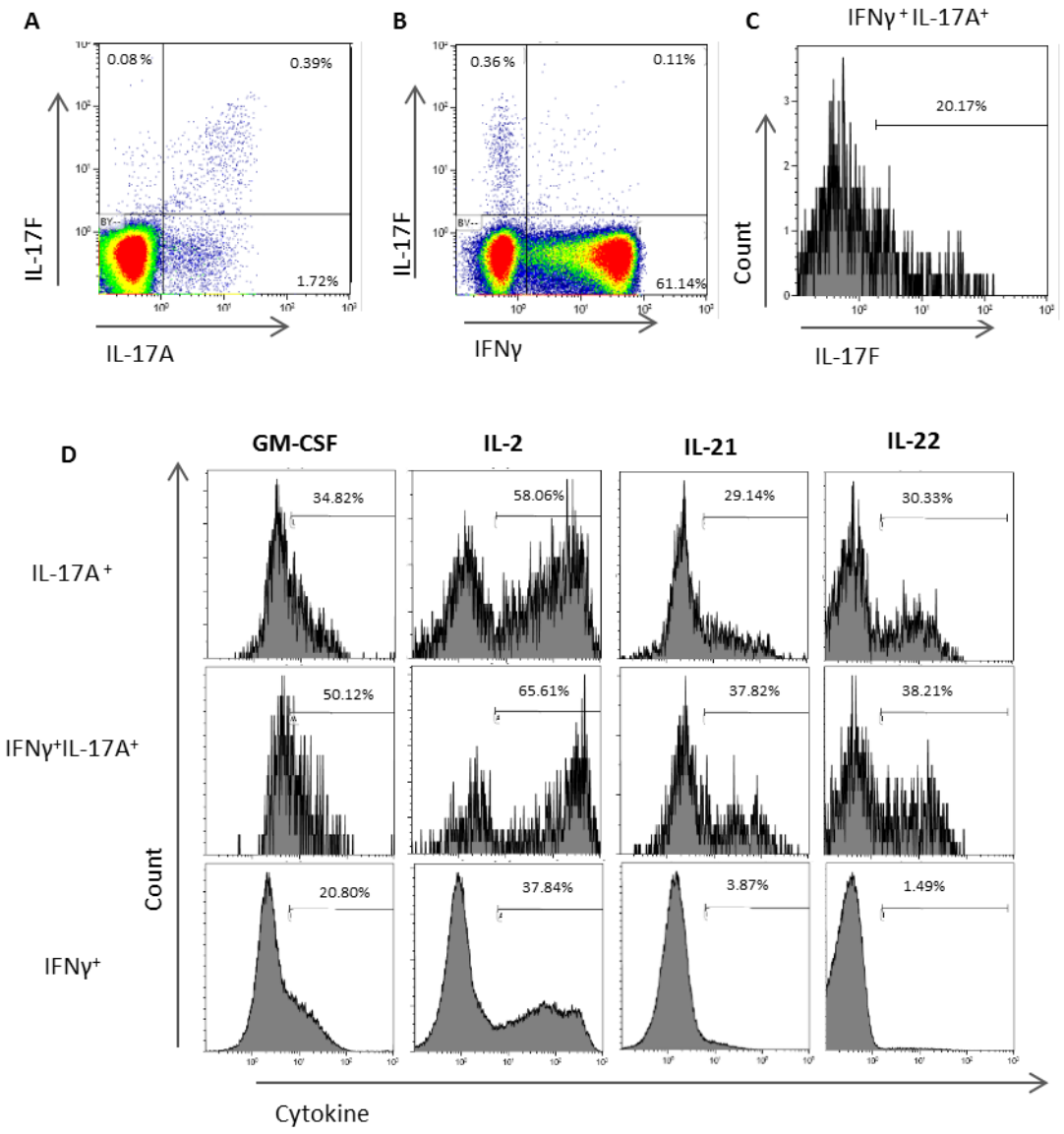

Figure 3.20. A similar percentage of IFNγ+IL-17A+ cells express IL-22 and IL-21 compared to single IL-17A+ cells, while very few single IFNγ+ secrete IL-21 and IL-22. PBMC were stimulated for 3 hours with PMA and Ionomycin in the presence of Brefeldin A to analyse their co-expression of intracellular IFNγ, IL-17A and IL-17F. **(A)** Representative flow plots gated on the CD4+CD45RO+ T cells of IL-17A and IL-17F as well as **(B)** IL-17F and IFNγ expression. **(C)** The co-expression of IL-17F in IFNγ+IL-17A+ cells gated on CD4+CD45RO+ T cells. **(D)** Representative flow plots of GM-CSF, IL-2, IL-21 and IL-22 cytokine expressed by IL-17A +, IFNγ+IL-17+, and IFNγ+ secreting cells. Values represent percentage of cells within the gate. (n=3)

There are 6 isoforms of IL-17, IL-17A-F. IL-17A was expressed by CD4$^+$ T cells with IL-17F also expressed, but only by a small proportion of cells. The CD4$^+$ T cells were analysed for IFNγ, IL-17F and IL-17A to identify if co-expression of IFNγ and IL-17F occurs in a similar manner to IFNγ and IL-17A. **Figure 3.20 A** shows IL-17F was always co-expressed with IL-17A, although IL-17A was expressed alone. IL-17F and IFNγ was co-expressed in a population of CD4$^+$ T cells **(Figure 3.20 B)**. 20% of cells that co-expressed IL-17A and IFNγ also co-expressed IL-17F **(Figure 3.20 C)**, which was approximately the same percentage of IL-17A cells expressing IL-17F.

IL-21 and IL-22 have previously been described as T_H17 associated cytokine before they were attributed to a lineage of their own[116,199]. To determine how similar or different the IFNγ$^+$IL-17$^+$ cells were from the IL-17$^+$ cells, IL-21 and IL-22, as well as IL-2 and GM-CSF, were stained for **(Figure 3.20 D)**. More than 30% of both single IL-17$^+$ and IFNγ$^+$ IL-17$^+$ expressed IL-21 and IL-22. There was very little IL-21 or IL-22 expressing in single IFNγ$^+$ T cells. GM-CSF was more highly expressed in IFNγ$^+$IL-17$^+$ cells, while only 30% of IL-17$^+$ cells and 20% of IFNγ$^+$ cells co-expressed these cytokines. IL-2 was expressed in all populations, however approximately 60% of IL-17$^+$ and IFNγ$^+$IL-17$^+$ cells expressed IL-2 compared to the 40% of IFNγ$^+$ single secretors **(Figure 3.20 D)**.

The next step was to investigate if cells that secreted two lineage defining cytokines had been recently activated. This was achieved by staining for the markers CD71, which is a transferrin receptor that is up regulated upon activation to transport iron into the cell, and CD69 which plays a role in negatively regulating the activation of T cells. CD4$^+$ T cells

expressing CD45RO and CD69 **(Figure 3.21 A)** or CD71 **(Figure 3.21 B)** were isolated using the MoFlo cell sorter from *ex vivo* PBMC. The cells could not be stimulated with PMA and ionomycin as this would up-regulate CD69 and CD71 expression on all cells. The isolated populations were then stimulated and their expression of IFNγ and IL-17 was analysed **(Figure 3.21)**. Initially, a ratio of the percentage of IFNγ$^+$, IL-17$^+$ and IFNγ$^+$IL-17$^+$ cells in the CD69$^+$ and CD69$^-$ was calculated. The ratio for the IL-17$^+$ and IFNγ$^+$ populations were all below 1, showing that these single cytokine secreting populations were not enriched in the recently activated populations **(Figure 3.22 A, D)**. This experiment also showed that there was no enrichment of dual IFNγ$^+$IL-17$^+$ cells in the recently activated CD69$^+$ or CD71$^+$ population **(Figure 3.22 A, D)**. This was also the case for cells co-secreting IL-10 and IFNγ **(Figure 3.22 B, E)**. Since all the ratios for these cytokine secreting populations was less than 1 it suggests that there was a reduction in cytokine secreting populations in CD69$^+$ or CD71$^+$ recently activated T cells. When looking at IL-5 and IFNγ expression in recently activated cells there appeared to be an enrichment of single IL-5 secreting cells in both the CD69$^+$ and CD71$^+$ populations, and the ratio for two out of the three replicates for IFNγ$^+$IL-5$^+$ in the CD69$^+$ population were greater than 1 **(Figure 3.22 C, F)**. This result shows that dual cytokine secreting cells do not represent recently activated T cells.

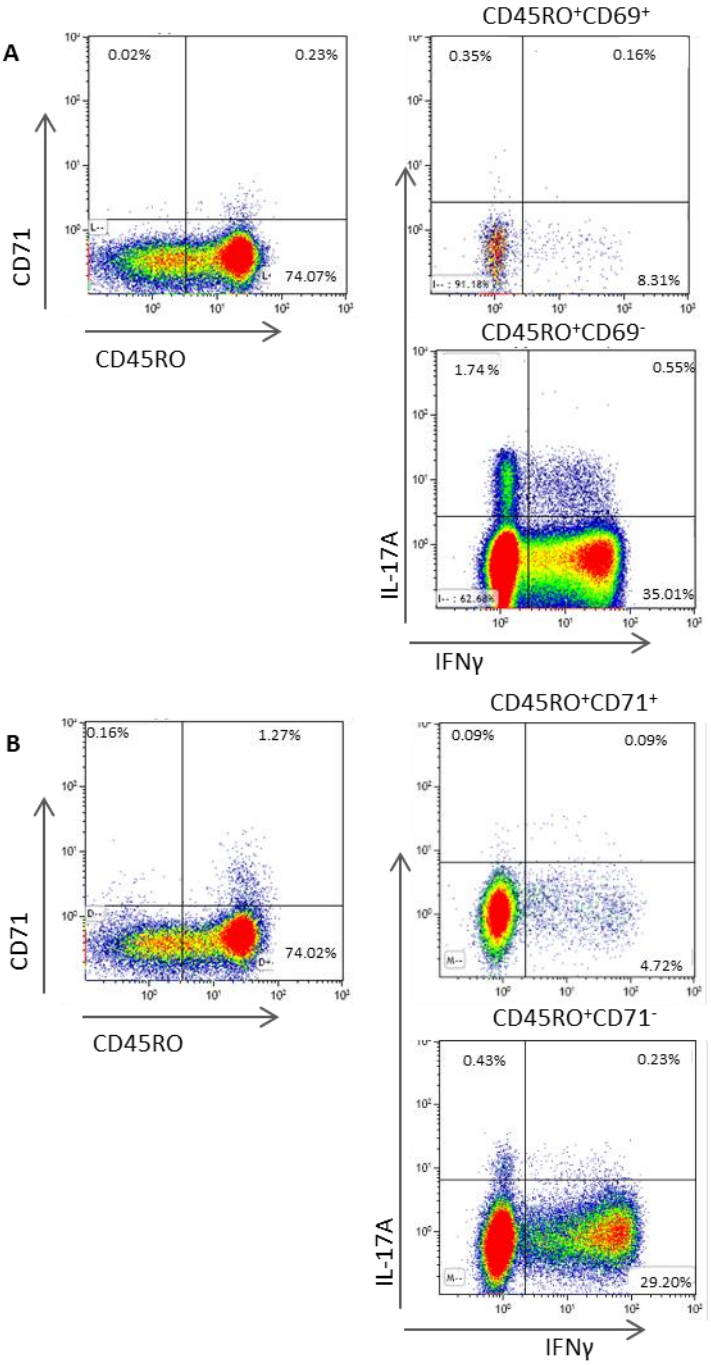

Figure 3.21. Memory CD4+ T cells that express both IFNγ and IL-17 are not enriched in a recently activated population. Freshly isolated PBMC were MoFlo cell sorted based on CD45RO and either CD69 or CD71 expression. Once isolated these populations were stimulated for 3 hours with PMA and Ionomycin in the presence of Brefeldin A to analyse their expression of IFNγ and IL-17A. **(A)** Representative flow plot of CD45RO and CD69 expression in *ex vivo* CD4+ T cells. Flow pots of IFNγ and IL-17 expression in the isolated populations. (n=3) **(B)** Representative flow plot of CD45RO and CD71 expression in *ex vivo* CD4+ T cells. FACS pots of IFNγ and IL-17 expression in the isolated populations. Values represent percentage of cells within the gate. (n=3)

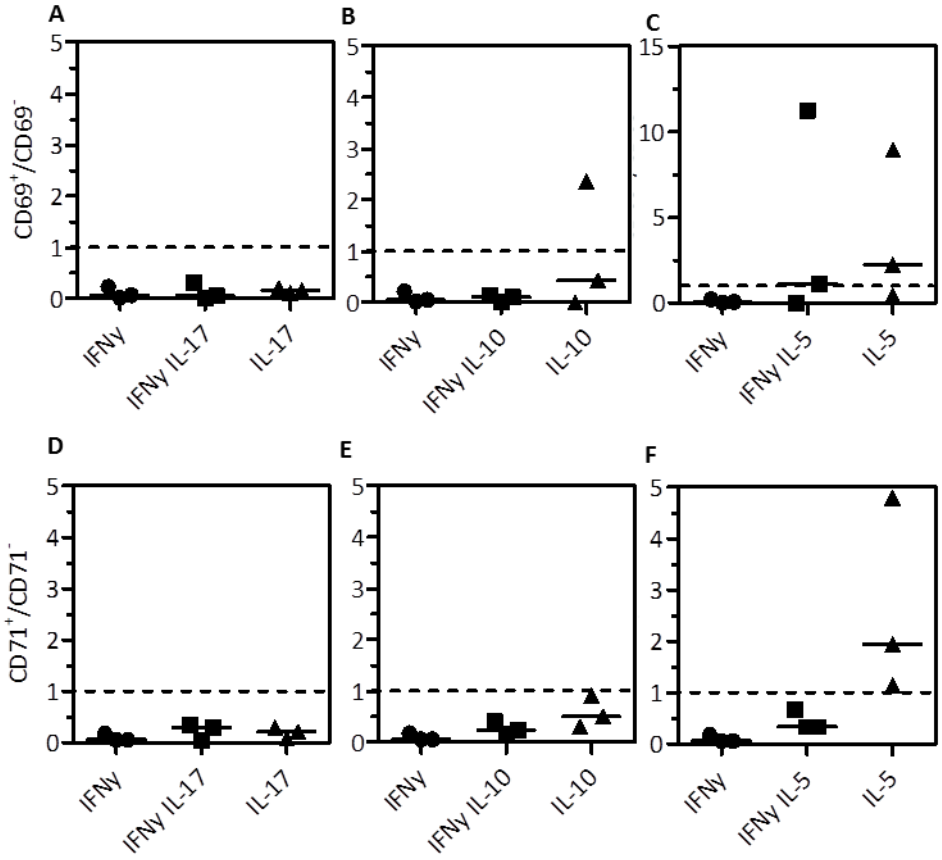

Figure 3.22. Memory CD4+ T cells that express two lineage defining cytokines are not enriched in a recently activated population. (A) The ratio of the percentage of CD4+CD45RO+ IFNγ and IL-17 secreting cells in CD69+/CD69- populations. **(B)** The ratio of the percentage of CD4+CD45RO+ IFNγ and IL-10 and **(C)** IFNγ and IL-5 secreting cells in CD69+/CD69- population. **(D)** Ratio of the percentage of CD4+CD45RO+ IFNγ and IL-17 secreting cells in CD71+/CD71- population. **(E)** Ratio of the percentage of CD4+CD45RO+ IFNγ and IL-10 and **(F)** IFNγ and IL-5 secreting cells in CD71+/CD71- population. Dotted line represents 1, the point at which there is an equal percentage of cells in each population. Median value shown of three independent experiments.

3.6 Analysis of Co-expression of Lineage Defining Transcription Factors

It is well documented that T-bet controls IFNγ secretion in CD4+ T cells[47], as RORC controls IL-17 expression[84]. Flow cytometry and qRT-PCR analysis were undertaken to analyse the expression of these two transcription factors within the IFNγ and IL-17 secreting populations **(Figure 3.23)**. T-bet was analysed in *ex vivo* memory CD4+ T cells. It showed that there was no significant difference in the level of T-bet protein in single IFNγ+ cells (median % T-bet+= 81.27), compared to IFNγ+IL-17+ cells (median % T-bet+=73.92). There was a trend for a decrease in the mRNA levels of T-bet in IFNγ+IL-17+ compared to IFNγ+ cells, however this was not significant. There was a significant difference in the protein and mRNA levels of T-bet between IFNγ+ and IL-17+ T cells (p=0.0156 - **Figure 3.23 A, C)**.

RORC protein analysis on *in vitro* cultured CD4+ T cells showed a significant reduction in the levels of RORC in IFNγ cells (median % RORC+ = 32.8%) compared to both IFNγ+IL-17+ and IL-17+ T cells (median % RORC+ = 69.87%, 69.38% respectively). The levels of RORC, both protein and mRNA, between IFNγ+IL-17+ and IL-17+ T cells were not different **(Figure 3.23 B, D)**.

Further protein analysis of T-bet was undertaken in IFNγ cells co-expressing IL-5 or IL-10. **Figure 3.24 B** and **C** highlights that even when IFNγ was co-expressed with other lineage defining cytokines, there was no significant difference in the levels of T-bet expressed. This was also the case for GATA-3 when IL-5 was co-expressed with IL-5.

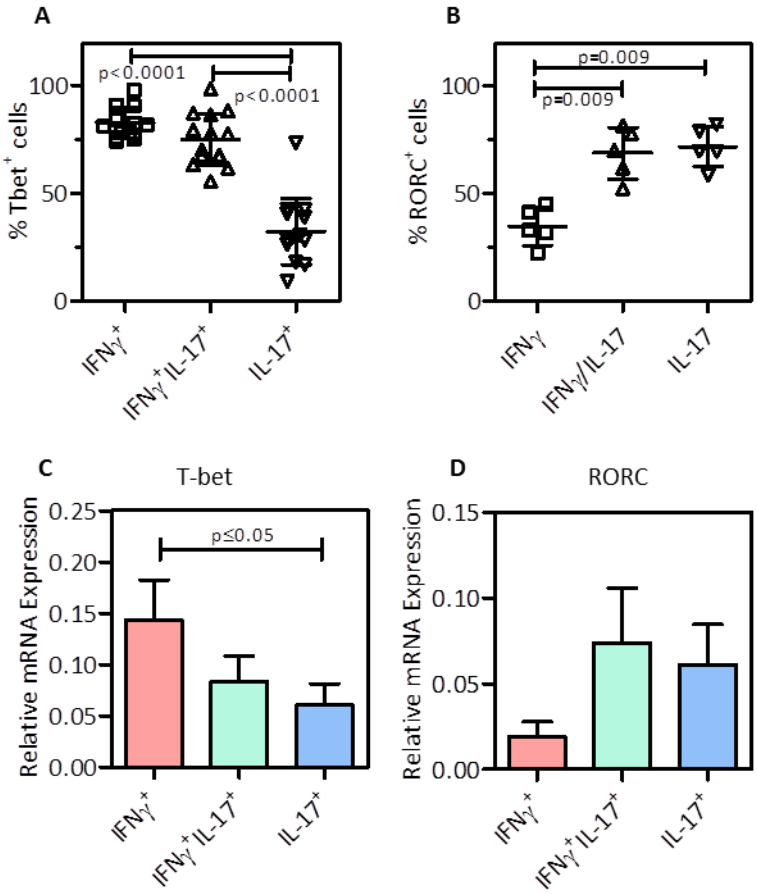

Figure 3.23. Cells that secrete both IFNγ and IL-17 protein express the transcription factors RORC and T-bet to a similar level to single secretors at mRNA level. (A) Flow cytometry analysis of the percentage of T-bet expressing cells *ex vivo* in IFNγ+, IFNγ+IL-17+, IL-17+ populations, gates based on matched isotype control. (n=11) **(B)** Flow cytometry analysis of percentage of RORC expressing CD4+ T cells in IFNγ+, IFNγ+IL-17+, IL-17+, population after 7 days culture in T_H17 polarising environment. (n=5) Cytokine secreting populations were isolated from CD4+CD25- bead purified cells using cytokine capture and a MoFlo cell sorter. qRT-PCR was used to assess mRNA expression of **(C)** T-bet (p=0.0156) and **(D)** RORC, relative to GAPDH. (n=4) Mean and standard error of the mean (SEM) represented by bars. A Kruskal-Wallis with a Dunns multiple comparison post test was used to identify significance.

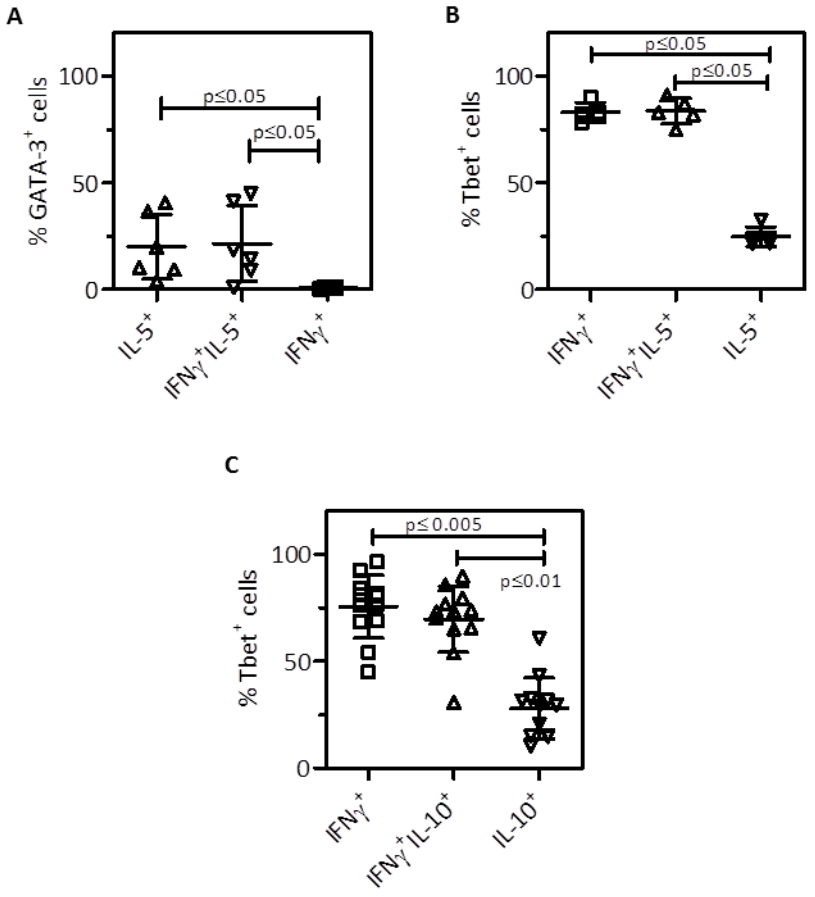

Figure 3.24. CD4+ memory T cells that secrete both IFNγ and IL-5 express the transcription factors GATA-3 and T-bet to a similar level to single secretors. The percentage of **(A)** GATA-3+ (p=0.0084, n=5) and **(B)** T-bet+ (p=0.009, n=4) expressing cells *ex vivo* in IFNγ+, IFNγ+IL-5+, IL-5+, populations. **(C)** Percentage of T-bet expressing cells in IFNγ+, IFNγ+IL-10+, IL-10+ populations, (p<0.0001, n=12). Mean and standard error of the mean (SEM) represented by bars. A Kruskal-Wallis with a Dunns multiple comparison post test was used to identify significance.

3.7 Discussion

In this chapter it has been demonstrated that IL-17 can be co-secreted with IFNγ, consistent with published data from several groups[1,144,145]. A reduction in the amount of IFNγ being produced by the IFNγ$^+$IL-17$^+$ cells compared to single IFNγ secreting cells has been identified in this work. The data within this chapter supports the literature [77,116] that these cells co-express both lineage defining transcription factors, RORC and T-bet, and are a stable phenotype. Dual secreting cells are not recently activated cells, suggesting that the co-expression of two cytokines such as IFNγ and IL-17 is not a transient phenotype. IFNγ$^+$IL-17$^+$ cells express IL-17A, IL-17F, IL-22 and IL-21 to a similar degree to T_H17 cells, but reduced IFNγ per cell, suggesting that these cells have a phenotype closer to a T_H17 cell than a T_H1. This concept is supported in the literature[1,144,200].

3.7.1 Similarities between T_H17 Cells and IFNγ$^+$IL-17$^+$ Cells

T_H17 cells have been implicated in several autoimmune conditions. Additionally, JIA[145] and Crohns disease[1] patients have CD4$^+$ T cells that co-express IFNγ and IL-17 at higher frequencies within affected tissues, compared to peripheral blood control cells. Within JIA joints the percentage of cells that expressed CD161, IFNγ and IL-17 correlate with parameters of disease activity suggesting these cells were involved in the disease process.

Within an inflammatory environment GM-CSF is thought to be a powerful inflammatory mediator released by T_H17 cells in both health and disease. It is thought to play a role in the disease pathogenesis in MS[173,201,202]. It has been shown in this work that three populations

of CD4$^+$ T cells, IFNγ$^+$, IFNγ$^+$IL-17$^+$ and IL-17$^+$, have the ability to secrete GM-CSF. However, a higher percentage of IFNγ$^+$IL-17$^+$ and IL-17$^+$ cells secreted GM-CSF compared to IFNγ$^+$ cells. This identifies a similarity in the two populations (IFNγ$^+$IL-17$^+$ and IL-17$^+$).

CD4$^+$ T cells in mice that co-secrete IFNγ and IL-17 have been shown to develop from T_H17 cells that had become responsive to environmental IL-12 (i.e. expressed IL-12R)[144]. In humans CD161$^+$IL-17$^+$IFNγ$^-$ cells cultured in synovial fluid (SF) from JIA patients acquired the ability to produce IFNγ. CD161$^+$IL-17$^+$IFNγ$^-$ cells cultured with SF from these patients, along with an antibody to neutralise IL-12, resulted in reduced expression of IFNγ. This suggests that in this pathogenic environment IL-12 has the ability to switch on IFNγ production in T_H17 cells, and this plasticity in T_H17 cells is a physiological phenomenon [145]. Conversely, T_H1 could not be converted to switch on IL-17 production in T_H17 polarising conditions. This information suggests that IFNγ$^+$IL-17$^+$ T cells may be more closely linked to T_H17 cells than T_H1 cells.

This work shows that IFNγ$^+$IL-17$^+$ cells can co-express other T_H17 related cytokines, IL-17F, IL-22 and IL-21 to a similar degree to IL-17$^+$ cells and to a greater extent than IFNγ$^+$ cells. Annunziato *et. al* [1] also showed other similarities between IFNγ$^+$IL-17$^+$ cells and T_H17 cells by demonstrating that human clones of IFNγ$^+$IL-17$^+$ cells maintained the ability to proliferate in the presence of T_{REG} suppression. IFNγ$^+$IL-17$^+$ could also aid B cell class switching and had low cytotoxic potential similar to T_H17 cells [1].

3.7.2 T-bet and RORC Expression in IFNγ+IL-17+ Cells

The results shown suggest that IFNγ+IL-17+ cells have a reduced ability to secrete IFNγ compared to single IFNγ+ cells, whereas they are able to secrete a similar level of IL-17 to single IL-17+ cells. Furthermore, there is a reduction in T-bet levels in IFNγ+IL-17+ cells compared to IFNγ+ cells, although this did not reach significance. There is a strong RORC signal within IFNγ+IL-17+ cells. If these cells had developed from T_H17 cells the RORC transcriptional profile would be well established.

Sustained stimulation of cells by IL-12 plays an important role in the development of T_H1 cells[203]. As mentioned IL-12 also plays a role in IFNγ induction in T_H17 cells, therefore the level of IL-12R expression could play a vital role in T-bet and IFNγ induction in these T_H17 cells. The literature shows that on IFNγ+IL-17+ clones there was a similar IL-12R expression to IL-17+ cells[1]. However, Lexberg *et al* [143] have revealed in mice that culturing cells makes T_H17 cells more likely to switch on IFNγ, so using clones may not give us a clear idea of the true expression of IL-12R *in vivo* on these cells. In equal measures, IL-23 is important for maintenance of a T_H17 phenotype so the balance between signals from IL-12 and IL-23 may play an important role in the phenotype of IFNγ+IL-17+ cells.

Transcriptional mechanisms have been identified in which the T_H1 phenotype can suppress a T_H17 profile. T-bet has been shown to suppress RORC activity by interaction with RUNX1. Blocking RUNX1 mediated transactivation of RORC. When RUNX1 was overexpressed in T-bet expressing T_H17 cells, then IL-17 expression was restored[137]. Conversely, there have been no mechanisms identified for T_H17 cells to suppress T-bet and the T_H1 profile. The

emergence of miRNAs offers a potential mechanism. miR155 has been identified as playing a role in T_H17 and T_H1 induction in mice[192], and miR-29ab1 has been shown to be involved in a negative feedback loop for T-bet and IFNγ expression[191]. These are potential candidates that may be controlling IFNγ and T-bet expression in IFNγ$^+$IL-17$^+$ cells.

3.7.3 Are Dual Cytokine Secreting Cells a Transitional Phenotype Induced by Recent Activation?

One hypothesis was that IFNγ$^+$IL-17$^+$ cells acquired the ability to secrete IFNγ after re-activation, and that the ability to co-express IFNγ was therefore a transient phenotype associated with TcR activation. To test this hypothesis the recent activation status of IFNγ$^+$IL-17$^+$ cells was analysed. The CD4$^+$ T cells that secrete IFNγ and IL-17 were not enriched in recently activated populations of CD69$^+$ or CD71$^+$. Furthermore, it was later shown Annunziato *et al.* that these cells have a stable phenotype[1], as the cells could be cultured and cloned. The fact that these cells up-regulate T-bet suggests that this phenotype is controlled at a transcriptional level. Identification of epigenetic alterations in T_H17 cells after IL-12 treatments suggest that IFNγ production by these cells may be a heritable, stable phenotype[204].

There did appear to be an enrichment of IL-5 and IFNγ$^+$IL-5$^+$ secreting cells in the CD69$^+$ and CD71$^+$CD45RO$^+$ population. In the individual donors this may be specific activation of T_H2 cells due to a recent allergic response or vaccination. This finding would need to be

investigated further in healthy and atopic subjects, and in a controlled study following vaccination and identification of antigen-specific cells.

When comparing the cytokine production in recently activated and non-activate CD4$^+$ T cells the ratios (**Figure 3.22)** were less than one, with the exception of IL-5. This result suggests there is a reduced cytokine production in the recently activated populations. This may mean that recently activated populations, CD69$^+$ or CD71$^+$, are refractory to PMA/ionomycin stimulation that normally induces production of IFNγ, IL-10 and IL-17. An alternative explanation may be that the cells are in a proliferative state and produce less inflammatory cytokines and more IL-2. CD69$^+$ and CD71$^+$ cells may have been proliferating at the time of stimulation, though the levels of IL-2 were not measured in this experiment.

If the cells are refractory to stimulation this may have consequences for the analysis of cytokine production using PMA/Ionomycin stimulation. There may be other T cell populations present that, although not still expressing CD69 or CD71, may be refractory to producing cytokines following a relatively recent activation.

A recent paper by Sallusto *et al.* stimulated antigen specific CD4$^+$ T_H17 cell clones with antigen and analysed their cytokine production over a number of days. This highlighted that when T cells were specific for an antigen from *C. albicans* the cells produced both IFNγ and IL-17A. However when the T cells were specific for an antigen from *S. aureus* they produced IL-17 but around the day 5 mark transiently down regulated expression and up regulated IL-10 production[147]. The CD69$^+$ or CD71$^+$ cells may be in this transient phase of cytokine down-regulation, which brings into question CD4$^+$ T cell plasticity. It will be

important in the future to identify if the dual cytokine production is a transient phenomenon or a committed lineage. It may also be possible that there cells that are committed to a dual phenotype (e.g. T_H1/T_H17) may at some point transiently down regulate one cytokine and appear to be a single cytokine secreting cell.

3.7.4 Cells that Secrete Both IFNγ and IL-5

In mice lymphocytic choriomeningitis virus specific T_H2 cells were stable when cultured in T_H1 polarising conditions, but they could be re-programmed to secrete IFNγ upon re-activation with LCMV. This phenotype was maintained over several months in culture. This work shows $CD4^+$ T cells that were $IFN\gamma^+IL\text{-}5^+$, and expressed T-bet and GATA-3 protein to a similar level as single $IFN\gamma^+$ and $IL\text{-}5^+$ cells respectively. Also, the amount of IFNγ and IL-5 in cells where they were co-expressed was significantly lower than single secretors. As I have shown that $IFN\gamma^+IL\text{-}5^+$ cells co-express T-bet and GATA-3, this might suggest a level of competition in the transcriptional profile of these cells. These two lineage defining cytokines have been shown to compete at certain genes, including the IFNG and IL4 gene[135].

3.7.5 $CD8^+$ T cell Cytokine Production

As expected the vast majority of CD8 T cells secreted IFNγ, apart from the small but detectable Tc17 cells. The Tc17, IL-17 secreting cells $CD8^+$ T cells, were within the $CD45RO^+$ population, showing Tc17 is not contained within the T_{EMRA} population. Within mice Tc17 expressed CCR6, which was needed for the recruitment to the lungs[205], as well as CXCR3.

The double secreting IFNγ+IL-17+ CD8+ T cells are more similar to Tc17 than conventional CD8+ T cells as neither population expressed lytic enzymes. Again, in mice there are similarities in the development of Tc17 and T_H17 cells, with STAT-3 activating cytokines being important in their induction, and RORγt being up-regulated [40,41].

3.7.6 Cytokines Not Co-expressed in CD4+ T cells

The co-expression of several cytokines was not detected. IL-5+IL-10+ cells and IL-10+IL-17+ or IL-5+IL-17+ cells could not be detected in this study. In humans T_H2 cells can, under T_H17 polarising conditions, be promoted to secrete IL-17. The IL-17+T_H2 cells in humans were isolated based on CRTH2 and CCR6, and expressed RORC. These cells were at an increased, but low, frequency in patients with atopic asthma[206]. T_H2 cells as well as secreting IL-5 also can co-secrete IL-4 and IL-13. Although the literature identified that the CCR6+CRTH2+ cell also can secrete IL-5 (using ELISA), the cells were identified based on the co-secretion using flow cytometry of IL-4 and IL-17. The overlap of IL-4, IL-5 and IL-13 within T_H2 cells has been shown to not always be homogeneous[207]. This suggests that if IL-4 had been stained for in this study there might have been some overlap with IL-17.

In naïve human T cells that have been primed with *Staphylococcus aureus* pulsed monocytes, a reciprocal production of IL-17 and IL-10 is seen. T_H17 cells are induced by the IL-1β, IL-6 and IL-23 produced by the *S.aureus* pulsed monocytes, however around 5 days after re-activation the cells down regulate IL-17 and RORC expression. Instead up-regulate IL-10 cytokine which is thought to be dependent on IL-2 activation of STAT-5 via CD25[147,208]. This

suggests that in an infectious environment there may be situations in which T_H17 cells can transiently co-express low levels of IL-10. This would support the flow data in **Figure 3.15 A** that shows these cells are not detectable in a healthy individual.

3.7.7 T_H17 Cultures

Within the T_H17 polarising cultures that were used there was a significant amount of variability in the percentage of IL-17 secretion obtained. Each experiment used different donors and was done on different days, though the culture conditions were kept the same. The activation strength via the TcR can make a difference to T_H17 induction. Using a low stimulating environment, such as low numbers of CD3/CD28 beads, leads to significantly more T_H17 induction. High activation leads to induction of FoxP3, transforming growth factor β–latency-associated peptide and inability of NAFTc1 (nuclear factor of activated T cells 1) to bind to the IL-17 promoter[101]. Within these experiments the amount of stimulation occurring via CD3/CD28 antibodies was not investigated.

Furthermore, by using total $CD4^+$ T cells it was not clear if T_H17 cells were being induced or if there was an expansion of a pre-existing T_H17 population. If within the cultures a pre-existing population of T_H17 cells was being expanded, and there was a difference in the starting population of T_H17 cells of each donor, this could account for some of the differences in percentage of T_H17 cells. Several groups have used antigen pulsed APC to induce T_H17 from naïve T cells which also would increase the yield of IL-17 producing cells[147].

T_{REG} cells have a reduced suppressive effect on T_H17 cells [1,209]. Interestingly, within the cultures when T_{REG} were titrated in at different ratios with effector cells, there was a relationship between IFNγ and T_H17 production. With more T_{REG} added there were less IFNγ secreting cells, and more cells secreting IL-17. Although this was only repeated once this supports T_{REG} ($CD25^+$) being unable to suppress T_H17 cells. Additionally, this could be due to the suppressive effect of T_{REG} on the T_H1 cell proliferation, resulting in less T_H1 cells, and less IFNγ to suppress T_H17 differentiation.

In mice, due to the high level of TGF-β produced, T_{REG} can induce IL-17 production in $CD25^-$ T cells in the presence of IL-6[210]. Furthermore, the same T_{REG} cultured in IL-6 rich environment are induced to secrete IL-17 themselves[211]. Within a human system in the presence of IL-2, IL-15 and IL-1β T_{REG} cells can start to secrete IL-17 and acquire CCR6 expression[212]. The cultures shown in **Figure 3.8** were not stained for FoxP3 or CCR6 so it cannot be determined how much the T_{REG} added to the $IL\text{-}17^+$ cells.

3.7.8 Cytokine Capture Purity

The cytokine capture protocol allows isolation of pure cytokine secreting cells, which have been used within the literature by several groups[143,213,214]. Using PMA and ionomycin to stimulate these cells, I was able to stimulate the whole population. However, the percentage of cells that were captured did not equate to the intracellular stained cells. This means that there are some cells that have either been missed or mis-labelled. The only population that might be contaminated to any degree would be the IL-17 cells. If $IFN\gamma^+IL\text{-}17^+$

cells were only labelled with IL-17, then this will contaminate the IL-17 population to a larger degree than if only IFNγ is picked up on the cell. The data for IFNγ gene expression levels gave only a very small signal in the single IL-17 population and the error bars were small. This result suggests only a small level of contamination of IFNγ expressing cells in the IL-17 population.

Several papers that use cytokine capture to isolate IL-17 secreting cells may suffer from this contamination due to inappropriate stimulation. For example, when using cytokine capture Unutmaz *et al.* stimulated their cells with anti-CD3 and anti-CD28 antibodies to isolate CCR6$^+$IL-17$^+$ and CCR6$^+$IL-17$^-$ cells, only picking up a small percentage of IL-17 secreting cells. It is not possible to completely rule out that there was contamination of the CCR6$^+$IL-17$^-$ populations with T_H17 cells. They go on to conclude that γ-chain cytokines can induce IL-17 expression in the CCR6$^+$IL-17$^-$ population. They may just be expanding an already existing population of IL-17 secreting cells that were not detected by the cytokine capture method.

In summary, the studies in this chapter have documented a stable population of cells that co-express IFNγ and IL-17 that retain features more similar to T_H17 cells. These cells have a strong RORC expression, and this T_H17 profile may be playing a role in maintaining a lower IFNγ production within the cell.

CHAPTER 4

PHENOTYPIC AND FUNCTIONAL FEATURES OF CCR6^{+}IFNγ^{+} CELLS

4.1 Introduction

A fate-mapping model in mice has shown that cells that initially secreted IL-17 became single IFNγ secreting cells. In humans there is no direct evidence this can happen. However there is a population of CD161^{+}T$_H$1 cells that express RORC. This information led to the hypothesis that these CD161^{+}T$_H$1 cells are differentiated from T$_H$17 cells[105,213].

Both CD161 and CCR6 can be used as a marker for T$_H$17 cells. CCR6 functions as a chemokine receptor, giving the T cell the potential to migrate into tissues expressing CCL20. CD161 is expressed on NK cells and the interaction of CD161 and its ligand LLT1 inhibits NK cell functions. The function of CD161 on T cells is less clear though it is thought to play a role in their co-stimulation[7].

CCR6 plays an important role in the initial wave of migration of inflammatory T cells into the CNS in multiple sclerosis. This led to the question of whether in multiple sclerosis there is a populations of CCR6^{+}T$_H$1 cells and if they also had characteristics of T$_H$17 cells

The aims of this chapter are:

- To investigate the relationship between CCR6 and CD161 and IFNγ in healthy controls.

- To characterise the phenotype of CCR6$^+$T$_H$1 cells in comparison to classical T$_H$1 and T$_H$17 cells.
- To investigate if CCR6$^+$T$_H$1 cells are present in the blood of and CSF of MS patients.

4.2 CCR6 and CD161 Expression in CD4$^+$ Memory T cells

Flow cytometry was used on *ex vivo* PBMC to investigate the relationship of the T$_H$17 associated markers, CCR6 and CD161, and the effector cytokines IFNγ and IL-17. CCR6, the chemokine receptor associated with T$_H$17 cells, is often used in cultures to enrich for T$_H$17 cells. CD161 is considered a T$_H$17 marker as all CD4$^+$CD161$^+$ cells from umbilical cord blood (UCB) can be converted into IL-17$^+$ cells[85]. The CCR6 staining needed to be optimised as upon stimulation with PMA and Ionomycin the CCR6 expression was down regulated. It was noted that if the cells were pre-stained for CCR6 antibody both before and after stimulation (both at room temperature), the down regulation of CCR6 was not observed (**Figure 4.1 A**).

The vast majority of IL-17A secreting memory CD4$^+$ T cells expressed CCR6 **(Figure 4.1 B).** There was a high expression level of CCR6 on these cells **(Figure 4.1 C).** Approximately 25% of IFNγ secreting memory CD4$^+$ T cells expressed CCR6. It was noticeable that the IFNγ MFI on CCR6$^+$ cells appeared to be reduced (MFI of IFNγ in CCR6$^-$= 3.54 CCR6$^+$= 3.18). The CCR6 expression on IFNγ$^+$ cells was reduced compared to the IL-17$^+$ and IFNγ$^+$IL-17$^+$ cells (Median CCR6 MFI for: IFNγ$^+$=4.69, IL-17$^+$=14.51, IFNγ$^+$IL-17$^+$=10.95) although this was not a significant difference ($p>0.05$). Cells that expressed IFNγ and IL-17 together expressed CCR6 to a similar MFI to single IL-17 expressing cells (**Figure 4.1 C)**.

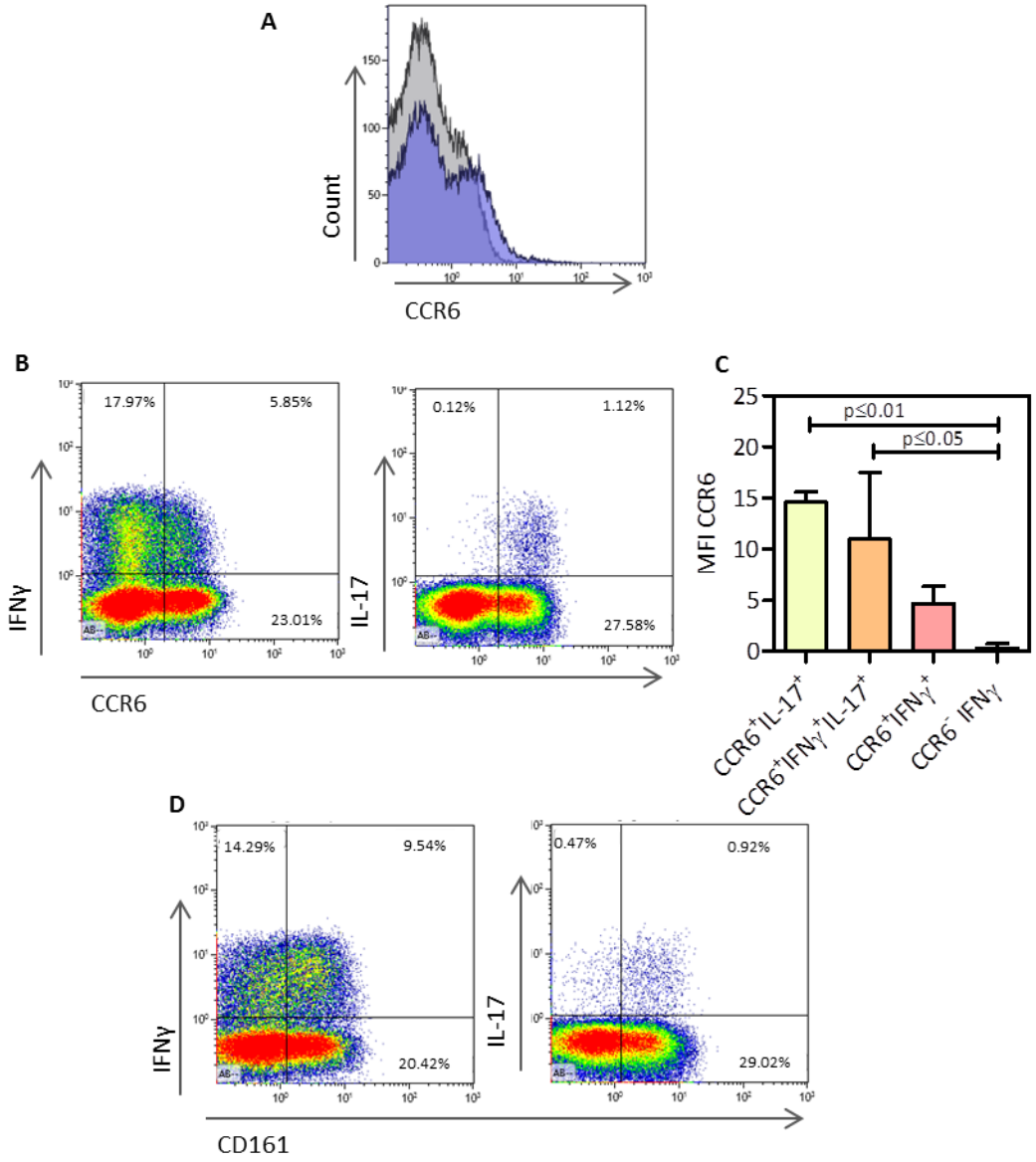

Figure 4.1. Relationship between CD161, CCR6 and IFNγ and IL-17 in CD4^{+} T cells. Total PBMC were stimulated with PMA and Ionomycin for 3 hours in the presence of Brefeldin A. Cells were stained for surface markers and intracellular cytokine expression and analysed by flow cytometry. **(A)** Optimisation of CCR6 staining. A comparison of PBMC pre-stained for CCR6 before stimulation (blue) and cells stained only after stimulation (grey), gated on CD4^{+}CD45RO^{+} **(B)** Representative flow plots gated on CD4^{+}CD45RO^{+} T cells, analysing expression of CCR6 on IFNγ and IL-17 secreting cells (n=8). **(C)** CCR6 MFI on cytokine secreting CD4^{+}CD45RO^{+} T cells (n=5-p<0.0001) **(D)** CD161 expression on IFNγ and IL-17 expressing cells (n=8). Values represent percentage of cells in the gate, negative gates were set based on a un-stimulated, stained control. To test significance a Friedman test with Dunn's Multiple Comparison Test was undertaken.

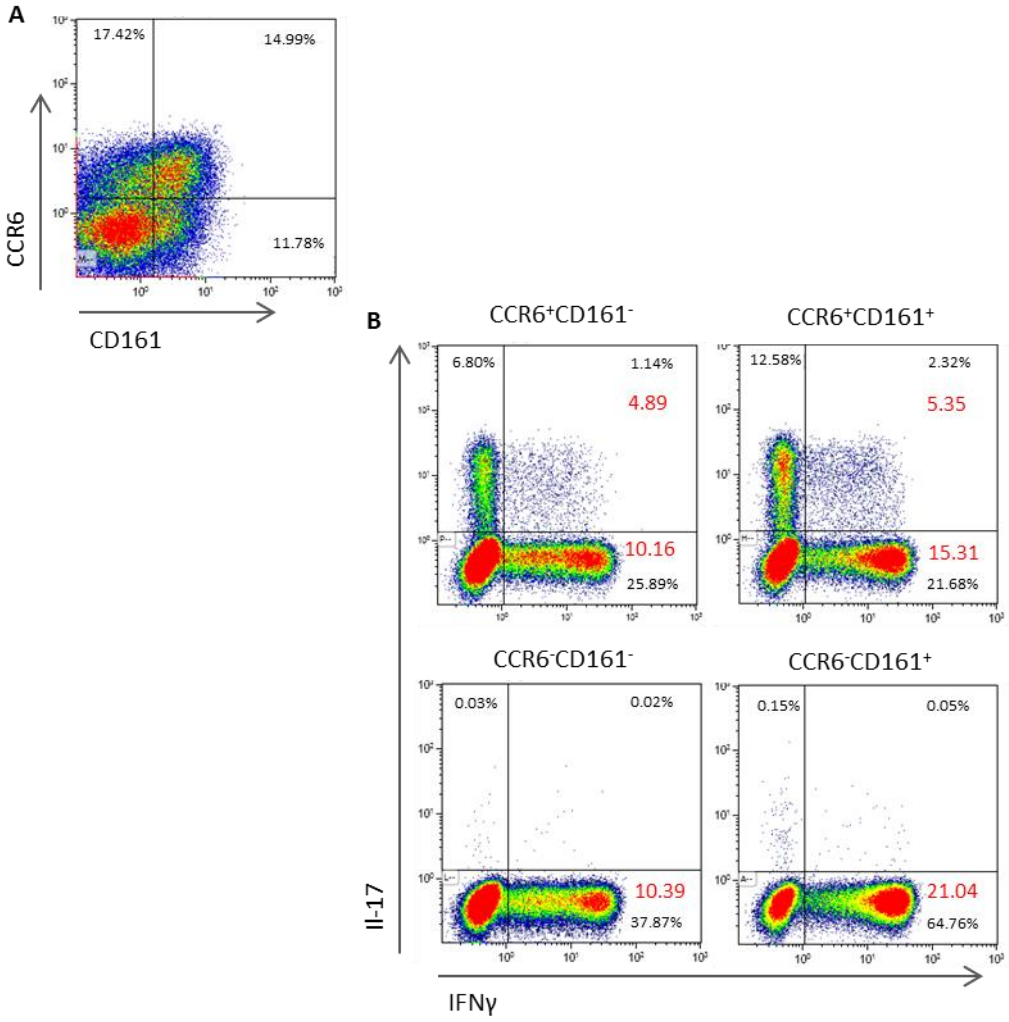

Figure 4.2. IFNγ and IL-17 expression by CCR6 and CD161 expressing populations. Total PBMC were stained for CD4, CD45RO along with CCR6 and CD161. Gated on CD4+CD45RO+ cells the populations shown were isolated using MoFlo cell sorter. Each population was stimulated with PMA and Ionomycin for 3 hours in the presence of Brefeldin A. Cells were stained for intracellular IFNγ and IL-17 expression and then analysed by flow cytometry. **(A)** Representative flow plot gated on CD4+CD45RO+ T cells showing the expression of CCR6 and CD161 (n=8). **(B)** Analysis of IFNγ and IL-17 expression in 4 isolated populations based on CCR6 and CD161 expression (labelled). Values in black show the percentage of cells within the gate, values in red are the IFNγ MFI for population within the gate. Negative gates were set based on a un-stimulated, stained control cells. (n=1)

Interestingly, when using this antibody and staining method, not all IL-17$^+$ expressing CD4$^+$ T cells expressed CD161. Approximately 35% (median % CD161$^-$IL-17$^+$=35.44%) of the IL-17$^+$ cells did not express CD161. There was a large percentage of IFNγ$^+$ cells that expressed CD161 (median=31.67%, range=7.28%-38.81%). The CD161$^+$IFNγ$^+$ cells expressed a higher amount of IFNγ per-cell (IFNγ MFI= 4.54) than the CD161$^-$ cells (MFI=2.90) **(Figure 4.1 D)**.

To identify the crossover of CCR6 and CD161 in the contribution of IL-17 secreting cells, *ex vivo* PBMC were stained for CCR6 and CD161 as well as CD4 and CD45RO. For one donor of CD4$^+$CD45RO$^+$ cells the four different populations based on CCR6 and CD161 expression were isolated using the MoFlo cell sorter. The isolated cells were stimulated and stained for the expression of IFNγ and IL-17 (**Figure 4.2**).

The results from this single experiment showed (**Figure 4.2 B**) that the CCR6$^+$CD161$^+$ and CCR6$^+$CD161$^-$ populations were enriched for IL-17$^+$ cells with respectively 14.9% and 7.95% of each population expressing IL-17. Interestingly, the CCR6$^-$CD161$^+$ population did not express a substantial number of IL-17 secreting cells. There were no IL-17 cells in the CD161$^-$CCR6$^-$ population. There were IFNγ secreting cells in all 4 populations. The largest enrichment of IFNγ cells was in the proportion of CCR6$^-$CD161$^+$ with 64.76% of the cells secreting only IFNγ. The IFNγ MFI for the CD161$^+$CCR6$^-$ population was a great deal higher than the IFNγ MFI for both the CCR6$^+$ populations and the CCR6$^-$CD161$^-$ population. There was an enrichment of IFNγ$^+$IL-17$^+$ cells in both the CCR6$^+$CD161$^-$ and CCR6$^+$CD161$^+$ populations.

It has been shown in the literature that CD161$^+$IFNγ$^+$ cells express RORC at the transcriptional level[105,213]. After identifying that all the IL-17 cells were within the CCR6

population and that there was a population of CD161$^+$CCR6$^-$ cells that only expressed IFNγ, it was decided to reconfirm this finding. CD161$^+$ cells were isolated based on IFNγ and IL-17 using cytokine capture. The gene expression of IFNγ, IL-17, T-bet and RORC were analysed in each population, relative to GAPDH. **(Figure 4.3 A-D)**.

The highest expression of the IFNγ gene was in the CD161$^+$IFNγ$^+$ cells, with a reduced but substantial expression in the CD161$^-$IFNγ$^+$ cells. Similar to results in Chapter 1 (**Figure 3.19 B**), the dual CD161$^+$IFNγ$^+$IL-17$^+$ cells expressed lower levels of IFNγ and there was no detectable level of IFNγ gene expression in the CD161$^+$IL-17$^+$ cells **(Figure 4.3 A)**. There was a detectable level of IL-17A gene expression in the CD161$^+$IL-17$^+$ and CD161$^+$IFNγ$^+$IL-17$^+$ populations **(Figure 4.3 B)**. There was no detectable IL-17A gene expression in the CD161$^+$IFNγ$^+$ and CD161$^-$IFNγ$^+$ cells, confirming expression detected at the level of protein.

The gene expression levels for T-bet were intriguing due to the similarities in the CD161$^+$IFNγ$^+$, CD161$^+$IFNγ$^+$IL-17$^+$ and CD161$^+$IL-17$^+$ cells. CD161$^-$IFNγ$^+$ cells expressed the highest levels of T-bet **(Figure 4.3 C)**. There was considerable RORC expression in the CD161$^+$IL-17$^+$ and CD161$^+$IFNγ$^+$IL-17$^+$ cells. There was equally low level of RORC in the CD161$^+$IFNγ$^+$ and CD161$^-$IFNγ$^+$ cells **(Figure 4.3 D).** These results do not agree with published data.

This data lead to the conclusion that CD161 was not specific enough in these experiments to identify IL-17 secreting cells and cells that expressed a 'T_H17' gene expression profile.

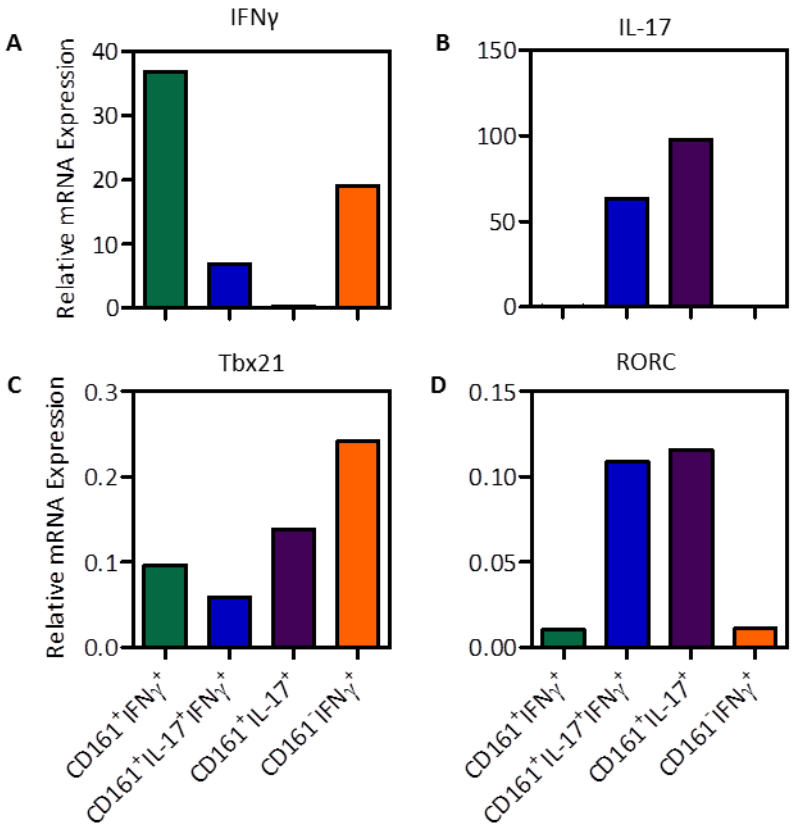

Figure 4.3. Gene expression of IFNγ, IL-17, T-bet and RORC in CD161^{+}IFNγ^{+} cells compared to CD161^{-}IFNγ^{+} cells and IL-17 secreting populations. CD161 expressing IFNγ and IL-17 secreting populations were isolated from CD4^{+}CD25^{-} bead purified cells using cytokine capture and a MoFlo cell sorter. qRT-PCR was used to assess the mRNA expression of **(A)** IFNγ, **(B)** IL-17, **(C)** T-bet and **(D)** RORC relative to GAPDH (n=1).

4.3 CCR6$^+$T$_H$1 Cells Express the Genes RORC, IL-23R, IL4I1 and IL-12Rβ2

A similar process of cytokine capture and cell sorting was undertaken using CCR6 to identify if it made any difference which marker was used to identify T_H17 cells. The cells were stained for CCR6 and cytokine capture was used to identify the IFNγ and IL-17 secreting cells **(Figure 4.4 A)**. The MoFlo cell sorter was used to isolate the cells which were then analysed for the gene expression of IFNγ, IL-17, RORC and T-bet, relative to GAPDH. There was a detectable level of IFNγ in all three IFNγ$^+$ populations, and although not statistically significant there was a reduction in the IFNγ gene expression in CCR6$^+$IFNγ$^+$IL-17$^+$, compared to CCR6$^+$IFNγ$^+$ and CCR6$^+$IFNγ$^-$ cells. This was comparable to results in the Chapter 1 (**Figure 3.19 B**).

In Chapter 1 no difference was identified in IL-17 mRNA levels between IL-17$^+$ and IFNγ$^+$IL-17$^+$ cells. The data in this chapter however identified a reduction in the level of mRNA for IL-17 in cells that co-expressed CCR6$^+$IFNγ$^+$IL-17$^+$ compared to single CCR6$^+$IL-17$^+$ cells (**Figure 3.19 B**). This reduction was not statistically significant. There was detectable expression of T-bet in all four populations. The T-bet mRNA expression was not significantly different in any population, though the highest level was in the CCR6$^+$IFNγ$^+$IL-17$^+$ and CCR6$^+$IFNγ$^+$ cells, and there was a reduced level in CCR6$^-$IFNγ$^+$ cells.

In **Figure 4.4 D** there was a slight increase in the expression level of T-bet in CCR6$^+$IFNγ$^+$ compared to CCR6$^-$IFNγ$^+$ cells. From *ex vivo* PBMC the protein expression of T-bet in CCR6$^+$ and CCR6$^-$ cells was analysed. **Figure 4.5** demonstrates that there was no significant difference in the T-bet expression at the protein level between CCR6$^+$IFNγ$^+$ and CCR6$^-$IFNγ$^+$.

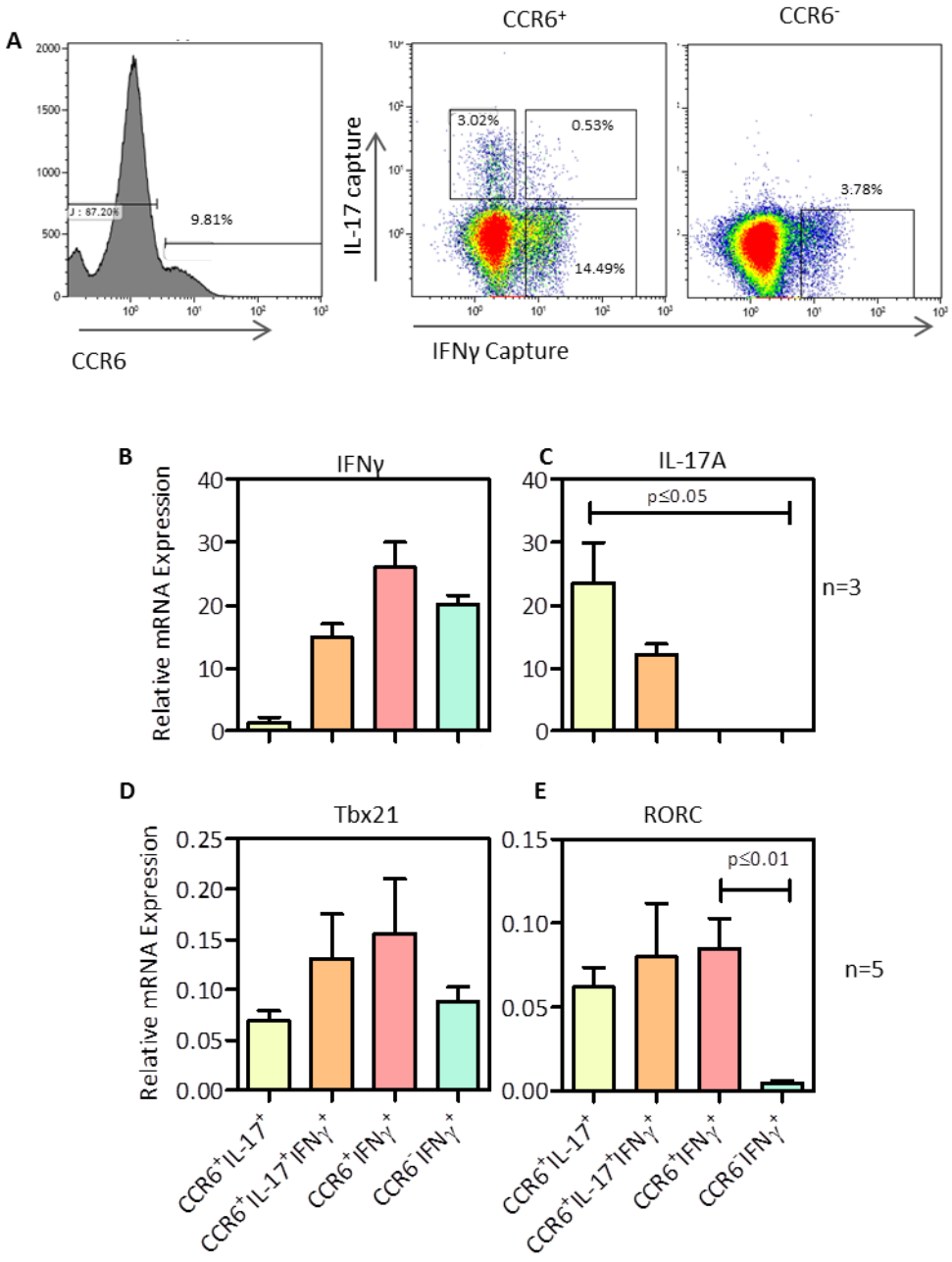

Figure 4.4. Gene expression of IFNγ, IL-17, T-bet and RORC in CCR6⁺IFNγ⁺ cells compared to CCR6⁻IFNγ⁺ cells and IL-17 secreting populations. CCR6 expressing IFNγ and IL-17 secreting populations were isolated from CD4⁺CD25⁻ bead purified cells using cytokine capture and a MoFlo cell sorter. **(A)** Gating strategy on the MoFlo cell sorter (CD45RO⁺ gate not shown) to isolate CCR6⁺ and CCR6⁻ populations based on IFNγ and IL-17 cytokine capture staining. qRT-PCR was used to assess the mRNA expression of **(B)** IFNγ (p=0.0174, n=3), **(C)** IL-17 (p=0.0017, n=3), **(D)** T-bet (n=5) and **(E)** RORC (p=0.0067, n=5) relative to GAPDH. To test significance a Friedman test with Dunn's Multiple Comparison Test was undertaken. Mean and standard error of the mean (SEM) are shown.

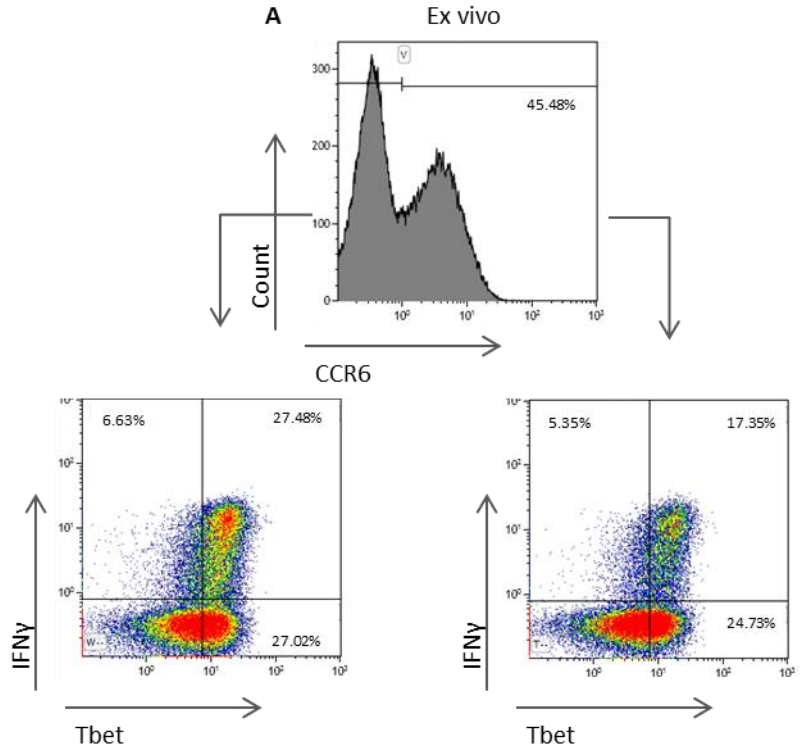

Figure 4.5. T-bet protein expression in CCR6⁺IFNγ⁺ cells compared to CCR6⁻IFNγ⁺ cells. Total PBMC were stimulated with PMA and Ionomycin for 3 hours in the presence of Brefeldin A. Cells were stained for surface markers and intracellular cytokine expression and analysed by flow cytometry. **(A)** Analysis of IFNγ and Tbet expression gated on CD4⁺CD45RO⁺ cells in the CCR6⁺ or CCR6⁻ cells. Values are percentage of cells in the gate, n=1.

The principal difference when looking at the $CCR6^+IFN\gamma^+$ expression data, compared to the $CD161^+IFN\gamma^+$ expression data, was that RORC was detectable in the $CCR6^+IFN\gamma^+$ population. The RORC expression level in $CCR6^+IFN\gamma^+$ cells was detectable to a similar level to $CCR6^+IFN\gamma^+IL\text{-}17^+$ and $CCR6^+IL\text{-}17^+$ cells. In addition there was a significant difference in RORC expression in the $CCR6^+IFN\gamma^+$ cells compared to the $CCD6^-IFN\gamma^+$ cells ($p=0.0067$). More gene expression was undertaken to identify if the $CCR6^+IFN\gamma^+$ cells expressed any other characteristics of T_H17 cells.

When using cytokine capture only a small number of cells can be isolated from large volumes of blood. The use of qRT-PCR would only have allowed investigation of a few T_H17 related genes. A novel method of Multiplex Gene Expression Assay using Luminex technology was tried. This method measured direct RNA quantity so no reverse transcription was required. It also reduced the loss of RNA material through inefficient conversion to cDNA. The process used luminex beads with a specific capture probe for the RNA sequence of interest. Once the RNA was captured the sequence was labelled and there was a series of signal amplification steps (using streptavidin phycoerythrin - SAPE) to allow detection of the quantity of RNA for the gene expressed. Each bead has a second distinct fluorochrome signature to allow detection of the different genes of interest. As all the beads can be put in one well of an analysis plate less material was needed. In principle up to eighty target genes can measure per well.

Eight genes of interest were initially chosen to test the luminex technology; RORC, T-bet, IL-17A, IFNγ, IL-17F, RUNX1, IL-12Rβ2 and IL-23R. RUNX1 was chosen as it is known to interact

with RORC to aid IL-17 expression. T-bet is known to bind RUNX1 to suppress RORC activation[137]. Finally, as IL-12 and IL-23 responsiveness is important for T_H1 and T_H17 induction respectively, IL-12Rβ2 and IL-23R were chosen. IL-12Rβ2 was chosen as this subunit of IL-12R is up regulated by IFNγ, while IL-12R1 is constitutively expressed by T cells.

Figure 4.6 shows the experimental triplicates of the gene of interest relative to a reference gene (delta MFI of the SAPE signal). Although all the genes gave a signal, there was a large variation in the triplicates resulting in large error bars. This was especially noticeable for the smaller CCR6$^+$IL-17$^+$ and CCR6$^+$IFNγ$^+$IL-17$^+$ populations. There were some similar patterns for T-bet, RORC, IL-17A and IFNγ compared to previous qRT-PCR data. IL-17A and IL-17F expression was found in both CCR6$^+$IL-17$^+$ and CCR6$^+$IFNγ$^+$IL-17$^+$ populations as expected (**Figure 4.6 A, B)** as was IFNγ (**Figure 4.6 C**). RORC was detectable in CCR6$^+$IFNγ$^+$ cells, alongside CCR6$^+$IL-17$^+$ and CCR6$^+$IFNγ$^+$IL-17$^+$ populations (**Figure 4.6 E**). Using this method RUNX1 appeared to be expressed in all subsets (**Figure 4.6 F**). The error bars for IL-12Rβ2 and IL-23R were too large to make any firm conclusions about their expression. Overall the method was not consistent. Using a different control gene, HPRT, gave very different results (not shown). This suggests a level of inconsistency in the experimental results. Several genes that were probably important for T_H17 and T_H1 profiling were identified and qRT-PCR was used again to identify any difference in the CCR6 expressing populations.

IL-12Rβ2, IL-23R, IL-1R1 (IL-1 receptor, type 1) and IL4I1 (interleukin 4 induced 1) were identified in the literature as differentially expressed in T_H1 cells compared to T_H17 cells[105]. IL-1R1 has been shown to be related to the ability of a CD4$^+$ T cell to secrete IL-17[103]. IL4I1 is

a phenylalanine oxidase that is thought to be only expressed on T_H17 cells and reduces the cells ability to proliferate[104]. The expression of these genes in CCR6$^+$ populations was investigated using qRT-PCR relative to GAPDH expression. IL-12Rβ2 was expressed to the highest degree in the CCR6$^+$IFNγ$^+$ cells. There was low expression in the other three subsets, with the lowest expression in the CCR6$^+$IFNγ$^+$IL-17$^+$ subset **(Figure 4.7 A)**. IL-23R expression was only detectible in CCR6$^+$IL-17$^+$ cells and a low but detectable expression in CCR6$^+$IFNγ$^+$ cells **(Figure 4.7 B)**. IL-1R1 was expressed in both CCR6$^+$IL-17$^+$ and CCR6$^+$IFNγ$^+$IL-17$^+$ subsets, although on the CCR6$^+$IFNγ$^+$IL-17$^+$ cells the expression was lower **(Figure 4.7 C)**. IL4I1 was expressed in all three CCR6$^+$ subsets, although with lower expression within the CCR6$^+$IFNγ$^+$ subset **(Figure 4.7 D)**.

4.5 T_H17 Related Cytokine Expression in CCR6$^+$$T_H1$ Cells

IL-17F, IL-22 and IL-21 are all T_H17 related cytokines and are expressed at a higher frequency in cells that expressed IL-17A. To identify if any of these cytokines were more highly expressed in the CCR6$^+$IFNγ$^+$ populations, PBMC were stimulated and stained for these cytokines, as well as IFNγ, IL-17 and CCR6. Approximately 30% (CCR6$^+$ IFNγ$^+$IL-17$^+$ median=28.57%, CCR6$^+$IL-17$^+$ median=33.05) of the CCR6$^+$IL-17$^+$ and CCR6$^+$IFNγ$^+$IL-17$^+$ co-expressed IL-17F, whereas there was very low expression of IL-17F by CCR6$^+$IFNγ$^+$ and CCR6$^-$ IFNγ$^+$ cells **(Figure 4.8 A)**. This was also the case with IL-22 (CCR6$^+$IFNγ$^+$IL-17$^+$ median=32.46%, CCR6$^+$IL-17$^+$ median=17.20%) **(Figure 4.8 B)** and IL-21(CCR6$^+$IFNγ$^+$IL-17$^+$ median=30.05%, CCR6$^+$IL-17$^+$=16.92% - **Figure 4.8 C**).

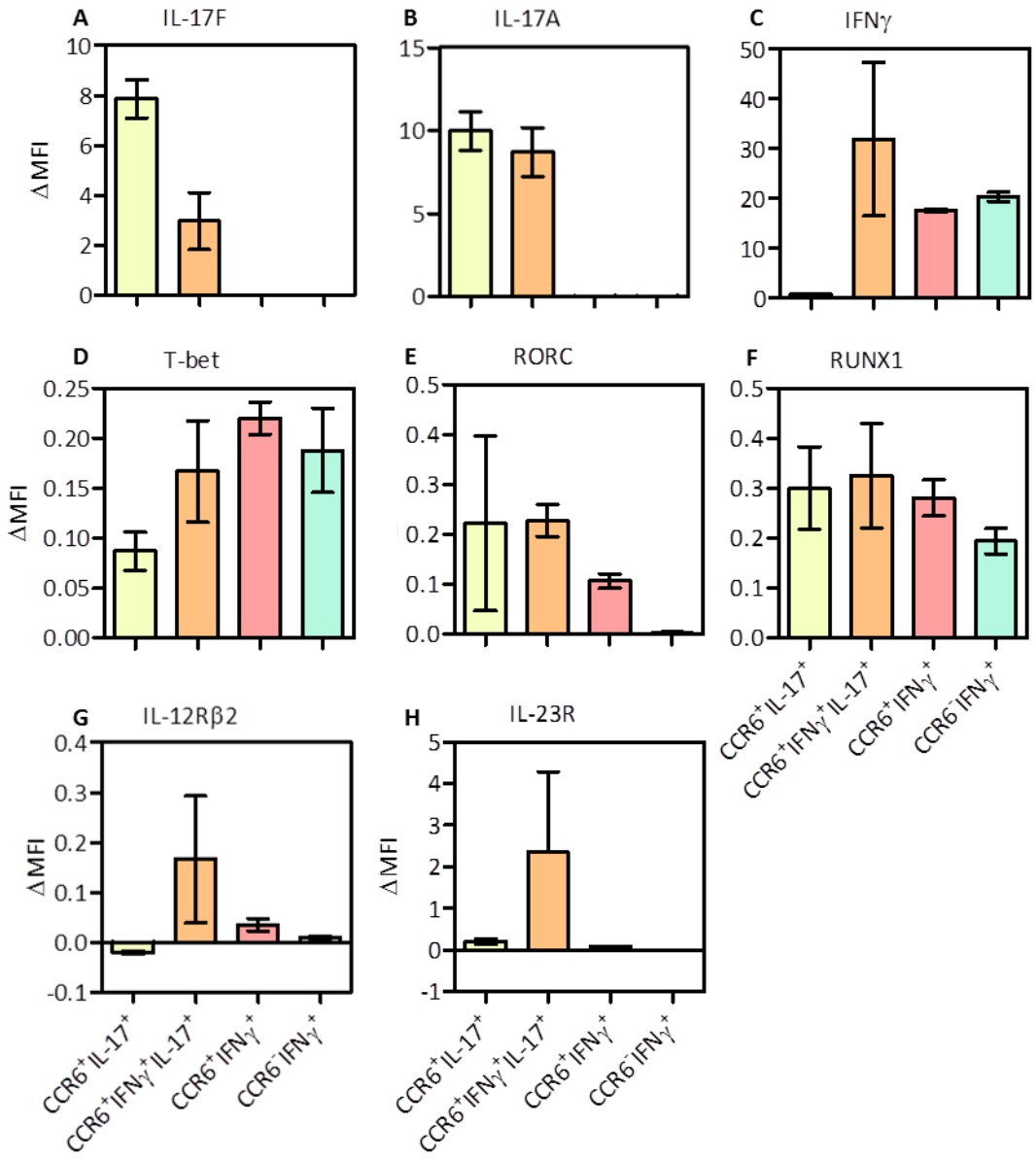

Figure 4.6. Analysis of T_H17 related gene in CCR6 expressing populations using QuantiGene Plex 2.0 Multiplex Assay. Memory (CD45RO$^+$) cells expressing CCR6, IFNγ and IL-17 were isolated from CD4$^+$CD25$^-$ bead purified cells using cytokine capture and a MoFlo cell sorter. The isolated populations were then analysed for the quantity of RNA for the genes of interest, using QuantiGene Plex 2.0 Multiplex Assay and Luminex technology. The SAPE signal for the gene of interest was made relative to signal of GAPDH within the sample (ΔMFI). Genes analysed were **(A)** IL-17A, **(B)** IL-17F, **(C)** IFNγ, **(D)** T-bet, **(E)** RORC, **(F)** RUNX1, **(G)** IL-12Rβ2, **(H)** IL-23R, based on triplicates of one experiment. Mean and standard error of the mean (SEM) shown.

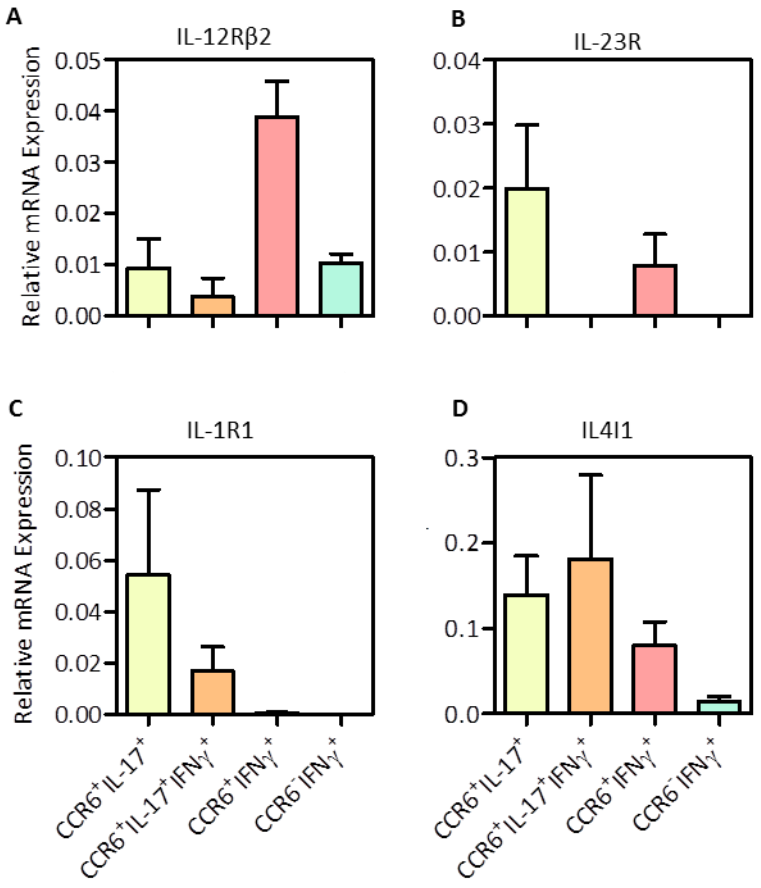

Figure 4.7. Gene expression of IL-12Rβ2, IL-23R, IL-1R1 and IL4I1 in CCR6^{+}IFNγ^{+} cells compared to CCR6^{-}IFNγ^{+} cells and IL-17 secreting populations. Memory (CD45RO^{+}) cells expressing CCR6, IFNγ and IL-17 were isolated from CD4^{+}CD25^{-} bead purified cells using cytokine capture and a MoFlo cell sorter. qRT-PCR was used to assess the mRNA expression of **(B)** IL-12Rβ2, **(C)** IL-23R, **(D)** IL-1R1 and **(E)** IL4I1 expression relative to GAPDH.. To test significance a Friedman test with Dunn's Multiple Comparison Test was undertaken. (n=3)

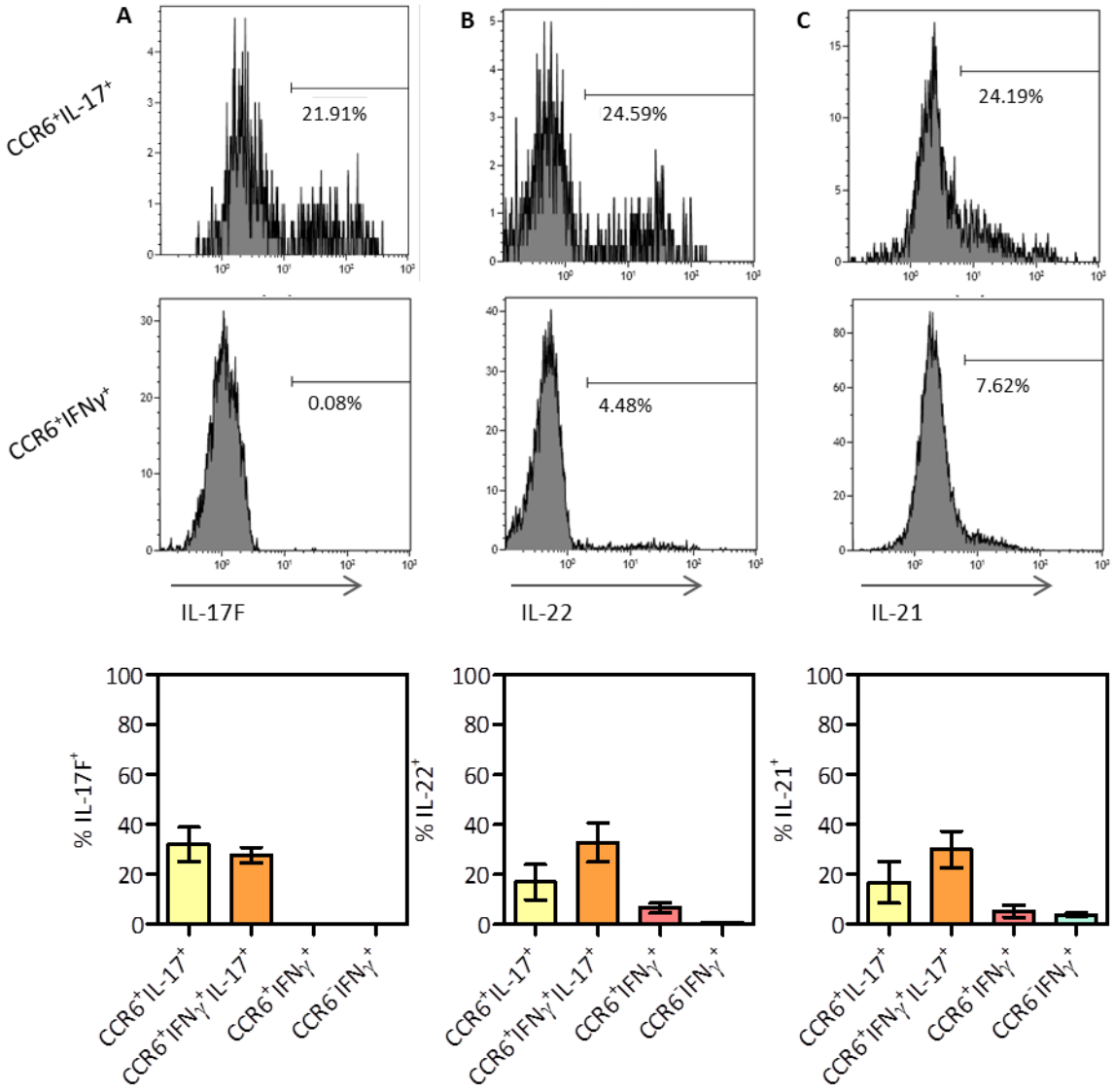

Figure 4.8. Expression of IL-17F, IL-22 and IL-21 in CCR6⁺IFNγ⁺ cells compared to CCR6⁻IFNγ⁺ cells and IL-17 secreting populations. Total PBMC were stimulated with PMA and Ionomycin for 3 hours in the presence of Brefeldin A. Cells were stained for surface markers and intracellular cytokine expression and analysed by flow cytometry. **(A)** Representative flow plots gated on CD4⁺CD45RO⁺ T cells and either CCR6⁺IFNγ⁺ or CCR6⁺IL-17⁺ cells. Values represent percentage of cells in the gate, negative gates were set based on a un-stimulated, stained control cells. The expression of **(A)** IL-17F, **(B)** IL-22 and **(C)** IL-21 from 4 independent donor. Mean and standard error of the mean (SEM) shown on graph.

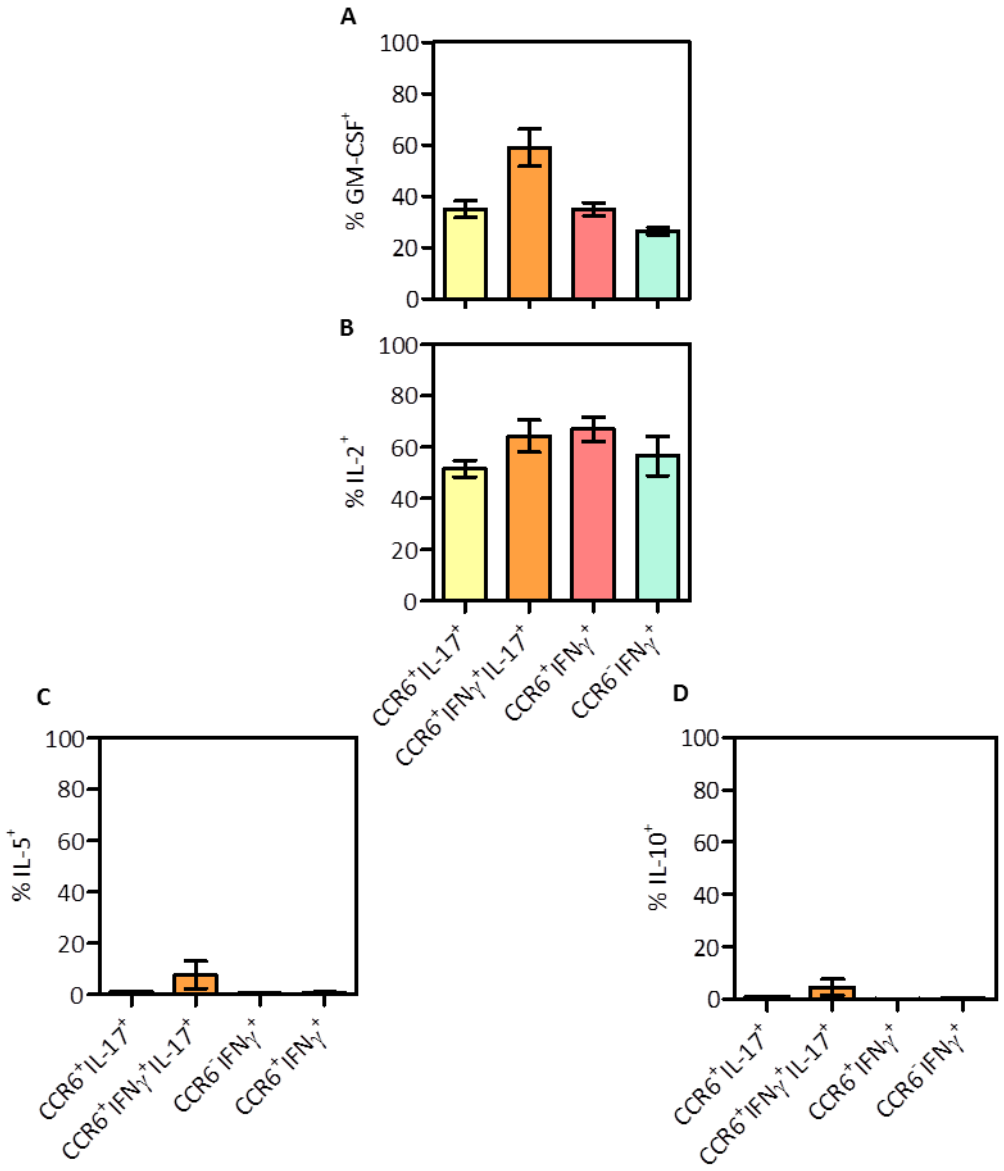

Figure 4.9. Expression of GM-CSF, IL-2, IL-5 and IL-10 in CCR6⁺IFNγ⁺ cells compared to CCR6⁻IFNγ⁺ cells and IL-17 secreting populations. Total PBMC were stimulated with PMA and Ionomycin for 3 hours in the presence of Brefeldin A. Cells were stained for surface markers and intracellular cytokine expression and analysed by flow cytometry. The percentage of CD4⁺CD45RO⁺ cells expressing **(A)** GM-CSF, **(B)** IL-2, **(C)** IL-5 and **(D)** IL-10 in the difference CCR6 expressing populations from 4 independent donor. Mean and standard error of the mean (SEM) shown.

GM-CSF, IL-2, IL-5 and IL-10 expression was also analysed **(Figure 4.9)** to identify if there were any other similarities or differences in the other cytokines these populations secreted. GM-CSF was expressed across the board at a similar percentage in three of the populations. There was an increase in the percentage to 63.77% (median) in CCR6$^+$IFNγ$^+$IL-17$^+$ cells **(Figure 4.9 A)**. The expression of IL-2 was uniform in all populations **(Figure 4.9 B)** and there was very little detectible expression of IL-10 **(Figure 4.9 C)** and IL-5 **(Figure 4.9 D)** in any of the populations.

4.6 CCR6$^+$T$_H$1 Cells Express CXCR3 to the Same Level as CCR6$^-$T$_H$1

CCR6 is a chemokine receptor that gives the cells the potential to migrate towards CCL20 (also known as Macrophage Inflammatory Protein-3). As mentioned before CCR6 is associated with T$_H$17 cells while CXCR3 is a chemokine receptor associated with T$_H$1 cells. Stimulated PBMC were co-stained with CCR6 and CXCR3, alongside IFNγ and IL-17 to identify if there was any difference in the expression of CXCR3 in CCR6$^+$IFNγ$^+$ cells compared to CCR6$^-$ IFNγ$^+$ cells. **Figure 4.10 A** shows the strong co-association of IFNγ and CXCR3. There was also a small subset of IL-17 secreting cells that had high expressed CXCR3, although the majority of cells had low CXCR3 expression. There was a relatively even split of memory CD4$^+$ T cells expressing CCR6 and CXCR3, with approximately 18% of cells co-expressing both chemokine receptors **(Figure 4.10 B). Figure 4.10 C** shows representative plots gated on the CXCR3 and CCR6 expressing populations. When gating on CCR6$^+$ cells that do not express CXCR3, there was very little IFNγ expression. There was an enrichment of IL-17 secreting

cells, although a large proportion of cells do not secrete either cytokine. When gated on $CXCR3^+CCR6^+$ cells, there was noticeably more IFNγ secreting cells, cells expressing IL-17 alone, and IL-17 with IFNγ. The $CXCR3^+CCR6^-$ population produced IFNγ or were $IFN\gamma^-IL\text{-}17^-$. **Figure 4.10 D and E** highlights that the majority of both $CCR6^+$ and $CCR6^-$ IFNγ secreting cells expressed CXCR3, and to a similar level per cell. Approximately 60% of the $CCR6^+IFN\gamma^+IL\text{-}17^+$ cells expressed CXCR3, although at a lower level than single IFNγ secreting cells.

4.7 $CCR6^+T_H1$ can Migrate Towards CCL20

The levels of CCR6 expressed on $CCR6^+IFN\gamma^+$ cells was reduced **(Figure 4.1 B)** compared to IL-17 expressing cells. To investigate if this made a difference to the migration of CCR6 expressing IFNγ cells, compared to IL-17 cells, a migration assay using a trans-well plate was set up. Initially, to test if $CCR6^+$ cells could be isolated before the migration assay, total $CD4^+$ T cells were either stained for CCR6 or left unstained. These were added to the top well of the transwell plate, while CCL20 was added to the bottom well. A control well in which no CCL20 was added to the bottom well was also constructed. After the cells were collected and stimulated for IFNγ and IL-17 expression the percentage migration was calculated for the total cells and the individual cytokine secreting populations. **Figure 4.11 A and B** demonstrates that staining for CCR6 reduces the ability of the cells to migrate towards CCL20. This reduced migration was not specific to one population. This meant that for the migration assay an assumption was made that the amount of CCL20 specific migration was considered to be the degree of migration above medium alone.

A 10 fold dilution of CCL20 and CXCL12, ranging from 0 – 1000ng was added to the bottom wells of a migration assay. CXCL12, the chemo-attractant for CXCR4 expressing cells, was used as a control, as a large percentage of cells can migrate towards CXCL12. There was a background migration of total CD4$^+$ T cells independently of any chemotactic gradient being added to the wells. This was considered non-specific migration and the CCL20/CXCL12 specific migration was considered to be anything above medium alone, indicated by the line across the graphs. **(Figure 4.12)**. There was a gradual dose dependent increase in total CD4$^+$ T cells that migrated towards CCL20. 15.40% of the CD4$^+$ T cells migrating towards 1000ng of CCL20 (above baseline - **Figure 4.12 A**). CXCL12 being present resulted in more CD4$^+$ T cells migrating in response. Up to 58.94% (above baseline) of the CD4$^+$ T cells migrated towards 100ng of CXCL12. At 1000ng of CXCL12 there was a reduction in the percentage of cells that migrate (14.53% above baseline - **Figure 4.12 D**). This is a known phenomenon in which the chemokine receptor is down regulated at high concentrations of chemokine[215]. When the cells were stimulated and stained for cytokine production there was a great deal of IL-17 specific migration in a dose dependent fashion. The migration of IL-17 cells plateaued at 100ng and remained at approximately 48.33% above baseline at 1000ng **(Figure 4.12 B)**. There was an increase in the percentage of IL-17$^+$ cells that migrated up to 100ng of CXCL12. At 100ng there were 61.34% of IL-17$^+$ cells migrating (above baseline) which reduced to 11.84% at 1000ng of CXCL12 **(Figure 4.12 E)**. Only 17.59% of IFNγ$^+$ cells migrate towards CCL20 at 1000ng (above baseline **- Figure 4.12 C)**. This was in the region of the percentage of IFNγ$^+$ cells that expressed CCR6. There was a large percentage of IFNγ$^+$ cells that migrate towards CXCL12 at 100ng. Again there was a reduction in the percentage

of IFNγ cells that migrated to 1000ng **(Figure 4.12 F)**. Overall, these data suggest that CCD6$^+$IFNγ$^+$ cells have a similar ability as CCR6$^+$IL-17$^+$ cells to migrate towards CCL20.

It has been shown above that there was less CCR6 expression on IFNγ$^+$ cells compared to IL-17$^+$ T cells. To investigate if the CCR6 expression on the IFNγ$^+$ cells was stably expressed in culture, the CCR6 expression levels of the cells were analysed after 7 days in different culture conditions. CCR6$^+$ and CCR6$^-$ cells were isolated from CD4$^+$CD45RO$^+$ cells and cultured with IL-2, IL-23 or no cytokines, and with TcR stimulation. After 7 days the CCR6 expression levels for all the CCR6$^-$ cells were negative, with the MFI never surpassing 0.39. Within the CCR6$^+$ population the CCR6 MFI was maintained (**Figure 4.13 C)**. The higher CCR6 expression is maintained on IL-17$^+$ cells compared to IFNγ$^+$ cells **(Figure 4.13 D)**. The CCR6 expression is also maintained on IFNγ$^+$ cells **(Figure 4.13 E)**. The maintenance of CCR6 does not appear to be cytokine dependent. However this is an experiment that needs repeating as there was an increase in CCR6 MFI compared to IL-2 and no cytokine culture in one experiment, but this was not seen in the second repeat.

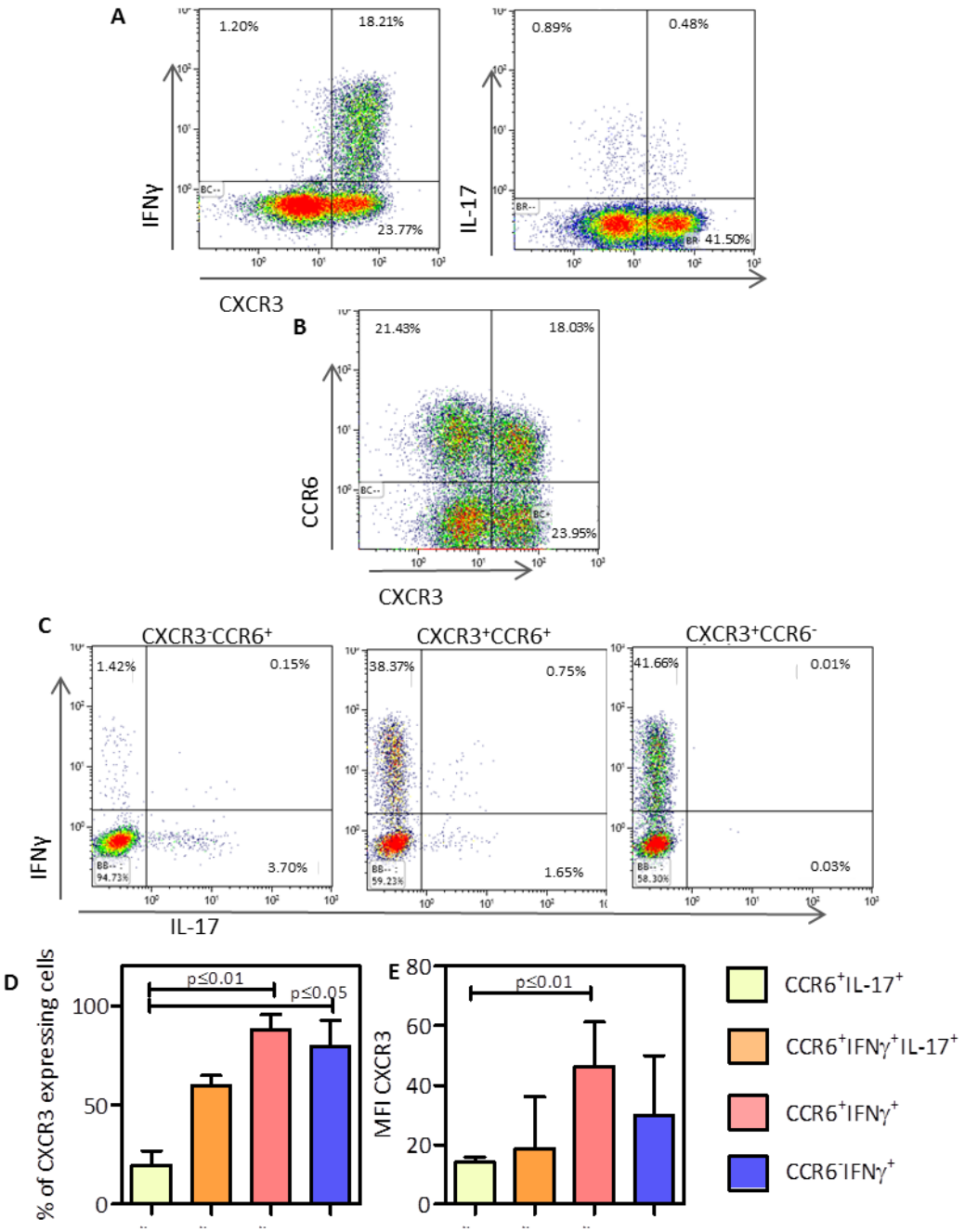

Figure 4.10. Expression of CXCR3 in CCR6^{+}IFNγ^{+} cells compared to CCR6^{-}IFNγ^{+} cells and IL-17 secreting populations. Total PBMC were stimulated with PMA and Ionomycin for 3 hours in the presence of Brefeldin A. Cells were stained for CXCR3 and CCR6 and intracellular IFNγ and IL-17 expression and analysed by flow cytometry. **(A)** Representative flow plots of CXCR3 expression in IFNγ and IL-17 expressing populations gated on CD4^{+}CD45RO^{+} cells. **(B)** Co-staining of CXCR3 and CCR6 in CD4^{+}CD45RO^{+}, cells and the **(C)** IFNγ and IL-17 expression gated on CXCR3^{-}CCR6^{+}, CXCR3^{+}CCR6^{+} and CXCR3^{+}CCR6^{-} populations. Values represent percentage of cells in the gate. **(D)** Percentage of CXCR3^{+} cells (p=0.0009) and **(E)** the MFI of CXCR3 in CD4^{+}CD45RO^{+} cells gated on CCR6 expressing populations (p=0.0016). To test significance a Friedman test with Dunn's Multiple Comparison Test was undertaken. Mean and standard error of the mean (SEM) shown.

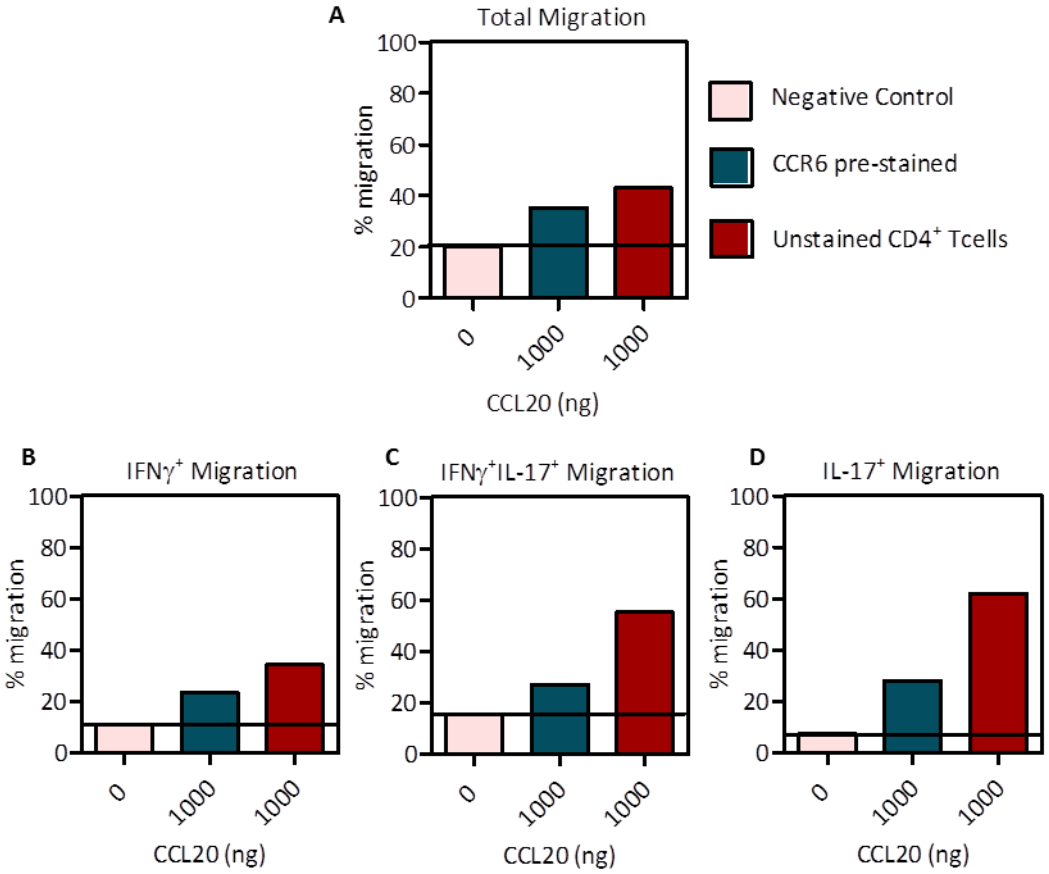

Figure 4.11. Cells pre-stained for CCR6 have a reduced ability to migrate towards CCL20. CD4$^+$ T cells were bead isolated and either pre-stained for CCR6 or left unstained. The cells were added to the top well of a transwell plate with either no CCL20 or 1000ng added to the bottom well. The cells were left for three hours and the number of cells in the top and bottom well were counted. The cells were then stimulated with PMA and Ionomycin for 3 hours in the presence of Brefeldin A. IFNγ and IL-17 expression by each population was analysed and the percentage of cells in each population was calculated. **(A)** Percentage of total cells migrate towards CCL20 in CCR6 stained CD4$^+$ T cells compared to unstained CD4$^+$ T cells. Percentage of **(B)** IFNγ$^+$, **(C)** IFNγ$^+$IL-17$^+$ and **(D)** IL-17$^+$ cells migrated towards CCL20 in CCR6 stained CD4$^+$ T cells compared to unstained cells. Line representing baseline migration towards no CCL20. Data represents mean of experimental duplicates of n=1.

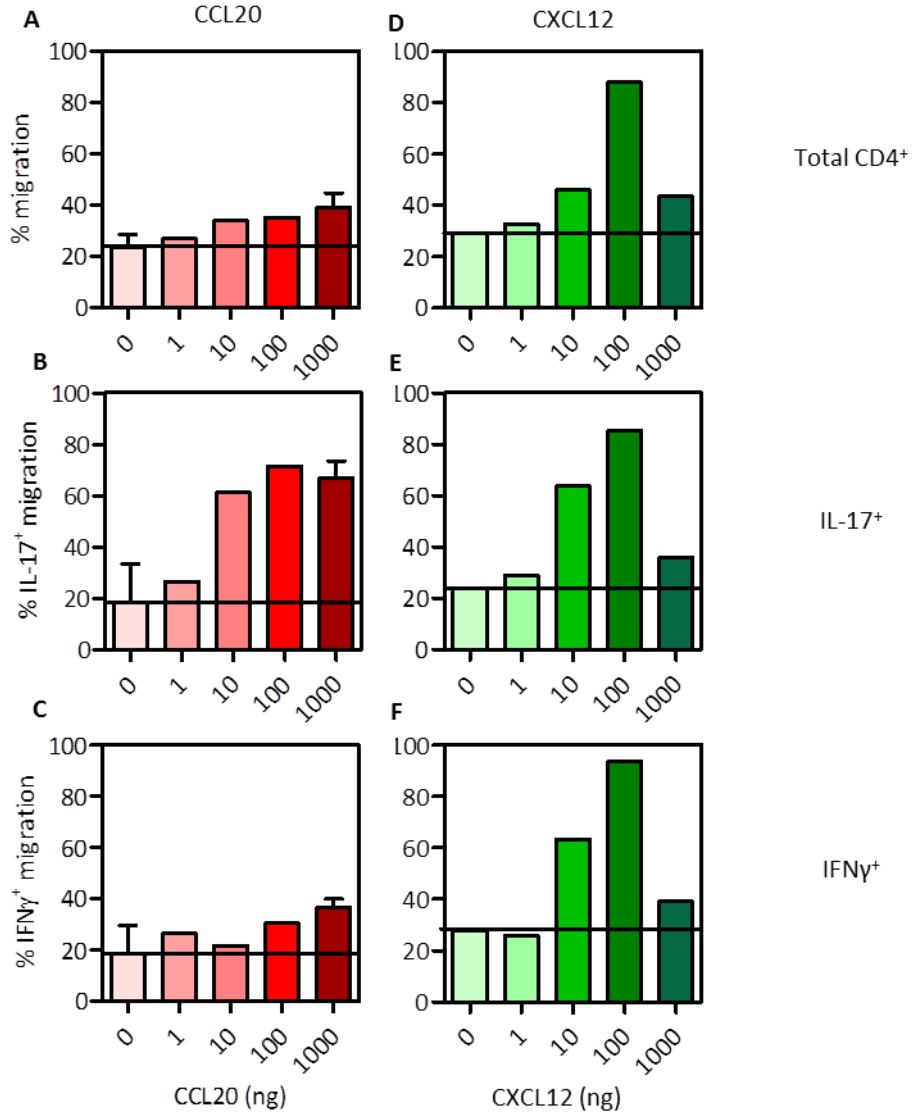

Figure 4.12. CCR6+IFNγ+ cells can migrate towards CCL20 in a dose dependent manner. CD4+ T cells were bead isolated and added to the top well of a transwell plate with either CCL20 or CXCL12 at different concentrations added to the bottom well. The cells were left for three hours and the number of cells in the top and bottom well were collected and counted. The cells were then stimulated with PMA and Ionomycin for 3 hours in the presence of Brefeldin A. IFNγ and IL-17 expression by each population was analysed and the percentage of cells in each population was calculated. Percentage of CD4+ total cells migrated towards **(A)** CCL20 or **(D)** CXCL12 at different concentrations. Percentage of **(B, E)** IFNγ+ and **(C, F)** IL-17+ cells migrated towards CCL20 or CXCL12. Line representing baseline migration towards no CCL20 or CXCL12. Data represents mean of experimental triplicates, apart from CCL20 1ng and 1000ng, which is mean and standard error of the mean (SEM) of two independent experiments.

4.8 Functional Consequences of IL-23R Expression on CCR6$^+$IFNγ$^+$ Cells

The IL-23R gene was expressed in CCR6$^+$IFNγ$^+$ cells. In an effort to confirm this expression *ex vivo* stimulated CD4$^+$ T cells were analysed for IL-23R expression by flow cytometry. There was very little detectable IL-23R expression on the CD4$^+$ T cells. Analyses of CD45RO expression showed an intermediate level of expression on the IL-23R$^+$ cells **(Figure 4.14 A)**. All the cells that expressed IL-23R were CCR6$^+$, but these cells did not express either IL-17 or IFNγ **(Figure 4.14 B)**. IL-23R expression was increased on the CD45RO$^+$ population after culture with IL-1β, IL-6 and IL-23. Approximately half of the IL-23R expression was on CCR6$^-$ cells. There was a small overlap of IL-23R expression on the IL-17 and IFNγ cells **(Figure 4.14 C)**.

To identify if there was any effect of IL-23 on the different populations, isolated CCR6$^+$ IFNγ$^+$, CCR6$^+$IL-17$^+$ and CCR6$^-$IFNγ$^+$ cells were cultured with IL-23 and compared to a culture with IL-7 and IL-15. The CCR6$^+$IFNγ$^+$ cells maintained their IFNγ expression, with a few cells losing the ability to produce IFNγ or IL-17 after stimulation. There was conversion of the CCR6$^+$IL-17$^+$ cells to secreting IFNγ with IL-17 or just IFNγ alone, but this was not differentially affected by IL-7/IL-15 and IL-23. In both cultures with IL-23 and IL-7/IL-15 there were a small percentage of CCR6$^+$IFNγ$^+$ cells that secreted IL-17 **(Figure 4.15)**.

Data from this study **(Figure 4.7 D)** have shown that CCR6$^+$IFNγ$^+$ cells expressed IL4I1 to a similar level to CCR6$^+$IL-17$^+$ cells. IL4I1 is a gene for secreted L-phenyl-alanine oxidase, associated with the reduced ability of T_H17 cells to proliferate in humans[104]. Cytokine capture could not be used to isolate the cells as they would have to be stimulated with

PMA/ionomycin. This stimulation has been shown to remove any effect of IL4I1 on proliferation. Instead, isolated CCR6$^+$ and CCR6$^-$ CD4$^+$ T cells were stimulated with anti-CD3/anti-CD28 antibody, and then cultured with either no-cytokines, IL-2 or IL-23.

There appeared to be no difference in the proliferation between the CCR6$^+$ and CCR6$^-$ populations when the cells were treated with different cytokines **(Figure 4.16 A-C)**. There was a difference in the percentage of undivided cells, with a higher percentage in the CCR6$^-$ fraction. It cannot be ruled out that this was due to higher mortality of the cells in the CCR6$^+$ cells rather than more proliferation.

4.9 CCR6 T_H1 cells are Found in the CSF of MS Patients

As previously described in **Section 1.8.3**, CCR6$^+$$T_H17$ expressing cells play an important role in the first wave of migration of T cells into the CNS in EAE, the murine model of autoimmune disease MS[157]. Some T_{REG} also express CCR6 and it has been suggested that CCR6 is involved in the migration of T_{REG} into the CNS to control EAE[2]. However to our knowledge there has been very little analysis of IFNγ expression in CCR6$^+$ cells in RR-MS patients. In this study the cellular components of the blood of 17 patients with suspected MS, 9 of which had matching CSF samples, was analysed. The CSF fluid was taken through a diagnostic lumbar puncture which meant that there was very little chance that the patient was in relapse at the time. The blood from 8 healthy controls was also analysed, but were not age or sex matched to the RR-MS patients. **Table 4.1** gives the diagnosis of the patient, received after analysis.

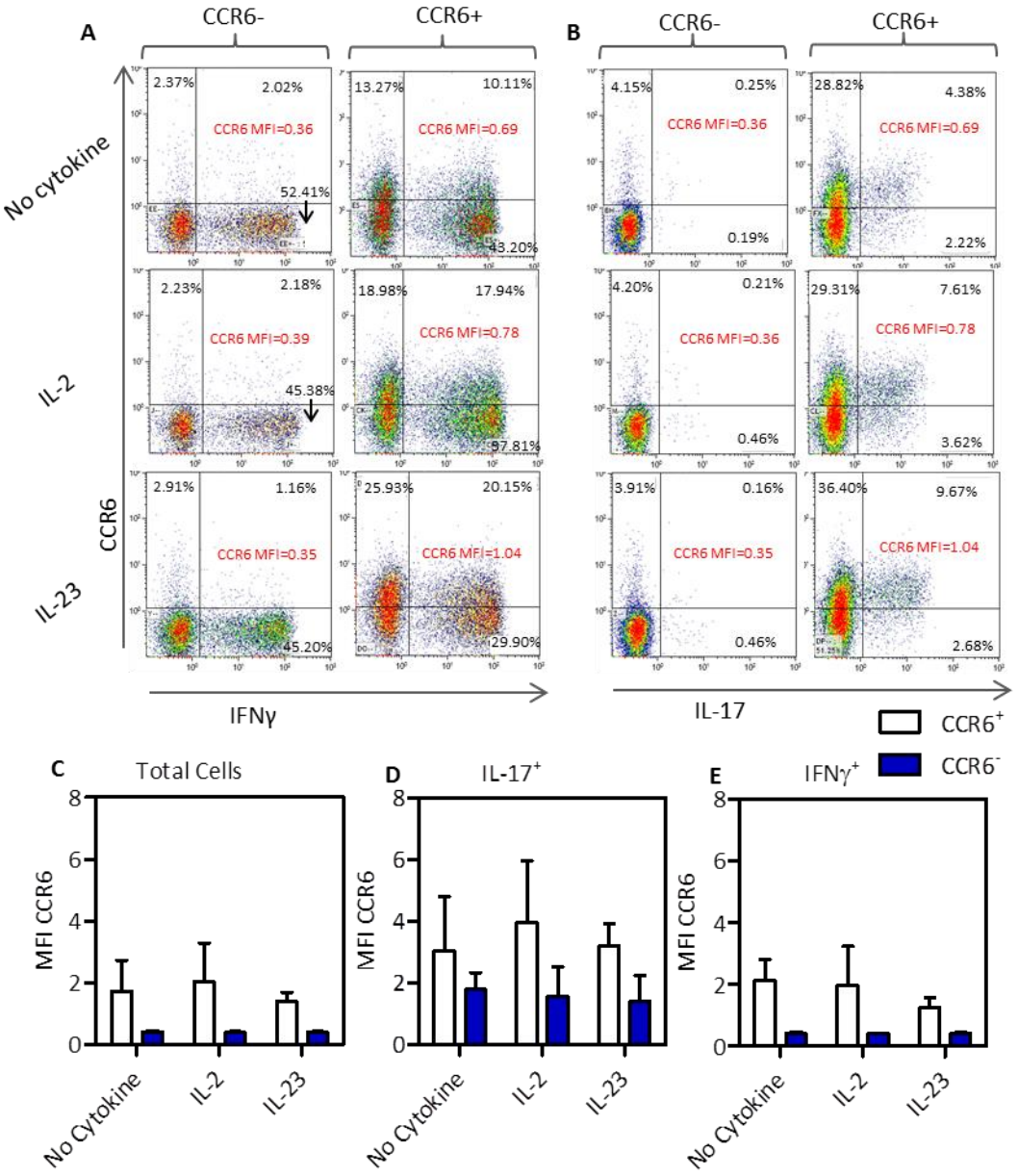

Figure 4.13. CCR6 expression is stable in culture: CD4+CD45RO+CCR6+ and CD4+CD45RO+CCR6- cells were isolated from PBMC**.** The cells were placed in culture and stimulated with anti-CD3/anti-CD28 antibodies, which was removed after 3 days, and the cytokines indicated, either no cytokine, IL-2 or IL-23 for the full 7 days. At day 7 the cells were stimulated with PMA and Ionomycin for 3 hours in the presence of Brefeldin A and analysed for CCR6, IFNγ and IL-17 expression by flow cytometry. **(A)** An example of analysis of CCR6 MFI in CCR6+ and CCR6- cells against **(A)** IFNγ **(B)** and IL-17. Red values shown are the CCR6 MFI for the total population. Analysis of duplicates from two independent experiments of CCR6 MFI in **(C)** the total, **(D)** IL-17+ and **(E)** IFNγ populations in cells cultured with no cytokine, IL-2 or IL-23. Mean and standard error of the mean (SEM) are shown on graph. Values represent percentage of cells in the gate

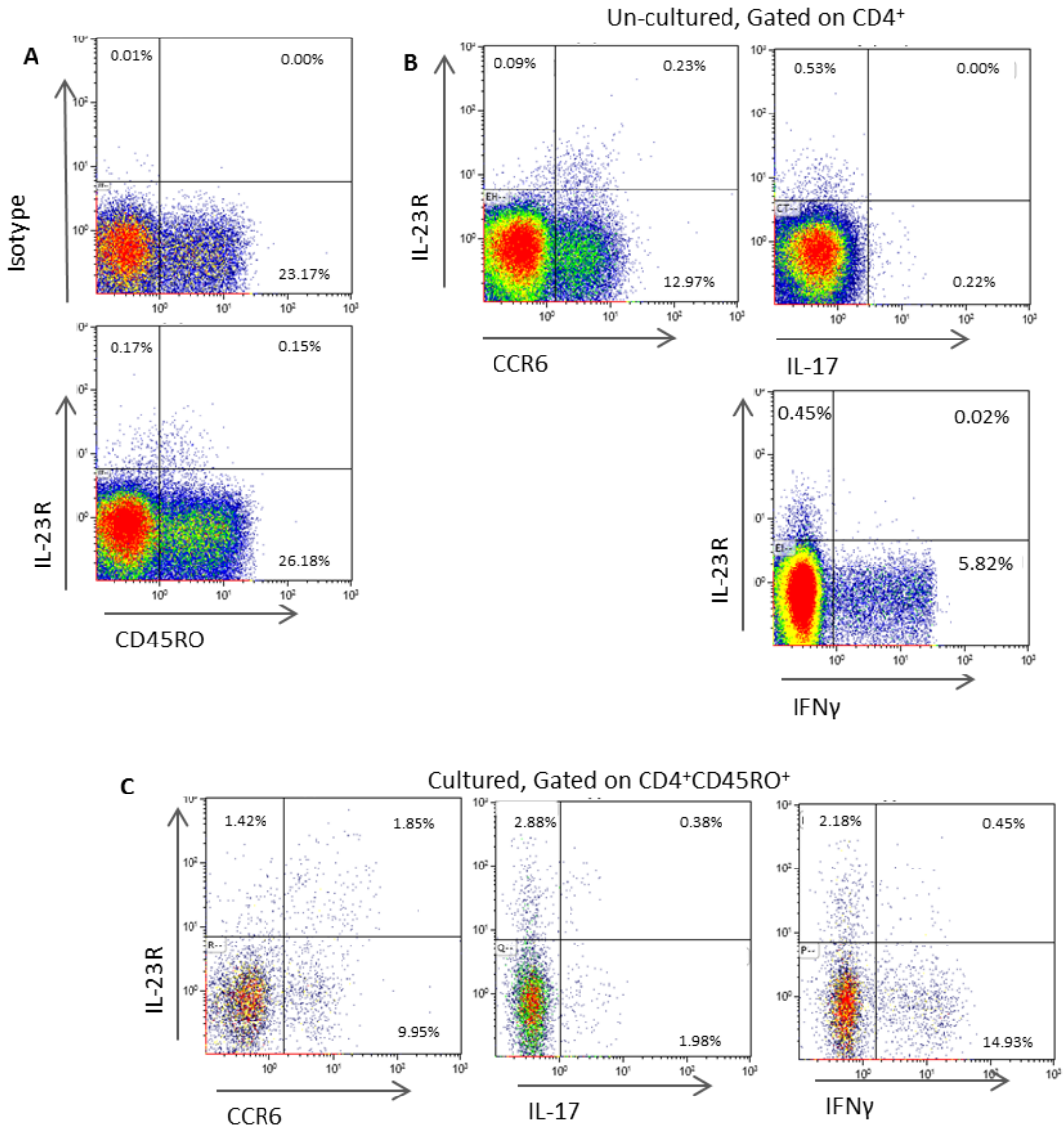

Figure 4.14. IL-23 receptor expression on *ex vivo* and *in vitro* CD4+ T cells. PBMC were stimulated with PMA and Ionomycin for 3 hours in the presence of Brefeldin A and analysed for IL-23R,CCR6, IFNγ and IL-17 expression by flow cytometry. **(A)** Representative flow plots gated on CD4+ T cells of the expression of IL-23R against CD45RO, gates based on isotype control shown. **(B)** IL-23R expression against CCR6, IL-17 and IFNγ expressing total CD4+ T cells. n=2 **(C)** Total CD4+ T cells were cultured with anti-CD3/ anti-CD28 antibodies which were removed after 3 days. IL-1β, IL-6 and IL-23 was present for 7 days. Day 7 the cells were stimulated with PMA and Ionomycin for 3 hours in the presence of Brefeldin A and analysed for IL-23R,CCR6, IFNγ and IL-17 expression by flow cytometry. Values represent percentage of cells in the gate. n=1

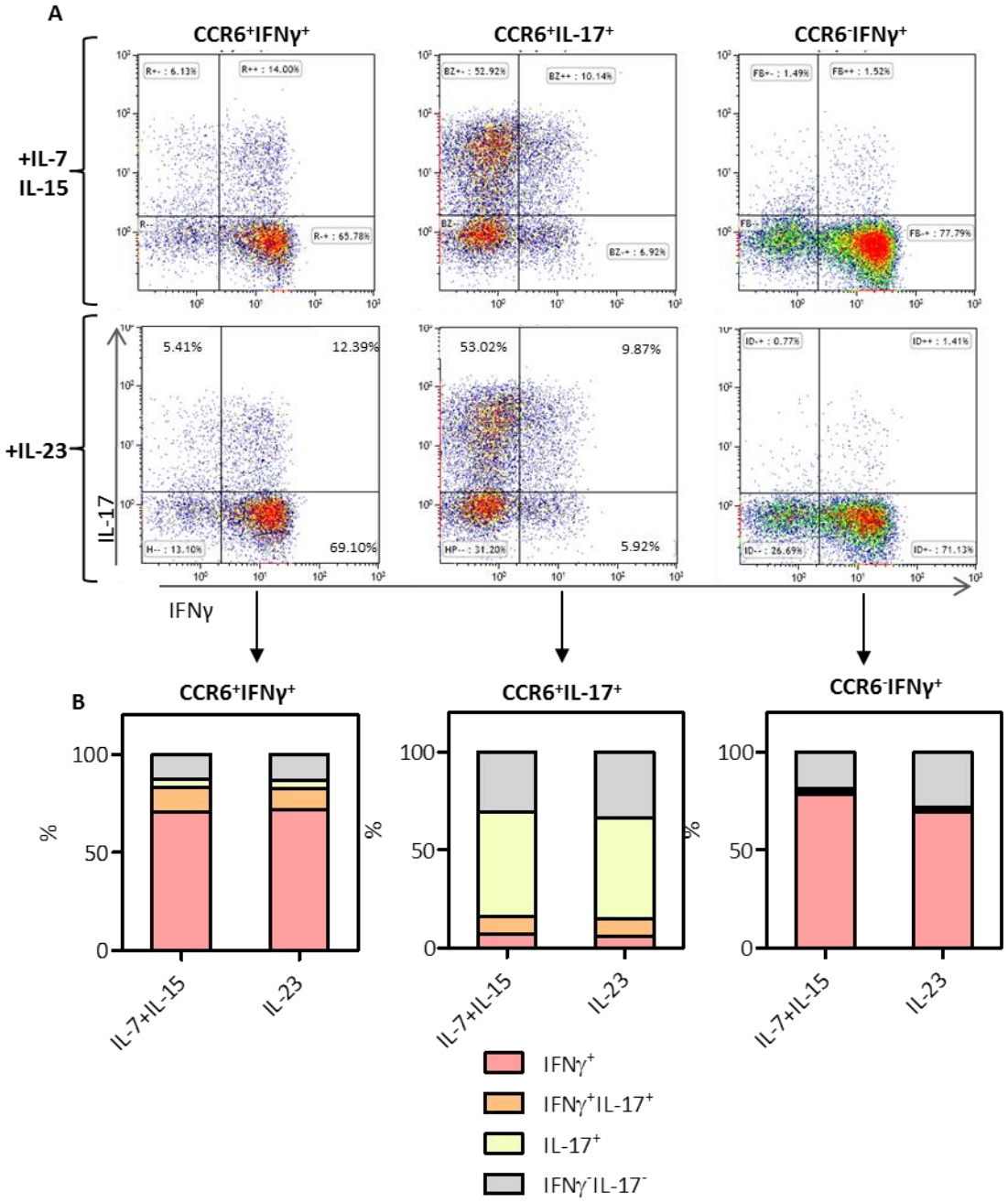

Figure 4.15. Culturing with IL-23 does not change the phenotype of CCR6^{+}IFNγ^{+} cells. Memory (CD45RO^{+}) cells expressing CCR6, IFNγ and IL-17 were isolated from CD4^{+}CD25^{-} bead purified cells using cytokine capture and a MoFlo cell sorter. The cells were cultured without stimulation in the presence of either IL-7/IL-15 or IL-23. At day 7 the cells were stimulated with PMA and Ionomycin for 3 hours in the presence of Brefeldin A and analysed for IFNγ and IL-17 expression by flow cytometry. **(A)** Representative flow cytometry plots of IFNγ and IL-17 expression in CCR6^{+}IFNγ^{+}, CCR6^{+}IL-17^{+} and CCR6^{-}IFNγ^{+} cells after culture with IL-2 or IL-23. n=1 of two replicates, median shown.

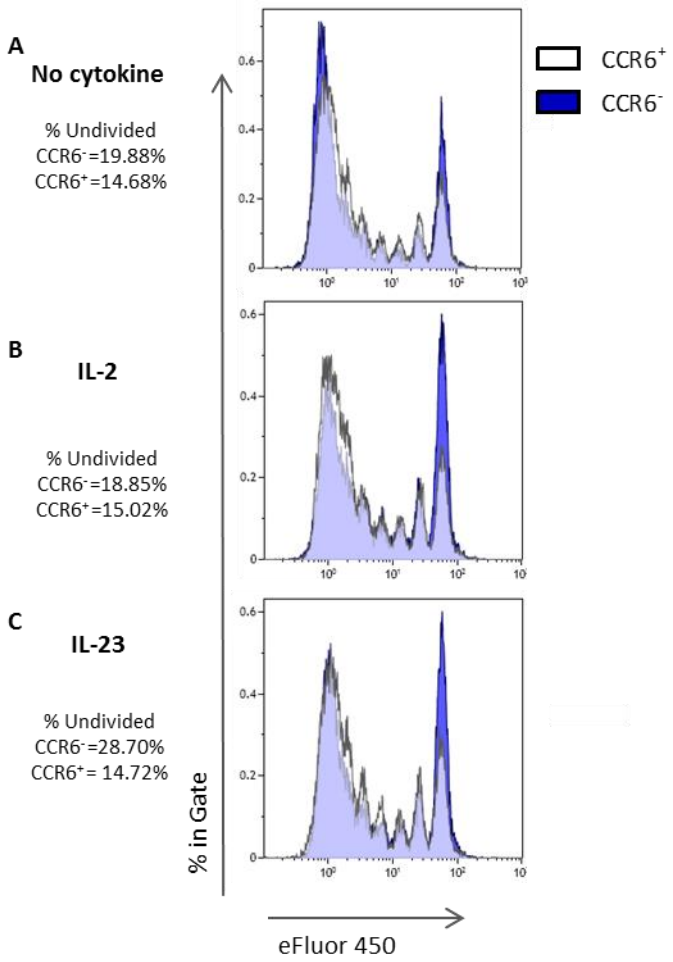

Figure 4.16. Analysis of proliferative ability of CCR6^{+} and CCR6^{-} populations. PBMC were pre-stained with eFLuor 450, a nuclear stain to analyse proliferation. CD4^{+}CD45RO^{+}CCR6^{+} and CD4^{+}CD45RO^{+}CCR6^{-} cells were isolated from the stained PBMC using MoFlo cell sorter**.** The cells were placed in culture and stimulated with plate bound anti-CD3/ soluble anti-CD28 antibodies, which was removed after 3 days, and the cytokines indicated, either **(A)** no cytokine, **(B)** IL-2 or **(C)** IL-23 for the full 7 days. On day 7 the cells were analysed for proliferation on the flow cytometer. The percentage of undivided cells is shown on the left. Representative plots shown of duplicates within same experiment. n=1

CCR6 expression was analysed alongside the IFNγ and IL-17 secretion in the $CD4^+$ memory cells within each sample. **Figure 4.17** shows the CCR6 expression within the bloods of (**Figure 4.17 B**) MS and (**Figure 4.17 A**) healthy controls, and (**Figure 4.17 C**) CSF from MS patients. Furthermore the IFNγ and IL-17 expression in both $CCR6^-$ and $CCR6^+$ populations are shown.

Figure 4.18 A analyses the overall IFNγ and IL-17A secretion within the samples, highlighting that the majority of the $CD4^+$ T cells within the CSF are IFNγ secreting. There are very few IL-17A secreting cells within the CSF. There appears to be a reduction in the number of IL-17 secreting cells in the blood of MS patients compared to controls, although not significantly different. The proportion of IFNγ cells that express CCR6 was analysed. Within the MS blood there was a reduced presence of $CCR6^+IFN\gamma^+$ cells compared to control blood (MS Blood, median=13.91% and range=1.47%-22.78%, Control blood, median= 37.22%, range= 1.08%-46.60%). Within the CSF there was a large presence of $CCR6^+IFN\gamma^+$ (median=44.5% of IFNγ cell expressing CCR6) and $CCR6^-IFN\gamma^+$ cells **(Figure 4.17 B and Figure 4.18 B)**. There was significantly higher percentage of $CD4^+CD45RO^+CCR6^+$ cells in the CSF compared to both the peripheral blood of healthy and MS samples **(Figure 4.17 C and Figure 4.18 C)**. The MFI of CCR6 was similar in all the populations **(Figure 4.18 D)**. There was a reduction in the percentage of $CCR6^+IFN\gamma^+$ cells in the MS blood compared to healthy controls, although this was not significant. However, there was a significant increase in the percentage of IFNγ cells expressing CCR6 in the CSF compared to matched peripheral blood of MS patients **(Figure 4.18 E)**. Where there were cells that expressed IL-17 within the blood and CSF of MS patients, the large majority were $CCR6^+$ **(Figure 4.18 F)**.

Correlation analysis of the CCR6^{+}IFNγ^{+} , CCR6^{+}IL-17^{+} and CCR6^{-}IFNγ^{+} populations showed that there was only a statistical correlation between CCR6^{+}IFNγ^{+} and CCR6^{-}IFNγ^{+} in healthy bloods, MS bloods and MS CSF **(Figure 4.19 A-C)**.

GM-CSF can be produced by T_H17 cells and in the context of MS is thought to be one of the molecules that cause the pathology within the CNS. Within T_H17 cells the expression of GM-CSF is induced by IL-23. To identify if CCR6^{+}IFNγ^{+} cells could also be a source of GM-CSF within the CNS the expression of this cytokine was analysed in MS bloods and CSF fluid. In the previous chapter it was shown that both CD4^{+} CCR6^{+} and CCR6^{-} T_H1 cells can secrete GM-CSF (**Figure 3.20 D**). As expected within the blood of MS patients both CCR6^{+} and CCR6^{-} IFNγ cells secreted GM-CSF. Roughly half of the CCR6^{+}IFNγ^{+} cells secreted GM-CSF. All the IL-17^{+} cells were within the CCR6^{+} population and roughly half of these cells co-secreted GM-CSF **(Figure 4.20 A, C)**.

The CSF contained very few IL-17 cells, but the few cells that did secrete IL-17 were GM-CSF^{+}. Of the CCR6^{+}IFNγ^{+} cells roughly 60% expressed GM-CSF, while approximately 50% of the CCR6^{-}IFNγ^{+} cells co-expressed GM-CSF **(Figure 4.20 B, C)**.

This data highlights that the IFNγ secreting cells within the CSF of RR-MS patients can be a significant source of GM-CSF, a potentially pathologically active cytokine.

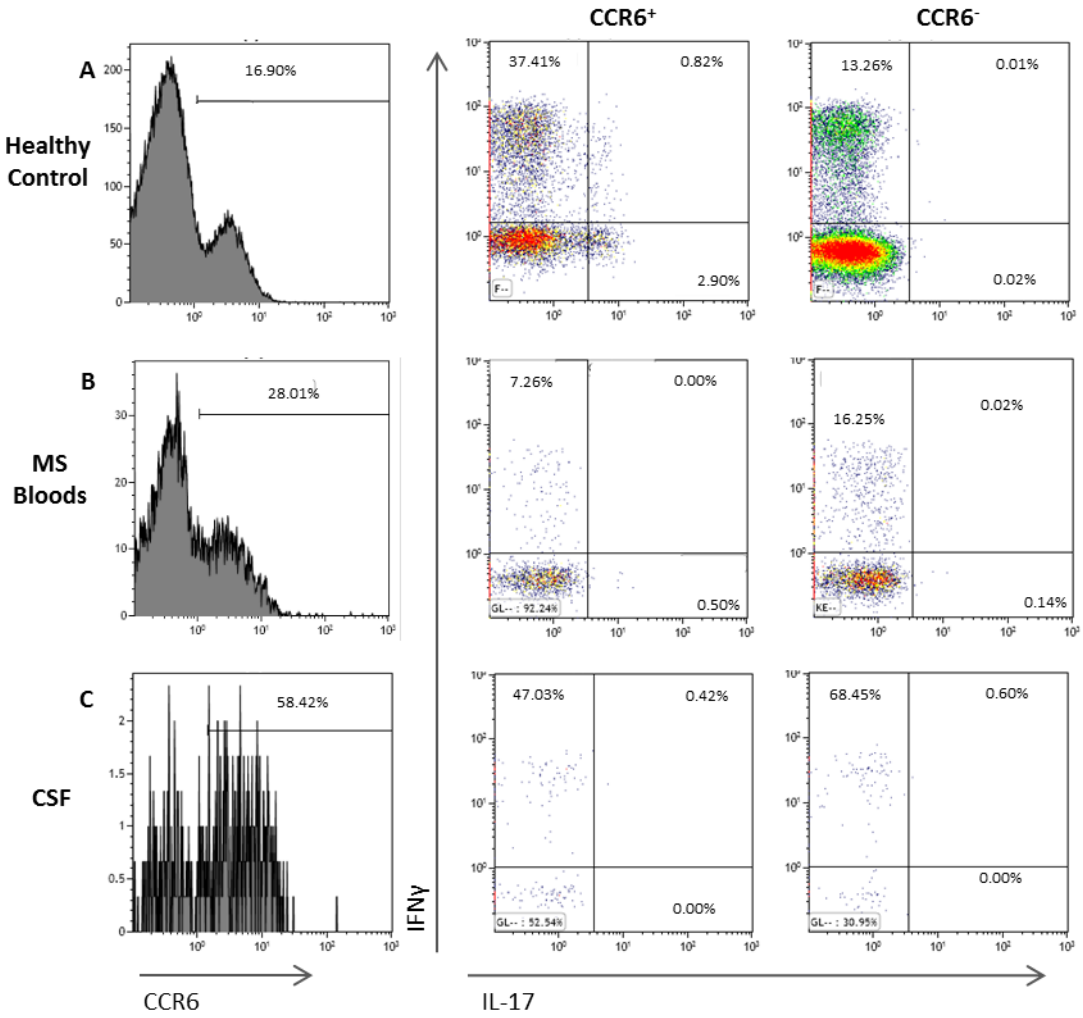

Figure 4.17 CCR6+IFNγ cells can be found in the CSF of MS patients. PBMC or cells isolated from CSF of MS patients were stimulated with PMA and Ionomycin for 3 hours in the presence of Brefeldin A. From these samples gated on CD4+CD45RO+ the IFNγ and IL-17 expression in the CCR6+ and CCR6- populations were analysed by flow cytometry. Representative plots show the expression in the blood of **(A)** healthy controls, **(B)** MS patients and **(C)** cell from the cerebral spinal fluid (CSF) of MS patient. Values represent percentage of cells in the gate. Images representative of one patient and one control.

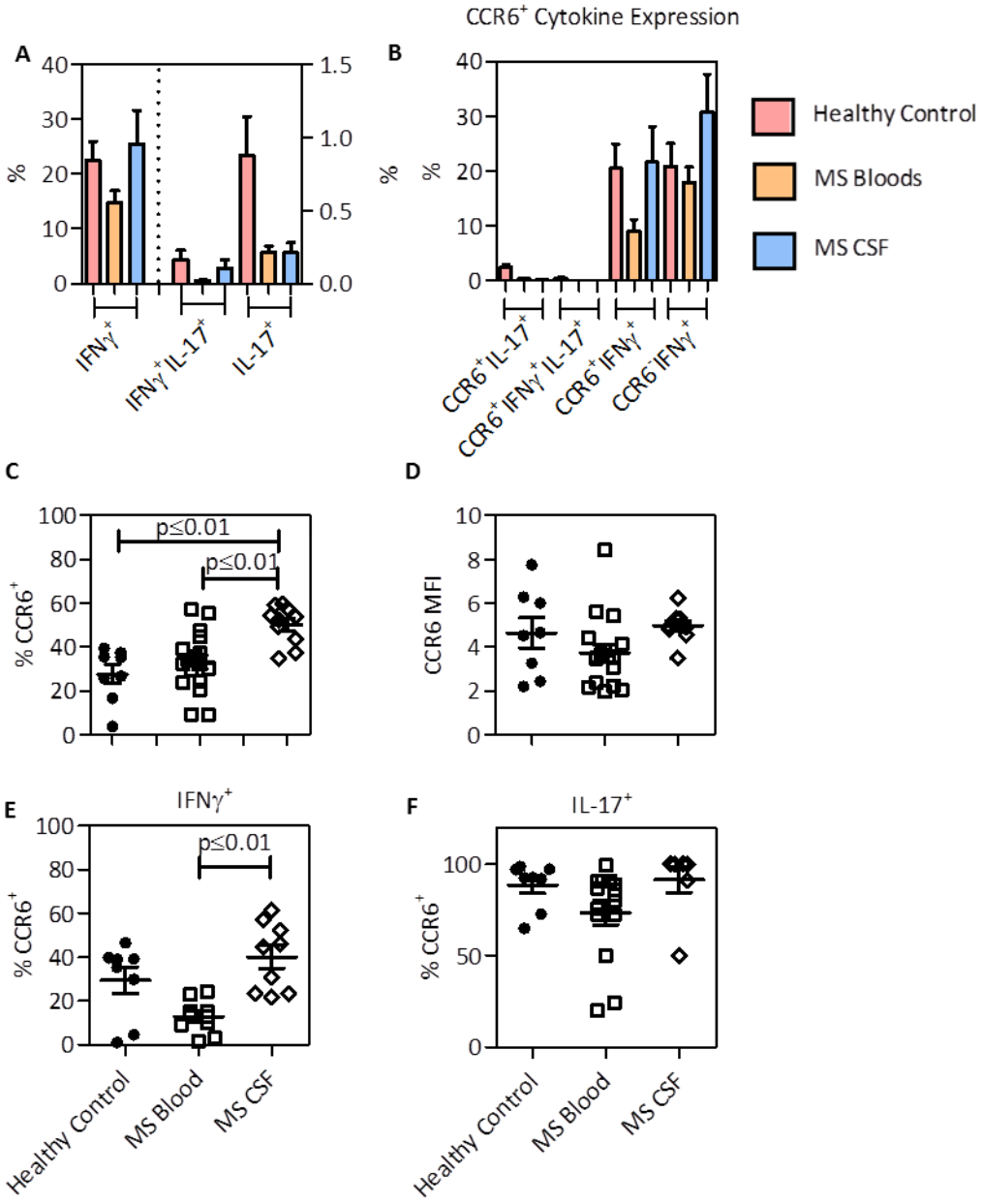

Figure 4.18 CCR6+T_H1 are found at a higher frequency in the CSF of MS patients compared to the peripheral blood: a) Multiple Sclerosis patients cytokine and chemokine expression – healthy vs. MS blood vs. MS CSF: PBMC or cells isolated from CSF were stimulated with PMA and Ionomycin for 3 hours in the presence of Brefeldin A. **(A)** Gated on CD4+CD45RO+ cells the percentage secreting IFNγ, IFNγ and IL-17 and IL-17 in healthy control blood, MS patients blood or cells from the CSF of MS patients. Within each compartment the **(B)** gated on either CCR6- or CCR6+ and cytokine expression .**(C)** Percentage of CCR6+ cells in each sample (p=0.0024) **(D)** MFI of CCR6 gated on CD4+CD45RO+CCR6+ **(E)** Gated on CD4+CD45RO+IFNγ+ (p=0.006) the percentage of CCR6+ and CD4+CD45RO+IL-17+ percentage of CCR6+ (mean and standard error of the mean (SEM) shown on all the graphs. Healthy controls n=8, MS Bloods n=20, CSF n=10) To test significance a Friedman test with Dunn's Multiple Comparison Test was undertaken.

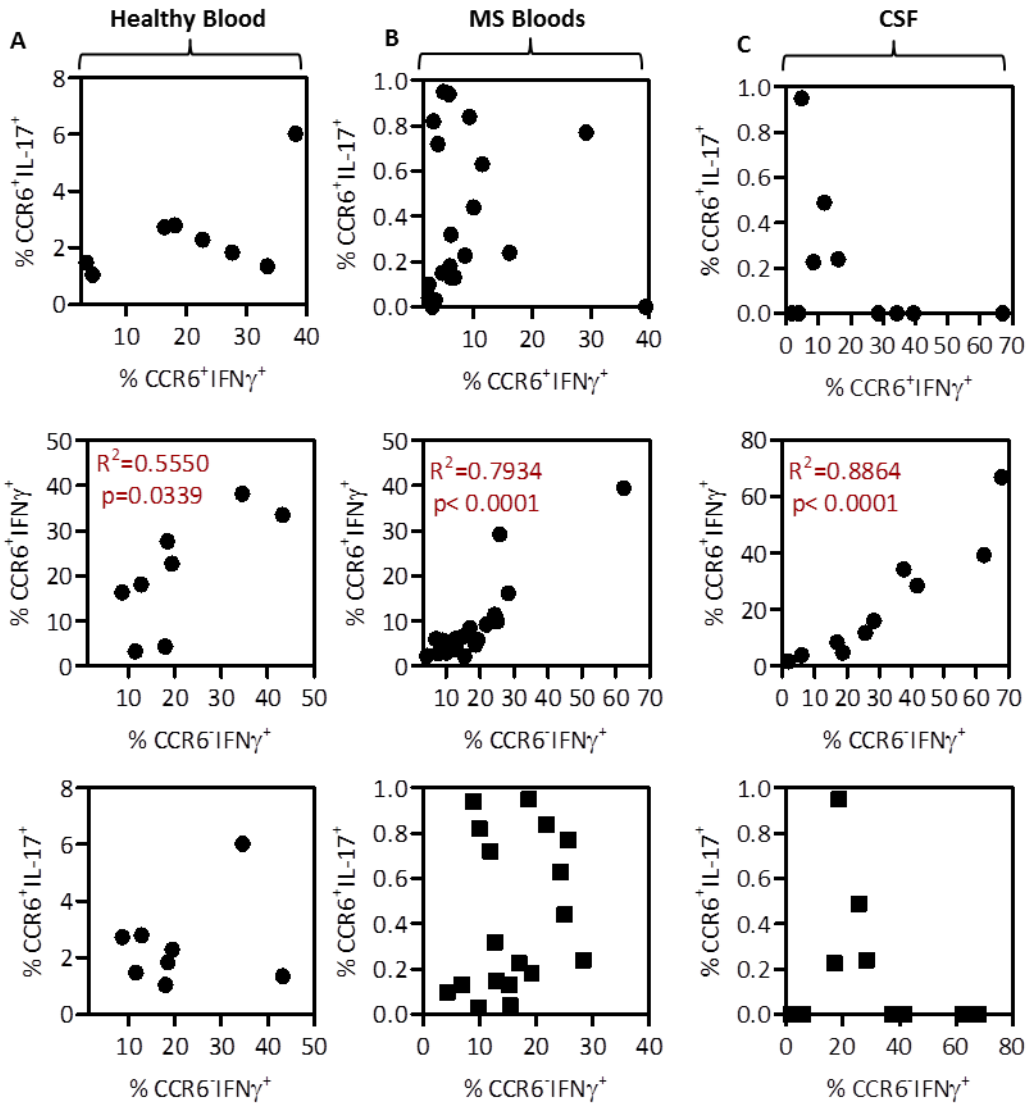

Figure 4.19. There is a positive correlation between the percentage of CCR6^{+} and CCR6^{-} IFNγ secreting cells in health controls, MS Bloods and CSF fluid. The correlation of CCR6^{+}IFNγ^{+} CCR6^{-}IFNγ^{+} and CCR6^{+}IL-17^{+} cells in **(A)** healthy control peripheral blood, **(B)** MS patients peripheral blood and **(C)** cells from CSF. Correlation R^2 and P values shown where significant.

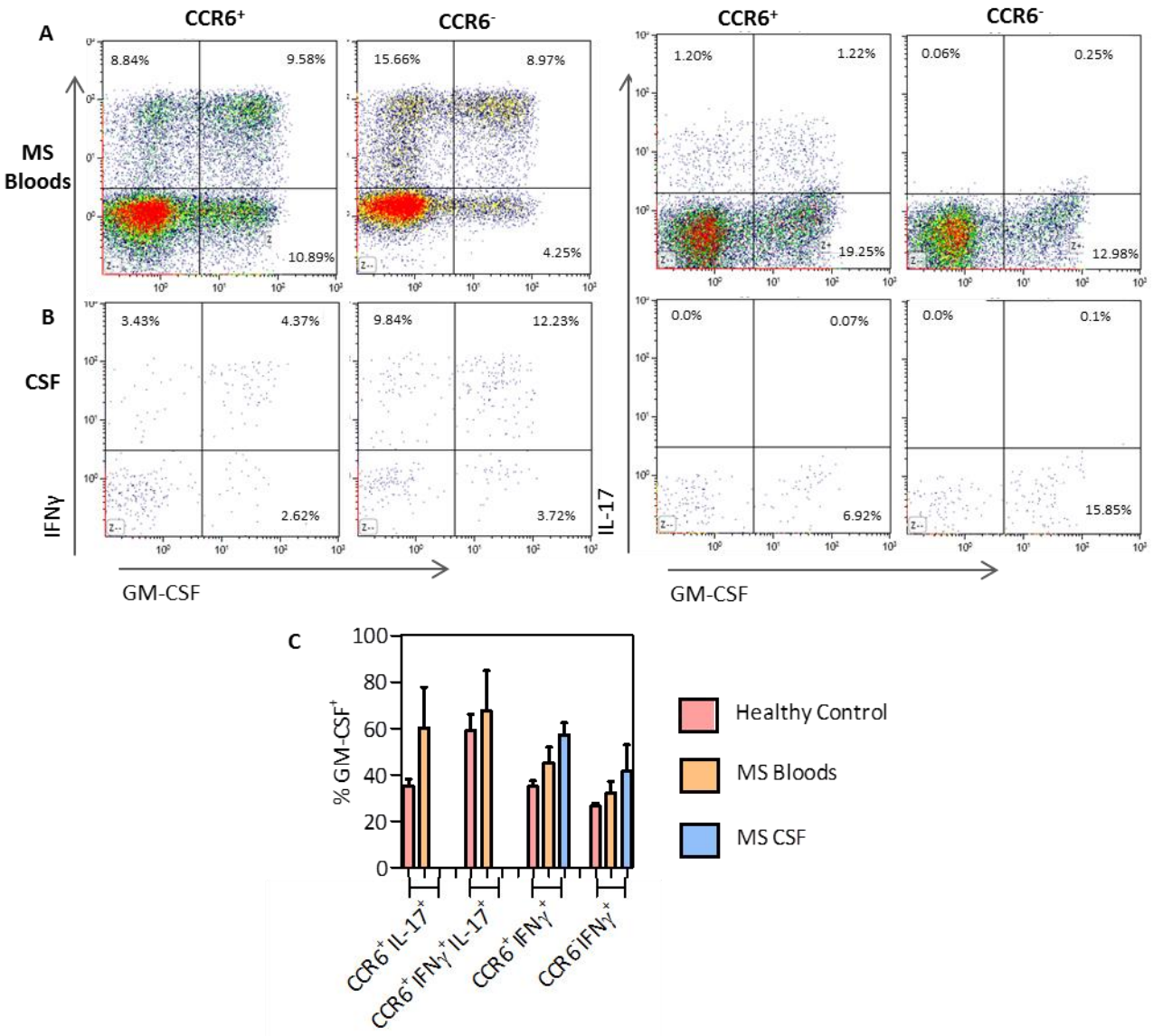

Figure 4.20 A proportion of CCR6+IFNγ+ cells express GM-CSF in the blood and CSF of MS patients. PBMC or cells were isolated from the blood and CSF from MS patients. The cells were stimulated with PMA and ionomycin for 3 hours along with Brefeldin A. Gated on CD4+CD45RO+ cells the expression of CCR6, IFNγ , IL-17 and GM-CSF Was analysed by intracellular flow cytometry. **(A)** Representative plot from the blood of MS patient **(B)** or cells from the CSF analysed the IFNγ and GM-CSF or IL-17 and GM-CSF secretion in the CCR6+ and CCR6- populations. **(C)** Analysis of the percentage of GM-CSF secreting cells in CCR6 expressing populations. n=2 MS Bloods and CSF, Healthy control n=4. Representative plots of one MS patient. Mean and standard error of the mean (SEM) shown on the graph.

4.10 Discussion

4.10.1 Is CD161 or CCR6 a Better Marker for T_H17 cells?

Within the literature CCR6 and CD161 are quoted as markers for T_H17 cells, although neither is solely specific to IL-17^+ cells. Within this study CCR6 was used to describe T_H1 cells with 'T_H17' characteristics. However Annunziato *et al*. use CD161 as a marker to identify these cells T_H1 cells. In $CD161^+IFN\gamma^+$ cells Annunziato demonstrated expression of T_H17 related genes[105]. The expression pattern of these genes was very similar to the gene expression data presented in this study in $CCR6^+IFN\gamma^+$ cells. This is to be expected as on T cells there is large overlap of expression of CD161 and CCR6.

From our experiments the vast majority of the $CD161^+CCR6^-$ population expressed IFNγ but no IL-17. The IFNγ MFI on these cells is greater than the IFNγ MFI on $CCR6^+$ cells. The difference characteristic of $CD161^+CCR6^-$ cells compared to $CCR6^+$ cells may suggest they are separate populations. This is something that would be worth investigating by isolating $CD161^+CCR6^-IFN\gamma^+$ and $CCR6^+CD161^-IFN\gamma^+$ cells and identifying if there were any differences in T-bet or RORC expression. The $CD161^+CCR6^-IFN\gamma^+$ population may have been why there was very little RORC expression found in $CD161^+$ cells (**Figure 4.3 D**). There are variations in the CD161 and CCR6 expression between donors. As the experiment was only done on one donor this particular donor might have had a large $CD161^+CCR6^-$ population. If this hypothesis is right, and $CD161^+CCR6^+$ cells do not express RORC, these cells would dilute the RORC signal of the $CD161^+CCR6^+$ population. From these data the CCR6 appears to be a better marker for T_H17 cells and cells with 'T_H17' gene expressions.

4.10.2 Similarities and Differences when Comparing CCR6^{+}IFNγ^{+} Cells to T_H17 and T_H1 Cells

The literature suggests that T_H1 cells that express the marker CD161 are derived from a T_H17 cell and are known as non-classical T_H1[105,213]. The hypothesis is that non-classical T_H1 cells have lost the ability to secrete IL-17 and instead secrete IFNγ. However, because of the transcriptional history, they maintain CD161 and RORC expression as well as other features of T_H17 cells. Within this chapter the phenotypic and functional characteristics of CCR6^{-}IFNγ^{+} cells and CCR6^{+}IL-17^{+} cells are compared to CCR6^{+}IFNγ^{+} cells. The aim was to identify similarities and differences in the different populations to try to better understand the CCR6^{+}IFNγ^{+} cell.

Wedderburn and Annunziato both showed that CD161^{+}IFNγ^{+} cells express IL-23R alongside RORC[105,213]. Annunziato went on to show that they also expressed other T_H17 related markers (IL4I1, IL-17RE and CCR6) to a greater extent than 'classical' T_H1 (CD161^{-}IFNγ^{+})[105]. Their paper did not show the expression of these genes compared to T_H17 cells. Although CCR6 was used in this study to identify 'non-classical' T_H1, the data presented in this chapter are very similar to Annunziato's work. The CCR6^{+}IFNγ^{+} cells have a significantly higher expression of RORC compared to CCR6^{-}IFNγ^{+} cells, with a comparable level of expression in both IL-17^{+} populations. This raises the possibility that RORC, either directly or indirectly, may be controlling the CCR6 expression. In RORγt$^{-/-}$ mice there is still CCR6 expression on T_H17 cells. However a RORγt/α$^{-/-}$ mouse does not express CCR6[216], suggesting RORα may control or be able to replace RORγt in controlling CCR6 expression. There is no evidence in

these mice of the effects on CCR6 expression in T_H1 cells. It has not been identified if the CCR6$^+$IFNγ$^+$ cells express RORα.

The expression level of CCR6 is lower on T_H1 cells compared to T_H17 cells. Nevertheless, the receptor is functional on CCR6$^+$IFNγ$^+$ cells. It was shown (**Figure 4.13**) that CCR6 expression was maintained in culture, though the expression level on T_H1 cells after culture was still at a lower level compared to T_H17 cells. CCR6 expression could not be induced on CCR6$^-$ cells, with the culture conditions tried. A non-coding region of the human CCR6 locus has been identified to be fully unmethylated in CCR6$^+$ lymphocytes. Even when the CCR6 expression was down regulated by TcR activation there was no alteration in the methylation status of this region, suggesting a level of stability in CCR6 expression. In cells where CCR6 expression had been induced the expression was unstable[217] due to the fact that the non-coding region was only partly demethylated. As the expression of CCR6 on the CCR6$^+$IFNγ$^+$ cells was stable, this suggests that the methylation status of non-coding region of the CCR6 gene was unmethylated.

At a transcriptional level there was expression of T-bet in all the IL-17$^+$ and IFNγ$^+$ CD4$^+$ T cells (**Figure 4.4**), although notably lower in the IL-17$^+$ cells compared to IFNγ$^+$ cells. As expected, when the protein expression of T-bet was analysed all the IFNγ$^+$ cells had high expression of T-bet (**Figure 4.5**). In the IFNγ$^-$ cells there was a gradual spread of expression of T-bet, not two distinct populations of T-bet$^+$ and T-bet$^-$ cells. This protein and PCR data suggests that most cells express some level of T-bet. IL-17 cells that express T-bet are said to be more pathogenic in an EAE model[218]. This raises the possibility that there is a spectrum of T-bet

expression in T_H17 cells. In the EAE model this gives the T_H17 cells that ability to induce worse EAE, highlighting the expression of T-bet can change the phenotype of these cells.

It is intriguing that the highest levels of T-bet are within the CCR6$^+$IFNγ$^+$IL-17$^+$ cell and CCR6$^+$IFNγ$^+$ cells. One possibility for this phenomenon may be that high T-bet expression is in response to competition with RORC. The CCR6$^+$IFNγ$^+$IL-17$^+$ cells may need a stronger T-bet presence to express IFNγ in a dominant T_H17 transcriptional phenotype. In the CCR6$^+$IFNγ$^+$ cells higher levels of T-bet may be needed to suppress the RORC transcriptional profile to prevent IL-17 expression. It would be interesting to investigate if a T_H17 phenotype would develop in a CCR6$^+$IFNγ$^+$ cells if T-bet was knocked-down.

There was also expression of IL-23R, IL4I1, but not IL-1R1 in CCR6$^+$IFNγ$^+$ cells at a transcriptional level. IL-23R expression by protein could not be detected in any IL-17$^+$ or IFNγ$^+$ cells *ex vivo.* IL-23 is an important cytokine in maintaining the T_H17 phenotype[73]. In CCR6$^+$IFNγ$^+$ cells the binding of IL-23 to IL-23R may be maintaining the RORC expression. T-bet has been proposed to directly affect IL-23R expression on T_H17 cells[219]. T-bet expression was found in both populations that expressed IL-23R. There was no detectable expression of IL-23R on CCR6$^+$IFNγ$^+$IL-17$^+$ cells. Conversely, in the literature IL-23R gene expression has been shown in IFNγ$^+$IL-17$^+$ cells[1,220], although both of these situations were after culture.

On naïve T cells the expression of IL-1R1 has been shown to be an important factor in the induction of a T_H17 phenotype[103]. The lack of IL-1R1 expression on the CCR6$^+$IFNγ$^+$ cells may be the reason why these cells cannot express IL-17, but due to their IL-23R can express other

T_H17 related genes such as RORC. It is important to determine if both IL-23R and IL-1R are functional on these cells.

A preliminary experiment was done to see if in culture with IL-23 there was any change in the cytokines expressed by CCR6$^+$IFNγ$^+$, CCR6$^-$IFNγ$^+$ and CCR6$^+$IL-17$^+$ cells. However, none of the populations were altered in culture with IL-23, compared to a culture with IL-7/IL-15 present. The CCR6$^+$IFNγ$^+$ cells, after culture, contained more IL-17 secreting cells compared to CCR6$^-$IFNγ$^+$ cells. Also after culture there were IL-17$^-$IFNγ$^+$ cells in the CCR6$^+$IL-17$^+$ population. It is very difficult, using the cytokine capture method, to be sure that a true homogeneous population has been isolated. This means that in these cultures (**Figure 4.15**) it cannot be rule out that the cells that have changed phenotype were not contaminating the original cell population.

IL-12Rβ2 was highly expressed on the CCR6$^+$IFNγ$^+$ cells. However the levels of IL-12Rβ2 were on the border of detection in the other subsets studied. This expression data mirrors Annunziato's data, as there was higher expression of IL-12Rβ2 in CD161$^+$IFNγ$^+$ cells compared to CD161$^-$IFNγ$^+$ cells[105]. The CCR6$^+$IFNγ$^+$ cells may need to be responsive to IL-12 to maintain the T-bet expression as there could possibly be competition with the RORC transcriptional programme. In comparison the reason there may be very little IL-12Rβ2 expression in the CCR6$^-$IFNγ$^+$ cell is they express no RORC and so do not require IL-12 signalling to stabilise T-bet expression. IFNγ$^+$IL-17$^+$ cells have been shown to be induced from T_H17 cells by IL-12 [1]. However, the data presented in **Figure 4.7 A** suggests at a

transcriptional level there is very little IL-12Rβ2 expression on these cells. It is not known if the receptor is down regulated on the dual secreting cells once IFNγ expression is induced.

The expression of the gene IL4I1, which codes for the secreted protein L-phenyl-alanine oxidase, is associated with reduced proliferative ability specifically in T_H17 cells[104]. The expressions of this molecule at a gene level in all the CCR6$^+$ populations led to an investigation into whether its expression affected the proliferation of CCR6$^+$IFNγ$^+$ compared to CCR6$^-$IFNγ$^+$ cells. It was not possible to directly isolate CCR6$^+$IFNγ$^+$ cells as cytokine capture involves PMA/Ionomycin stimulation, which has been shown to overcome the effects of IL4I1 on proliferation. Instead, CCR6$^+$ and CCR6$^-$ cells were isolated. Anti-CD3/CD28 stimulating antibodies were used and their proliferative ability compared. Annunziato *et al* isolated the CD161$^+$IFNγ$^-$IL-17$^+$ population and showed there was a significant reduction in proliferation compared to CD161$^-$IFNγ$^+$IL-17$^-$ cells[104]. However, in the culture conditions used in this study there was very little difference in the proliferative ability of CCR6$^+$ and CCR6$^-$ populations. This discrepancy may have been due to the strength of the stimulation used. PMA/ionomycin stimulation is strong enough to overcome the effects of IL4I1 which may have occurred with the amount of anti-CD3/28 used in this study.

The CCR6$^+$IFNγ$^+$ cells do not express other T_H17 related cytokines, such as IL-22, IL-21 and IL-17F, to the same degree as T_H17 cells. This suggest that based on this cytokine co-expression data the CCR6$^+$IFNγ$^+$ cells are more like T_H1 than T_H17 cells. In contrast, due to the expression of RORC, IL-23R and IL4I1, transcriptionally the CCR6$^+$IFNγ$^+$ cells have some features of T_H17 cells.

4.10.3 Are CCR6$^+$T$_H$1 Cells 'ex-T$_H$17' or T$_H$1 Cells with T$_H$17 Phenotypic Characteristics?

There is a murine fate mapping model that suggest that the transition of a T$_H$17 to a T$_H$1 cell is possible in response to specific inflammatory cues. IL-17 expressions induced the expression of YFP in the T cells. After the induction of EAE there were cells that were negative for IL-17A protein, positive for YFP and secreted IFNγ. Conversely, these cells were not found when the mice were infected with *Candida albicans,* a resolving model of inflammation. Within the paper the level of IL-17 gene expression that was needed to activate the YFP expression was not determined. This means that there is no evidence that the YFP$^+$ cells had been truly committed to a T$_H$17 lineage, and not just transiently expressed IL-17, before switching on IFNγ expression.

In humans it is not possible to map the development of T$_H$17 cells. *In vitro* there have been experiments demonstrating IFNγ expression can be induced in T$_H$17 cells, but IL-17 expression cannot be induced in T$_H$1 cells[221] . Wedderburn and Annunziato both suggest that CD161 in humans is a marker that tracks the passage of T$_H$17 cells to a T$_H$1 phenotype. Both these papers identify RORC expression in CD161$^+$T$_H$1 cells[105,213]. No significant expression of RORC was found in CD161$^+$IFNγ$^+$ cells in this study, although no conclusions can be drawn from this as it was from one donor. As mentioned in **Section 4.10.1** there is variation in the percentage of cells expressing CD161 and CCR6 between donors. There might have been very few CCR6$^+$ cells within the CD161$^+$ population within this donor, resulting in a reduced RORC signal.

Wedderburn cultured CD161$^+$T$_H$17 cells with IL-12 and the cells were induced to secrete IFNγ, with a small population only secreting IFNγ. They showed that all these cells still expressed CD161. It is difficult with this type of work to ensure there is no contamination of the IFNγ$^+$ cells in the population before culture. Wedderburn *et al* analysed the TcR sequence of one donor in the different populations. The data showed shared sequences between CD161$^+$IFNγ$^+$ cells and CD161$^+$IL-17$^+$ cells. Their repertoire overlap was relatively low[213]. This is something that could be interesting to identify if CCR6$^+$IFNγ$^+$ and CCR6$^+$IL-17$^+$ cells had similar TcR sequences, although it is not a conclusive test as there are situations in which different subsets can share TcR. An example of this is when one cell divides and the two cells differentiated down different lineages.

Overall there has not been conclusive evidence in humans that a T$_H$17 cell can convert to become a full T$_H$1 cell, that either expresses CD161 or CCR6. The data reported here cannot support or refute the hypothesis that CCR6$^+$IFNγ$^+$ cells are ex-T$_H$17 cells. To support the idea that CCD6$^+$IFNγ$^+$ were related to T$_H$1 cells there is a correlation in the percentage of CCR6$^+$IFNγ$^+$ cells and CCR6$^-$IFNγ$^+$ cells in both healthy controls and MS patients. However the data reported here does not prove this. It would be interesting to further look, at a transcriptional level, at the CCR6$^+$IFNγ$^+$ cells. Methylation of genes can, in some cases, be an indicator of the history of the cells. An example of this is the methylation status of the FoxP3 gene, which can identify if a cell was a natural T$_{REG}$ of inducible T$_{REG}$[132,222]. It would be interesting to investigate the methylation status of IL-17 within CCR6$^+$IFNγ$^+$ cells compared to CCR6$^+$IL-17$^+$ and CCR6$^-$IFNγ$^+$.

4.10.4 Multiple Sclerosis

CCR6 is a vital molecule for the induction of EAE, in that inflammatory T cells use CCL20 to migrate across the choroid plexus[157]. It is unknown if this is also the case in MS. T_H17 cells switch on IFNγ production in a chronic inflammatory environment[145,147]. The link that was suggested between non-classical T_H1 (CD161^{+}IFNγ^{+} or CCR6^{+}IFNγ^{+}) and T_H17 cells led to the hypothesis that CCR6^{+}T_H1 cells may be present in MS.

We have shown there is a significant enrichment of CCR6^{+} T_H1 cell in the CSF of MS patients compared to peripheral blood. Furthermore CCR6^{+}IFNγ^{+} cells were significantly enriched within the CSF fluid compared to matched blood. There could have got there in at least three possible ways. Firstly, CCR6 dependent migration is said to be the first wave of migration of inflammatory cells into the CNS. The data presented in Chapter 4 showed that at least in healthy blood these cells have the potential to migrate towards CCL20 to a similar extent as T_H17 cells. In a CCR6$^{-/-}$ model of EAE there is a reduction in both IL-17 and IFNγ production by the cells in the brain, which is only restored with the introduction of wild-type CD4^{+} T cells[157]. These data suggest that CCR6 dependent migration of IFNγ cells into the CNS is possible.

Secondly, the cells could have differentiated from T_H17 cells that were already present in the CSF. To determine if this was the case the TcR pattern could be sequenced, to determine the overlap of TcR sequences in CCR6^{+}T_H1 and CCR6^{+}T_H17 cells.

Thirdly, the cells could have migrated in the secondary wave of cells, independently from CCR6. This would be dependent on CCR6^{+}T_H17 cells migrating in to the CNS. Unfortunately

these patients were most likely in the relapsing-remitting stage of MS so there has most likely been inflammation in the CNS for a while. There are $CCR6^{-}$ cells present in all the CSF samples suggesting that the BBB is already letting cells into the CNS through other migratory pathways.

It has been published that there is an expansion in the percentage of T_H17 cells within the CSF in relapse in MS patients, which is not seen in the blood [223]. Unfortunately in this study due to timing and logistics by the time the lumber puncture samples are taken for analyses of the CSF the patients are most likely back in remission. This could be why there were virtually undetectable levels of T_H17 cells. It would be intriguing to see if there was an expansion in the percentage of $CCR6^{+}T_H1$ in relapse as well as T_H17 cells, to suggest a common differentiation factor.

Correlations between the cells within the CSF shown there may be a developmental relationship between $CCR6^{+}IFN\gamma^{+}$ and $CCR6^{-}IFN\gamma^{+}$. There was no correlation between $CCR6^{+}IFN\gamma^{+}$ and $CCR6^{+}IL\text{-}17^{+}$ cells. However, because there were so few cells that expressed IL-17 in CSF any conclusions drawn from this data may be unreliable.

The data presented in this chapter highlights that GM-CSF can be produced by the $CCR6^{+}IFN\gamma^{+}$ and $CCR6^{-}IFN\gamma^{+}$ $CD4^{+}$ cells within the CSF of MS patients. In $CSF2^{-/-}$ mice, that cannot produce GM-CSF, there is a reduced morbidity within an EAE model. In another murine model $IL\text{-}17^{-/-}IFN\gamma^{-/-}$ MOG-specific T cells were introduced into a wild type mice and EAE was induced[201]. This data suggested that the cells induced disease through their production of GM-CSF.

The production of GM-CSF by T_H17 cells is part of an amplification loop for inflammation. T-bet is proposed to induce IL-23R expression in T_H17 cells[219]. IL-23 induces GM-CSF production in T_H17 cells and in turn the GM-CSF induces IL-23 expression in APC. Microglial cell activation has been shown to be GM-CSF dependent which is important for the induction of EAE[202]. It was thought that GM-CSF in T_H17 cells was dependent on RORγt[201], however RORγt$^{-/-}$ mice can secrete GM-CSF. T_H17 cells that express T-bet have the potential to secrete IFNγ and it has been postulated that these are the pathogenic T cells. TGF-β3 and IL-6 are thought , independently of IFNγ, to be able to induce a 'pathogenic' T_H17 cell phenotype and induce EAE in mice[174]. IL-1β and IL-6 are said to induce T_H1 and T_H17 cells to secret GM-CSF[173].

All of this data on GM-CSF uses an EAE model which is known to be strongly T_H17 biased. It is important to recognised the there is a possibility of T_H1 cells playing a role in the pathogenesis of this disease. If this is overlooked therapies to target T_H17 cells might fall short of expected therapeutic value as it is not also treating T_H1 cells based pathologies. This data set needs to be repeated on more donors but clearly shows that T_H1 cells, both CCR6$^-$ and CCR6$^+$, will be a source of GM-CSF within the CNS.

In summary this study highlights that CCR6 expression on T_H1 cells distinguishes a stable population of T_H1 cells expressing parts of a T_H17 transcriptional programme. There is no direct evidence that these CCR6$^+$$T_H1$ cells develop from either a T_H1 or T_H17 background. Further work is needed to determine the heritage of these cells. Within the CSF of MS patients there is a statistical increase in the percentage of CCR6 cells compared to matched

blood. Furthermore, there are statistically a higher percentage of $CCR6^{+}IFN\gamma^{+}$ cells within the CSF compared to the peripheral blood of MS patients. These cells are a source of GM-CSF within the CNS, which raises the possibility that these cells contribute to the pathogenesis of MS.

CHAPTER 5

MICRO-RNA EXPRESSION IN CCR6$^+$T$_H$1 CELLS IN COMPARISON TO CCR6$^-$T$_H$1 and CCR6$^+$T$_H$17 CELLS

5.1 Introduction

MicroRNAs are small, endogenous, non-coding molecules that alter the expression of genes post-transcriptionally by targeting mRNA for degradation. Research into these conserved molecules has uncovered several fundamental cellular processes that are controlled by microRNAs including cell proliferation, differentiation and death. As a result, microRNAs have been directly implicated in the development and progression of human diseases, including cancer and autoimmune diseases. The critical regulatory role of microRNAs suggests they offer an enormous potential for therapeutic targeting.

MicroRNAs have been shown to play a particularly important role in relation to T$_H$17 cells, especially in their differentiation. The microRNA miR-326 mediates T$_H$17 differentiation through inhibiting the expression of a negative regulator of T$_H$17 differentiation (Ets-1)[194]. However, currently there is no known role for microRNAs in CD4$^+$ T$_H$ plasticity.

Within this chapter the aims are to:

- identify microRNAs that are differentially expressed in CCR6$^+$IL-17$^+$, CCR6$^+$IFNγ$^+$IL-17$^+$ cells compared to CCR6$^+$IFNγ$^+$ and CCR6$^-$IFNγ$^+$ cells and that may play a role in controlling the T$_H$17/RORC or T$_H$1/T-bet phenotype.
- identify microRNAs that are differentially expressed in CCR6$^+$IL-17$^+$, CCR6$^+$IFNγ$^+$IL-17$^+$ and CCR6$^+$IFNγ$^+$ cells compared to CCR6$^-$IFNγ$^+$ cells and that may play a role in controlling the CCR6 phenotype.
- identify microRNAs that are differentially expressed in CCR6$^+$IL-17$^+$ compared to CCR6$^+$IFNγ$^+$IL-17$^+$, CCR6$^+$IFNγ$^+$ and CCR6$^-$IFNγ$^+$ cells than may play a role in controlling the IFNγ expression.

There were two major challenges to achieving these aims. Firstly as the cell populations *ex vivo* are relatively rare, only a small quantity of RNA material was available. Secondly, there are now many hundreds of miRNAs that have been identified. This would have limited us to only analysing a few miRNAs.

These challenges were overcome using a method of amplification of material using microfluidic cards, which made it possible to screen the expression levels of 384 miRNAs. The amplification used miRNA specific primers to amplify up only the required transcripts. A microfluidic card is a 384 well card in which TaqMan miRNA Assays have been dried in the array well. Up to 8 cDNA samples per array can be added to 8 loading ports, allowing delivery of a single sample-specific reaction mix to 48 wells. Within this screen one microfluidic card was used per sample.

5.2 Data Analysis

5.2.1. Normalising the Data

From total PBMC from 3 different donors the CCR6$^+$IL-17$^+$, CCR6$^+$IL-17$^+$IFNγ$^+$, CCR6$^+$ IFNγ$^+$, and CCR6$^-$IFNγ$^+$ populations were isolated using cytokine capture and cell sorting (**Figure 4.4 A**).

For the three different donors **Figure 5.1** shows the spread of cycle values (Cp) across each subset. A cycle value limit of 40 was chosen as a cut off for miRNAs that were below the detection limit. The range was similar for most samples suggesting a good spread of expression levels in each subset. The CCR6$^+$IFNγ$^+$IL-17$^+$ population in Donor 3 does appear to have a very short range of expression suggesting either that this sample did not amplify well or that the quality of amplification was not optimum. However the two other CCR6$^+$IFNγ$^+$IL-17$^+$ populations from the other donors have a good spread of Cp values. The red line in **Figure 5.1** indicates the average expression of the endogenous control, which in this experiment was U6 snRNA. This is a small non-coding nuclear RNA component of U6 snRNP (small nuclear ribonucleoprotein), part of a larger complex involved in splicing pre-mRNA. There is a large variability in the expression levels of the endogenous control, suggesting that this is possibly not a good control to use.

To analyse the similarity of the expression levels between the different subsets, correlation plots between each subset were produced. **Figure 5.2** is these plots from a representative donor. There is a strong positive correlation between the expressions for the miRNAs in each subset. The coefficient of determination **(**R^2) value gives a measure of the relative

association between different samples. R^2 values of 1 means the samples exactly matched to each other. All the correlations were significant, with R^2 values of 0.59 and above. However on some of the correlation graphs there is a shift away from the line for one population (e.g. in **Figure 5.2** between CCR6$^-$IFNγ$^+$ and CCR6$^+$IL-17$^+$ there is a shift to the right of the line). Any spot that is not on the line means that there is a differential expression. If the samples were not normalised, this would mean that all the miRNA would be more highly expressed in one sample.

The average expression of the endogenous control was initially used to normalise the Cp values. This was done to account for variation introduced to the system between samples and between runs. By using this endogenous control there is an assumption that the expression of U6 snRNA is in no way different between the different subsets. The box and whisker diagrams after normalisation shows that the process has introduced more variation in the range of the samples (**Figure 5.3**). These box and whisker plots are representative of all the samples run.

Figure 5.4 shows representative correlation plots of the different subsets for Donor 1. There was very little difference in the correlation of the normalised samples compared to the unaltered samples.

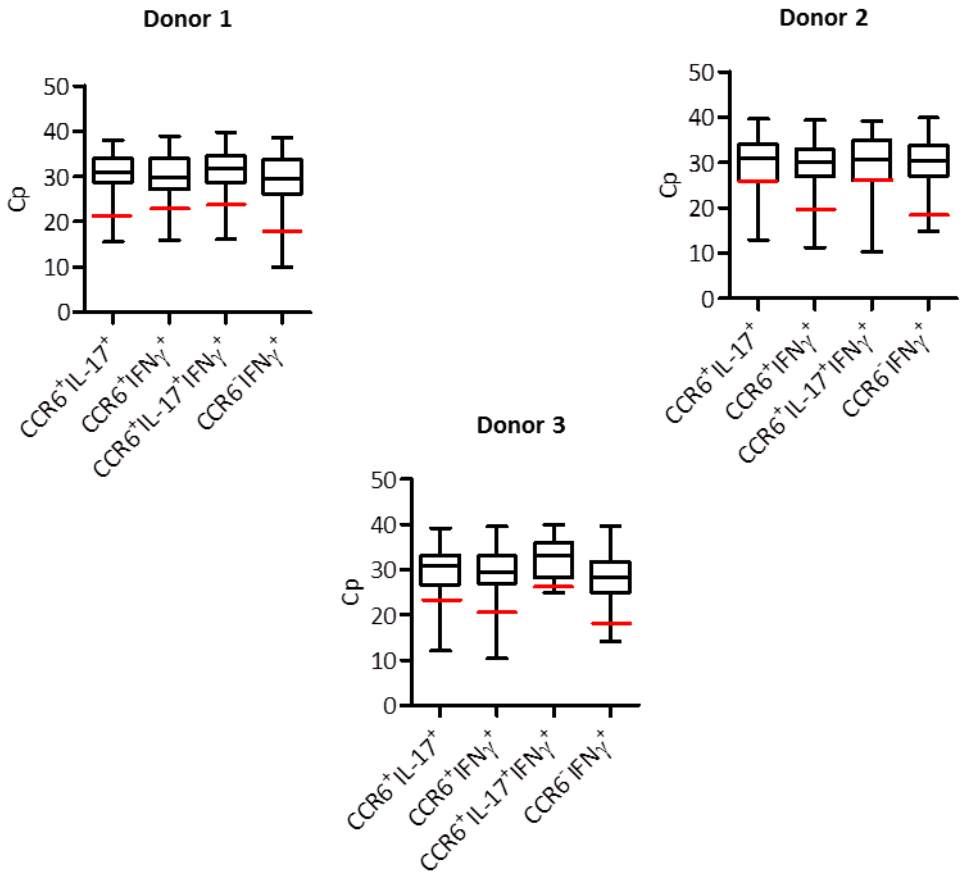

Figure 5.1. Cycle value (cp) of 384 miRNAs in CD4^{+} T$_{H}$1 and T$_{H}$17 subsets The maximum, minimum, median and interquartile range for the Cp of 384 miRNAs expressed in CCR6^{+}IL-17^{+} CCR6^{+}IFNγ^{+}IL-17^{+}, CCR6^{+}IFNγ^{+} and CCR6^{-}IFNγ^{+} populations, from 3 different donors. Red line represents the average Cp for reference gene in each subset.

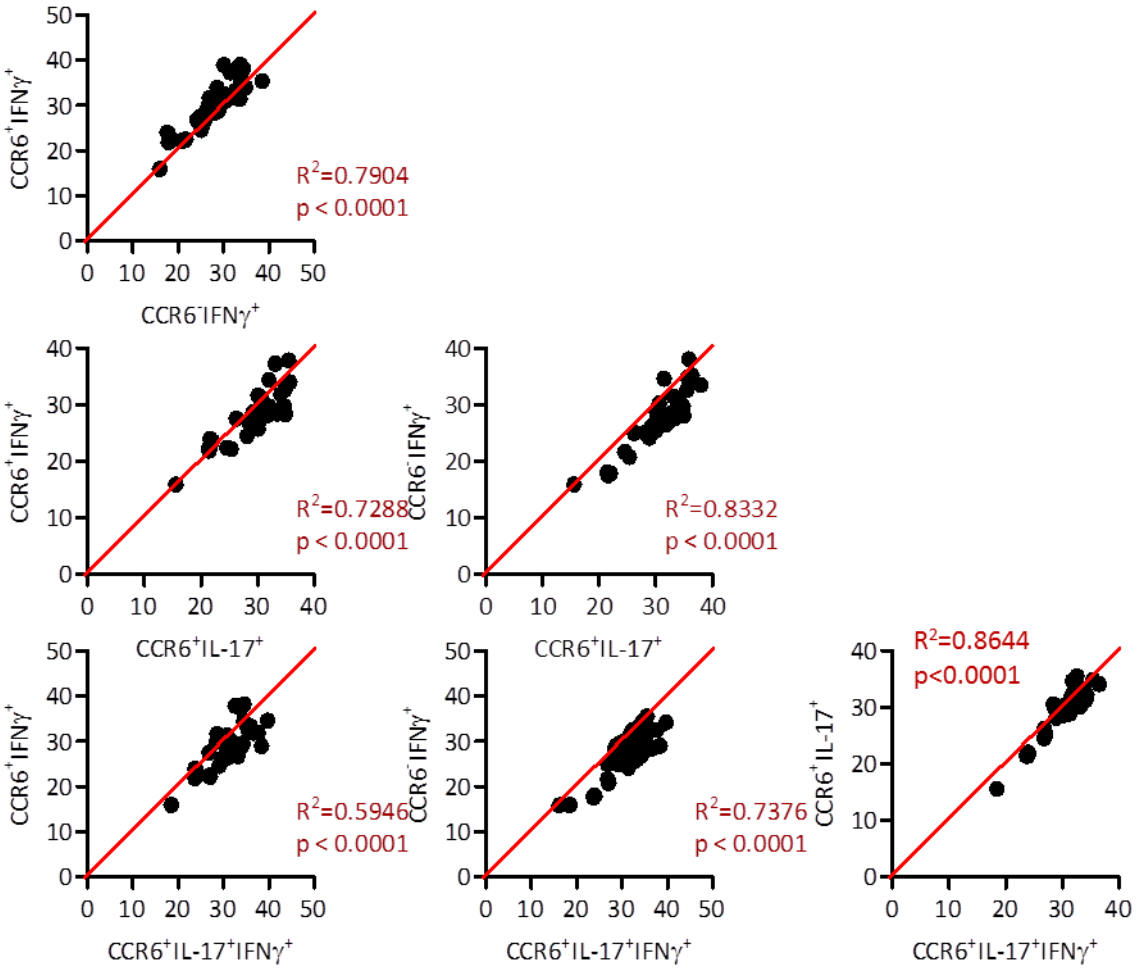

Figure 5.2. Correlation of the cycle value of the detectible miRNAs between T$_H$ populations, before normalisation. The Cycle values (Cp) were determined for CCR6$^-$IFNγ$^+$, CCR6$^+$IFNγ$^+$, CCR6$^+$IL-17$^+$ and CCR6$^+$IFNγ$^+$IL-17$^+$ cells for 384 miRNA. Using a microarray. The expression of detectible miRNA for each population was plotted against each of the other populations to determine if there was a correlation of miRNA expression between the groups. Plots from Donor 1, representative of 3 different donors. To analyse the level of correlation a Pearson's two tails correlation was undertaken, p value and R^2 shown in red. Red line is reference in which x=y.

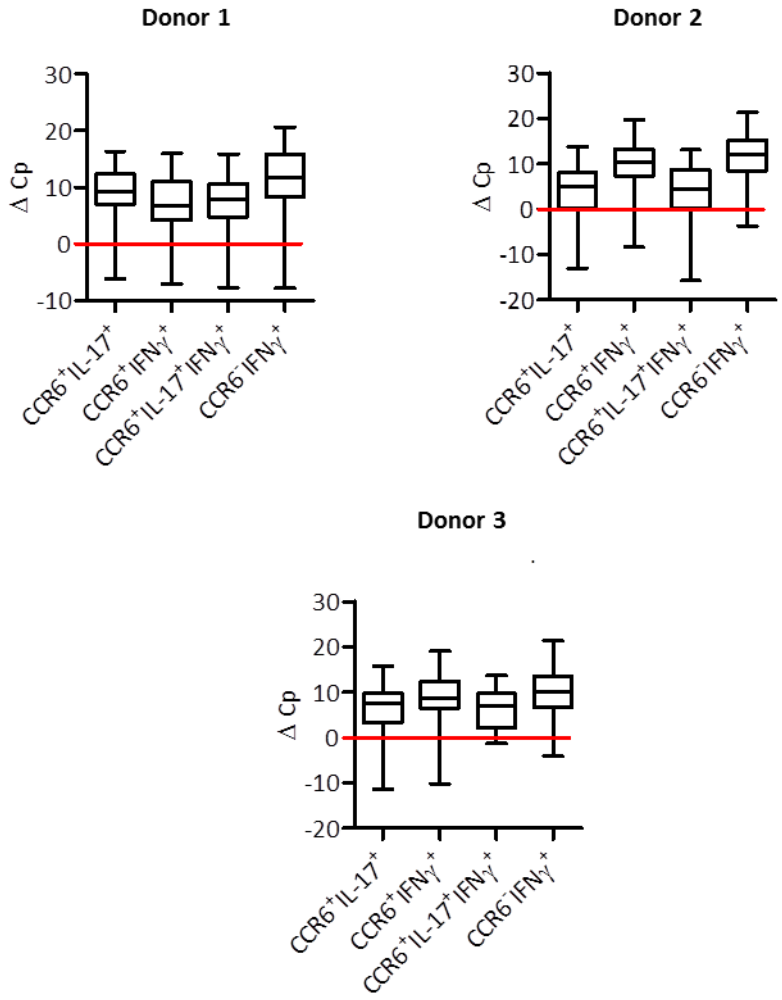

Figure 5.3. Analysis of 384 miRNA expressed in CCR6 expressing samples, normalised to the reference genes U6 snRNA The maximum, minimum, median and interquartile range for the Cycle value (Cp) of 384 miRNAs expressed in CCR6^{+}IL-17^{+} CCR6^{+}IFNγ^{+}IL-17^{+}, CCR6^{+}IFNγ^{+} and CCR6^{-}IFNγ^{+} populations from 3 different donors. Values normalised to average Cp of the reference gene (ΔCp) . (n=4 for the reference on same plate)

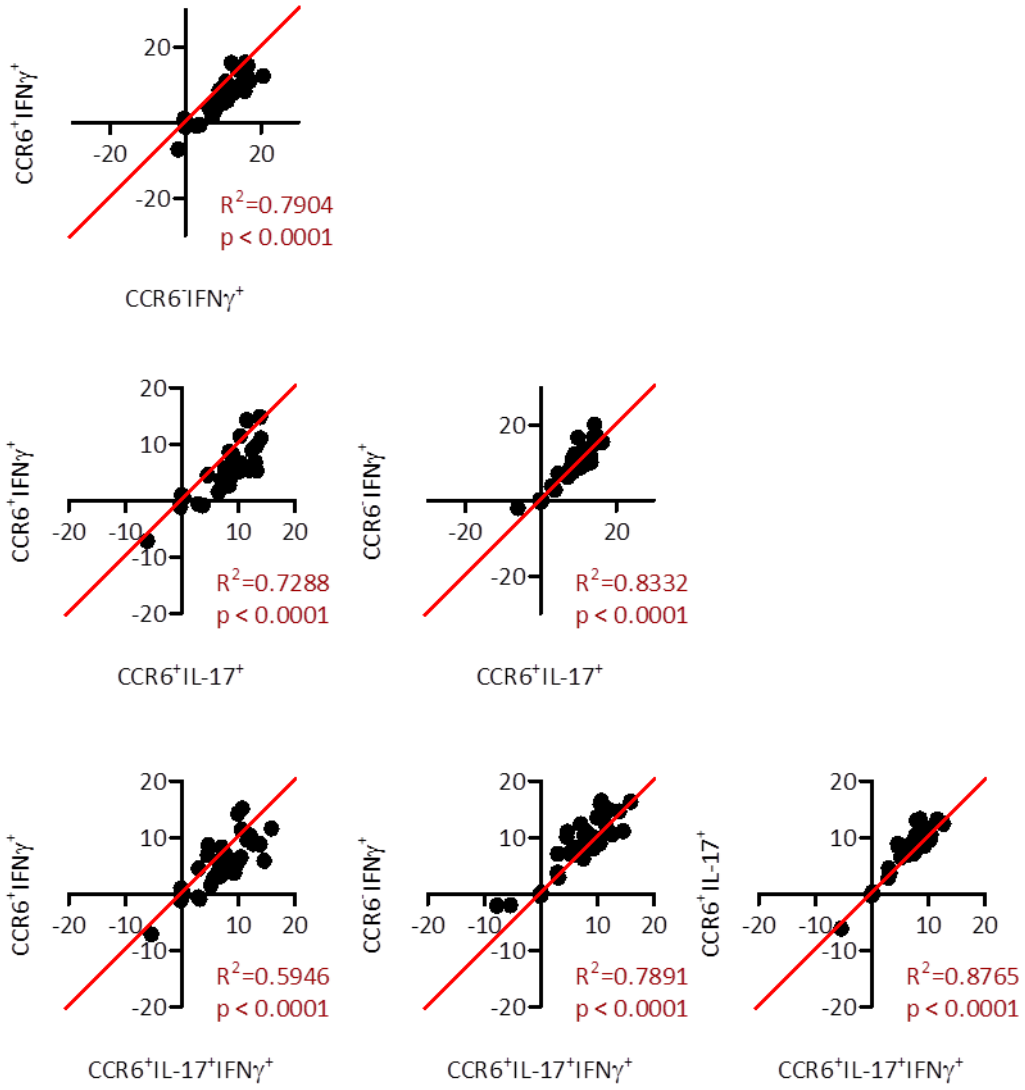

Figure 5.4. Correlation of 384 miRNA normalised using average of reference genes U6 snRNA: Correlation of the normalised cycle value (ΔCp) with the reference gene Plots from donor 1, representative of 3 different donors. To analyse the level of correlation a Pearson's two tails correlation was undertake, p value and R^2 shown in red.

A second way to normalise the samples was tested to identify if this was more appropriate than the endogenous control. The median of all the Cp values for a sample was used to normalise the sample. The box and whisker plots showed that there was more uniformity in the range for the samples **(Figure 5.5)**. The correlations between each samples for each donor show a small improvement, shown by the R^2 value being closer to 1. Representative correlations plots for Donor 1 are shown in **Figure 5.6.** Because of this reduced variation in the range of expression, it was decided use data that was normalised with the median Cp in the analysis.

5.2.2 Differential Expression Between Subsets

To identify the miRNAs of interest that were differentially expressed between the different subsets the relative expression (E) was analysed (**Appendix**). The difference in normalised Cp between each combination of subsets was analysed (ΔCp). The relative difference for each miRNA was calculated ($2^{-\Delta Cp}$). The miRNAs that were differentially expressed more than two fold between the subsets were selected ($0.5 \leq E \leq 2$). The selected miRNAs were then manually checked to confirm that there was detectable expression of the miRNA in more than two replicates. This gave a list of 79 miRNA that were differentially expressed between the different subsets (**Appendix**).

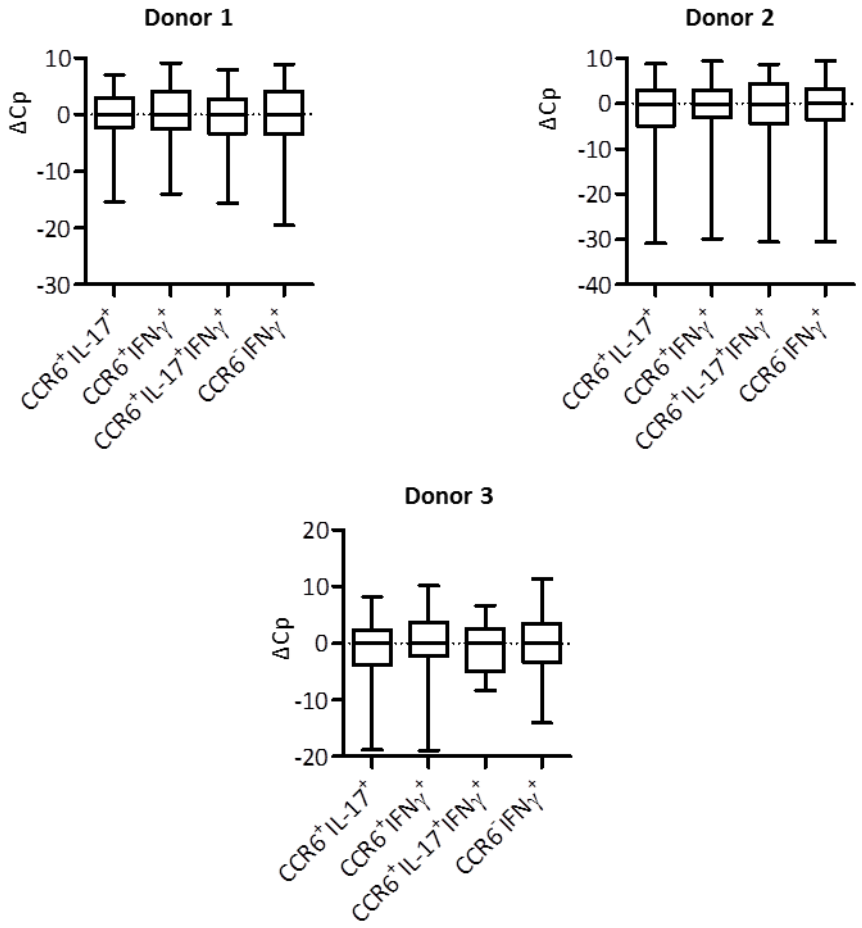

Figure 5.5. Analysis of 384 miRNA expressed in CCR6 expressing samples, normalised with median value of all Cp. The maximum, minimum, median and interquartile range for the Cycle value (Cp) of 384 miRNAs expressed in CCR6^{+}IL-17^{+} CCR6^{+}IFNγ^{+}IL-17^{+}, CCR6^{+}IFNγ^{+}, CCR6^{-}IFNγ^{+} populations from 3 different donors. Values normalised with median Cp value of the subset (ΔCp).

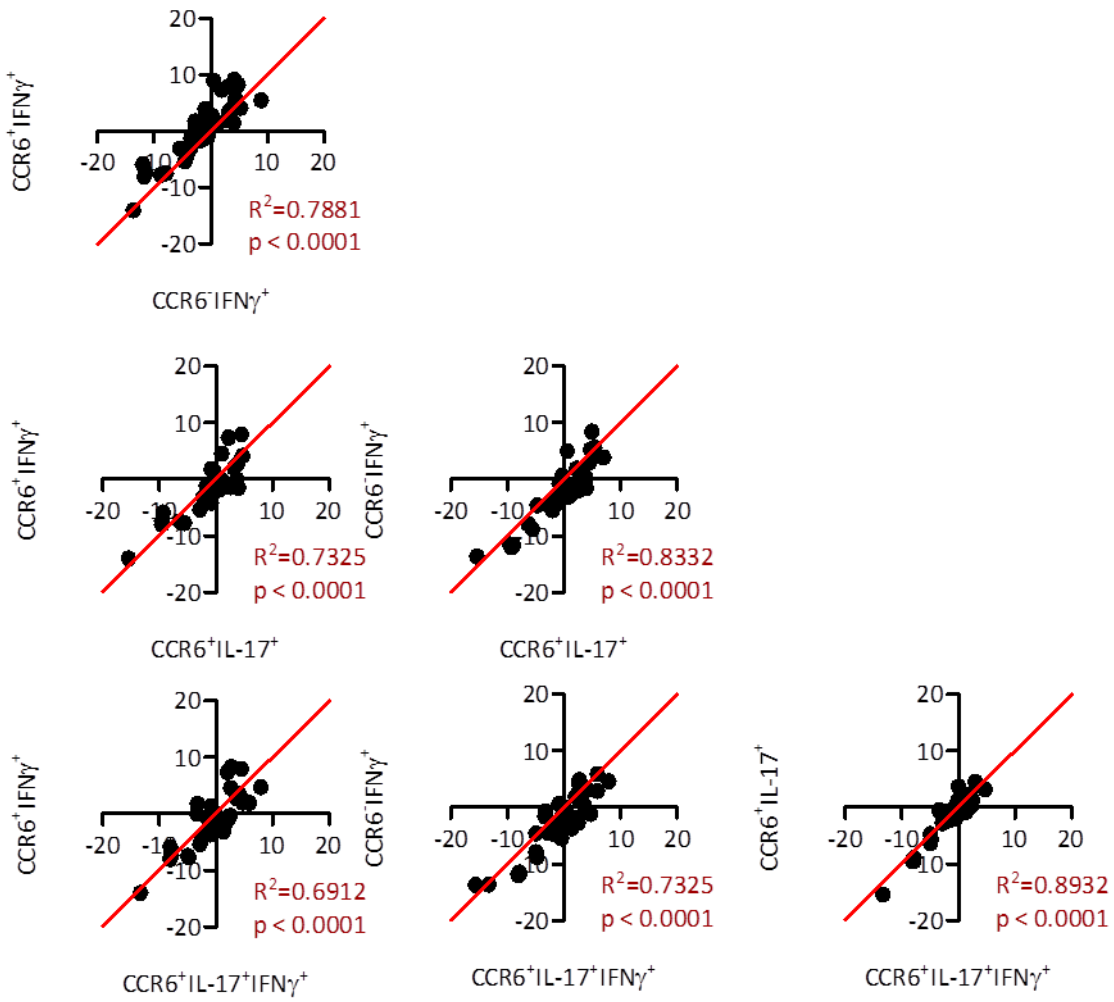

Figure 5.6. Correlation of 384 miRNA normalised to the median. Correlation of Cycle value (Cp) normalised with the median Cp for miRNA expression within the different subsets. Plots from donor 1, representative of 3 different donors. To analyse the level of correlation a Pearson's two tails correlation was undertake, p value and R^2 shown in red.

5.3 MicroRNAs Highlighted as Playing a Role in T Helper Differentiation

Within the list of 79 miRNAs of interest were several that have previously been associated in the literature with T$_H$17 or T$_H$1 cell differentiation. Three miRNAs, miR-155, miR-150, and miR- 146a[193], which play a role in lymphocyte activation and differentiation, all came up in the screen. miR-155 has been shown the inhibit IFNγ signalling[193] and when knocked out in mice with EAE leads to a reduction in the severity of the disease[192,224,225]. The miR-155 T$_H$17 cells were shown to be hypo-responsive to IL-23 and had increased expression of the transcriptional repressor Ets-1 which reduced their pathogenic potential in EAE[224]. For effective T$_{REG}$ effectively suppression of T$_H$1 cells miR-146a is an important miRNA, possibly due to effects on STAT-1[226], a direct target. With STAT-1 being an important factor in T$_H$1 induction and maintenance this microRNA could be important in T$_H$ cell induced inflammation. Within this study there was expression of these three miRNAs within the CCR6$^-$IFNγ$^+$, CCR6$^+$IL-17$^+$ and CCR6$^+$IFNγ$^+$ populations. The highest expression among them was within the CCR6$^-$IFNγ$^+$ population. CCR6$^+$IFNγ$^+$ cells had roughly half the expression, and the CCR6$^+$IL-17$^+$ cells had reduced expression again (**Figure 5.7 A)**. CCR6$^+$IFNγ$^+$IL-17$^+$ and CCR6$^+$IL-17$^+$ cells had a similar level of expression of miR-150. There was no detectable expression of miR-155 or miR-146a within the CCR6$^+$IFNγ$^+$IL-17$^+$ cells.

miR-181a was only detectable in CCR6$^-$IFNγ$^+$ cells, though at a very low level (**Figure 5.8 C)**. miR-181 has been associated with modulating TcR sensitivity to antigen[227]. The cluster of 6 microRNAs (miR-17-92, comprising miR-17, miR-18a, miR-20a, miR-19a, miR-19b-1, and miR-92a-1) have been associated with the control of proliferation in cells[189]. Within this screen miR-17, miR-19a, miR19b and miR92a were identified as differentially expressed. The

highest expression for all these miRNAs was within the CCR6^{-}IFNγ^{+} population, with a lower but detectable expression within the CCR6^{+}IFNγ^{+} cells. In most cases there was low but detectable expression of the microRNAs within the CCR6^{+}IL-17^{+} population, and only miR-19b and miR-92a had detectable expression within the CCR6^{+}IFNγ^{+}IL-17^{+} population (**Figure 5.7 B**).

Expression of miR-29a, b and c were all found in both T$_{H}$1 subsets. It is involved in the regulation of T-bet and IFNγ expression[191] (**Figure 5.7 A**). There are also several microRNAs that are associated with T$_{H}$17 cell phenotype. miR-21 and miR-301 were both, along with miR-155, shown to play a role in T$_{H}$17 cells differentiation in response to MOG antigen[195]. However, neither of these miRNAs was present in this screen at detectible level the IL-17 secreting populations. MicroRNA-21 was detectible in CCR6^{+}IFNγ^{+} and CCR6^{+}IFNγ^{+} cells, whereas miR-301 was barely detectable in any of the different subsets (**Figure 5.8 B**).

In mice overexpression of has-let-7e enhanced T$_{H}$1 and T$_{H}$17 cells and aggravated EAE[228]. Within the data set there was only expression of has-let-7e within the CCR6^{+}IFNγ^{+} and CCR6^{-} IFNγ^{+} populations (**Figure 5.8 D)**.

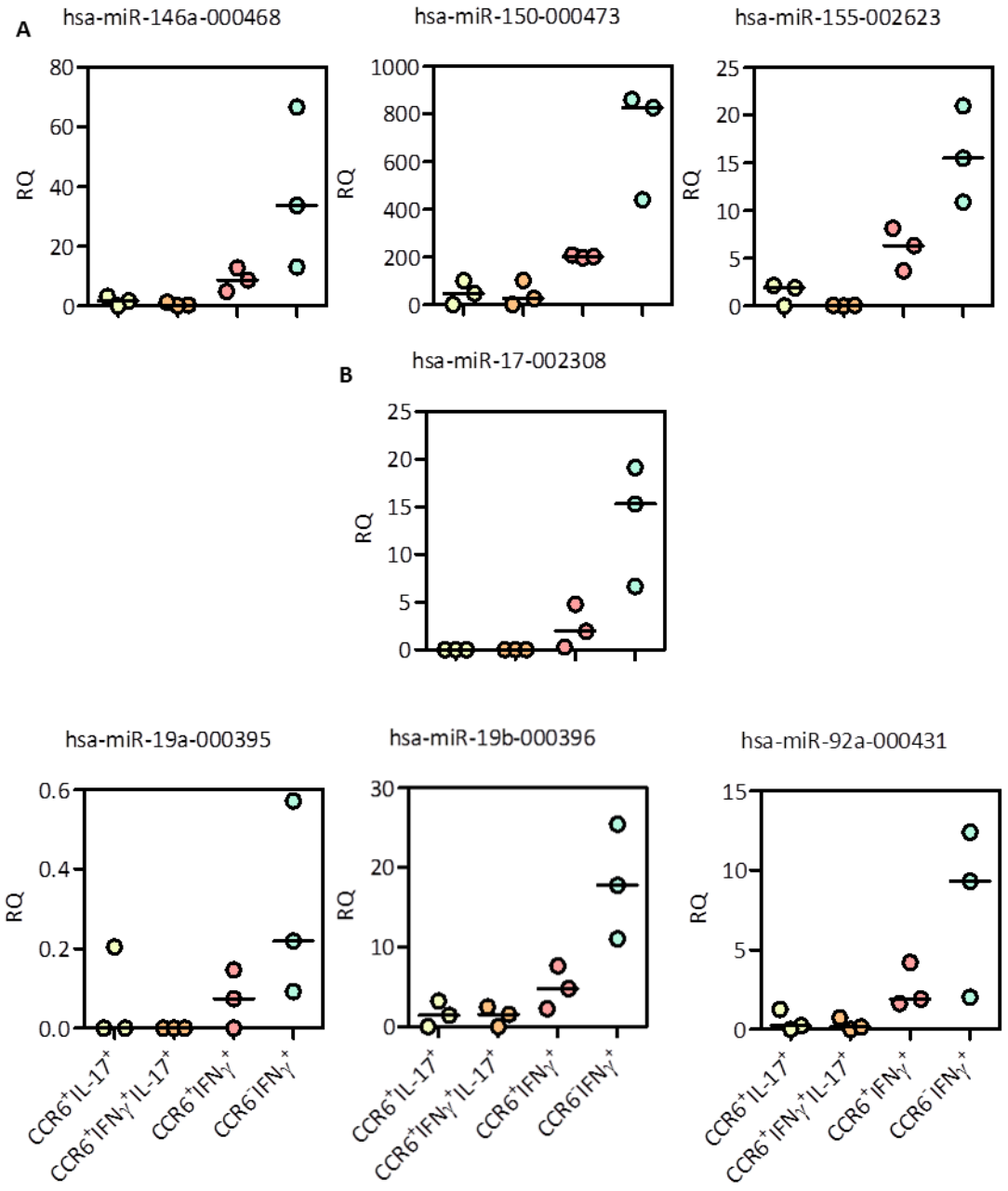

Figure 5.7 Known miRNAs involved in T helper cell differentiation, that were differentially expressed in CCR6$^+$IL-17$^+$ CCR6$^+$IFNγ$^+$IL-17$^+$, CCR6$^+$IFNγ$^+$ and CCR6$^-$IFNγ$^+$ cells. Relative Quantity (RQ) expression of miRNAs within CCR6$^+$IL-17$^+$ CCR6$^+$IFNγ$^+$IL-17$^+$, CCR6$^+$IFNγ$^+$, CCR6$^-$IFNγ$^+$ populations. RQ is the cycle value (Cp) normalised to the median Cp of all the miRNAs from one run. Line represents median RQ value. n=3

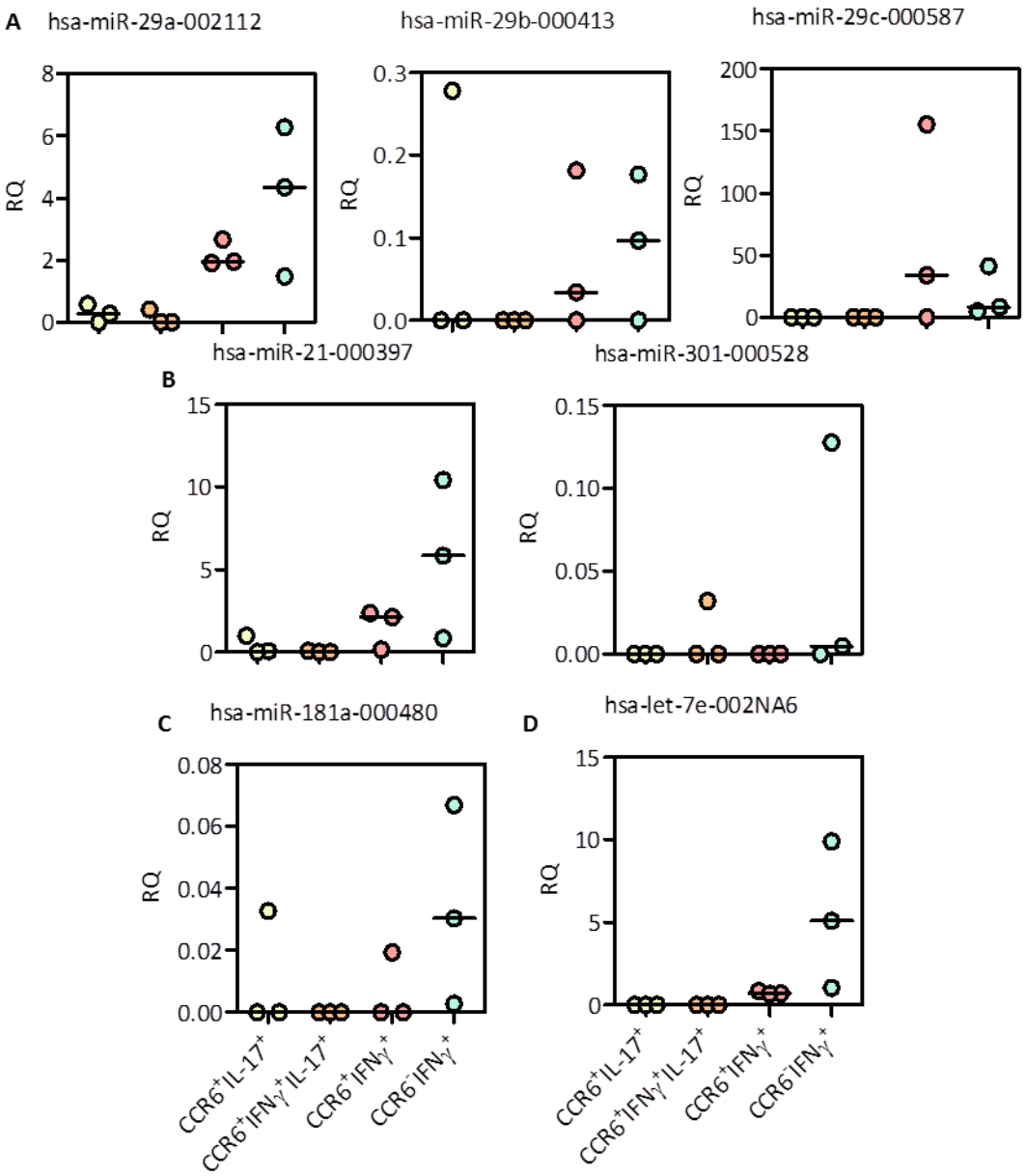

Figure 5.8 Known miRNAs involved in T helper cell differentiation, that were differentially expressed in CCR6$^+$IL-17$^+$ CCR6$^+$IFNγ$^+$IL-17$^+$, CCR6$^+$IFNγ$^+$, and CCR6$^-$IFNγ$^+$ cells: Relative Quantity (RQ) expression of miRNAs within CCR6$^+$IL-17$^+$ CCR6$^+$IFNγ$^+$IL-17$^+$, CCR6$^+$IFNγ$^+$, CCR6$^-$IFNγ$^+$ populations. RQ is the cycle value (Cp) normalised to the median Cp of all the miRNAs from one run. Line represents median RQ value. n=3

5.4 MicroRNAs Expressed in IL-17$^+$ Secreting Cells

Using information from a literature search, the remaining miRNAs were grouped based on their pattern of expression in the different subsets. There were 4 miRNAs that were highly expressed in IL-17 secreting cells compared to the IFNγ secreting populations. miR-184 expression was found in both CCR6$^+$IL-17$^+$ and CCR6$^+$IFNγ$^+$IL-17$^+$ cells. There was detectable expression in CCR6$^+$IFNγ$^+$ and CCR6$^-$IFNγ$^+$ cells, but it was lower than the IL-17 secreting populations (**Figure 5.9 A)**. Both miR-518 and miR-628 had similar expression patterns to miR-184 (**Figure 5.9 C, D**). There was very high expression of miR324-3p in all the subsets. However, the highest level of expression was in the CCR6$^+$IL-17$^+$ cells (**Figure 5.9 B**).

5.5 MicroRNAs Expressed in IFNγ$^+$ Secreting Cells

There were 3 miRNAs that were expressed to a similar level in both IFNγ secreting cell populations; miR-125a-5p, miR-195 and miR-598. There was no detectable expression of any of these miRNA within the CCR6$^+$IL-17$^+$ or CCR6$^+$IFNγ$^+$IL-17$^+$ populations (**Figure 5.10 A, B, C**). miR-106 was expressed in CCR6$^+$IFNγ$^+$, CCR6$^-$IFNγ$^+$, and CCR6$^-$IFNγ$^+$ cells. The highest expression was in the CCR6$^-$IFNγ$^+$ subsets with slightly lower expression in the CCR6$^+$IFNγ$^+$ cells. The lowest expression of miR-106b was in the CCR6$^+$IFNγ$^+$IL-17$^+$ cells. There was no detectable expression within the CCR6$^+$IL-17$^+$ population (**Figure 5.10 D**).

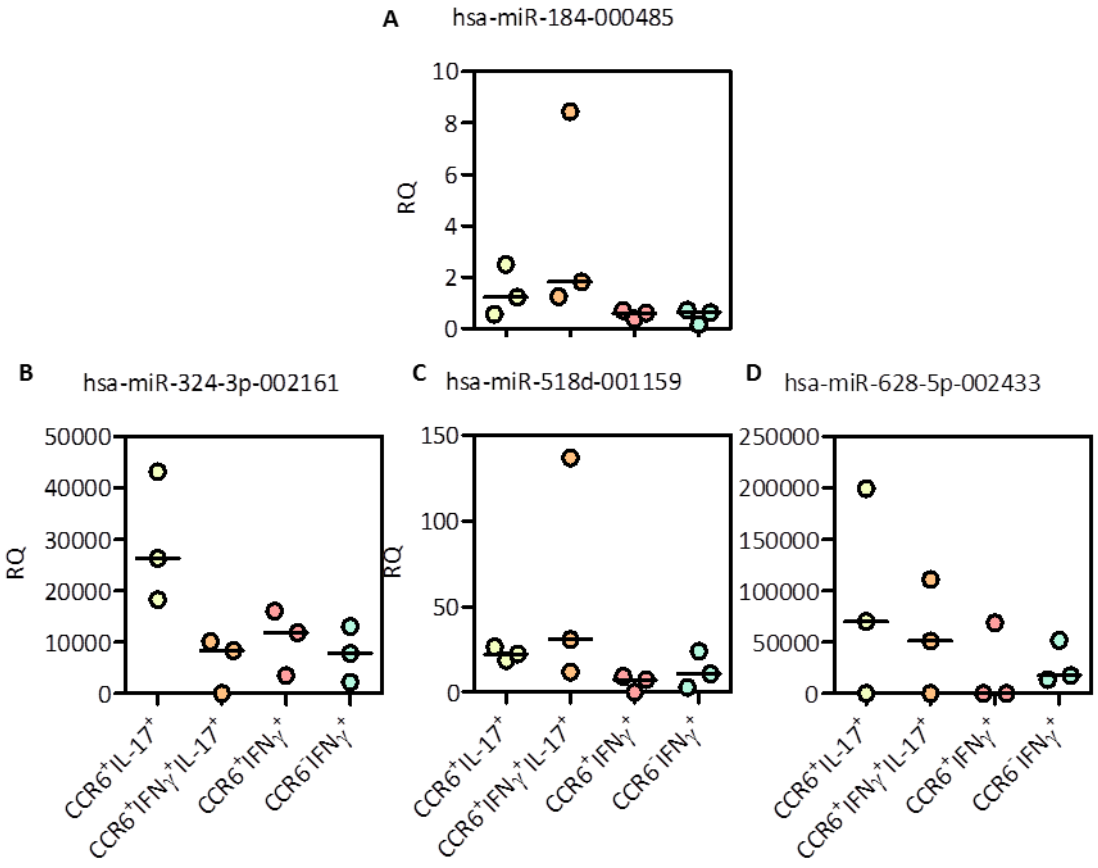

Figure 5.9 miRNAs expressed in IL-17$^+$ populations to a greater extent than IFNγ$^+$ CD4$^+$ T cells. Relative Quantity (RQ) of miRNAs within CCR6$^+$IL-17$^+$ CCR6$^+$IFNγ$^+$IL-17$^+$, CCR6$^+$IFNγ$^+$, CCR6$^-$ IFNγ$^+$ populations. RQ is the cycle value (Cp) normalised to the median Cp of all the miRNAs from one run. Line represents median RQ value. n=3

5.6 MicroRNAs Expressed in CCR6$^-$ or CCR6$^+$ Cells

There were many miRNAs within this screen that were just expressed within the CCR6$^-$ population. The majority of these miRNAs were expressed at a relatively low level. Further investigation will be needed to confirm that these miRNAs are solely expressed within the CCR6$^-$IFNγ$^+$ population (**Figure 5.11, Figure 5.12 and Appendix**).

Interestingly, there were two miRNAs that were expressed only within the CCR6$^+$IL-17$^+$ and CCR6$^+$IFNγ$^+$ populations (**Figure 5.13**), although the replicates were not all consistent. The expression within the CCR6$^+$IL-17$^+$ and CCR6$^+$IFNγ$^+$ populations of miR-136 and miR-454 were similar, with little or no expression in CCR6$^+$IFNγ$^+$IL-17$^+$ or CCR6$^+$IFNγ$^+$ cells.

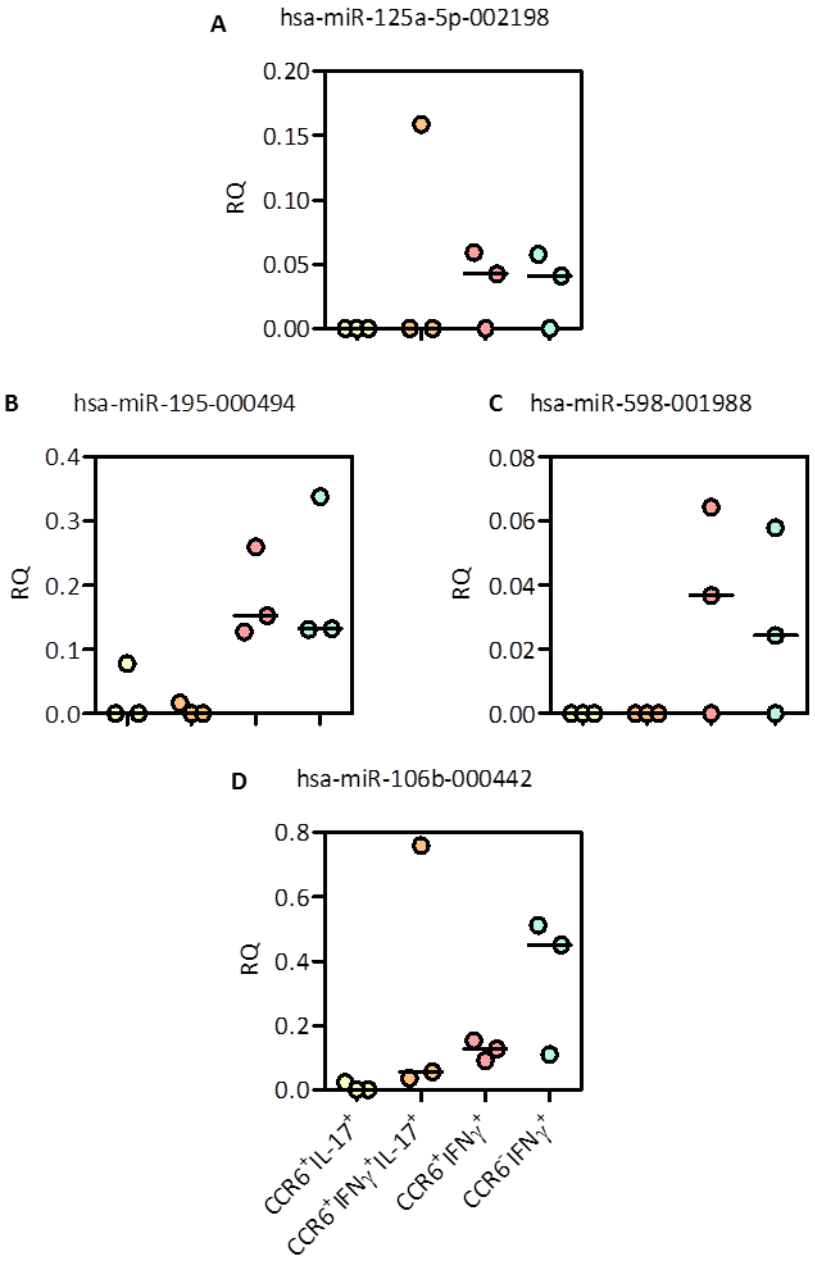

Figure 5.10 miRNAs expressed in CCR6^{+} and CCR6^{-} cells that secrete IFNγ^{+} to a greater extent than IL-17^{+} CD4^{+} T cells: Relative Quantity (RQ) expression of miRNAs within CCR6^{+}IL-17^{+} CCR6^{+}IFNγ^{+}IL-17^{+}, CCR6^{+}IFNγ^{+}, CCR6^{-}IFNγ^{+} populations. RQ is the cycle value (Cp) normalised to the median Cp of all the miRNAs from one run. Line represents median RQ value. n=3

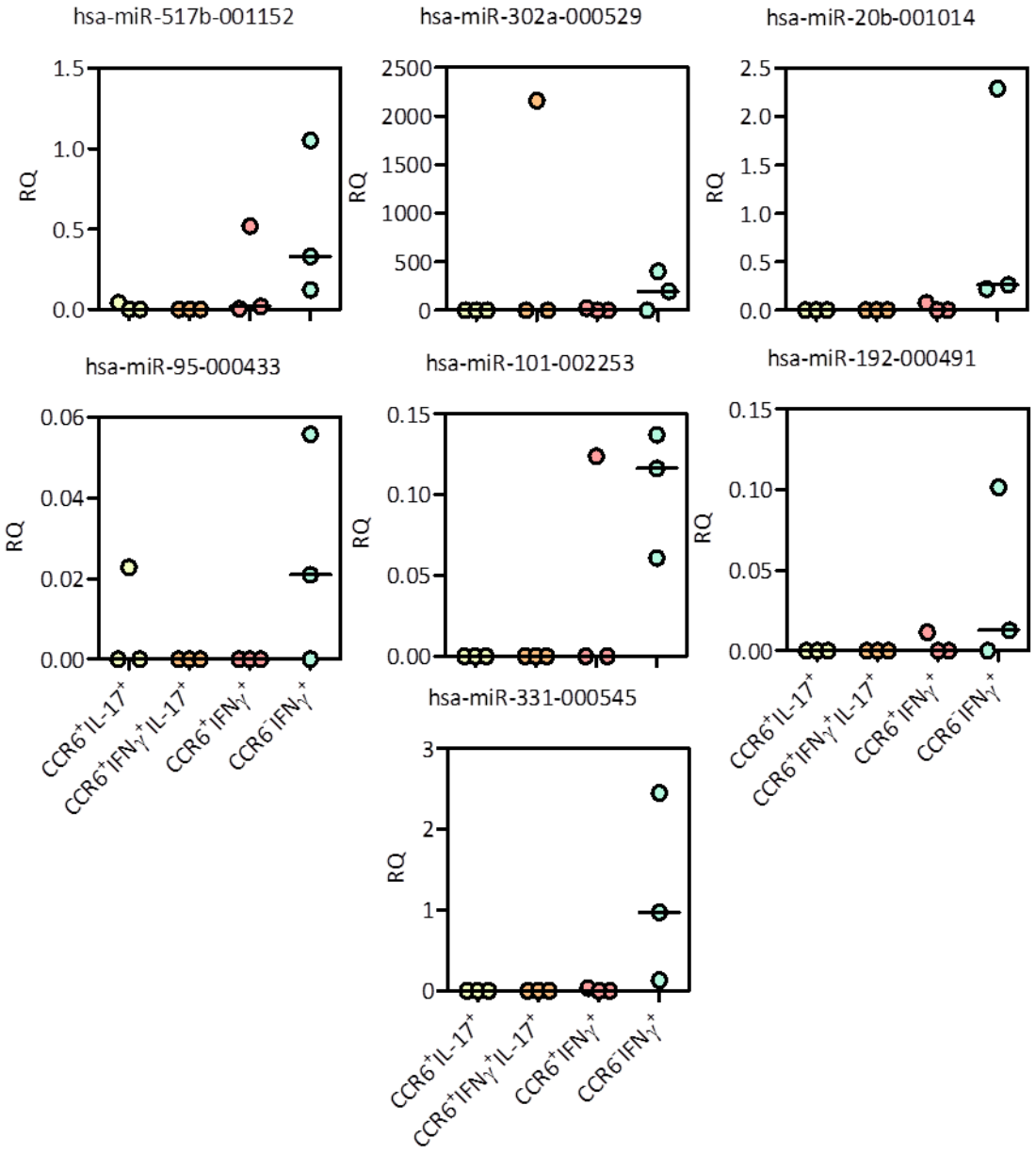

Figure 5.11 Detectible expression of miRNAs in CCR6^{-}IFNγ^{+} cells only: Relative Quantity (RQ) expression of miRNAs within CCR6^{+}IL-17^{+} CCR6^{+}IFNγ^{+}IL-17^{+}, CCR6^{+}IFNγ^{+}, CCR6^{-}IFNγ^{+} populations. RQ is the cycle value (Cp) normalised to the median Cp of all the miRNAs from one run. Line represents median RQ value. n=3

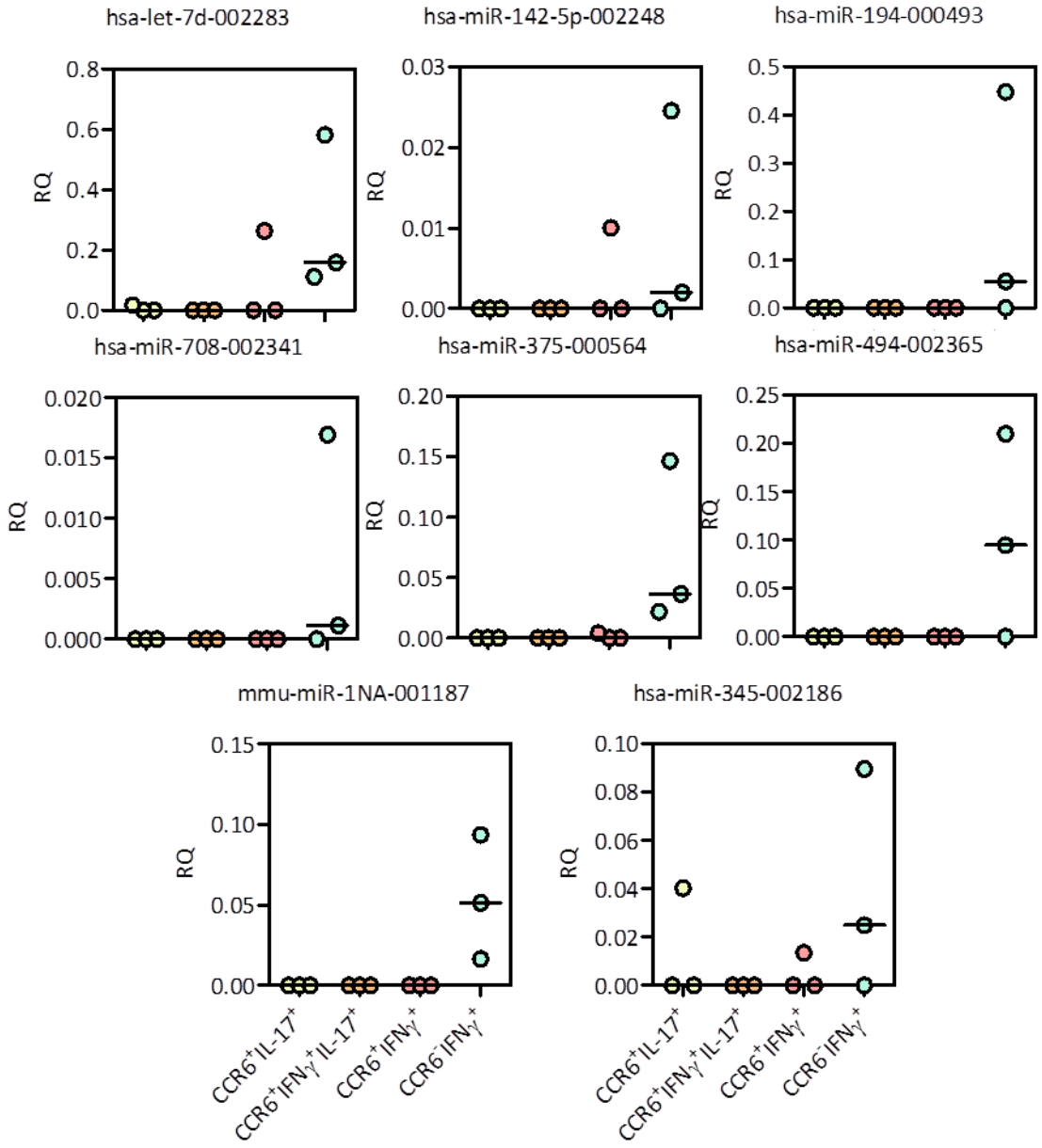

Figure 5.12 Detectible expression of miRNAs in CCR6^{-}IFNγ^{+} cells only: Relative Quantity (RQ) expression of miRNAs within CCR6^{+}IL-17^{+} CCR6^{+}IFNγ^{+}IL-17^{+}, CCR6^{+}IFNγ^{+}, CCR6^{-}IFNγ^{+} populations. RQ is the cycle value (Cp) normalised to the median Cp of all the miRNAs from one run. Line represents median RQ value. n=3.

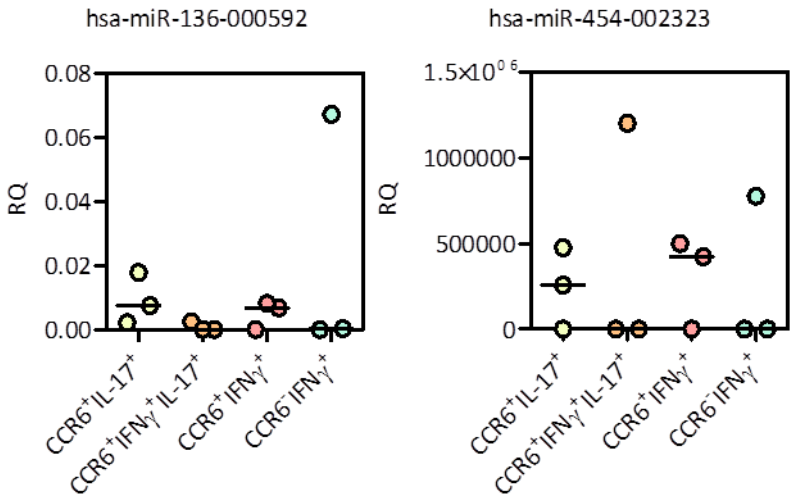

Figure 5.13 Detectible expression of miRNAs in CCR6^{+} cells but not CCR6^{-}IFNγ^{+} cells. Relative Quantity (RQ) expression of miRNAs within CCR6^{+}IL-17^{+} CCR6^{+}IFNγ^{+}IL-17^{+}, CCR6^{+}IFNγ^{+}, CCR6^{-}IFNγ^{+} populations. RQ is the cycle value (Cp) value normalised to the median Cp of all the miRNAs from one run. Line represents median RQ value. n=3

5.7 Other Expression Patterns of MicroRNAs

There were two other detectible expression patterns that occurred within this screen.

Firstly there were several miRNAs that were highly expressed within the CCR6$^-$IFNγ$^+$ population, with lower expression within the CCR6$^+$IFNγ$^+$ population, and no expression in either IL-17 secreting cell populations (**Figure 5.14 - Appendix**).

Secondly there was high expression of the miRNAs within the CCR6$^-$IFNγ$^+$ populations. Again, there was lower expression within the CCR6$^+$IFNγ$^+$ but also detectable expression within the CCR6$^+$IL-17$^+$ population (**Figure 5.15**).

This is only an initial screen of the expression of miRNAs within these subsets. Having only 3 donor's means there is a limit to the statistical tests that can be done and the reliability of the data. All of the interesting and novel expression of miRNA within these subsets will need to be validated. Due do it being a study in humans there is not normally distributed and there is high variability between donors. This means that more samples would be needed to reach significance and the appropriate controls needed to test the reliability.

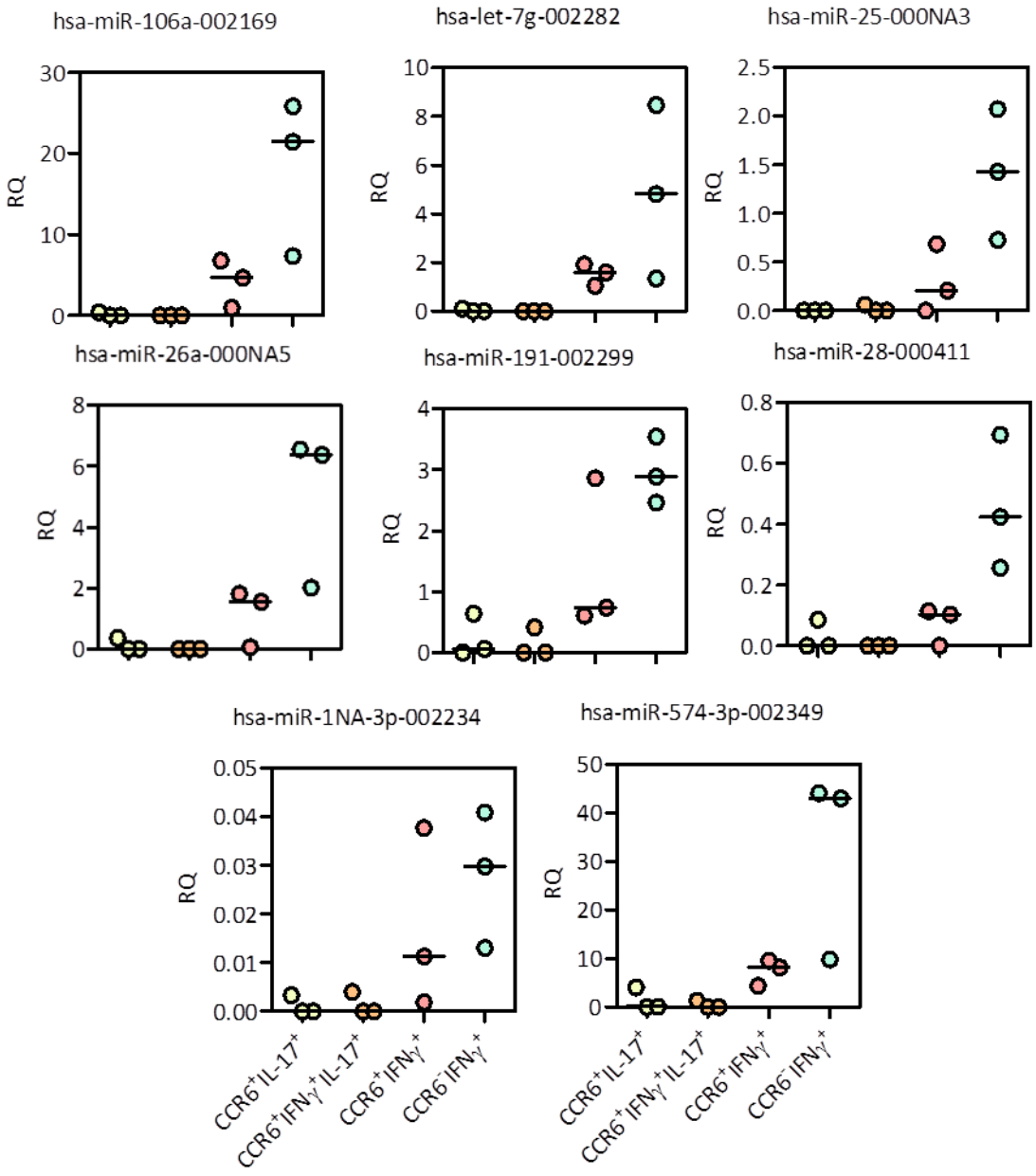

Figure 5.14 Detectible expression of miRNA in CCR6^{-}IFNγ^{+} cells with lower expression within CCR6^{+}IFNγ^{+} cells. Relative Quantity (RQ) expression of miRNAs within CCR6^{+}IL-17^{+} CCR6^{+}IFNγ^{+}IL-17^{+}, CCR6^{+}IFNγ^{+}, CCR6^{-}IFNγ^{+} populations. RQ is the Cycle value (Cp) normalised to the median Cp of all the miRNAs from one run. Line represents median RQ value. n=3

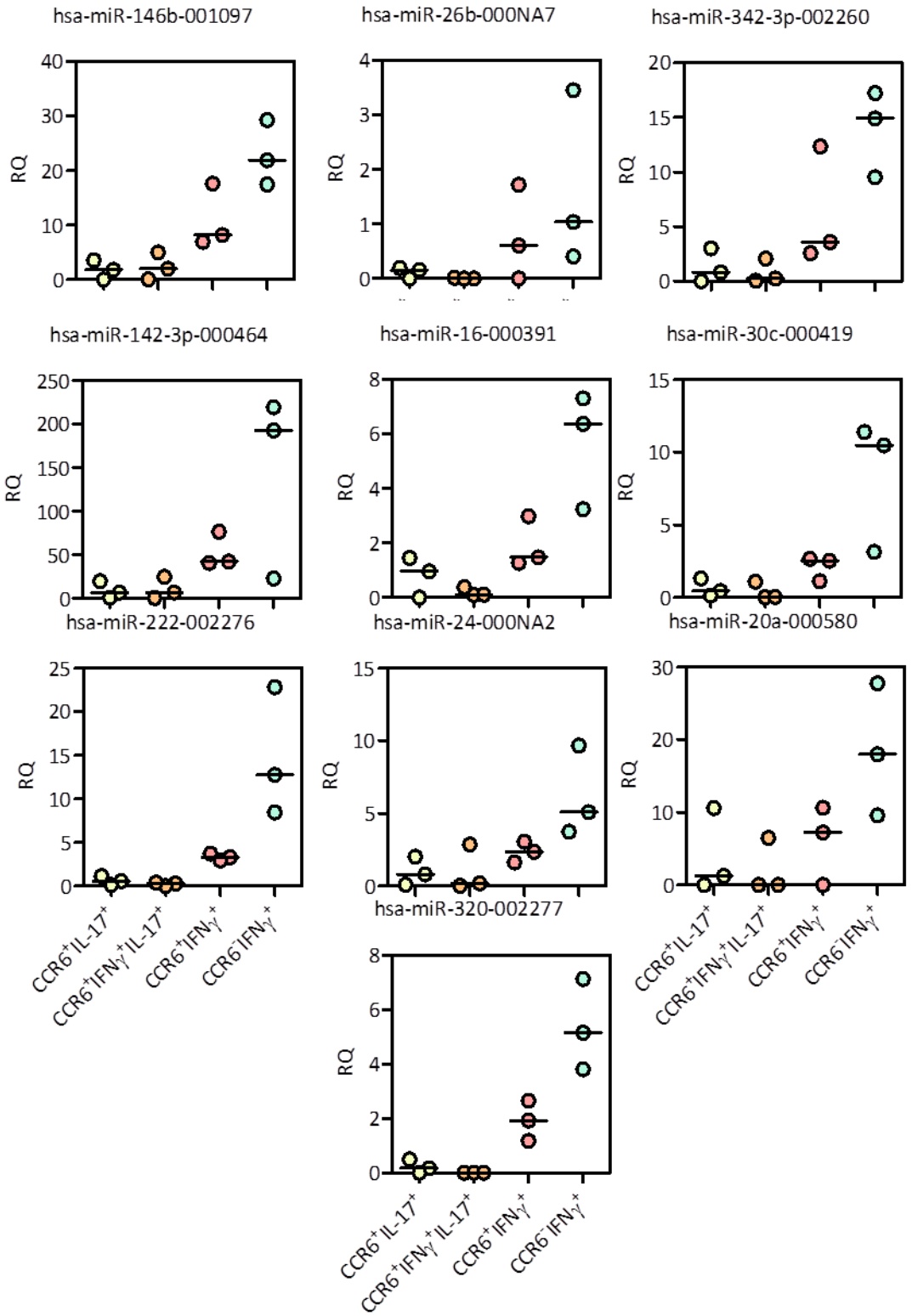

Figure 5.15 Detectible expression of miRNAs in CCR6^{-}IFNγ^{+} ,CCR6^{+}IFNγ^{+} cells and CCR6^{+}IL-17^{+} cells. Relative Quantity (RQ) expression of miRNAs within CCR6^{+}IL-17^{+} CCR6^{+}IFNγ^{+}IL-17^{+}, CCR6^{+}IFNγ^{+}, CCR6^{-}IFNγ^{+} populations. RQ is the Cycle value (Cp) normalised to the median Cp of all the miRNAs from one run. Line represents median RQ value. n=3

5.8 Discussion

5.8.1 Normalisation and Analysis of the Data Set

In most cases the highest expression of miRNA was in the CCR6$^-$IFNγ$^+$ populations. It has to be noted that the CCR6$^-$IFNγ$^+$ population was always the largest population from the sorts. This could skew the data as miRNAs that only have a few copies will be amplified more efficiently in samples with more material. The samples were normalised to the median expression to control for differences such as sample size.

Statistical test were not undertaken on this data set. The aim of this study was to identify interesting and novel miRNA which may be involved in T helper cell plasticity rather than finding significant differences in expression of the miRNA between subsets. Furthermore, although triplicates in some setting can be sufficient to extract accurate significant data in this setting there were large variations between data sets. These variations could either be the natural variation you get in humans or introduced by the amplification process. As this could not be controlled for we could not do reliable statistical test on the data set. Further analysis of miRNA expression in the T$_H$17 and T$_H$1 subsets will be needed to confirm any findings from this study.

5.8.2 Regulation of T Helper Cell Differentiation by Known MicroRNAs

miR-29 plays an important role in T$_H$1 differentiation[190,191] as it negatively regulates IFNγ production through interactions with Epsom and T-bet. miR-29a, b and c were expressed solely in the CCR6$^+$IFNγ$^+$ and CCR6$^-$IFNγ$^+$ populations. Most of the literature only gives the

data on the expression of miR-23a and miR-29b. With mice CD4$^+$ T cells, miR-29C is not highly expressed[190]. miR-29c was highly expressed and miR-29b had the lowest expression within the two IFNγ secreting populations (**Figure 5.8**). miR-29c was expressed more highly in CCR6$^+$IFNγ$^+$ cell compared to CCR6$^-$IFNγ$^+$ cells. Both miR-29a and miR-29b are more highly expressed in CCR6$^-$IFNγ$^+$ than CCR6$^+$IFNγ$^+$ cells. Within this human system it would be interesting to decipher if the different forms of miR-29 had any functional consequences on the T$_H$1 phenotype. Initially the expression levels of each miR-29 form would need to be confirmed. Due to its role in controlling T-bet expression it might be intriguing to knock down miR-29 in CCR6$^+$IFNγ$^+$ cells to identify if this had any effects on the 'T$_H$17' phenotype of the cell.

The miR-17-92 cluster has a host of different effects on the T helper cell, including roles in proliferation[189], supporting IFN-γ production and suppressing regulatory T-cell differentiation in the periphery[229]. The miRNAs miR-17 and miR-19b have been associated with having a pro-T$_H$1 influence through the antagonism of the PI3K-Akt pathway. Within this screen both miRNAs were detected in the CCR6$^-$IFNγ$^+$ with a lower expression within the CCR6$^+$IFNγ$^+$ population. miR-19b also had low but detectible expression within both IL-17 secreting populations.

The miR-17-92 cluster also has effects on T$_{FH}$ cell development independent of its effects on proliferation. What is intriguing about this is that removing the expression of miR-17-92 cluster in T$_{FH}$ cells led to the expression of genes that were normally not associated with a T$_{FH}$ phenotype. These genes included T$_H$17 and T$_H$22 associated genes, such as CCR6, IL1R1

and RORα. This model showed that RORα was the direct target for miR-17-92[230]. The suppression of RORα by miR17-92 has in part controlled the CCR6 expression.

Considering the CCR6 populations all the miR-17-92 cluster miRNAs are more highly expressed in CCR6$^-$ populations. This might also explain the lower expression of this cluster of miRNAs within the CCR6$^+$IFNγ$^+$ population. It was shown in the last chapter that these cells have a reduced level of CCR6 expression (**Figure 4.1 C**) which may in part be controlled by this cluster of miRNAs. It also highlights that the expression of RORα in the CCR6$^+$IFNγ$^+$ subset might be worth investigating, as it may control the CCR6 levels. hsa-let-7f is involved in IL-23R expression[231]. There was no detectable expression of hsa-let-7f in any of the subsets analysed.

The role of miR-155 within the immune system has been well characterised. It appears to have many different methods of action within a range of both innate and adaptive immune cells. Within T cells miR-155 has been shown to be important in the expression of IFNγRβ. This miRNA has been shown to down regulate the expression of the receptor early on in T$_H$1 cell differentiation. This suggests a potential role for miR-155 in controlling the pace of differentiation of T$_H$1 cells[193].

Within this data set it would appear that the expression of miR-155 is highest in classical T$_H$1 cells (CCR6-IFNγ$^+$) cells. When overexpressed in mice miR-155 has been shown to promote a T$_H$1 response. One target for miR-155 is SOCS1. A high level of SOCS1 is known to suppress T$_H$1 response and promote T$_H$2 differentiation, but also suppress T$_H$17 and T$_{REG}$ differentiation[232].

Within T$_H$17 differentiation miR-155 is involved in the regulation of Ets-1, a negative regulator of T$_H$17 differentiation. This miRNA is also shown to correlate with IL-23R expression. There was expression of miR-155 in both the subsets in which IL-23R gene expression was found in Chapter 4 (namely CCR6$^+$IL-17$^+$ and CCR6$^+$IFNγ$^+$). Further work is needed to identify the true targets of miR-155 in these different subsets in humans.

miR-326 also targets the negative regulator of T$_H$17 differentiation, Ets-1[194]. In this data set there was no detectable expression of miR-326 in any of the subsets analysed. miR-301a also enhances T$_H$17 induction by targeting an inhibitor of STAT-3[195]. miRNA was not highly expressed in any of the subsets in this screen, although in contrast to the literature[194] it was detected in the CCR6$^-$IFNγ$^+$ population.

5.8.3 Identification of Novel miRNA in T Helper Cell Subsets

MicroRNAs are involved in fundamental cellular processes, such as proliferation and death, in many different cell types. As a result, microRNAs have been directly implicated in the development of many cancers. The majority of the other differentially expressed miRNAs identified in this screen have at some point been implicated in controlling cancer, and a few target molecules have been identified which the miRNA bind to. In relation to the T helper subsets in this screen there is limited data. The next step in future work would be to validate the expression of the miRNAs on samples that have not been amplified using qRT-PCR. Using a system to knock-down the miRNA within the T cells could also be used to identify if the miRNAs have a significant impact on the cell phenotype.

The miRNAs that were highly expressed within IL-17 secreting cells were miR-184, miR-324-3p, miR-518d and miR-628-5p. miR-184 was expressed in both IL-17 secreting subsets. It has been suggested in mice that this controls the differentiation and proliferation of adult neural stem cells[233]. Within the stem cells high levels of miR-184 promote proliferation but prevent differentiation[233]. miR184 has been identified as targeting the nuclear factor(s) of activated T cells-1 (NFAT1) protein through its complementary sequence binding with NFATc2 mRNA (without transcriptional degradation). Expression of miR-184 in CD4^{+} T cells from the UCB has been associated with reduced inflammatory cytokine expression in these cells due to lower NFAT-1 expression[234]. A further target on miR-184 was found to be the microRNA miR-204. Interaction of these two miRNA led to increased SHIP2 expression in keratinocytes[235] and resulted in increased proliferation. Although direct targets for miR-324 and miR-518b have not been identified they are thought to be oncogenes. When expressed they suppress the proliferation of different cells types. It is known that T$_H$17 cells have reduced proliferative ability[103] so it may be possible that these miRNA are also involved in controlling the proliferation within the T cell subsets. Finally miR-628-5p has been associated with acute myeloid leukaemia and was up-regulated in response to GM-CSF, IL-3 or G-CSF[236]. One of the highly conserved predicted targets of miR-628-5p is Foxo3/Foxo3a.

Within the miRNAs expressed exclusively in the T$_H$1 cells, both CCR6^{-} and CCR6^{+}, some have a role in aiding the immune cells in protecting against infection. miR-125a-5p has been identified in the human liver to have an anti-viral role against HBV[237]. miR-598 has been postulated to be involved in the repair of lymphocytes after ionising radiation[238]. Aberrant expression of miR-195 has been associated with several different types of cancer. miR-106b

has an role in targeting Smad7 signalling to activate TGF-β signalling specifically in the setting of cancer[239]. TGF-β is known to be involved in differentiation of T helper cells, especially T_{REG} and T_H17 cells, although not specifically T_H1 cells.

There were only two miRNAs that were associated with CCR6$^+$ cells. These were miR-136 and miR-454. miR-136 targets Bcl-2 and AEG-1 within glioma[240], which are anti-apoptotic genes. miR-454 was a candidate miRNA found to be differentially expressed in the plasma of MS patients compared to controls. miR-454 was also differentially expressed in MS patients at different stages of disease suggesting a possible role in the progression of MS[241]. This would be an interesting candidate to take further considering that CCR6 is involved in T cell migration into the CNS in MS[157].

In summary, within this chapter miRNAs that are differentially expressed between CCR6$^+$IL-17$^+$, CCR6$^+$IFNγ$^+$IL-17$^+$, CCR6$^+$IFNγ$^+$, and CCR6$^-$IFNγ$^+$ cells have been identified. Using amplification of material and microfluidic cards has allowed analysis of the expression of over 300 miRNA in very small subsets of cells. Several miRNAs highlighted from this screen had previously been associated with T_H differentiation such as miR-155 and miR-29. Other miRNA that were expected to be differentially expressed were not, such as miR-326 involved in T_H17 differentiation[194]. Novel miRNAs that have not previously been associated with T_H differentiation have also been identified. The next stage for this screen will be to validate the expression of the miRNAs of interest using samples that have not been amplified. As the validation process has not yet been carried out, it cannot be ruled out that the amplification process has affected the expression levels in some samples.

CHAPTER 6

GENERAL DISCUSSION

6.1 Summary

The identification of T_H1 and T_H2 cells by Mosmann and Coffman[43] led to the recognition that $CD4^+$ T cells could differentiation down separate lineages. Since this discovery several other subsets of T_H cells have been identified, in the most part defined by the effector cytokines produced and the lineage defining transcription factor expressed (**Figure 1.1**). The different T_H phenotypes all play a part in controlling unwanted infection within the body. An example of this is T_H1 cells which are vital for immunity against intra-cellular infection. They produce IFNγ that drives the activation of macrophages. This phenotype is controlled by T-bet, the T_H1 lineage defining transcription factor[47,52]. T_H17 cell are important primarily for protection against fungal infections but also play a role in protection against some extracellular bacterial infections. They produce IL-17 and control neutrophil activity. The lineage defining transcription factor that is involved in the induction and maintenance of the T_H17 phenotype is RORC[86].

Although T_H1 and T_H17 cells are very distinct lineage with discrete properties, it has now been demonstrated that there are cells that have features and functions of both phenotypes. At the start of this study there was very little known about T_H17 cells and their ability to co-express IFNγ. $IFN\gamma^+IL\text{-}17^+$ cells have now been characterised, both within this study and in the literature[1,145,200,221]. However there are still questions to be answered as to

the level of plasticity exhibited by these T cells and in what situations they play an important role.

There are several groups now suggesting that T_H17 cells can fully convert to T_H1 cells. CD161 has been suggested as a marker for T_H1 cells that have a T_H17 heritage[105], though this has not been proven directly in humans. The data presented in this study has identified a novel subset of T_H1 cells that express functional CCR6 and have other features of a 'T_H17' transcriptional profile, although no IL-17 expression.

Multiple sclerosis affects 2.5 million people worldwide. If severely affects patient's quality of life and reduces their life expectancy. Both T_H1 and T_H17 cell are important in the initiation and maintenance of the disease[242,243]. Data from this study has demonstrated that $CCR6^+T_H1$ cells are present in the CSF of MS patients. The literature has shown the presence of T_H1 cells with T_H17 phenotypic markers in the joints of arthritis patients[213]. It will be important to understand if $CCR6^+T_H1$ cells play a role in the pathogenesis of MS.

6.2 Strength and Limitations of the Study

Investigating the biology of T_H cells within the human system lends this study both strengths and limitations. These are highlighted when this study is compared to murine studies of T_H cell plasticity and the murine model EAE. There are variations between human individuals that cannot be controlled for in the same way as in murine experiments. These variations are introduced both by genetic and environmental factors which in mice are tightly controlled. In humans it is not possible to control for these variations without using very

large cohorts of samples. This study only uses a small number of patients and controls. This leads to a lack of statistical significance in much of the data, such as in the miRNA study and some of the qRT-PCR data. To confirm the results further work will be needed to consolidate the findings.

In contrast to this however the use of human system means that the data is directly relevant and useful, especially in the study of MS. Murine models, although related to human immune system, are not the same, so findings may not translate to human disease. Although EAE does have characteristic of MS it is by no means a true representation. The requirement of an adjuvant to initiate EAE is one example that may be skewing the inflammatory process in this model. To initially find an interesting subset of T_H cells within the human system means it is a realistic therapeutic target to treat MS or other inflammatory diseases in humans. Human samples can be difficult to obtain, as they require ethical approval and consenting patients. The data from this study should be added to the pool of already published data on T cell plasticity and information on CSF T cell subsets.

A further strength of this study is that it uses ex vivo populations of cells. This highlights how the technology in this area is rapidly developing. The ability to isolate very small but pure populations of viable cytokine secreting T cells means that more reliable *ex vivo* analysis of the different cells types can be undertaken. At the start of the study a lot of the information in the literature about plasticity in T_H1 and T_H17 cells was based on in vitro and clone systems. T_H17 cells in culture appear to become more plastic with the up regulation of IL-12R, suggesting cultured cell may have altered biology to *ex vivo* cells. Throughout this study

all the transcriptional analysis was done on ex vivo populations suggesting this is a true snap shot of the genes expressed by these cells in the body.

Finally the use of PMA and ionomycin to stimulate cells to produce cytokines is a limitation of this study. There can be no certainty that stimulating cells by bypassing the antigen-TcR pathway gives a true representation of the cell's cytokine secreting potential. This study has identified that there was less cytokine produced by recently activated T cells when they were stimulated by PMA/ionomycin than cells that had not been recently activated. It is difficult to say if this phenomenon is real or an artefact of PMA/Ionomycin stimulation. Using antigen specific stimulation would not be a viable option in this human study as there are so few antigen specific cells. Many papers use antigen stimulation by using clones. It was felt in this study that this would lead to undesirable consequences with the gene expression within these cells.

Overall in this study there are some interesting, novel findings about T helper cell plasticity, both in health and disease. However further research is needed to confirm the relationship in humans between T_H17 and T_H1 cells, and their potential role in MS.

6.3 Identification of T_H17-like T_H1 Cells

As mentioned in **Section 4.10.1** there is evidence in Chapter 4 that CCR6 may be a better marker to identify cells with a 'T_H17' like phenotype and IL-17 secreting cells compared to

CD161. CD161 has been used by the Annunziato group to identify T_H1 cells with 'T_H17' phenotype[105,213].

In this study CD161 appears to be associated with a significant increase of IFNγ in T cells (**Figure 6.1**). T_H1 cells that express CCR6 have a reduced IFNγ MFI in comparison to $CD4^+CD161^+CCR6^-$ cells. On T cells when CD161 is stimulated by its ligand, LLT1, IFNγ production is increased[244]. As $CD161^+CCR6^+$ cells secrete less IFNγ per cell than $CD161^+CCR6^-$ cells there may be an effect of CCR6, or the related transcriptional programme, affecting the way CD161 is acting when it binds to its ligand. LLT1 is known to be expressed by activated DC, B cells and T cells[7] meaning it is possible that LLT1 was present in the cultures used in this study. Although there is a large overlap in the expression of CCR6 and CD161, this suggests that T_H1 $CD161^+CCR6^-$ cells may have a separate phenotype to T_H1 cells expressing CCR6. It would be intriguing to identify if $CD161^+CCR6^-$ cells did in fact have a separate transcriptional profile to $CD161^+CCR6^+$ cells.

Throughout the literature PMA/ionomycin is used to establish the cytokines produced by T cells. In the experiments within this thesis PMA/ionomycin has also been used. By using this type of TcR-independent stimulation there is an assumption that it is revealing the true phenotype of the T cells. PMA/ionomycin has been shown to induce IFNγ secretion in anergic T cells[245] and our data shows that recently activated cells produce less cytokine than cell that have not been activated recently. It was not determined if this was a PMA/ionomycin specific effect or a true reduction in cytokine production. Using a system of

anti-CD3 anti-CD28 stimulating antibodies or antigen pulsed DC would allow for a more physiological TcR –dependent stimulation.

6.4 Are CCR6$^+$T$_H$1 cells Derived From a T$_H$1 or T$_H$17 Cell?

The literature has taken plasticity in T$_H$17 cells a step further to infer that T$_H$17 cells can fully convert to a T$_H$1 cell, and that expression of CD161 or CCR6 on T$_H$1 cells infers that the cells were once T$_H$17 cells[105,145].

Within the literature there are three main data sets that suggest that T$_H$17 cells can convert to T$_H$1 cells. A murine fate mapping model labelled IL-17A expressing cells with YFP[146]. When EAE was induced in the mice there were YFP$^+$ cells that expressed only IFNγ suggesting a phenotype switch from T$_H$17 to T$_H$1. Furthermore, in humans there was work on CD161$^+$IFNγ$^+$ cells that suggested RORC expression and other features such as IL-23R and IL4I1 expression inferred the cells were ex-T$_H$17 cells. CD161$^+$IL-17$^+$ cells were isolated and cultured, and they showed that CD161$^+$IFNγ$^+$ cells arose in these conditions[105]. Finally, it is argued that T$_H$1 cells have come from a T$_H$17 background as *in vitro* T$_H$1 cells cannot be converted to T$_H$17 phenotype, but T$_H$17 cell can be induced to switch on IFNγ[221].

There is an issue with the fate mapping model in that there is no indication of what level of IL-17 expression is needed to induce the expression of YFP, and that therefore YFP expression may not indicate a committed T$_H$17 cell[146]. A recent paper by Sallusto *et al.* has shown T cells stimulated with different pathogens transiently express certain cytokines depending on the pathogen[147]. The cells that were IFNγ$^+$YFP$^+$ may have transiently expressed IL-17 and never been fully committed to the T$_H$17 lineage.

The finding that *in vitro* T_H1 cells cannot be converted to a T_H17 phenotype does not prove that the conversion is not possible. These $CCR6^+IFN\gamma^+$ cells have not switched on IL-17 expression, just expression of what are considered 'T_H17-related' genes. It is also possible that the conditions needed to switch on 'T_H17' gene expression in T_H1 cells have not yet been found. Several recent publications have demonstrated that a high salt environment boosts the induction of T_H17 cells[246]. Serum/glucocorticoid-regulated kinase 1 (SGK1) was up regulated in cells treated to a high NaCl concentration. SGK1 phosphorylates the transcription factor forkhead box protein O1 (FOXO1)[247]. The phosphorylation of FOXO1 deactivates its suppressive effect on RORγt. SGK1 is critical for IL-23R expression. The increased salt concentration results in the up-regulation of IL-23R, CCR6, RORα and RORC expression. It would be interesting to investigate the possible effects of salt on T_H1 cells (**Figure 6.1**). It is possible that under these conditions RORC, IL-23R and CCR6 are up regulated. RORα is a gene that would be interesting to investigate the in $CCR6^+IFN\gamma^+$ cells, as it is also been suggested to control CCR6 expression[216].

In conclusion there is no solid evidence in this study or in the literature that in humans T_H17 cells can switch to become T_H1 cells. Identifying the methylation status of the IL-17A gene in the $CCR6^+IFN\gamma^+$ cells might hint at the cells history of IL-17A production. A gene expressed in a cell that was fully de-methylated never becomes fully re-methylated. This was demonstrated in experiments investigating the methylation status of the CD8 gene in $CD4^+$ T cells that have developed from a $CD8^+CD4^+$ precursor in the thymus. Within the $CD4^+$ T cells the gene for CD8 was still partially de-methylated[16]. Within the $CCR6^+IFN\gamma^+$ populations

there would be an expectation that the IL-17A gene will be only partially methylated if the cells came from a T_H17 background, and mostly methylated if it was from a T_H1 background.

The next step for the study of $CCR6^+IFN\gamma^+$ cells would be to identify if there were any effects of knocking down RORC expression (**Figure 6.1**). The hypothesis being that the cells would lose CCR6 expression, along with the expression of other 'T_H17'related genes, and develop a phenotype more closely related to the $CCR6^-IFN\gamma^+$ cells. Following on from this the knockdown of T-bet within the $CCR6^+IFN\gamma^+$ cells might determine if it is possible for RORC to become the dominant transcription factor in these cells. If T-bet is knocked down in $CCR6^+IFN\gamma^+$ cells, would they lose the ability to produce IFNγ and gain the ability to produce IL-17?

Within this study there is evidence that the T_H1 population is not homogeneous in their gene expression. Based on this information can cytokine and transcription factor expression still be used to define T_H subsets, and are these cells terminally differentiated?

John J. O'Shea and William Paul developed the hypothesis that within $CD4^+$ T cells there is a dynamic transcription factor expression[248]. The plasticity is no doubt driven by the lineage defining transcription factors but must be tightly controlled by other factors. The next stage is to understand what is controlling the plasticity of different $CD4^+$ T cells.

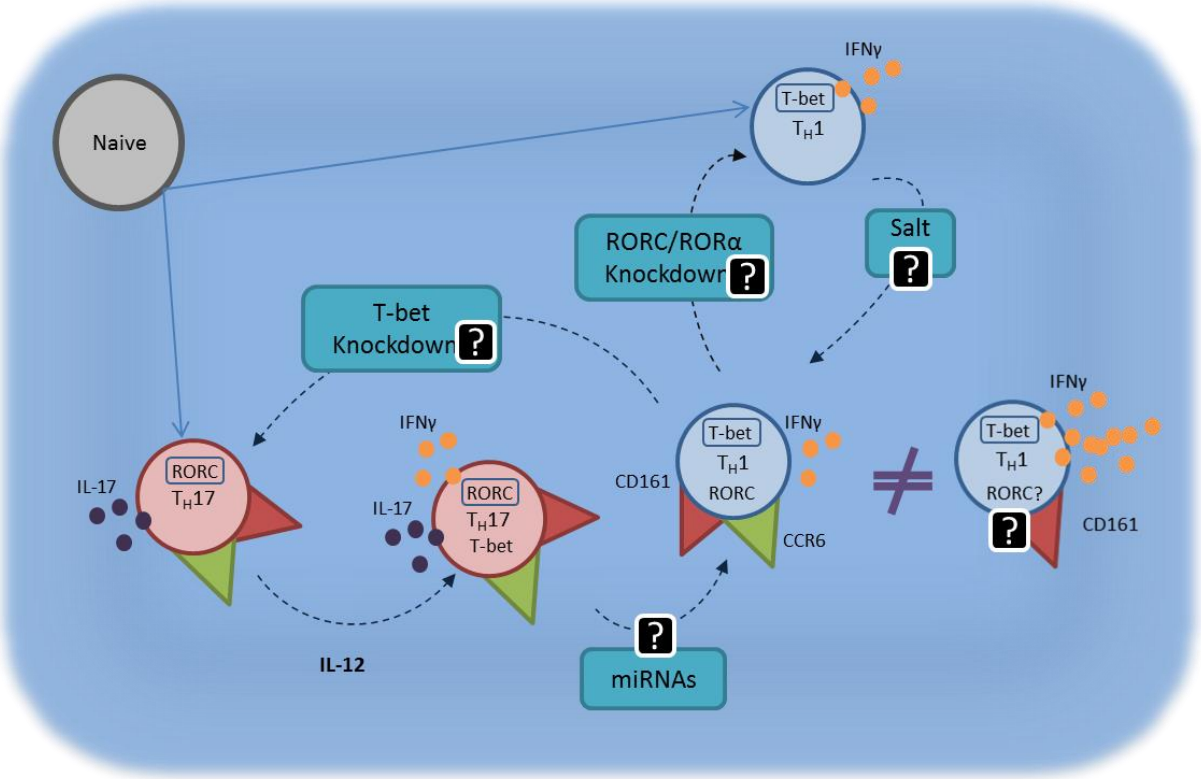

Figure 6.1. Proposed model of T_H1 and T_H17 cell plasticity. T_H17 cells are defined by IL-17 secretion and RORC expression, while T_H1 cells secrete IFNγ and express T-bet. $IFN\gamma^+IL\text{-}17^+$ cells have been shown to differentiate from T_H17 cells in response to IL-12. These cells express RORC and T-bet. Cells expressing CCR6 and CD161, T_H17 related markers, also express RORC and T-bet but only secret IFNγ. It is not known if the $CCR6^+IFN\gamma^+$ cells differentiate from a T_H1 or T_H17 cell. There may be miRNAs that suppress the IL-17 expression in the $CCR6^+IFN\gamma^+$ cells. Salt can induce a 'T_H17' gene expression pattern in naïve T cell. The effect of salt on T_H1 cells is not known and if it may play a role in the induction of CCR6 and RORC in T_H1 cells. The effects of RORC/RORα or T-bet knockdown in $CCR6^+IFN\gamma^+$ cells is not known but will establish the role the transcription factors play in the phenotype of the cell. $CD161^+CCR6^-$ cells secrete more IFNγ than CCR6 expressing T_H1 cells. Further work is needed to understand if these cells have the same 'T_H17 related' phenotype as $CD161^+CCR6^+$ cells.

Comparisons between the different $CD4^+$ T cell subsets are a vital tool to further understand plasticity in humans. The difference between the $IFN\gamma^+IL\text{-}17^+$ cells and $CCR6^+T_H1^+$ will lead to a better understanding of what is specifically controlling IL-17 expression, for example (**Figure 6.1**). This was one of the aims of the miRNA study, to identify specific miRNAs that may be controlling IL-17 expression. If there was a miRNA that was differentially expressed between $CCR6^+IFN\gamma^+IL\text{-}17^+$ cells and $CCR6^+IFN\gamma^+IL\text{-}17^-$cells this could be a candidate for controlling IL-17 expression.

Figure 5.9 and 5.10 shows either miRNAs that were highly expressed in $CCR6^-IFN\gamma^+$ and $CCR6^+IFN\gamma^+$ cells compared to CCR6 $IFN\gamma^+IL\text{-}17^+$ and $CCR6^+IL\text{-}17^+$ cells, or vice versa. $CCR6^+IFN\gamma^+IL\text{-}17^+$ and $CCR6^+IL\text{-}17^+$ cells were associated in this comparison as it has been suggested from data presented in this study and in the literature that $CCR6^+IFN\gamma^+IL\text{-}17^+$ cells are more related to T_H17 cells[1]. These differentially expressed miRNAs may be involved in the T_H17 and T_H1 transcriptional profiles rather than controlling the cytokine expression. Conversely miR-324 was highly expressed in $CCR6^+IL\text{-}17^+$ cells with lower expression in all three IFNγ secreting populations. This could be a candidate miRNA to control the expression of either IL-17 or IFNγ.

Many of the miRNAs are only expressed in $CCR6^-IFN\gamma^+$ cells (**Figure 5.11 and 5.12**). These candidates could be controlling IFNγ/IL-17 expression. Conversely this could be an erroneous result introduced by the amplification process. As the $CCR6^+IFN\gamma^+$ started with more material, genes expressed at a low level, they could be amplified more reliably than genes expressed at a low level in a population with less material. A proportion of the miRNAs that

were only expressed in the $CCR6^{+}IFN\gamma^{+}$ cells have a very low relative expression. The only way to verify if this is the case is to validate the expression of the miRNA by qRT-PCR on samples that have not been amplified.

It may be hypothesised that the $CCR6^{+}IFN\gamma^{+}$ cells may up-regulate RORC or possibly RORα as a way to gain migratory ability into certain tissues. There are many autoimmune disease such as MS[157] and psoriasis[249] where CCR6 has been shown to play a role in T cell migration in to the effected tissue. If a miRNA was identified that targeted either the T_H17 transcriptional profile or specifically the CCR6 transcription it could have real therapeutic potential for these diseases. However, as T_{REG} also use CCR6 to migrate into the CNS[216], the effects of also removing these regulatory cells, as well as inflammatory T_H cell, from the CNS must be taken into account.

6.5 The Presence of $CCR6^{+}IFN\gamma$ Cells in RR-MS

In MS patients, T_H17 cells have been shown to be increased with in the CSF compared to peripheral blood[223]. It has been shown within this thesis that there is also an increase in the percentage of $CCR6^{+}IFN\gamma^{+}$ cells in the CSF compared to peripheral blood of RR-MS patients.

In EAE, the murine model of MS, there is an initial wave of T_H17 cells using CCR6-dependent migration into the CNS via the choroid plexus. As T_H17 cells are considered the pathogenic cells in EAE, they attributed the attenuated EAE in $CCR6^{-/-}$ mice to the reduced ability of T_H17 cell to migrate into the CNS[157]. However, the presence of $CCR6^{+}T_H1$ cells, which far outnumbers the T_H17 cells, may also be important in the disease pathogenesis. In the

$CCR6^{-/-}$ mice both the IL-17 and IFNγ secreting cells were reduced in the CNS after EAE induction[157].

However, the presence of $CCR6^{+}IFN\gamma^{+}$ cells does not prove that their method of entry into the CSF was CCR6 dependent. Firstly almost half of the IFNγ cells did not express CCR6. It has been shown in mice that only the first wave of cells migrating into the CSF are CCR6 dependent. As the patients used in this study were either RR-MS or SP-MS, the initial wave of cells infiltrating the CNS will have already occurred. After the initial wave of CCR6 dependent migration the inflammatory cells cause damage to the BBB allowing a second CCR6 independent wave of T cell migration to occur[157]. This could be the reason why only half of the $IFN\gamma^{+}$ cells are $CCR6^{+}$, and so does not give any clues as to how the $CCR6^{+}$ cells entered the CSF.

IL-17 secreting cells have been heavily implicated in the pathogenesis of MS. In humans the percentage of $IL\text{-}17^{+}$ cells in the CSF and blood have been shown to increase in relapse and then reduce back to baseline again upon remission[223,250]. This reference show there was no difference in the percentage of T_H1 cells in either relapse or remission in MS patients [223], however the percentage of $CCR6^{+}IFN\gamma^{+}$ cells was not directly studied. It would be interesting to see if there is any change in the $CCR6^{+}IFN\gamma^{+}$ population upon relapse. Due to the way in which the samples were collected for this study all the CSF samples were from patients who were likely to be in remission.

Whether the $CCR6^{+}IFN\gamma^{+}$ cells are playing a role in the pathogenesis of MS is difficult to determine. GM-CSF has been implicated as having pathogenic activity in MS[173,201,202]. T_H17

cells have been shown to be a source of GM-CSF within the brain parenchyma. Within the data presented in this study $CCR6^{+}IFN\gamma^{+}$ and $CCR6^{-}IFN\gamma^{+}$ cells in the CSF can produce GM-CSF. All the samples from this data set are from RR-MS patients in remission, but this shows that T_H1 cells rather than T_H17 cells are probably the major source of GM-CSF.

Within humans determining if any of the $CCR6^{+}IFN\gamma^{+}$ cells reacted against known auto-antigens involved in MS would be an important step forward. Using a murine model EAE, a conditional knockout of CCR6 in IFNγ secreting T cells, might give an indication if the cells were entering the CNS in a CCR6 dependent fashion, and if the cells were playing any sort of role in the pathogenesis of EAE. This experiment has limitations in that the $CCR6^{+}IFN\gamma^{+}IL\text{-}17^{+}$ cells would also lose CCR6 expression. This would mean that the effects of the knockout could not be attributed to just one individual subset of $CD4^{+}$ T cells.

Identification of the antigen specificity of the $CCR6^{+}IFN\gamma^{+}$ cells within the CSF samples would also give an indication as to their role in disease pathogenesis. Identifying $CCR6^{+}IFN\gamma^{+}$ cells with specificity for antigens such as myelin basic protein (MBP), Myelin oligodendrocyte glycoprotein (MOG) and myelin proteolipid protein (PLP) would point towards them playing a role in the destruction of myelin[251].

There are several other autoimmune diseases where $CCR6^{+}IFN\gamma^{+}$ T cells may also play a role. The pathogenesis of psoriasis[252], Crohns disease[1] and JIA[145] has been associated with both T_H17 and T_H1 cells, as well as $IFN\gamma^{+}IL\text{-}17^{+}$ cells. It may be interesting to see if there is an increased presence in these diseases of $CCR6^{+}IFN\gamma^{+}$ cells. The presence of RORC in $CCR6^{+}T_H1$ cells leads to the conclusion that this is the transcription factor that is controlling the 'T_H17'

like phenotype in the T_H1 cells, as it does in T_H17 cells[99]. This suggest that in settings such as MS, and the other autoimmune disease, the knockdown of RORC in both T_H17 and T_H1 cells may have an impact on the pathogenesis of the disease, but still leave a fully functional T_H1 response. However, there would be consequences for other cell types if RORC was knocked down. CCR6 T_{REG} cells also express RORC, and they have a CCR6 dependent migration in EAE. The reduction of these cells may cause uninhibited inflammation within the brain. RORC antagonists are already being considered as treatments for T_H17 related disease[253].

It is important to take into account the stages of the disease when assessing treatments such as a CCR6 targeted therapy. Within MS there is the initial wave of CCR6 dependent migration of T cells through the choroid plexus[157]. If the treatment to target CCR6 was given after this initial wave would there be any effect on inflammation within the brain? However it is possible that entry of CCR6 expressing cells is still needed to maintain inflammation. It will be important to understand if the expansion of the T_H17 cell population in relapse was due to more cells migrating into the CSF or if it was due to T_H17 cell proliferation within the tissue. This would have important implications for future treatments. Furthermore, it has still not been ruled out that T_H17 cells within the CSF are converting to $CCR6^+T_H1$ cells, or vice versa.

Situations such as this make it clear that understanding T cell biology in health is just as important as understanding T cell biology in disease settings. Understanding the true plastic nature of T cells will be vital to producing more target therapies that have a greater chance of having long lasting effects.

So can cytokine and transcription factors still be used to define lineages? These markers are still an important aspect of a T cell's phenotype. After all it is the cytokine that the cell produces that defines its ability to control an immune response. However, now that it is becoming obvious there is overlap in cytokine secretion, it is going to be the level of expression and the combinations of transcription factors that are expressed that becomes important. Other factors, such as miRNAs, will become important in understanding what may be controlling a T cell. Technology such as mRNA-seq[254] (analysis of the transcriptome of a single cell), and Chip-Seq[255] (analysis of protein and DNA interactions) will move the field of T cell plasticity forward. Rather than trying to define a T cell by how it acts *in vitro,* it will become more important to understand how T cells act *in vivo,* both in disease and health, to truly understand what role T cells have within the immune system.

LIST OF REFERENCES

1. Annunziato, F. *et al.* Phenotypic and functional features of human Th17 cells. *J. Exp. Med.* **204,** 1849–61 (2007).

2. Villares, R. *et al.* CCR6 regulates EAE pathogenesis by controlling regulatory CD4+ T-cell recruitment to target tissues. *Eur. J. Immunol.* **39,** 1671–81 (2009).

3. Kondo, M., Weissman, I. L. & Akashi, K. Identification of clonogenic common lymphoid progenitors in mouse bone marrow. *Cell* **91,** 661–72 (1997).

4. Akashi, K., Traver, D., Miyamoto, T. & Weissman, I. L. A clonogenic common myeloid progenitor that gives rise to all myeloid lineages. *Nature* **404,** 193–7 (2000).

5. Takeuchi, O. & Akira, S. Pattern recognition receptors and inflammation. *Cell* **140,** 805–20 (2010).

6. Nathan, C. Neutrophils and immunity: challenges and opportunities. *Nat. Rev. Immunol.* **6,** 173–82 (2006).

7. Germain, C. *et al.* Induction of lectin-like transcript 1 (LLT1) protein cell surface expression by pathogens and interferon-γ contributes to modulate immune responses. *J. Biol. Chem.* **286,** 37964–75 (2011).

8. Cosmi, L. *et al.* Human interleukin 17-producing cells originate from a CD161+CD4+ T cell precursor. *J. Exp. Med.* **205,** 1903–16 (2008).

9. Randolph, G. J., Inaba, K., Robbiani, D. F., Steinman, R. M. & Muller, W. a. Differentiation of phagocytic monocytes into lymph node dendritic cells in vivo. *Immunity* **11,** 753–61 (1999).

10. Merad, M., Sathe, P., Helft, J., Miller, J. & Mortha, A. The dendritic cell lineage: ontogeny and function of dendritic cells and their subsets in the steady state and the inflamed setting. *Annu. Rev. Immunol.* **31,** 563–604 (2013).

11. Neefjes, J., Jongsma, M. L. M., Paul, P. & Bakke, O. Towards a systems understanding of MHC class I and MHC class II antigen presentation. *Nat. Rev. Immunol.* **11,** 823–36 (2011).

12. Allman, D. & Pillai, S. Peripheral B cell subsets. *Curr. Opin. Immunol.* **20,** 149–157 (2008).

13. Wolf, S. D., Dittel, B. N., Hardardottir, F. & Janeway, C. a. Experimental autoimmune encephalomyelitis induction in genetically B cell-deficient mice. *J. Exp. Med.* **184,** 2271–8 (1996).

14. Kessel, A. *et al.* Human CD19(+)CD25(high) B regulatory cells suppress proliferation of CD4(+) T cells and enhance Foxp3 and CTLA-4 expression in T-regulatory cells. *Autoimmun. Rev.* **11,** 670–7 (2012).

15. Starr, T. K., Jameson, S. C. & Hogquist, K. a. Positive and negative selection of T cells. *Annu. Rev. Immunol.* **21,** 139–76 (2003).

16. Carbone, A., Marrack, P. & Kappler, J. Demethylated CD8 gene in CD4+ T cells suggests that CD4+ cells develop from CD8+ precursors. *Science (80-.).* **242,** 1174–1176 (1988).

17. Förster, R., Schubel, A. & Breitfeld, D. CCR7 coordinates the primary immune response by establishing functional microenvironments in secondary lymphoid organs. *Cell* **99,** 23–33 (1999).

18. Inaba, B. K., Metlay, J. P., Crowley, M. T. & Steinman, R. M. Dendritic Cells Pulsed with Protein Antigens In Vitro Can Prime Antigen-specific, MHC-restricted T Cells In Situ. *J. Exp. Med.* **172,** 631–640 (1990).

19. Levin, D., Constant, S., Pasqualini, T., Flavell, R. & Bottomly, K. Role of Dendritic Cells in the Priming of of CD4+ T Lymphocytes to Peptide Antigen In vivo. *J. Immunol.* **151,** 6742–6750 (1993).

20. Stoll, S., Delon, J., Brotz, T. M. & Germain, R. N. Dynamic imaging of T cell-dendritic cell interactions in lymph nodes. *Science (80-.).* **296,** 1873–6 (2002).

21. Tao, X., Constant, S., Jorritsma, P. & Bottomly, K. Strength of TCR Signal Determines the Costimulatory Requirements for Thl and Th2 CD4+ T Cell Differentiation. *J. Immunol.* **159,** 5956–5963 (1997).

22. Shahinian, A. *et al.* Differential T Cell Costimulatory Requirements in CD28-Deficient Mice AL-2. 28–31

23. Dong, C. *et al.* ICOS co-stimulatory receptor is essential for T-cell activation and function. *Nature* **409,** 97–101 (2001).

24. Murphy, K. M. & Reiner, S. L. The lineage decisions of helper T cells. *Nat. Rev. Immunol.* **2,** 933–44 (2002).

25. Helper, H. P. T., Sallusto, B. F., Lenig, D., Mackay, C. R. & Lanzavecchia, A. Flexible Programs of Chemokine Receptor Expression on Human Polarized T Helper1 and 2 Lymphocytes. *J. Exp. Med.* **187,** 875–883 (1998).

26. Razzaq, T. M. *et al.* Regulation of T-cell receptor signalling by membrane microdomains. *Immunology* **113,** 413–26 (2004).

27. Schwartz, B. R. H. Models o f T Cell Anergy: Is There A Common Molecular Mechanism? *J. Exp. Med.* **184,** 1–8 (1996).

28. Ostergaard, H. L. *et al.* Expression of CD45 alters phosphorylation of the lck-encoded tyrosine protein kinase in murine lymphoma T-cell lines. *Proc. Natl. Acad. Sci. U. S. A.* **86,** 8959–63 (1989).

29. Shaw, a S. & Dustin, M. L. Making the T cell receptor go the distance: a topological view of T cell activation. *Immunity* **6,** 361–9 (1997).

30. Greenlund, a C. *et al.* Stat recruitment by tyrosine-phosphorylated cytokine receptors: an ordered reversible affinity-driven process. *Immunity* **2,** 677–87 (1995).

31. Sallusto, F., Geginat, J. & Lanzavecchia, A. Central memory and effector memory T cell subsets: function, generation, and maintenance. *Annu. Rev. Immunol.* **22,** 745–63 (2004).

32. Unutmaz, D, Pileri, P and Abrignani, S. Antigen-independent Activation of Naive and Memory Resting T Cells by a Cytokine Combination. *J. Exp. Med.* **180,** 1–6 (1994).

33. Allen, S. J., Crown, S. E. & Handel, T. M. Chemokine: receptor structure, interactions, and antagonism. *Annu. Rev. Immunol.* **25,** 787–820 (2007).

34. Murphy, P. The molecular biology of leukocyte chemoattractant receptors. *Annu. Rev. Immunol.* **12,** 593–633 (1994).

35. Premont, R., Inglese, J. & Lefkowitz, R. Protein kinases that phosphorylate activated G protein-coupled receptors. *FASEB J.* **9,** 175–182 (1995).

36. Bonecchi, B. R. *et al.* Differential Expression of Chemokine Receptors and Chemotactic Responsiveness of Type 1 T Helper Cells. *J. Exp. Med.* **187,** 129–134 (1998).

37. Singh, S. P., Zhang, H. H., Foley, J. F., Hedrick, M. N. & Farber, J. M. Human T cells that are able to produce IL-17 express the chemokine receptor CCR6. *J. Immunol.* **180,** 214–21 (2008).

38. Peters, P. J. *et al.* Cytotoxic T lymphocyte granules are secretory lysosomes, containing both perforin and granzymes. *J. Exp. Med.* **173,** 1099–109 (1991).

39. Rouvier, E., Luciani, M. F. & Golstein, P. Fas involvement in Ca(2+)-independent T cell-mediated cytotoxicity. *J. Exp. Med.* **177,** 195–200 (1993).

40. Huber, M. *et al.* A Th17-like developmental process leads to CD8(+) Tc17 cells with reduced cytotoxic activity. *Eur. J. Immunol.* **39,** 1716–25 (2009).

41. Yen, H.-R. H. *et al.* Tc17 CD8 T cells: functional plasticity and subset diversity. *J. Immunol.* **183,** 7161–8 (2009).

42. Hamada, H. *et al.* Tc17, a unique subset of CD8 T cells that can protect against lethal influenza challenge. *J. Immunol.* **182,** 3469–81 (2009).

43. Mosmann, T. R., Cherwinski, H., Bond, M. W., Giedlin, M. a & Coffman, R. L. Two types of murine helper T cell clone. I. Definition according to profiles of lymphokine activities and secreted proteins. 1986. *J. Immunol.* **175,** 5–14 (1986).

44. Nathan, C. & Murray, H. Identification of interferon-gamma as the lymphokine that activates human macrophage oxidative metabolism and antimicrobial activity. *J. Exp. Med.* **158,** 670–689 (1983).

45. Milstone, L. & Waksman, B. Release of virus inhibitor from tuberculin-sensitized peritoneal cells stimulated by antigen. *J. Immunol.* **2,** 1068–1071 (1970).

46. Ahn, H.-J. *et al.* A Mechanism Underlying Synergy Between IL-12 and IFN-γ-Inducing Factor in Enhanced Production of IFN-γ. *J. Immunol.* (1997).

47. Szabo, S. J. *et al.* A novel transcription factor, T-bet, directs Th1 lineage commitment. *Cell* **100,** 655–69 (2000).

48. Jouanguy, E. *et al.* Interferon-γ–receptor deficiency in an Infant with Fatal Bacille Calmette-Guerin Infection. *N. Engl. J. Med.* **335,** 1956–1961 (1996).

49. Newport, M. *et al.* A mutation in the interferon-γ–receptor gene and susceptibility to mycobacterial infection. *N. Engl. J. Med.* **335,** 1941–1949 (1996).

50. Dupuis, S. *et al.* Impairment of mycobacterial but not viral immunity by a germline human STAT1 mutation. *Science (80-.).* **293,** 300–3 (2001).

51. Finotto, S. *et al.* Development of spontaneous airway changes consistent with human asthma in mice lacking T-bet. *Science (80-.).* **295,** 336–8 (2002).

52. Szabo, S. J. *et al.* Distinct effects of T-bet in TH1 lineage commitment and IFN-gamma production in CD4 and CD8 T cells. *Science (80-.).* **295,** 338–42 (2002).

53. Mullen, A. C. *et al.* Hlx is induced by and genetically interacts with T-bet to promote heritable T(H)1 gene induction. *Nat. Immunol.* **3,** 652–8 (2002).

54. Afkarian, M. *et al.* T-bet is a STAT1-induced regulator of IL-12R expression in naïve CD4+ T cells. *Nat. Immunol.* **3,** 549–57 (2002).

55. Mullen, a C. *et al.* Role of T-bet in commitment of TH1 cells before IL-12-dependent selection. *Science (80-.).* **292,** 1907–10 (2001).

56. Szabo, S. J., Dighe, a S., Gubler, U. & Murphy, K. M. Regulation of the interleukin (IL)-12R beta 2 subunit expression in developing T helper 1 (Th1) and Th2 cells. *J. Exp. Med.* **185,** 817–24 (1997).

57. Cua, D. J. *et al.* Interleukin-23 rather than interleukin-12 is the critical cytokine for autoimmune inflammation of the brain. *Nature* **421,** 744–8 (2003).

58. Sadick, H., Holaday, B., Coffman, R. & Locksley, R. Reciprocal expression of interferon gamma or interleukin 4 during the resolution or progression of murine leishmaniasis. *J Exp Med* **169,** 59–72 (1989).

59. Coffman, R. L. *et al.* B cell stimulatory factor-1 enhances the IgE response of lipopolysaccharide-activated B cells. *J. Immunol.* **136,** 4538–41 (1986).

60. Zheng, W. & Flavell, R. a. The transcription factor GATA-3 is necessary and sufficient for Th2 cytokine gene expression in CD4 T cells. *Cell* **89,** 587–96 (1997).

61. Takemoto, N. *et al.* Cutting edge: chromatin remodeling at the IL-4/IL-13 intergenic regulatory region for Th2-specific cytokine gene cluster. *J. Immunol.* **165,** 6687–91 (2000).

62. Zhu, J., Cote-Sierra, J., Guo, L. & Paul, W. E. Stat5 activation plays a critical role in Th2 differentiation. *Immunity* **19,** 739–48 (2003).

63. Ouyang, W. *et al.* Stat6-independent GATA-3 autoactivation directs IL-4-independent Th2 development and commitment. *Immunity* **12,** 27–37 (2000).

64. Cote-Sierra, J. *et al.* Interleukin 2 plays a central role in Th2 differentiation. *Proc. Natl. Acad. Sci. U. S. A.* **101,** 3880–5 (2004).

65. Quirion, M. R., Gregory, G. D., Umetsu, S. E., Winandy, S. & Brown, M. a. Cutting edge: Ikaros is a regulator of Th2 cell differentiation. *J. Immunol.* **182,** 741–5 (2009).

66. Zhu, J. *et al.* Conditional deletion of Gata3 shows its essential function in T(H)1-T(H)2 responses. *Nat. Immunol.* **5,** 1157–65 (2004).

67. Willenborg, D., Fordham, S., Cowden, W. B. & Ramshawt, I. A. IFN-y Plays a Critical Down-Regulatory Role in the Induction and Effector Phase of Myelin Oligodendrocyte Glycoprotein-Induced Autoimmune Encephalomyelitis. *J. Immunol.* **157,** 3223–3227 (1996).

68. Gran, B. *et al.* IL-12p35-Deficient Mice Are Susceptible to Central Nervous System Autoimmune in the IL-12 System in the Induction of Encephalomyelitis: Evidence for Redundancy Experimental Autoimmune Demyelination. *J. Immunol.* **169,** 7104–7110 (2002).

69. Langrish, C. L. *et al.* IL-23 drives a pathogenic T cell population that induces autoimmune inflammation. *J. Exp. Med.* **201,** 233–40 (2005).

70. Bettelli, E. *et al.* Loss of T-bet, but not STAT1, prevents the development of experimental autoimmune encephalomyelitis. *J. Exp. Med.* **200,** 79–87 (2004).

71. Aggarwal, S., Ghilardi, N., Xie, M.-H., de Sauvage, F. J. & Gurney, A. L. Interleukin-23 promotes a distinct CD4 T cell activation state characterized by the production of interleukin-17. *J. Biol. Chem.* **278,** 1910–4 (2003).

72. Zhou, L. *et al.* IL-6 programs T(H)-17 cell differentiation by promoting sequential engagement of the IL-21 and IL-23 pathways. *Nat. Immunol.* **8,** 967–74 (2007).

73. McGeachy, M. J. *et al.* The interleukin 23 receptor is essential for the terminal differentiation of interleukin 17-producing effector T helper cells in vivo. *Nat. Immunol.* **10,** 314–24 (2009).

74. Rouvier, E., Luciani, M., Mattei, M., Denizot, F. & Golstein, P. CTLA-8, cloned from an activated T cell, bearing AU-rich messenger RNA instability sequences, and homologous to a herpesvirus saimiri gene. *J. Immunol.* **150,** 5445–5456 (1993).

75. Chang, S. H. & Dong, C. A novel heterodimeric cytokine consisting of IL-17 and IL-17F regulates inflammatory responses. *Cell Res.* **17,** 435–40 (2007).

76. Moseley, T. a., Haudenschild, D. R., Rose, L. & Reddi, a. H. Interleukin-17 family and IL-17 receptors. *Cytokine Growth Factor Rev.* **14,** 155–174 (2003).

77. Kagami, S., Rizzo, H. L., Kurtz, S. E., Miller, L. S. & Blauvelt, A. IL-23 and IL-17A, but not IL-12 and IL-22, are required for optimal skin host defense against Candida albicans. *J. Immunol.* **185,** 5453–62 (2010).

78. Ishigame, H. *et al.* Differential roles of interleukin-17A and -17F in host defense against mucoepithelial bacterial infection and allergic responses. *Immunity* **30,** 108–19 (2009).

79. Kolls, J. & Lindén, A. Interleukin-17 family members and inflammation. *Immunity* **21,** 467–476 (2004).

80. Infante-Duarte, C., Horton, H. F., Byrne, M. C. & Kamradt, T. Microbial Lipopeptides Induce the Production of IL-17 in Th Cells. *J. Immunol.* **165,** 6107–6115 (2000).

81. Fossiez, F. *et al.* T cell interleukin-17 induces stromal cells to produce proinflammatory and hematopoietic cytokines. *J. Exp. Med.* **183,** 2593–603 (1996).

82. Chang, H. *et al.* Causes of Death in Adults With Acute Leukemia. *Medicine (Baltimore).* **55,** 259–268 (1976).

83. Huang, W., Na, L., Fidel, P. L. & Schwarzenberger, P. Requirement of interleukin-17A for systemic anti-Candida albicans host defense in mice. *J. Infect. Dis.* **190,** 624–31 (2004).

84. Ivanov, I. I. *et al.* The orphan nuclear receptor RORgammat directs the differentiation program of proinflammatory IL-17+ T helper cells. *Cell* **126,** 1121–33 (2006).

85. Maggi, L. *et al.* CD161 is a marker of all human IL-17-producing T-cell subsets and is induced by RORC. *Eur. J. Immunol.* **40,** 2174–81 (2010).

86. Yang, X. O. *et al.* T helper 17 lineage differentiation is programmed by orphan nuclear receptors ROR alpha and ROR gamma. *Immunity* **28,** 29–39 (2008).

87. Veldhoen, M., Hirota, K., Christensen, J., O'Garra, A. & Stockinger, B. Natural agonists for aryl hydrocarbon receptor in culture medium are essential for optimal differentiation of Th17 T cells. *J. Exp. Med.* **206,** 43–9 (2009).

88. Sun, Z. *et al.* Requirement for RORgamma in Thymocyte Survival and Lymphoid Organ Development. *Science (80-.).* **288,** 2369–2373 (2000).

89. Eberl, G. *et al.* An essential function for the nuclear receptor RORgamma(t) in the generation of fetal lymphoid tissue inducer cells. *Nat. Immunol.* **5,** 64–73 (2004).

90. Harrington, L. E. *et al.* Interleukin 17-producing CD4+ effector T cells develop via a lineage distinct from the T helper type 1 and 2 lineages. *Nat. Immunol.* **6,** 1123–32 (2005).

91. Stockinger, B., Veldhoen, M. & Martin, B. Th17 T cells: linking innate and adaptive immunity. *Semin. Immunol.* **19,** 353–61 (2007).

92. Veldhoen, M., Hocking, R. J., Atkins, C. J., Locksley, R. M. & Stockinger, B. TGFbeta in the context of an inflammatory cytokine milieu supports de novo differentiation of IL-17-producing T cells. *Immunity* **24,** 179–89 (2006).

93. Nurieva, R. *et al.* Essential autocrine regulation by IL-21 in the generation of inflammatory T cells. *Nature* **448,** 480–3 (2007).

94. Sutton, C., Brereton, C., Keogh, B., Mills, K. H. G. & Lavelle, E. C. A crucial role for interleukin (IL)-1 in the induction of IL-17-producing T cells that mediate autoimmune encephalomyelitis. *J. Exp. Med.* **203,** 1685–91 (2006).

95. Hu, W., Troutman, T. D., Edukulla, R. & Pasare, C. Priming microenvironments dictate cytokine requirements for T helper 17 cell lineage commitment. *Immunity* **35,** 1010–22 (2011).

96. Zhou, L. *et al.* TGF-beta-induced Foxp3 inhibits T(H)17 cell differentiation by antagonizing RORgammat function. *Nature* **453,** 236–40 (2008).

97. Das, J. *et al.* Transforming growth factor beta is dispensable for the molecular orchestration of Th17 cell differentiation. *J. Exp. Med.* **206,** 2407–16 (2009).

98. Acosta-Rodriguez, E. V, Napolitani, G., Lanzavecchia, A. & Sallusto, F. Interleukins 1beta and 6 but not transforming growth factor-beta are essential for the differentiation of interleukin 17-producing human T helper cells. *Nat. Immunol.* **8,** 942–9 (2007).

99. Manel, N., Unutmaz, D. & Littman, D. R. The differentiation of human T(H)-17 cells requires transforming growth factor-beta and induction of the nuclear receptor RORgammat. *Nat. Immunol.* **9,** 641–9 (2008).

100. Ma, C. S. *et al.* Deficiency of Th17 cells in hyper IgE syndrome due to mutations in STAT3. *J. Exp. Med.* **205,** 1551–7 (2008).

101. Purvis, H. a *et al.* Low-strength T-cell activation promotes Th17 responses. *Blood* **116,** 4829–37 (2010).

102. Evans, H. G. *et al.* In vivo activated monocytes from the site of inflammation in humans specifically promote Th17 responses. *Proc. Natl. Acad. Sci. U. S. A.* **106,** 6232–7 (2009).

103. Lee, W.-W. *et al.* Regulating human Th17 cells via differential expression of IL-1 receptor. *Blood* **115,** 530–40 (2010).

104. Santarlasci, V. *et al.* Rarity of Human T Helper 17 Cells Is due to Retinoic Acid Orphan Receptor-Dependent Mechanisms that Limit Their Expansion. *Immunity* **36,** 201–214 (2012).

105. Maggi, L. *et al.* Distinctive features of classic and nonclassic (Th17 derived) human Th1 cells. *Eur. J. Immunol.* **42,** 1–9 (2012).

106. Boulland, M.-L. *et al.* Human IL4I1 is a secreted L-phenylalanine oxidase expressed by mature dendritic cells that inhibits T-lymphocyte proliferation. *Blood* **110,** 220–7 (2007).

107. Billerbeck, E. *et al.* Analysis of CD161 expression on human CD8+ T cells defines a distinct functional subset with tissue-homing properties. *Proc. Natl. Acad. Sci. U. S. A.* **107,** 3006–11 (2010).

108. Rosen, D. B. *et al.* Functional consequences of interactions between human NKR-P1A and its ligand LLT1 expressed on activated dendritic cells and B cells. *J. Immunol.* **180,** 6508–17 (2008).

109. Poggi, a, Costa, P., Zocchi, M. R. & Moretta, L. Phenotypic and functional analysis of CD4+ NKRP1A+ human T lymphocytes. Direct evidence that the NKRP1A molecule is involved in transendothelial migration. *Eur. J. Immunol.* **27,** 2345–50 (1997).

110. Liao, F. *et al.* CC-chemokine receptor 6 is expressed on diverse memory subsets of T cells and determines responsiveness to macrophage inflammatory protein 3 alpha. *J. Immunol.* **162,** 186–194 (2013).

111. Voo, K. S. *et al.* Identification of IL-17-producing FOXP3+ regulatory T cells in humans. *Proc. Natl. Acad. Sci. U. S. A.* **106,** 4793–8 (2009).

112. Krzysiek, R. & Lefevre, E. Regulation of CCR6 chemokine receptor expression and responsiveness to macrophage inflammatory protein-3α/CCL20 in human B cells. *Blood* **96,** 2338–2345 (2000).

113. Liang, S. C. *et al.* Interleukin (IL)-22 and IL-17 are coexpressed by Th17 cells and cooperatively enhance expression of antimicrobial peptides. *J. Exp. Med.* **203,** 2271–9 (2006).

114. Duhen, T., Geiger, R., Jarrossay, D., Lanzavecchia, A. & Sallusto, F. Production of interleukin 22 but not interleukin 17 by a subset of human skin-homing memory T cells. *Nat. Immunol.* **10,** 857–63 (2009).

115. Wolk, K. *et al.* IL-22 increases the innate immunity of tissues. *Immunity* **21,** 241–54 (2004).

116. Eyerich, S. *et al.* Th22 cells represent a distinct human T cell subset involved in epidermal immunity and remodeling. *J. Clin. Invest.* **119,** 3573–3585 (2009).

117. Cella, M. *et al.* A human natural killer cell subset provides an innate source of IL-22 for mucosal immunity. *Nature* **457,** 722–5 (2009).

118. Breitfeld, D. *et al.* Follicular B helper T cells express CXC chemokine receptor 5, localize to B cell follicles, and support immunoglobulin production. *J. Exp. Med.* **192,** 1545–52 (2000).

119. Fontenot, J. D., Gavin, M. a & Rudensky, A. Y. Foxp3 programs the development and function of CD4+CD25+ regulatory T cells. *Nat. Immunol.* **4,** 330–6 (2003).

120. Sakaguchi, S., Sakaguchi, N., Asano, M., Itoh, M. & Toda, M. Immunologic Self-Tolerance Maintained by Activated T Cells Expressing 11-2 Receptor. *J. Immunol.* **155,** 1151–1164 (1995).

121. Wildin, R. S. *et al.* The immune dysregulation , polyendocrinopathy , enteropathy , X-linked syndrome (IPEX) is caused by mutations of FOXP3. *Nat. Genet.* **27,** 20–21 (2001).

122. Qureshi, O. S. *et al.* Trans-endocytosis of CD80 and CD86: a molecular basis for the cell-extrinsic function of CTLA-4. *Science (80-.).* **332,** 600–3 (2011).

123. Vignali, D. a a, Collison, L. W. & Workman, C. J. How regulatory T cells work. *Nat. Rev. Immunol.* **8,** 523–32 (2008).

124. Cowan, J. E. *et al.* The thymic medulla is required for Foxp3+ regulatory but not conventional CD4+ thymocyte development. *J. Exp. Med.* **210,** 675–681 (2013).

125. Lafaille, M. de. CD25− T cells generate CD25+ Foxp3+ regulatory T cells by peripheral expansion. *J. Immunol.* **173,** 7259–7268 (2004).

126. Fantini, M. C. *et al.* Cutting edge: TGF-beta induces a regulatory phenotype in CD4+CD25- T cells through Foxp3 induction and down-regulation of Smad7. *J. Immunol.* **172,** 5149–53 (2004).

127. Furtado, G. C., de Lafaille, M. a. C., Kutchukhidze, N. & Lafaille, J. J. Interleukin 2 Signaling Is Required for CD4+ Regulatory T Cell Function. *J. Exp. Med.* **196,** 851–857 (2002).

128. Battaglia, M., Gregori, S., Bacchetta, R. & Roncarolo, M.-G. Tr1 cells: from discovery to their clinical application. *Semin. Immunol.* **18,** 120–7 (2006).

129. Chen, Y., Kuchroo, V. K., Inobe, J., Hafler, D. a & Weiner, H. L. Regulatory T cell clones induced by oral tolerance: suppression of autoimmune encephalomyelitis. *Science (80-.).* **265,** 1237–40 (1994).

130. Coombes, J. L. *et al.* A functionally specialized population of mucosal CD103+ DCs induces Foxp3+ regulatory T cells via a TGF-beta and retinoic acid-dependent mechanism. *J. Exp. Med.* **204,** 1757–64 (2007).

131. Sun, C.-M. *et al.* Small intestine lamina propria dendritic cells promote de novo generation of Foxp3 T reg cells via retinoic acid. *J. Exp. Med.* **204,** 1775–85 (2007).

132. Lal, G. *et al.* Epigenetic Regulation of Foxp3 Expression in Regulatory T cells by DNA Methylation. *J. Immunol.* **182,** 259–273 (2009).

133. Janson, P. C. J. *et al.* FOXP3 promoter demethylation reveals the committed Treg population in humans. *PLoS One* **3,** e1612 (2008).

134. Liao, W., Lin, J.-X., Wang, L., Li, P. & Leonard, W. J. Modulation of cytokine receptors by IL-2 broadly regulates differentiation into helper T cell lineages. *Nat. Immunol.* **12,** 551–9 (2011).

135. Jenner, R. G. *et al.* The transcription factors T-bet and GATA-3 control alternative pathways of T-cell differentiation through a shared set of target genes. *Proc. Natl. Acad. Sci. U. S. A.* **106,** 17876–81 (2009).

136. Djuretic, I. M. *et al.* Transcription factors T-bet and Runx3 cooperate to activate Ifng and silence Il4 in T helper type 1 cells. *Nat. Immunol.* **8,** 145–53 (2007).

137. Lazarevic, V. *et al.* T-bet represses T(H)17 differentiation by preventing Runx1-mediated activation of the gene encoding RORγt. *Nat. Immunol.* **12,** 96–104 (2011).

138. Zhou, L., Chong, M. M. W. & Littman, D. R. Plasticity of CD4+ T cell lineage differentiation. *Immunity* **30,** 646–55 (2009).

139. Yang, X. O. *et al.* Molecular antagonism and plasticity of regulatory and inflammatory T cell programs. *Immunity* **29,** 44–56 (2008).

140. Koch, M. a *et al.* The transcription factor T-bet controls regulatory T cell homeostasis and function during type 1 inflammation. *Nat. Immunol.* **10,** 595–602 (2009).

141. Chen, J. & Liu, X. S. Development and function of IL-10 IFN-gamma-secreting CD4(+) T cells. *J. Leukoc. Biol.* **86,** 1305–10 (2009).

142. Hegazy, A. N. *et al.* Interferons direct Th2 cell reprogramming to generate a stable GATA-3(+)T-bet(+) cell subset with combined Th2 and Th1 cell functions. *Immunity* **32,** 116–28 (2010).

143. Lexberg, M. H. *et al.* Frontline: Th memory for interleukin-17 expression is stable in vivo. *Eur. J. Immunol.* **38,** 2654–2664 (2008).

144. Lexberg, M. H. *et al.* IFN-γ and IL-12 synergize to convert in vivo generated Th17 into Th1/Th17 cells. *Eur. J. Immunol.* **40,** 3017–27 (2010).

145. Cosmi, L. *et al.* Evidence of the transient nature of the Th17 phenotype of CD4+CD161+ T cells in the synovial fluid of patients with juvenile idiopathic arthritis. *Arthritis Rheum.* **63,** 2504–15 (2011).

146. Hirota, K. *et al.* Fate mapping of IL-17-producing T cells in inflammatory responses. *Nat. Immunol.* **12,** 255–63 (2011).

147. Zielinski, C. E. *et al.* Pathogen-induced human T(H)17 cells produce IFN-γ or IL-10 and are regulated by IL-1β. *Nature* **484,** 514–518 (2012).

148. Cohen, C. J. *et al.* Human Th1 and Th17 cells exhibit epigenetic stability at signature cytokine and transcription factor loci. *J. Immunol.* **187,** 5615–26 (2011).

149. Han, Q. *et al.* Polyfunctional responses by human T cells result from sequential release of cytokines. *PNAS* **109,** 1–6 (2011).

150. Korn, T. *et al.* Myelin-specific regulatory T cells accumulate in the CNS but fail to control autoimmune inflammation. *Nat. Med.* **13,** 423–31 (2007).

151. Stevenson, P. G., Hawke, S., Sloan, D. J. & Bangham, C. R. The immunogenicity of intracerebral virus infection depends on anatomical site. *J. Virol.* **71,** 145–51 (1997).

152. Matyszak, M. K. & Perry, V. H. Bacillus Calmette-Guérin sequestered in the brain parenchyma escapes immune recognition. *J. Neuroimmunol.* **82,** 73–80 (1998).

153. Matyszak, M. & Perry, V. Demyelination in the central nervous system following a delayed-type hypersensitivity response to bacillus Calmette-Guerin. *Neuroscience* **64,** (1995).

154. Yamada, S., DePasquale, M., Patlak, C. & Cserr, H. Albumin outflow into deep cervical lymph from different regions of rabbit brain. *Am. J. Physiol. - Hear. Circ. Physiol.* **261,** H1197–204 (1991).

155. Giulian, D., Li, J., Bartel, S. & Broker, J. Cell surface morphology identifies microglia as a distinct class of mononuclear phagocyte. *J. Neurosci.* **15,** 7712–7726 (1995).

156. Mendez-Fernandez, Y., MJ, H., Rodriguez, M. & Pease, L. Anatomical and cellular requirements for the activation and migration of virus-specific CD8+ T cells to the brain during Theiler's virus infection. *J. Virol.* **79,** 3063–3070 (2005).

157. Reboldi, A. *et al.* C-C chemokine receptor 6-regulated entry of TH-17 cells into the CNS through the choroid plexus is required for the initiation of EAE. *Nat. Immunol.* **10,** 514–23 (2009).

158. Carrithers, M. D., Visintin, I., Kang, S. J. & Janeway, C. a. Differential adhesion molecule requirements for immune surveillance and inflammatory recruitment. *Brain* **123 (Pt 6,** 1092–101 (2000).

159. González-Amaro, R., Mittelbrunn, M. & Sánchez-Madrid, F. Therapeutic anti-integrin (alpha4 and alphaL) monoclonal antibodies: two-edged swords? *Immunology* **116,** 289–96 (2005).

160. Bartholomäus, I. *et al.* Effector T cell interactions with meningeal vascular structures in nascent autoimmune CNS lesions. *Nature* **462,** 94–8 (2009).

161. Charcot, J. Histologie de la sclerose en plaque. *Gaz. Hop.* **41,** 554–566 (1868).

162. Kabat, E., Glusman, M. & Knaub, V. Quantitative estimation of the albumin and gamma globulin in normal and pathologic cerebrospinal fluid by immunochemical methods. *Am. J. Med.* **4,** 653–662 (1948).

163. Ebers, G. C., Sadovnick, a D. & Veith, R. Vitamin D intake and incidence of multiple sclerosis. *Neurology* **63,** 60–65 (2004).

164. Marrie, R. A. Reviews Environmental risk factors in multiple sclerosis aetiology. *Lancet Neurol.* **3,** 709–718 (2004).

165. Fingerprinting, G. Risk alleles for multiple sclerosis identified by a genomewide study. *N Engl J Med* (2007). at <http://www.nejm.org/doi/full/10.1056/NEJMoa073493>

166. Cantorna, M., Yu, S. & Bruce, D. The paradoxical effects of vitamin D on type 1 mediated immunity. *Mol. Aspects Med.* **29,** 369–375 (2008).

167. Smolders, J. *et al.* Vitamin D status is positively correlated with regulatory T cell function in patients with multiple sclerosis. *PLoS One* **4,** e6635 (2009).

168. Haahr, S. & Koch-Henriksen, N. Increased risk of multiple sclerosis after late Epstein-Barr virus infection: a historical prospective study. *Mult. Scler.* 73–77 (1995).

169. Prineas, J. & Graham, J. Multiple sclerosis: capping of surface immunoglobulin G on macrophages engaged in myelin breakdown. *Ann. Neurol.* **10,** 149–158 (1981).

170. Serafini, B., Rosicarelli, B., Magliozzi, R., Stigliano, E. & Aloisi, F. Detection of ectopic B-cell follicles with germinal centers in the meninges of patients with secondary progressive multiple sclerosis. *Brain Pathol.* **14,** 164–74 (2004).

171. Yednock, T., Cannon, C. & Fritz, L. Prevention of experimental autoimmune encephalomyelitis by antibodies against α4β1 integrin. *Nature* **5,** 63–66 (1992).

172. Miller, D. H. *et al.* A randomized, placebo-controlled trial of natalizumab for relapsing multiple sclerosis. *N. Engl. J. Med.* **354,** 899–910 (2006).

173. El-Behi, M. *et al.* The encephalitogenicity of T(H)17 cells is dependent on IL-1- and IL-23-induced production of the cytokine GM-CSF. *Nat. Immunol.* **12,** 568–75 (2011).

174. Lee, Y. *et al.* Induction and molecular signature of pathogenic TH17 cells. *Nat. Immunol.* **13,** 991–999 (2012).

175. Yang, L., Anderson, D. E., Kuchroo, J. & Hafler, D. a. Lack of TIM-3 immunoregulation in multiple sclerosis. *J. Immunol.* **180,** 4409–14 (2008).

176. Koguchi, K. *et al.* Dysregulated T cell expression of TIM3 in multiple sclerosis. *J. Exp. Med.* **203,** 1413–8 (2006).

177. Fletcher, J. M. *et al.* CD39+Foxp3+ regulatory T Cells suppress pathogenic Th17 cells and are impaired in multiple sclerosis. *J. Immunol.* **183,** 7602–10 (2009).

178. Atarashi, K. *et al.* ATP drives lamina propria T(H)17 cell differentiation. *Nature* **455,** 808–12 (2008).

179. Ye, Z.-J. *et al.* CD39+ regulatory T cells suppress generation and differentiation of Th17 cells in human malignant pleural effusion via a LAP-dependent mechanism. *Respir. Res.* **12,** 77 (2011).

180. Dominguez-Villar, M., Baecher-Allan, C. M. & Hafler, D. a. Identification of T helper type 1-like, Foxp3+ regulatory T cells in human autoimmune disease. *Nat. Med.* **17,** 673–5 (2011).

181. Hammond, S. M. Dicing and slicing: the core machinery of the RNA interference pathway. *FEBS Lett.* **579,** 5822–9 (2005).

182. Lee, Y. *et al.* MicroRNA genes are transcribed by RNA polymerase II. *EMBO J.* **23,** 4051–60 (2004).

183. Lee, Y. *et al.* The nuclear RNase III Drosha initiates microRNA processing. *Nature* **425,** 415–9 (2003).

184. Denli, A. M., Tops, B. B. J., Plasterk, R. H. a, Ketting, R. F. & Hannon, G. J. Processing of primary microRNAs by the Microprocessor complex. *Nature* **432,** 231–5 (2004).

185. Filipowicz, W., Jaskiewicz, L., Kolb, F. a & Pillai, R. S. Post-transcriptional gene silencing by siRNAs and miRNAs. *Curr. Opin. Struct. Biol.* **15,** 331–41 (2005).

186. Chong, M. M. W., Rasmussen, J. P., Rudensky, A. Y., Rundensky, A. Y. & Littman, D. R. The RNAseIII enzyme Drosha is critical in T cells for preventing lethal inflammatory disease. *J. Exp. Med.* **205,** 2005–17 (2008).

187. Muljo, S. a *et al.* Aberrant T cell differentiation in the absence of Dicer. *J. Exp. Med.* **202,** 261–9 (2005).

188. Zhou, X. *et al.* Selective miRNA disruption in T reg cells leads to uncontrolled autoimmunity. *J. Exp. Med.* **205,** 1983–91 (2008).

189. Xiao, C. *et al.* Lymphoproliferative disease and autoimmunity in mice with increased miR-17-92 expression in lymphocytes. *Nat. Immunol.* **9,** 405–14 (2008).

190. Steiner, D., Thomas, M., Hu, J. & Yang, Z. MicroRNA-29 regulates T-box transcription factors and interferon-γ production in helper T cells. *Immunity* **35,** 169–181 (2011).

191. Smith, K. M. *et al.* miR-29ab1 deficiency identifies a negative feedback loop controlling Th1 bias that is dysregulated in multiple sclerosis. *J. Immunol.* **189,** 1567–76 (2012).

192. O'Connell, R. M. *et al.* MicroRNA-155 promotes autoimmune inflammation by enhancing inflammatory T cell development. *Immunity* **33,** 607–19 (2010).

193. Banerjee, A., Schambach, F., DeJong, C. S., Hammond, S. M. & Reiner, S. L. Micro-RNA-155 inhibits IFN-gamma signaling in CD4+ T cells. *Eur. J. Immunol.* **40,** 225–31 (2010).

194. Du, C. *et al.* MicroRNA miR-326 regulates TH-17 differentiation and is associated with the pathogenesis of multiple sclerosis. *Nat. Immunol.* **10,** 1252–9 (2009).

195. Mycko, M. P. *et al.* MicroRNA-301a regulation of a T-helper 17 immune response controls autoimmune demyelination. *Proc. Natl. Acad. Sci. U. S. A.* **109,** E1248–57 (2012).

196. Zhao, F. *et al.* Human CCR4+ CCR6+ Th17 cells suppress autologous CD8+ T cell responses. *J. Immunol.* **188,** 6055–62 (2012).

197. Irie-Sasaki, J. *et al.* CD45 is a JAK phosphatase and negatively regulates cytokine receptor signalling. *Nature* **409,** 349–54 (2001).

198. Chatila, T., Silverman, L., Miller, R. & Geha, R. Mechanisms of T cell activation by the calcium ionophore ionomycin. *J. Immunol.* **143,** 1283–9 (1989).

199. Chtanova, T. *et al.* T follicular helper cells express a distinctive transcriptional profile, reflecting their role as non-Th1/Th2 effector cells that provide help for B cells. *J. Immunol.* **173,** 68–78 (2004).

200. Boniface, K. *et al.* Human Th17 cells comprise heterogeneous subsets including IFN-gamma-producing cells with distinct properties from the Th1 lineage. *J. Immunol.* **185,** 679–87 (2010).

201. Codarri, L. *et al.* RORγt drives production of the cytokine GM-CSF in helper T cells, which is essential for the effector phase of autoimmune neuroinflammation. *Nat. Immunol.* **12,** 560–7 (2011).

202. Ponomarev, E. & Shriver, L. GM-CSF production by autoreactive T cells is required for the activation of microglial cells and the onset of experimental autoimmune encephalomyelitis. *J. Immunol.* 39–48 (2007).

203. Athie-Morales, V., Smits, H. H., Cantrell, D. a & Hilkens, C. M. U. Sustained IL-12 signaling is required for Th1 development. *J. Immunol.* **172,** 61–9 (2004).

204. Mukasa, R. *et al.* Epigenetic instability of cytokine and transcription factor gene loci underlies plasticity of the T helper 17 cell lineage. *Immunity* **32,** 616–27 (2010).

205. Nanjappa, S. G., Heninger, E., Wüthrich, M., Gasper, D. J. & Klein, B. S. Tc17 cells mediate vaccine immunity against lethal fungal pneumonia in immune deficient hosts lacking CD4+ T cells. *PLoS Pathog.* **8,** e1002771 (2012).

206. Wang, Y.-H. *et al.* A novel subset of CD4(+) T(H)2 memory/effector cells that produce inflammatory IL-17 cytokine and promote the exacerbation of chronic allergic asthma. *J. Exp. Med.* **207,** 2479–91 (2010).

207. Kelly, B. L. & Locksley, R. M. Coordinate regulation of the IL-4, IL-13, and IL-5 cytokine cluster in Th2 clones revealed by allelic expression patterns. *J. Immunol.* **165,** 2982–6 (2000).

208. Laurence, A. *et al.* Interleukin-2 signaling via STAT5 constrains T helper 17 cell generation. *Immunity* **26,** 371–81 (2007).

209. Evans, H. G., Suddason, T., Jackson, I., Taams, L. S. & Lord, G. M. Optimal induction of T helper 17 cells in humans requires T cell receptor ligation in the context of Toll-like receptor-activated monocytes. *Proc. Natl. Acad. Sci. U. S. A.* **104,** 17034–9 (2007).

210. Zheng, S. G., Wang, J. & Horwitz, D. a. Cutting edge: Foxp3+CD4+CD25+ regulatory T cells induced by IL-2 and TGF-beta are resistant to Th17 conversion by IL-6. *J. Immunol.* **180,** 7112–6 (2008).

211. Xu, L., Kitani, A., Fuss, I. & Strober, W. Cutting edge: regulatory T cells induce CD4+ CD25− Foxp3− T cells or are self-induced to become Th17 cells in the absence of exogenous TGF-β. *J. Immunol.* **178,** 6725–6729 (2007).

212. Koenen, H. J. P. M. *et al.* Human CD25highFoxp3pos regulatory T cells differentiate into IL-17-producing cells. *Blood* **112,** 2340–52 (2008).

213. Nistala, K. *et al.* Th17 plasticity in human autoimmune arthritis is driven by the inflammatory environment. *Proc. Natl. Acad. Sci. U. S. A.* **107,** 14751–6 (2010).

214. Wan, Q. *et al.* Cytokine signals through PI-3 kinase pathway modulate Th17 cytokine production by CCR6+ human memory T cells. *J. Exp. Med.* **208,** 1875–87 (2011).

215. Sallusto, F. *et al.* Rapid and coordinated switch in chemokine receptor expression during dendritic cell maturation. *Eur. J. Immunol.* **28,** 2760–9 (1998).

216. Yamazaki, T. *et al.* CCR6 regulates the migration of inflammatory and regulatory T cells. *J. Immunol.* **181,** 8391–401 (2008).

217. Steinfelder, S. *et al.* Epigenetic modification of the human CCR6 gene is associated with stable CCR6 expression in T cells. *Blood* **117,** 2839–46 (2011).

218. Yang, Y. *et al.* T-bet is essential for encephalitogenicity of both Th1 and Th17 cells. *J. Exp. Med.* **206,** 1549–64 (2009).

219. Gocke, A. R. *et al.* T-bet regulates the fate of Th1 and Th17 lymphocytes in autoimmunity. *J. Immunol.* **178,** 1341–8 (2007).

220. Bending, D. & Newland, S. Epigenetic changes at Il12rb2 and Tbx21 in relation to plasticity behavior of Th17 cells. *J. Immunol.* **186,** 3373–3382 (2011).

221. Shi, G. *et al.* Phenotype switching by inflammation-inducing polarized Th17 cells, but not by Th1 cells. *J. Immunol.* **181,** 7205–13 (2008).

222. Baron, U. *et al.* DNA demethylation in the human FOXP3 locus discriminates regulatory T cells from activated FOXP3(+) conventional T cells. *Eur. J. Immunol.* **37,** 2378–89 (2007).

223. Brucklacher-Waldert, V., Stuerner, K., Kolster, M., Wolthausen, J. & Tolosa, E. Phenotypical and functional characterization of T helper 17 cells in multiple sclerosis. *Brain* **132,** 3329–41 (2009).

224. Murugaiyan, G., Beynon, V., Mittal, A., Joller, N. & Weiner, H. L. Silencing microRNA-155 ameliorates experimental autoimmune encephalomyelitis. *J. Immunol.* **187,** 2213–21 (2011).

225. Hu, R. *et al.* MicroRNA-155 Confers Encephalogenic Potential to Th17 Cells by Promoting Effector Gene Expression. *J. Immunol.* (2013). doi:10.4049/jimmunol.1300351

226. Lu, L.-F. *et al.* Function of miR-146a in controlling Treg cell-mediated regulation of Th1 responses. *Cell* **142,** 914–29 (2010).

227. Li, Q.-J. *et al.* miR-181a is an intrinsic modulator of T cell sensitivity and selection. *Cell* **129,** 147–61 (2007).

228. Guan, H. *et al.* MicroRNA let-7e is associated with the pathogenesis of experimental autoimmune encephalomyelitis. *Eur. J. Immunol.* **43,** 104–14 (2013).

229. Jiang, S. *et al.* Molecular dissection of the miR-17-92 cluster's critical dual roles in promoting Th1 responses and preventing inducible Treg differentiation. *Blood* **118,** 5487–97 (2011).

230. Baumjohann, D. *et al.* The microRNA cluster miR-17∼92 promotes TFH cell differentiation and represses subset-inappropriate gene expression. *Nat. Immunol.* **14,** 840–8 (2013).

231. Li, Z., Wu, F., Brant, S. R. & Kwon, J. H. IL-23 receptor regulation by Let-7f in human CD4+ memory T cells. *J. Immunol.* **186,** 6182–90 (2011).

232. Yao, R. *et al.* MicroRNA-155 modulates Treg and Th17 cells differentiation and Th17 cell function by targeting SOCS1. *PLoS One* **7,** e46082 (2012).

233. Liu, C., Teng, Z., Santistevan, N. & Szulwach, K. Epigenetic regulation of miR-184 by MBD1 governs neural stem cell proliferation and differentiation. *Cell Stem Cell* **6,** 433–444 (2010).

234. Weitzel, R. P. *et al.* microRNA 184 regulates expression of NFAT1 in umbilical cord blood CD4+ T cells. *Blood* **113,** 6648–57 (2009).

235. Yu, J. *et al.* MicroRNA-184 antagonizes microRNA-205 to maintain SHIP2 levels in epithelia. *Proc. Natl. Acad. Sci. U. S. A.* **105,** 19300–5 (2008).

236. Favreau, A. J. & Sathyanarayana, P. miR-590-5p, miR-219-5p, miR-15b and miR-628-5p are commonly regulated by IL-3, GM-CSF and G-CSF in acute myeloid leukemia. *Leuk. Res.* **36,** 334–41 (2012).

237. Potenza, N. *et al.* Human microRNA hsa-miR-125a-5p interferes with expression of hepatitis B virus surface antigen. *Nucleic Acids Res.* **39,** 5157–63 (2011).

238. Girardi, C. *et al.* Analysis of miRNA and mRNA expression profiles highlights alterations in ionizing radiation response of human lymphocytes under modeled microgravity. *PLoS One* **7,** e31293 (2012).

239. Smith, a L. *et al.* The miR-106b-25 cluster targets Smad7, activates TGF-β signaling, and induces EMT and tumor initiating cell characteristics downstream of Six1 in human breast cancer. *Oncogene* **31,** 5162–71 (2012).

240. Yang, Y. *et al.* MiR-136 promotes apoptosis of glioma cells by targeting AEG-1 and Bcl-2. *FEBS Lett.* **586,** 3608–12 (2012).

241. Gandhi, R. *et al.* Circulating MicroRNAs as biomarkers for disease staging in multiple sclerosis. *Ann. Neurol.* **73,** 729–40 (2013).

242. Lovett-Racke, A. E. *et al.* Silencing T-bet defines a critical role in the differentiation of autoreactive T lymphocytes. *Immunity* **21,** 719–31 (2004).

243. Komiyama, Y. *et al.* IL-17 plays an important role in the development of experimental autoimmune encephalomyelitis. *J. Immunol.* **177,** 566–73 (2006).

244. Aldemir, H. *et al.* Cutting edge: lectin-like transcript 1 is a ligand for the CD161 receptor. *J. Immunol.* **175,** 7791–5 (2005).

245. Macián, F., García-Cózar, F., Im, S. & Horton, H. Transcriptional mechanisms underlying lymphocyte tolerance. *Cell* **109,** 719–731 (2002).

246. Kleinewietfeld, M. *et al.* Sodium chloride drives autoimmune disease by the induction of pathogenic TH17 cells. *Nature* 1–7 (2013). doi:10.1038/nature11868

247. Wu, C. *et al.* Induction of pathogenic TH17 cells by inducible salt-sensing kinase SGK1. *Nature* (2013). doi:10.1038/nature11984

248. O'Shea, J. J. & Paul, W. E. Mechanisms underlying lineage commitment and plasticity of helper CD4+ T cells. *Science (80-.).* **327,** 1098–102 (2010).

249. Harper, E. G. *et al.* Th17 cytokines stimulate CCL20 expression in keratinocytes in vitro and in vivo: implications for psoriasis pathogenesis. *J. Invest. Dermatol.* **129,** 2175–83 (2009).

250. Durelli, L. *et al.* T-helper 17 cells expand in multiple sclerosis and are inhibited by interferon-beta. *Ann. Neurol.* **65,** 499–509 (2009).

251. Schmidt, S. Candidate autoantigens in multiple sclerosis. *Mult. Scler.* **5,** 147–160 (1999).

252. Kryczek, I. & Bruce, A. Induction of IL-17+ T cell trafficking and development by IFN-γ: mechanism and pathological relevance in psoriasis. *J. Immunol.* **181,** 4733–4741 (2008).

253. Huh, J. R. *et al.* Digoxin and its derivatives suppress TH17 cell differentiation by antagonizing RORγt activity. *Nature* **472,** 486–90 (2011).

254. Ramsköld, D. *et al.* Full-length mRNA-Seq from single-cell levels of RNA and individual circulating tumor cells. *Nat. Biotechnol.* **30,** 777–82 (2012).

255. Lu, K. T. *et al.* Functional and epigenetic studies reveal multistep differentiation and plasticity of in vitro-generated and in vivo-derived follicular T helper cells. *Immunity* **35,** 622–32 (2011).

APPENDIX

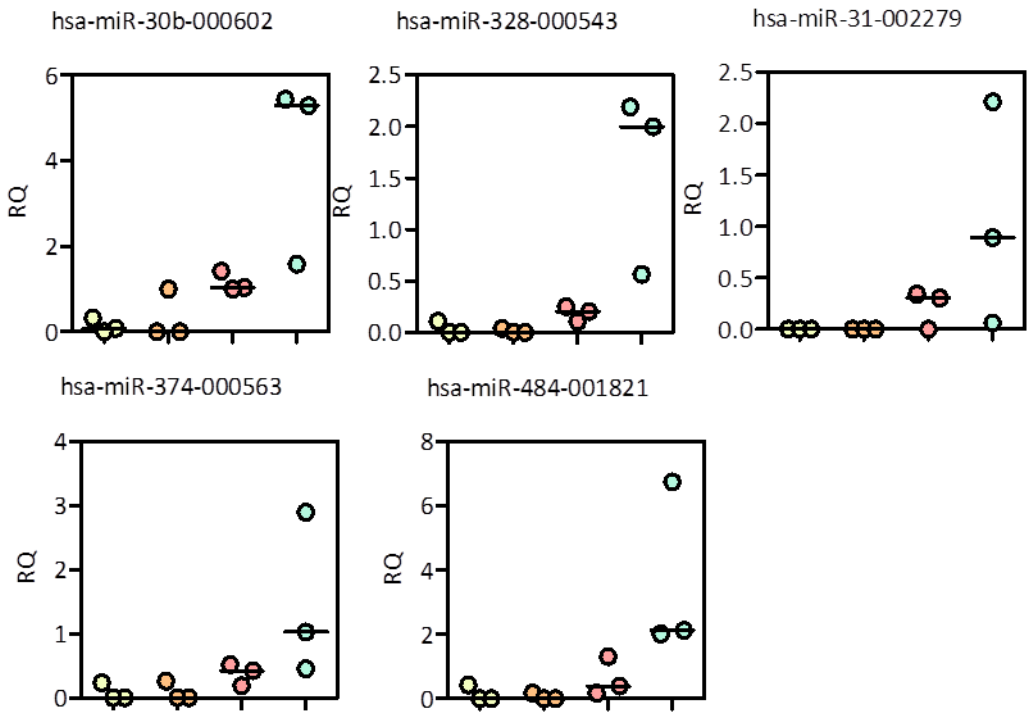

Figure 8.1 Remaining miRNAs differentially expressed between the susbets. Relative Quantity (RQ) expression of miRNAs within CCR6^{+}IL-17^{+} CCR6^{+}IFNγ^{+}IL-17^{+}, CCR6^{+}IFNγ^{+}, CCR6^{-}IFNγ^{+} populations. RQ is the Cycle value (Cp) normalised to the median Cp of all the miRNAs from one run. Line represents median RQ value. n=3

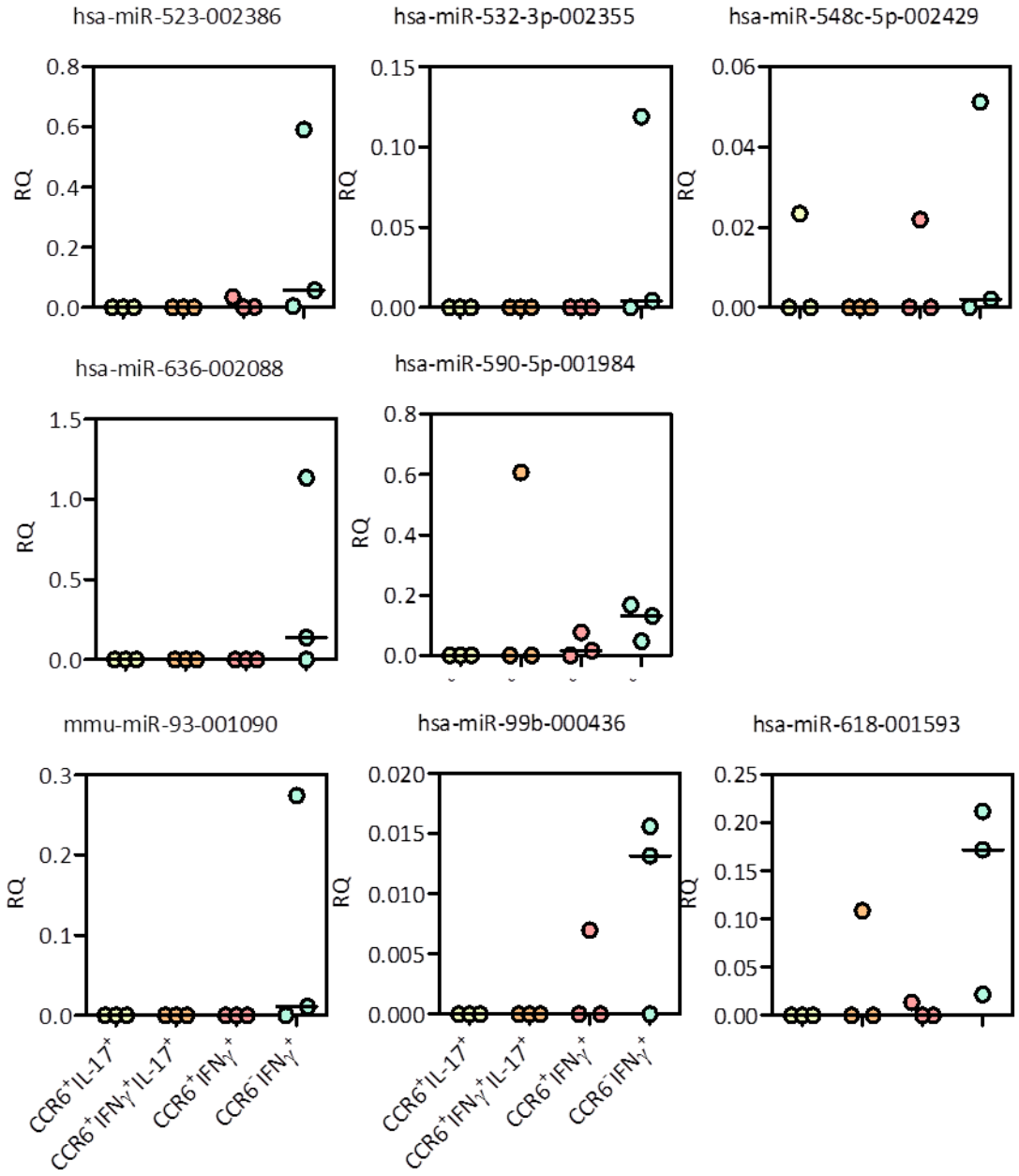

Figure 8.2 Remaining miRNAs differentially expressed between the susbets. Relative Quantity (RQ) expression of miRNAs within $CCR6^{+}IL\text{-}17^{+}$ $CCR6^{+}IFN\gamma^{+}IL\text{-}17^{+}$, $CCR6^{+}IFN\gamma^{+}$, $CCR6^{-}IFN\gamma^{+}$ populations. RQ is the Cycle value (Cp) normalised to the median Cp of all the miRNAs from one run. Line represents median RQ value. n=3

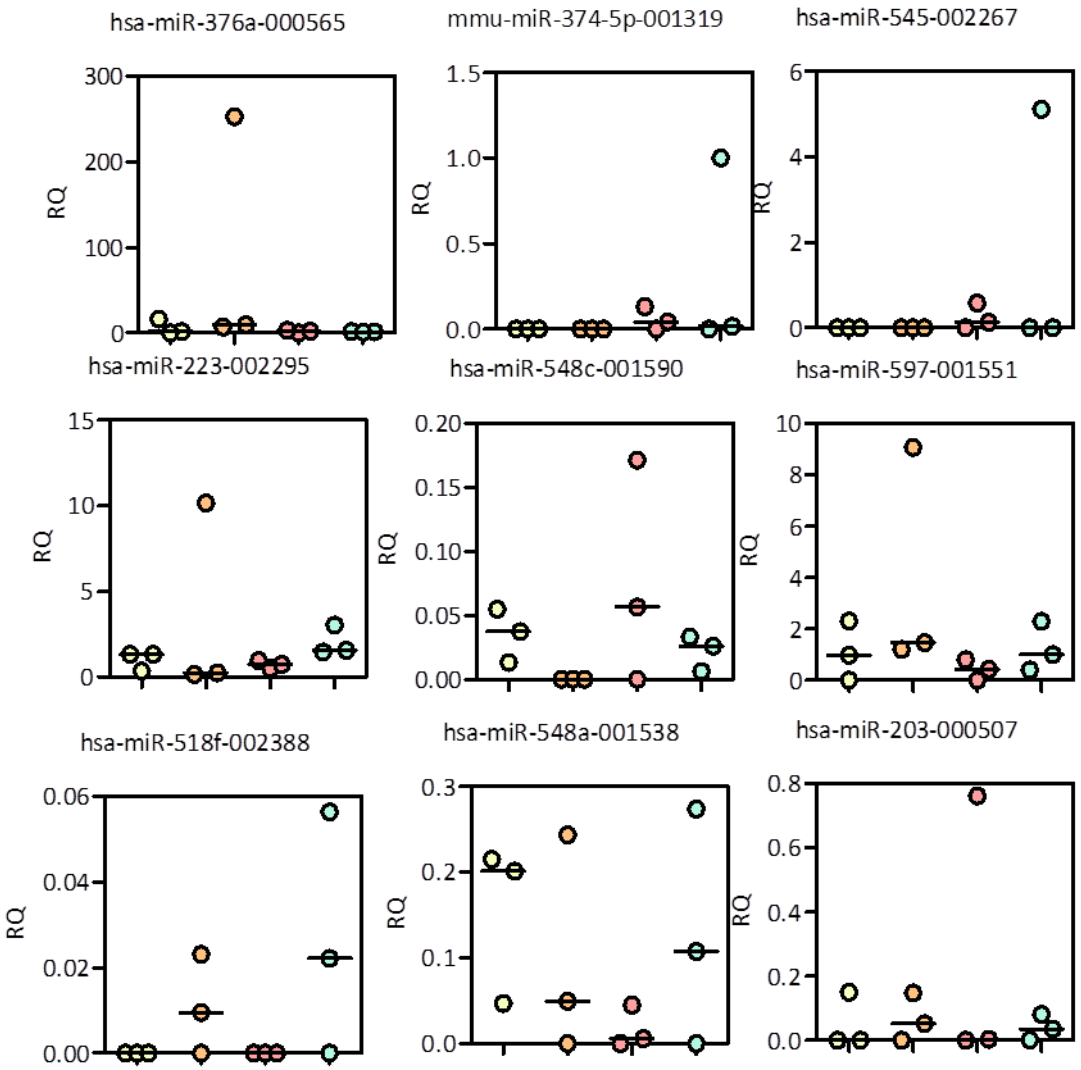

Figure 8.3 Remaining miRNAs differentially expressed between the susbets. Relative Quantity (RQ) expression of miRNAs within CCR6^{+}IL-17^{+} CCR6^{+}IFNγ^{+}IL-17^{+}, CCR6^{+}IFNγ^{+}, CCR6^{-}IFNγ^{+} populations. RQ is the Cycle value (Cp) normalised to the median Cp of all the miRNAs from one run. Line represents median RQ value. n=3

	CCR6$^+$IL-17$^+$ vs. CCR6$^+$IFNγ$^+$	CCR6$^+$IL-17$^+$ vs. CCR6$^-$IFNγ$^+$	CCR6$^+$IL-17$^+$ vs. CCR6$^+$IFNγ$^+$IL-17$^+$	CCR6$^-$IFNγ$^+$ vs. CCR6$^+$IFNγ$^+$	CCR6$^-$IFNγ$^+$ vs. CCR6$^+$IFNγ$^+$IL-17$^+$	CCR6$^+$IFNγ$^+$ vs. CCR6$^+$IFNγ$^+$IL-17$^+$
hsa-let-7d-002283		0.014638637		27.69942157	160.4566476	
hsa-let-7e-002NA6	0.001831413	0.00036343		5.03924407	2751.560656	546.0264711
hsa-let-7g-002282	0.003878387	0.001509688		2.568999602	2807.077312	1092.673315
hsa-miR-101-002253		0.01370484		16.21028194	72.96692495	
hsa-miR-106a-002169	0.00284539	0.000556425		5.113695773	11765.14992	2300.713699
hsa-miR-106b-000442	0.029074417	0.011984712	0.030527291	2.425958717	2.547186038	
hsa-miR-125a-5p-002198	0.090127534	0.09200976			2.221453289	2.267846204
hsa-miR-126-002228					4.593989666	
hsa-miR-136-000592		2.052618442	4.044026015			2.543126934
hsa-miR-142-3p-000464	0.10116721	0.05206174			19.14524654	9.852350821
hsa-miR-142-5p-002248		0.333855579			2.995307139	
hsa-miR-146a-000468	0.023993474	0.006351056	0.453185161	3.777871594	71.35587605	18.88785108
hsa-miR-146b-001097	0.020547284	0.009200973	0.257661852	2.2331642	28.00376047	12.53994689
hsa-miR-150-000473	0.091425283	0.027280735		3.351276371	37.90991544	11.31208269
hsa-miR-155-002623	0.031000612	0.011707979	8.844412622	2.647819296	755.4175403	285.2979965
hsa-miR-16-000391	0.069725935	0.023272041		2.996124692	34.41877072	11.48776311
hsa-miR-17-002308	0.000969151	0.000108679		8.917590797	9201.447286	1031.831074
hsa-miR-181a-000480		0.218389246		5.450482483	13.22660369	
hsa-miR-184-000485	2.185750406	2.848295181	0.448850529		0.157585679	0.205353058
hsa-miR-186-002285	0.004667959					
hsa-miR-191-002299	0.034863733	0.012916433	4.135359651	2.699176528	320.1626665	118.6149417
hsa-miR-192-000491		0.1125949		4.36448614	8.881396927	
hsa-miR-194-000493		0.042098979		23.75354518	23.75354518	
hsa-miR-195-000494	0.030495392	0.028993589			57.60557802	54.76868278
hsa-miR-19a-000395	0.293585617	0.031942641		9.191025275	166.6525309	18.13209363
hsa-miR-19b-000396	0.042551413	0.010832156		3.928249779	98.76555924	25.14238269
hsa-miR-1NA-3p-002234	0.1965928	0.072844847		2.698788027	12.8949262	4.778043355
hsa-miR-203-000507	0.438065305	0.397523868	0.296210399			
hsa-miR-20a-000580		0.015560039	11.46155703	35.8072414	736.6020547	20.57131535
hsa-miR-20b-001014		0.002653456		97.75473037	376.866936	
hsa-miR-21-000397	0.049720129	0.012122137	3.65128766	4.101597717	301.2082494	73.43680929
hsa-miR-212-000515					9.03445019	
hsa-miR-222-002276	0.14061665	0.03456384	8.308483298	4.068316726	240.3807913	59.08605636
hsa-miR-223-002295		0.451632016		2.654638967	2.569814102	
hsa-miR-24-000NA2	0.243807599	0.097330515	2.098144441	2.504945127	21.55690268	8.605738487
hsa-miR-25-000NA3	0.02090121	0.00105011		19.90382775	267.2961556	13.42938449
hsa-miR-26a-000NA5	0.015596067	0.00199442		7.819850357	3233.810483	413.5386657
hsa-miR-26b-000NA7	0.307918617	0.030462606	11.81325915	10.10808507	387.7954173	38.36487473
hsa-miR-27a-000NA8				6.191894136		
hsa-miR-28-000411	0.214217641	0.012795908		16.74110447	311.497135	18.60672547
hsa-miR-29a-002112	0.028013101	0.01757267	6.61653613		376.5242423	236.1943446
hsa-miR-29b-000413	0.39299055	0.280408735			21.01982779	14.99818076
hsa-miR-29c-000587	0.000703949	0.000115004		6.121089541		1420.557268
hsa-miR-301-000528		0.144478466		6.921446672	2.411738475	

Table 8.1 List of 79 differentially expressed miRNAs in T_H1 and T_H17 CD4$^+$ T cell subsets. Relative expression of miRNAs between each subset ($2^{-\Delta\Delta Cp}$), normalised to median Cycle value (Cp).

		CCR6$^+$IL-17$^+$ vs. CCR6$^+$IFNγ$^+$	CCR6$^+$IL-17$^+$ vs. CCR6$^-$IFNγ$^+$	CCR6$^+$IL-17$^+$ vs. CCR6$^+$IFNγ$^+$IL-17$^+$	CCR6$^-$IFNγ$^+$ vs. CCR6$^+$IFNγ$^+$	CCR6$^-$IFNγ$^+$ vs. CCR6$^+$IFNγ$^+$IL-17$^+$	CCR6$^+$IFNγ$^+$ vs. CCR6$^+$IFNγ$^+$IL-17$^+$
hsa-miR-302a-000529			0.000284283		138.7228345	30.12956222	
hsa-miR-30b-000602		0.028040156	0.008931925	2.600941839	3.139318344	291.196111	92.75775157
hsa-miR-30c-000419		0.220841366	0.060379558	4.424986335	3.657551893	73.28616672	20.03694516
hsa-miR-31-002279		0.026130376	0.002735821		9.551200902	365.5209829	38.26963611
hsa-miR-320-002277		0.026748853	0.009407618	36.01140405	2.843318406	3827.898207	1346.278419
hsa-miR-324-3p-002161		3.136205293	4.508459828	564.3385679		125.1732497	179.9431208
hsa-miR-328-000543		0.033476737	0.004358565		7.680677992	329.9885779	42.96346992
hsa-miR-331-000545			0.00199463		166.8084941	501.3462139	
hsa-miR-342-3p-002260		0.031112444	0.011209496	0.457088849	2.775543556	40.77693215	14.69151225
hsa-miR-345-002186			0.290119504		4.969472793	10.67854325	
hsa-miR-374-000563		0.021806027	0.006857612		3.179827859	140.9178877	44.31620012
hsa-miR-375-000564			0.027702505		25.10305328	36.09781855	
hsa-miR-376a-000565		0.275665736	0.263754911	0.013256054		0.050258985	0.04808742
hsa-miR-454-002323			487.6713716	421.4832453	0.00170825		505.9430317
hsa-miR-484-001821		0.020551451	0.0030024		6.84500692	450.5240393	65.81790852
hsa-miR-494-002365			0.045195086		22.12629942	22.12629942	
hsa-miR-517b-001152		0.12535737	0.012211925		10.26516088	257.3281988	25.06811162
hsa-miR-518d-001159		49.27316158	2.433386244		20.24880419	0.247685274	0.012232094
hsa-miR-518f-002388			0.11375512	0.202828467	8.790813092		0.202828467
hsa-miR-523-002386		0.307620749	0.025201817		12.2062923	39.6796781	3.250756013
hsa-miR-532-3p-002355			0.153872187		6.49890028	6.49890028	
hsa-miR-545-002267		0.028961592			0.450611132		34.52848855
hsa-miR-548a-001538		17.76421631	3.70480636	4.986364934	4.794910877		0.280697152
hsa-miR-548c-001590				22.18094742		13.07614538	17.41539888
hsa-miR-548c-5p-002429						3.856506684	
hsa-miR-574-3p-002349		0.012633389	0.003334466	6.552256367	3.78872913	1965.0091	518.6459713
hsa-miR-590-5p-001984			0.01338881		8.401402224	9.7631404	
hsa-miR-597-001551			0.147603571	0.057527644	12.63414508	0.389744256	0.030848487
hsa-miR-598-001988		0.091885311	0.109162208			9.160679475	10.88313236
hsa-miR-618-001593			0.014641389		31.82287507	15.8395006	
hsa-miR-628-5p-002433		531.1438412	0.011570566		45904.74323	116.6822639	0.002541835
hsa-miR-636-002088			0.022738166		43.97892022	43.97892022	
hsa-miR-708-002341					2.179368684	2.179368684	
hsa-miR-92a-000431		0.032175778	0.012299381		2.616048583	113.3129919	43.31455946
hsa-miR-95-000433			0.298075257		8.600764748	8.600764748	
hsa-miR-99b-000436			0.207686362		2.788274256	4.814952652	
mmu-miR-1NA-001187			0.031512774		31.73316285	31.73316285	
mmu-miR-374-5p-001319		0.069524457	0.04819987			20.74694407	14.38342763
mmu-miR-93-001090			0.085227553		11.73329474	11.73329474	

	CCR6$^+$IL-17$^+$			CCR6$^+$IL-17$^+$IFNγ$^+$			CCR6$^+$IFNγ$^+$			CCR6$^-$IFNγ$^+$		
hsa-let-7a-000377	0.000	0.000	0.000	0.000	0.000	0.000	0.000	0.000	0.000	0.000	0.000	0.000
hsa-let-7c-000379	0.000	0.000	0.000	0.000	0.000	0.000	0.000	0.000	0.000	0.000	0.000	0.000
hsa-let-7d-002283	0.000	0.000	0.018	0.000	0.000	0.000	0.000	0.000	0.264	0.111	0.159	0.583
hsa-let-7e-002NA6	0.000	0.000	0.000	0.000	0.000	0.000	0.701	0.844	0.686	1.034	9.889	5.081
hsa-let-7f-000382	0.000	0.000	0.000	0.000	0.000	0.000	0.000	0.000	0.000	0.000	0.000	0.000
hsa-let-7g-002282	0.000	0.000	0.103	0.000	0.000	0.000	1.055	1.926	1.602	1.354	8.459	4.817
hsa-miR-1-002222	0.000	0.000	0.000	0.000	0.000	0.000	0.000	0.000	0.000	0.000	0.121	0.000
hsa-miR-9-000583	0.000	0.000	0.000	0.000	0.000	0.000	0.000	0.000	0.000	0.000	0.000	0.000
hsa-miR-10a-000387	0.000	0.000	0.000	0.000	0.000	0.000	0.000	0.000	0.000	0.000	0.000	0.000
hsa-miR-10b-002218	0.000	0.000	0.000	0.000	0.000	0.000	0.000	0.000	0.000	0.000	0.000	0.000
U6 snRNA-001973	638.914	28.155	151.439	266.838	25.308	154.916	58.274	1386.041	519.962	4131.569	2809.621	1326.055
U6 snRNA-001973	722.808	34.138	178.659	276.018	20.466	60.916	253.606	1214.039	638.852	3415.391	5066.789	1002.528
hsa-miR-15a-000389	0.000	0.000	0.000	0.000	0.000	0.000	0.000	0.000	0.000	0.000	0.000	0.000
hsa-miR-15b-000390	0.000	0.000	0.009	0.000	0.000	0.000	0.000	0.000	0.000	0.000	0.000	0.164
hsa-miR-16-000391	1.464	0.000	0.959	0.381	0.096	0.102	2.983	1.272	1.481	3.245	7.309	6.370
hsa-miR-17-002308	0.000	0.000	0.000	0.000	0.000	0.000	0.293	1.955	4.785	6.637	15.312	19.117
hsa-miR-18a-002422	0.000	0.000	0.000	0.000	0.000	0.000	0.000	0.000	0.000	0.000	0.000	0.000
hsa-miR-18b-002217	0.000	0.000	0.000	0.000	0.000	0.000	0.000	0.000	0.000	0.000	0.000	0.000
hsa-miR-19a-000395	0.000	0.000	0.205	0.000	0.000	0.000	0.000	0.075	0.147	0.219	0.092	0.571
hsa-miR-19b-000396	3.218	0.000	1.455	2.467	0.000	1.550	2.255	7.622	4.796	11.057	17.777	25.420
hsa-miR-20a-000580	0.000	1.254	10.578	0.000	6.497	0.000	0.000	10.632	7.214	9.572	17.986	27.738
hsa-miR-20b-001014	0.000	0.000	0.000	0.000	0.000	0.000	0.000	0.000	0.078	0.264	0.221	2.290
hsa-miR-21-000397	0.068	0.000	1.000	0.079	0.018	0.000	0.150	2.361	2.112	0.847	10.416	5.833
hsa-miR-22-000398	0.000	0.000	0.000	0.000	0.000	0.000	0.000	0.000	0.000	0.000	0.000	0.000
hsa-miR-23a-000399	0.000	0.000	0.000	0.000	0.000	0.000	0.000	0.000	0.000	0.000	0.000	0.000
hsa-miR-23b-000NA0	0.000	0.000	0.000	0.000	0.000	0.000	0.000	0.000	0.000	0.000	0.000	0.000
hsa-miR-24-000NA2	0.811	0.104	2.019	0.193	0.033	2.860	1.629	2.359	3.051	3.746	5.087	9.668
hsa-miR-25-000NA3	0.000	0.000	0.000	0.000	0.000	0.061	0.002	0.685	0.209	0.727	2.073	1.429
hsa-miR-26a-000NA5	0.000	0.000	0.364	0.000	0.000	0.000	0.062	1.822	1.552	2.022	6.367	6.552
hsa-miR-26b-000NA7	0.156	0.000	0.194	0.000	0.014	0.000	0.000	0.603	1.721	0.406	1.036	3.454

Table 8.2 Relative expression ($2^{-\Delta Cp}$) of 384 miRNAs, normalised to median Cycle value (Cp)

	CCR6^{+} IL-17^{+}			CCR6^{+} IFNγ^{+} IL-17^{+}			CCR6^{+} IFNγ^{+}			CCR6^{-} IFNγ^{+}		
hsa-miR-27a-000NA8	0.000	0.000	0.000	0.849	0.000	0.000	0.000	0.000	0.000	0.000	0.000	0.322
hsa-miR-27b-000NA9	0.000	0.000	0.000	0.000	0.000	0.000	0.000	0.000	0.000	0.000	0.000	0.011
hsa-miR-28-3p-002446	0.000	0.000	0.000	0.000	0.000	0.000	0.000	0.000	0.000	0.000	0.000	0.000
hsa-miR-28-000411	0.000	0.000	0.086	0.000	0.000	0.000	0.000	0.114	0.104	0.256	0.424	0.694
U6 snRNA-001973	720.530	30.224	205.337	232.757	20.769	97.063	168.076	1491.644	488.805	2891.365	3402.662	1458.761
U6 snRNA-001973	493.375	35.019	168.206	223.158	23.028	317.427	0.000	1095.472	236.895	3297.342	5382.423	641.586
hsa-miR-29a-002112	0.000	0.279	0.580	0.000	0.000	0.411	1.961	2.666	1.906	1.478	6.283	4.348
hsa-miR-29b-000413	0.000	0.000	0.278	0.000	0.000	0.000	0.000	0.034	0.181	0.000	0.097	0.177
hsa-miR-29c-000587	0.000	0.000	0.000	0.000	0.000	0.000	0.000	33.974	155.175	41.107	4.817	8.281
hsa-miR-30b-000602	0.075	0.000	0.316	1.000	0.000	0.000	1.034	1.419	1.000	1.584	5.428	5.281
hsa-miR-30c-000419	0.458	0.136	1.324	1.089	0.022	0.040	1.139	2.658	2.537	3.154	11.378	10.473
hsa-miR-31-002279	0.000	0.000	0.000	0.000	0.000	0.000	0.341	0.302	0.000	0.062	0.893	2.212
hsa-miR-32-002109	0.000	0.000	0.000	0.000	0.000	0.000	0.000	0.000	0.000	0.000	0.000	0.000
hsa-miR-33b-002085	0.000	0.000	0.000	0.000	0.000	0.000	0.000	0.000	0.000	0.000	0.000	0.000
hsa-miR-34a-000426	0.000	0.000	0.000	0.000	0.000	0.000	0.000	0.000	0.000	0.000	0.000	0.000
hsa-miR-34c-000428	0.000	0.000	0.000	0.000	0.000	0.000	0.000	0.000	0.000	0.000	0.000	0.000
hsa-miR-92a-000431	0.254	0.000	1.264	0.742	0.000	0.160	1.911	4.208	1.625	2.026	9.320	12.394
mmu-miR-93-001090	0.000	0.000	0.000	0.000	0.000	0.000	0.000	0.000	0.000	0.011	0.000	0.274
hsa-miR-95-000433	0.023	0.000	0.000	0.000	0.000	0.000	0.000	0.000	0.000	0.021	0.000	0.056
mmu-miR-96-000186	0.000	0.000	0.000	0.000	0.000	0.000	0.000	0.000	0.000	0.000	0.000	0.000
hsa-miR-98-000577	0.000	0.000	0.000	0.000	0.000	0.000	0.000	0.000	0.000	0.000	0.000	0.000
hsa-miR-99a-000435	0.000	0.000	0.000	0.000	0.000	0.000	0.000	0.000	0.000	0.000	0.000	0.000
hsa-miR-99b-000436	0.000	0.000	0.000	0.000	0.000	0.000	0.000	0.000	0.007	0.013	0.000	0.016
hsa-miR-100-000437	0.000	0.000	0.000	0.000	0.000	0.000	0.000	0.000	0.000	0.000	0.000	0.000
hsa-miR-101-002253	0.000	0.000	0.000	0.000	0.000	0.000	0.000	0.000	0.124	0.116	0.061	0.137
hsa-miR-103-000439	0.000	0.000	0.000	0.000	0.000	0.000	0.000	0.000	0.000	0.000	0.000	0.000
hsa-miR-105-002167	0.000	0.000	0.000	0.000	0.000	0.000	0.000	0.000	0.000	0.000	0.000	0.000
hsa-miR-106a-002169	0.000	0.000	0.380	0.000	0.000	0.000	0.962	6.798	4.642	7.346	25.804	21.425
RNU44-001094	4.930	0.000	10.157	3.051	0.000	0.000	9.386	33.502	23.144	26.760	75.957	59.366
hsa-miR-106b-000442	0.000	0.024	0.000	0.056	0.036	0.760	0.091	0.153	0.127	0.110	0.511	0.451
hsa-miR-107-000443	0.000	0.000	0.000	0.000	0.000	0.000	0.000	0.000	0.000	0.000	0.000	0.000
hsa-miR-122-002245	0.000	0.000	0.000	0.000	0.000	0.000	0.000	0.000	0.000	0.000	0.000	0.000
mmu-miR-124a-001182	0.000	0.000	0.000	0.000	0.000	0.000	0.000	0.000	0.000	0.000	0.000	0.000

	CCR6$^+$ IL-17$^+$			CCR6$^+$ IFNγ$^+$ IL-17$^+$			CCR6$^+$ IFNγ$^+$			CCR6$^-$ IFNγ$^+$		
hsa-miR-125a-3p-002199	0.000	0.000	0.000	0.000	0.000	0.000	0.000	0.000	0.000	0.000	0.000	0.000
hsa-miR-125a-5p-002198	0.000	0.000	0.000	0.159	0.000	0.000	0.042	0.000	0.059	0.058	0.000	0.041
hsa-miR-125b-000449	0.000	0.000	0.000	0.000	0.000	0.000	0.000	0.000	0.000	0.000	0.000	0.000
hsa-miR-126-002228	0.476	0.000	0.000	0.000	0.000	0.000	0.043	0.000	0.000	0.000	0.023	0.008
hsa-miR-127-000452	0.000	0.000	0.000	0.000	0.000	0.000	0.056	0.000	0.000	0.000	0.000	0.000
hsa-miR-127-5p-002229	0.000	0.000	0.000	0.000	0.000	0.000	0.000	0.000	0.000	0.000	0.000	0.000
hsa-miR-128a-002216	0.000	0.000	0.000	0.000	0.000	0.000	0.000	0.058	0.000	0.000	0.000	0.000
mmu-miR-129-3p-001184	0.000	0.000	0.000	0.000	0.000	0.000	0.000	0.000	0.000	0.000	0.000	0.000
hsa-miR-129-000590	0.000	0.000	0.000	0.000	0.000	0.000	0.000	0.000	0.000	0.000	0.000	0.000
hsa-miR-130a-000454	0.000	0.000	0.000	0.000	0.000	0.000	0.000	0.000	0.000	0.000	0.000	0.000
hsa-miR-130b-000456	0.000	0.000	0.000	0.000	0.000	0.000	0.000	0.000	0.000	0.000	0.000	0.000
hsa-miR-132-000457	0.000	0.000	0.000	0.000	0.000	0.000	0.000	0.000	0.000	0.000	0.000	0.000
hsa-miR-133a-002246	0.000	0.000	0.000	0.000	0.000	0.000	0.000	0.000	0.000	0.000	0.472	0.000
hsa-miR-133b-002247	0.000	0.000	0.000	0.000	0.000	0.000	0.000	0.000	0.000	0.000	0.000	0.000
mmu-miR-134-001186	0.000	0.000	0.000	0.000	0.000	0.000	0.000	0.000	0.000	0.000	0.000	0.000
hsa-miR-135a-000460	0.000	0.000	0.000	0.000	0.000	0.000	0.000	0.000	0.000	0.000	0.000	0.000
hsa-miR-135b-002261	0.000	0.000	0.000	0.000	0.000	0.000	0.000	0.000	0.000	0.000	0.000	0.000
hsa-miR-136-000592	0.008	0.002	0.018	0.000	0.003	0.000	0.000	0.007	0.008	0.067	0.000	0.000
mmu-miR-137-001129	0.000	0.000	0.000	0.000	0.000	0.000	0.000	0.000	0.000	0.000	0.000	0.000
hsa-miR-138-002284	0.000	0.000	0.000	0.000	0.000	0.000	0.000	0.000	0.000	0.000	0.000	0.000
hsa-miR-139-3p-002313	0.000	0.000	0.000	0.000	0.000	0.000	0.000	0.000	0.000	0.000	0.000	0.000
hsa-miR-139-5p-002289	0.000	0.000	0.000	0.000	0.000	0.000	0.000	0.000	0.000	0.000	0.000	0.000
hsa-miR-1NA-3p-002234	0.000	0.000	0.003	0.004	0.000	0.000	0.038	0.002	0.011	0.041	0.030	0.013
mmu-miR-1NA-001187	0.000	0.000	0.000	0.000	0.000	0.000	0.000	0.000	0.000	0.017	0.051	0.094
hsa-miR-141-000463	0.000	0.000	0.000	0.000	0.000	0.000	0.000	0.000	0.000	0.000	0.000	0.000
hsa-miR-142-3p-000464	6.919	1.000	19.964	6.987	0.797	25.046	40.847	76.667	42.600	23.147	192.868	219.269
hsa-miR-142-5p-002248	0.000	0.000	0.000	0.000	0.000	0.000	0.000	0.010	0.000	0.025	0.000	0.002
hsa-miR-143-002249	0.000	0.000	0.000	0.000	0.000	0.000	0.000	0.000	0.000	0.000	0.000	0.000
hsa-miR-145-002278	0.000	0.000	0.000	0.000	0.000	0.000	0.000	0.000	0.000	0.000	0.000	0.000
hsa-miR-146a-000468	1.715	0.000	3.240	0.379	0.162	1.316	8.704	12.753	4.915	13.059	66.731	33.761
hsa-miR-146b-3p-002361	0.000	0.000	0.000	0.000	0.000	0.000	0.000	0.000	0.000	0.000	0.000	0.000
hsa-miR-146b-001097	1.796	0.000	3.585	5.004	0.051	1.997	17.591	8.215	6.968	17.479	29.275	21.913
hsa-miR-147b-002262	0.000	0.000	0.000	0.000	0.000	0.000	0.000	0.000	0.000	0.000	0.000	0.000

	CCR6^{+} IL-17^{+}			CCR6^{+} IFNγ^{+} IL-17^{+}			CCR6^{+} IFNγ^{+}			CCR6^{-} IFNγ^{+}		
hsa-miR-148a-000470	0.000	0.000	0.000	0.000	0.000	0.000	0.000	0.000	0.027	0.000	0.000	0.000
hsa-miR-148b-000471	0.000	0.000	0.000	0.000	0.000	0.000	0.000	0.000	0.000	0.000	0.000	0.000
hsa-miR-149-002255	0.000	0.000	0.000	0.000	0.000	0.000	0.000	0.000	0.000	0.000	0.000	0.000
hsa-miR-150-000473	47.879	1.303	101.845	27.250	2.046	103.065	208.094	197.455	202.407	440.445	826.040	860.383
hsa-miR-152-000475	0.000	0.000	0.000	0.000	0.000	0.000	0.000	0.000	0.000	0.000	0.000	0.191
mmu-miR-153-001191	0.000	0.000	0.000	0.000	0.000	0.000	0.000	0.000	0.000	0.000	0.000	0.000
hsa-miR-154-000477	0.000	0.000	0.000	0.000	0.000	0.000	0.000	0.000	0.000	0.000	0.000	0.000
hsa-miR-181a-000480	0.033	0.000	0.000	0.000	0.000	0.000	0.000	0.000	0.019	0.003	0.067	0.030
hsa-miR-181c-000482	0.000	0.000	0.000	0.000	0.000	0.000	0.000	0.000	0.000	0.000	0.000	0.000
hsa-miR-182-002334	0.000	0.000	0.000	0.000	0.000	0.000	0.000	0.000	0.000	0.000	0.000	0.000
RNU48-001006	83.431	2.174	51.182	31.341	2.008	23.165	172.832	203.260	92.921	238.339	562.758	287.227
hsa-miR-183-002269	0.000	0.000	0.000	0.000	0.000	0.000	0.000	0.000	0.000	0.000	0.000	0.000
hsa-miR-184-000485	1.232	0.566	2.498	1.820	1.254	8.437	0.382	0.613	0.712	0.632	0.722	0.165
hsa-miR-185-002271	0.000	0.000	0.000	0.000	0.000	0.000	0.000	0.000	0.000	0.000	0.000	0.000
hsa-miR-186-002285	0.000	0.000	0.000	0.000	0.000	0.000	0.000	0.000	13332.567	5151.504	0.000	0.000
mmu-miR-187-001193	0.000	0.000	0.000	0.000	0.000	0.000	0.000	0.000	0.000	0.000	0.000	0.000
hsa-miR-188-3p-002106	0.000	0.000	0.000	0.000	0.000	0.000	0.000	0.000	0.000	0.000	0.000	0.000
hsa-miR-190-000489	0.000	0.000	0.000	0.000	0.000	0.000	0.000	0.000	0.000	0.000	0.000	0.000
hsa-miR-191-002299	0.063	0.000	0.638	0.000	0.000	0.418	2.864	0.605	0.740	2.887	3.544	2.463
hsa-miR-192-000491	0.000	0.000	0.000	0.000	0.000	0.000	0.000	0.011	0.000	0.000	0.013	0.101
hsa-miR-193a-3p-002250	0.000	0.000	0.000	0.000	0.000	0.000	0.000	0.000	0.000	0.000	0.000	0.000
hsa-miR-193a-5p-002281	0.000	0.000	0.000	0.000	0.000	0.000	0.000	0.000	0.000	0.000	0.000	0.000
hsa-miR-193b-002367	0.000	0.000	0.000	0.000	0.000	0.000	0.000	0.000	0.000	0.000	0.000	0.000
hsa-miR-194-000493	0.000	0.000	0.000	0.000	0.000	0.000	0.000	0.000	0.000	0.055	0.000	0.448
hsa-miR-195-000494	0.000	0.000	0.078	0.017	0.000	0.000	0.260	0.127	0.153	0.131	0.132	0.338
hsa-miR-196b-002215	0.000	0.000	0.000	0.000	0.000	0.000	0.000	0.000	0.000	0.000	0.000	0.000
hsa-miR-197-000497	0.000	0.000	0.000	0.000	0.000	0.000	0.000	0.000	0.000	0.000	0.000	0.000
hsa-miR-198-002273	0.000	0.000	0.000	0.000	0.000	0.000	0.000	0.000	0.000	0.000	0.000	0.000
hsa-miR-199a-000498	0.000	0.000	0.000	0.000	0.000	0.000	0.000	0.000	0.000	0.000	0.000	0.000
hsa-miR-199a-3p-002304	0.000	0.000	0.000	0.000	0.000	0.000	0.000	0.000	0.000	0.000	0.000	0.019
hsa-miR-199b-000500	0.000	0.000	0.000	0.000	0.000	0.000	0.000	0.000	0.000	0.000	0.000	0.000
hsa-miR-200a-000502	0.000	0.000	0.000	0.000	0.000	0.000	0.000	0.000	0.000	0.000	0.000	0.000
hsa-miR-200b-002251	0.000	0.000	0.000	0.000	0.000	0.000	0.000	0.000	0.000	0.000	0.000	0.000

	CCR6+ IL-17+			CCR6+ IFNγ+ IL-17+			CCR6+ IFNγ+			CCR6- IFNγ+		
hsa-miR-200c-002300	0.000	0.000	0.000	0.000	0.000	0.000	0.000	0.000	0.000	0.000	0.000	0.000
hsa-miR-202-002363	0.000	0.000	0.000	0.005	0.000	0.000	0.000	0.000	0.000	0.000	0.000	0.000
hsa-miR-203-000507	0.000	0.150	0.000	0.148	0.053	0.000	0.003	0.762	0.000	0.035	0.002	0.081
hsa-miR-204-000508	0.000	0.000	0.000	0.000	0.000	0.000	0.000	0.000	0.000	0.055	0.000	0.000
hsa-miR-205-000509	0.000	0.000	0.000	0.000	0.000	0.000	0.000	0.000	0.000	0.000	0.000	0.000
hsa-miR-208b-002290	0.000	0.000	0.000	0.000	0.000	0.000	0.000	0.000	0.000	0.000	0.000	0.000
hsa-miR-210-000512	0.000	0.000	0.000	0.000	0.000	0.000	0.000	0.000	0.000	0.000	0.000	0.000
hsa-miR-214-002306	0.000	0.000	0.000	0.000	0.000	0.000	0.000	0.000	0.000	0.000	0.000	0.000
hsa-miR-215-000518	0.000	0.000	0.000	0.000	0.000	0.000	0.000	0.000	0.000	0.000	0.000	0.000
hsa-miR-216a-002220	0.000	0.000	0.000	0.000	0.000	0.000	0.000	0.000	0.000	0.000	0.000	0.000
hsa-miR-216b-002326	0.000	0.000	0.000	0.000	0.000	0.000	0.000	0.000	0.000	0.000	0.000	0.000
hsa-miR-217-002337	0.000	0.000	0.000	0.000	0.000	0.000	0.000	0.000	0.000	0.000	0.000	0.000
hsa-miR-218-000521	0.674	0.000	0.000	0.000	0.000	0.000	0.000	0.000	0.000	0.031	0.000	0.000
hsa-miR-219-000522	0.000	0.000	0.000	0.000	0.000	0.000	0.000	0.000	0.000	0.000	0.000	0.000
hsa-miR-221-000524	0.000	0.000	0.000	0.000	0.000	0.000	0.000	0.000	0.000	0.000	0.000	0.000
hsa-miR-222-002276	0.586	0.148	1.168	0.305	0.000	0.426	3.314	2.952	3.722	8.443	22.794	12.739
hsa-miR-223-002295	1.332	1.328	0.361	10.160	0.254	0.158	0.967	0.517	0.740	3.044	1.464	1.555
hsa-miR-224-002099	0.000	0.000	0.000	0.000	0.000	0.000	0.000	0.000	0.000	0.000	0.000	0.000
hsa-miR-296-3p-002101	0.000	0.000	0.000	0.000	0.000	0.000	0.000	0.000	0.000	0.000	0.000	0.000
hsa-miR-296-000527	0.000	0.000	0.000	0.009	0.000	0.000	0.000	0.000	0.000	0.000	0.000	0.000
hsa-miR-299-3p-001015	0.000	0.000	0.000	0.000	0.000	0.000	0.000	0.000	0.000	0.000	0.000	0.000
hsa-miR-299-5p-000600	0.000	0.000	0.000	0.000	0.000	0.000	0.000	0.000	0.000	0.000	0.000	0.000
hsa-miR-301-000528	0.000	0.000	0.000	0.032	0.000	0.000	0.000	0.000	0.000	0.000	0.128	0.005
hsa-miR-301b-002392	0.000	0.000	0.000	0.000	0.000	0.000	0.000	0.000	0.000	0.000	0.000	0.000
hsa-miR-302a-000529	0.000	0.000	0.000	0.000	2158.057	0.000	0.000	0.000	22.110	403.472	0.000	198.391
ath-miR159a-000338	0.000	0.000	0.000	0.000	0.000	0.000	0.000	0.000	0.000	0.000	0.000	0.000
hsa-miR-302b-000531	0.000	0.000	0.000	0.000	0.000	0.000	0.000	0.000	0.000	0.000	0.000	0.000
hsa-miR-302c-000533	0.000	0.000	0.000	0.000	0.000	0.000	0.000	0.000	0.000	305.185	0.000	0.000
hsa-miR-320-002277	0.170	0.000	0.506	0.000	0.000	0.000	2.659	1.185	1.931	3.807	7.127	5.155
hsa-miR-323-3p-002227	0.000	0.000	0.000	0.000	0.000	0.000	0.000	0.000	0.017	0.000	0.000	0.000
hsa-miR-324-3p-002161	43176.270	26330.732	18254.455	10141.996	8395.363	0.000	16023.326	11854.909	3541.707	13024.424	7802.691	2228.381
hsa-miR-324-5p-000539	0.000	0.000	0.000	0.000	0.000	0.000	0.000	0.000	0.000	0.000	0.000	0.000
hsa-miR-326-000542	0.000	0.000	0.000	0.000	0.000	0.000	0.000	0.000	0.000	0.000	0.000	0.000

	CCR6$^+$ IL-17$^+$			CCR6$^+$ IFNγ$^+$ IL-17$^+$			CCR6$^+$ IFNγ$^+$			CCR6$^-$ IFNγ$^+$		
hsa-miR-328-000543	0.112	0.000	0.000	0.037	0.000	0.000	0.251	0.204	0.107	2.191	1.997	0.566
hsa-miR-329-001101	0.000	0.000	0.000	0.000	0.000	0.000	0.000	0.000	0.000	0.000	0.000	0.000
hsa-miR-330-000544	0.000	0.000	0.000	0.000	0.000	0.000	0.000	0.000	0.000	0.000	0.000	0.000
hsa-miR-330-5p-002230	0.000	0.000	0.000	0.000	0.000	0.000	0.000	0.000	0.000	0.000	0.000	0.000
hsa-miR-331-000545	0.000	0.000	0.000	0.000	0.000	0.000	0.000	0.037	0.000	0.132	0.973	2.448
hsa-miR-331-5p-002233	0.000	0.000	0.000	0.000	0.000	0.000	0.000	0.000	0.000	0.000	0.000	0.000
hsa-miR-335-000546	0.000	0.000	0.000	0.000	0.000	0.000	0.000	0.000	0.000	0.000	0.000	0.020
hsa-miR-337-5p-002156	0.000	0.000	0.000	0.000	0.000	0.000	0.000	0.000	0.001	0.000	0.017	0.000
hsa-miR-338-3p-002252	0.000	0.000	0.000	0.000	0.000	0.000	0.000	0.000	0.000	0.000	0.000	0.000
hsa-miR-339-3p-002184	0.000	0.000	0.000	0.000	0.000	0.000	0.000	0.000	0.000	0.000	0.000	0.000
hsa-miR-339-5p-002257	0.000	0.000	0.000	0.000	0.000	0.000	0.000	0.000	0.000	0.000	0.000	0.000
hsa-miR-3NA-002258	0.000	0.000	0.000	0.000	0.000	0.000	0.000	0.002	0.000	0.000	0.000	0.000
hsa-miR-155-002623	2.178	0.000	1.925	0.000	0.069	0.088	6.340	8.133	3.700	10.890	20.976	15.503
hsa-let-7b-002619	0.000	0.000	0.000	0.000	0.000	0.000	0.000	0.000	0.078	0.000	0.000	0.128
hsa-miR-342-3p-002260	3.034	0.000	0.837	2.089	0.068	0.252	12.348	3.588	2.580	17.217	14.903	9.527
hsa-miR-342-5p-002147	0.000	0.000	0.000	0.000	0.000	0.000	0.000	0.000	0.000	0.000	0.000	0.000
hsa-miR-345-002186	0.000	0.000	0.040	0.000	0.000	0.000	0.000	0.013	0.000	0.025	0.000	0.090
hsa-miR-361-000554	0.000	0.000	0.000	0.000	0.000	0.000	0.000	0.000	0.000	0.000	0.000	0.000
hsa-miR-362-3p-002117	0.000	0.000	0.000	0.000	0.000	0.000	0.000	0.000	0.000	0.000	0.000	0.000
hsa-miR-362-001273	0.000	0.000	0.000	0.000	0.000	0.000	0.000	0.020	0.000	0.000	0.181	0.000
hsa-miR-363-001271	0.000	0.000	0.000	0.000	0.000	0.000	0.000	0.000	0.000	0.000	0.000	0.000
hsa-miR-365-001020	0.000	0.010	0.000	0.000	0.000	0.000	0.000	0.000	0.000	0.000	0.000	0.000
hsa-miR-367-000555	0.000	0.000	2304.910	0.000	136.117	0.000	0.000	0.000	29.173	126.103	0.000	0.000
hsa-miR-369-3p-000557	0.000	0.000	0.000	0.000	0.000	0.000	0.000	0.000	0.000	0.000	0.000	0.000
hsa-miR-369-5p-001021	0.000	0.000	0.000	0.000	0.000	0.000	0.000	0.000	0.000	0.000	0.000	0.000
hsa-miR-370-002275	0.000	0.000	0.000	0.000	0.000	0.000	0.000	0.000	0.000	0.000	0.000	0.000
hsa-miR-371-3p-002124	0.000	0.000	0.000	0.000	0.000	0.000	0.000	0.000	0.000	0.000	0.000	0.000
hsa-miR-372-000560	0.000	0.000	0.000	0.000	0.000	0.000	0.000	0.000	0.000	0.000	0.000	0.000
hsa-miR-373-000561	0.000	0.000	0.000	0.000	0.000	0.000	0.000	0.000	0.000	0.000	0.000	0.000
hsa-miR-374-000563	0.000	0.000	0.238	0.000	0.000	0.264	0.427	0.519	0.191	0.456	2.895	1.028
mmu-miR-374-5p-001319	0.000	0.000	0.000	0.000	0.000	0.000	0.000	0.132	0.041	0.016	0.000	1.000
hsa-miR-375-000564	0.000	0.000	0.000	0.000	0.000	0.000	0.000	0.000	0.004	0.147	0.037	0.022
hsa-miR-376a-000565	1.791	0.000	16.205	9.423	7.088	252.912	0.292	2.044	3.143	1.635	1.218	1.077

	CCR6$^+$ IL-17$^+$			CCR6$^+$ IFNγ$^+$ IL-17$^+$			CCR6$^+$ IFNγ$^+$			CCR6$^-$ IFNγ$^+$		
hsa-miR-376b-001102	0.000	0.000	0.000	0.000	0.000	0.000	0.000	0.000	0.000	0.000	0.000	0.000
hsa-miR-377-000566	0.000	0.000	0.000	0.000	0.000	0.000	0.000	0.000	0.000	0.000	0.000	0.000
mmu-miR-379-001138	0.000	0.000	0.000	0.000	0.000	0.000	0.000	0.000	0.000	0.000	0.000	0.000
hsa-miR-380-3p-000569	0.000	0.000	0.000	0.000	0.000	0.000	0.000	0.000	0.000	0.000	0.000	0.000
hsa-miR-381-000571	0.000	0.000	0.000	0.000	0.000	0.000	0.000	0.000	0.000	0.000	0.040	0.000
hsa-miR-382-000572	0.000	0.000	0.000	0.000	0.000	0.000	0.000	0.000	0.000	0.000	0.000	0.000
hsa-miR-383-000573	0.000	0.000	0.000	0.000	0.000	0.000	0.000	0.000	0.000	0.000	0.000	0.000
hsa-miR-NA9-5p-002331	0.000	0.000	0.000	0.000	0.000	0.000	0.000	0.000	0.000	0.000	0.000	0.000
hsa-miR-410-001274	0.000	0.000	0.000	0.000	0.000	0.000	0.000	0.000	0.022	0.036	0.000	0.000
hsa-miR-411-001610	0.000	0.000	0.000	0.000	0.000	0.000	0.000	0.000	0.000	0.000	0.000	0.000
hsa-miR-422a-002297	0.000	0.000	0.000	0.000	0.000	0.000	0.000	0.142	0.000	0.000	0.177	0.000
hsa-miR-423-5p-0023NA	0.000	0.000	0.000	0.000	0.000	0.000	0.000	0.000	0.000	0.000	0.000	0.000
hsa-miR-424-000604	0.000	0.000	0.000	0.000	0.000	0.000	0.000	0.000	0.000	0.000	0.000	0.000
hsa-miR-425-5p-001516	0.000	0.000	0.000	0.000	0.000	0.000	0.000	0.000	0.000	0.000	0.000	0.000
hsa-miR-429-001024	0.000	0.000	0.000	0.000	0.000	0.000	0.000	0.000	0.000	0.000	0.000	0.000
hsa-miR-431-001979	0.000	0.000	0.000	0.000	0.000	0.000	0.000	0.000	0.000	0.000	0.000	0.000
hsa-miR-433-001028	0.000	0.000	0.000	0.000	0.000	0.000	0.000	0.000	0.000	0.000	0.000	0.000
hsa-miR-449-001030	0.000	0.000	0.000	0.000	0.000	0.000	0.000	0.000	0.000	0.000	0.000	0.000
hsa-miR-449b-001608	0.000	0.000	0.000	0.000	0.000	0.000	0.000	0.000	0.000	0.000	0.000	0.000
hsa-miR-450a-002303	0.000	0.000	0.000	0.000	0.000	0.000	0.000	0.000	0.000	0.000	0.000	0.000
hsa-miR-450b-3p-002208	0.000	0.000	0.000	0.000	0.000	0.000	0.000	0.000	0.000	0.000	0.043	0.000
hsa-miR-450b-5p-002207	0.000	0.000	0.000	0.000	0.000	0.000	0.000	0.000	0.000	0.000	0.000	0.000
mmu-miR-451-001141	0.000	0.000	0.000	0.000	0.000	0.000	0.000	0.000	0.000	0.000	0.731	0.000
hsa-miR-452-002329	0.000	0.000	0.000	0.000	0.000	0.000	0.000	0.000	0.000	0.000	0.000	0.000
hsa-miR-453-002318	0.000	0.000	0.000	0.000	0.000	0.000	0.000	0.000	0.000	0.000	0.000	0.000
hsa-miR-454-002323	0.000	256972.776	475011.198	0.000	1202140.425	0.000	0.000	422503.568	499717.425	776094.067	0.000	0.000
hsa-miR-455-3p-002244	0.000	0.000	0.000	0.000	0.000	0.000	0.000	0.000	0.000	0.000	0.000	0.000
hsa-miR-455-001280	0.000	0.000	0.000	0.000	0.000	0.000	0.000	0.000	0.000	0.000	0.000	0.000
hsa-miR-483-5p-002338	0.000	0.000	0.000	0.000	0.000	0.000	0.000	0.000	0.000	0.058	0.000	0.000
hsa-miR-484-001821	0.427	0.000	0.000	0.173	0.000	0.000	1.307	0.395	0.175	6.753	2.132	2.017
hsa-miR-485-3p-001277	0.000	0.000	0.000	0.000	0.000	0.000	0.000	0.000	0.000	0.000	0.000	0.000
hsa-miR-485-5p-001036	0.000	0.000	0.000	0.000	0.000	0.000	0.000	0.000	0.000	0.000	0.000	0.000
hsa-miR-486-3p-002093	0.000	0.000	0.000	0.000	0.000	0.000	0.000	0.000	0.000	0.000	0.000	0.000

	CCR6^{+} IL-17^{+}			CCR6^{+} IFNγ^{+} IL-17^{+}			CCR6^{+} IFNγ^{+}			CCR6^{-} IFNγ^{+}		
hsa-miR-486-001278	0.000	0.000	0.000	0.000	0.000	0.000	0.000	0.000	0.000	0.000	0.000	0.000
hsa-miR-487a-001279	0.000	0.000	0.000	0.000	0.000	0.000	0.000	0.000	0.000	0.000	0.000	0.000
hsa-miR-487b-001285	0.000	0.000	0.000	0.000	0.000	0.000	0.000	0.000	0.000	0.000	0.000	0.000
hsa-miR-488-002357	0.000	0.000	0.000	0.000	0.000	0.000	0.000	0.000	0.000	0.000	0.000	0.000
hsa-miR-489-002358	0.000	0.000	0.000	0.000	0.000	0.000	0.000	0.000	0.000	0.000	0.000	0.000
hsa-miR-490-001037	0.000	0.000	0.000	0.000	0.000	0.000	0.000	0.000	0.000	0.000	0.000	0.000
hsa-miR-491-3p-002360	0.000	0.000	0.000	0.000	0.000	0.000	0.000	0.000	0.000	0.000	0.000	0.000
mmu-miR-491-001630	0.000	0.000	0.000	0.000	0.000	0.000	0.000	0.000	0.075	0.000	0.000	0.000
hsa-miR-493-002364	0.000	0.000	0.000	0.000	0.000	0.000	0.000	0.000	0.000	0.000	0.000	0.000
hsa-miR-494-002365	0.000	0.000	0.000	0.000	0.000	0.000	0.000	0.000	0.000	0.095	0.210	0.000
mmu-miR-495-001663	0.000	0.000	0.000	0.000	0.000	0.000	0.000	0.000	0.000	0.000	0.000	0.000
mmu-miR-496-001953	0.000	0.000	0.000	0.000	0.000	0.000	0.000	0.000	0.000	0.000	0.000	0.000
hsa-miR-499-3p-002427	0.000	0.000	0.000	0.000	0.000	0.000	0.000	0.000	0.000	0.000	0.000	0.000
mmu-miR-499-001352	0.000	0.000	0.000	0.000	0.000	0.000	0.000	0.000	0.000	0.000	0.023	0.000
hsa-miR-500-002428	0.000	0.000	0.000	0.000	0.000	0.000	0.000	0.000	0.000	0.000	0.000	0.000
hsa-miR-501-3p-002435	0.000	0.000	0.000	0.000	0.000	0.000	0.000	0.000	0.000	0.000	0.000	0.000
hsa-miR-501-001047	0.000	0.000	0.000	0.000	0.000	0.000	0.000	0.000	0.000	0.000	0.000	0.000
hsa-miR-502-3p-002083	0.000	0.000	0.000	0.000	0.000	0.000	0.000	0.000	0.000	0.000	0.000	0.000
hsa-miR-502-001109	0.000	0.000	0.000	0.000	0.000	0.000	0.000	0.000	0.000	0.000	0.000	0.000
hsa-miR-503-001048	0.000	0.000	0.000	0.000	0.000	0.000	0.000	0.000	0.000	0.000	0.000	0.000
hsa-miR-504-002084	0.000	0.000	0.000	0.000	0.000	0.000	0.000	0.000	0.000	0.000	0.000	0.000
hsa-miR-505-002089	0.000	0.000	0.000	0.000	0.000	0.000	0.000	0.000	0.000	0.000	0.000	0.000
hsa-miR-507-001051	0.000	0.000	0.000	0.000	0.000	0.000	0.000	0.000	0.000	0.000	0.000	0.000
hsa-miR-508-001052	0.000	0.000	0.000	0.000	0.000	0.000	0.000	0.000	0.000	0.000	0.000	0.000
hsa-miR-508-5p-002092	0.000	0.000	0.000	0.000	0.000	0.000	0.000	0.000	0.000	0.000	0.000	0.000
hsa-miR-509-5p-002235	0.000	0.000	0.000	0.000	0.000	0.000	0.000	0.000	0.000	0.000	0.000	0.000
hsa-miR-510-002241	0.000	0.000	0.000	0.000	0.000	0.000	0.000	0.000	0.000	0.000	0.000	0.000
hsa-miR-512-3p-001823	0.000	0.000	0.000	0.000	0.000	0.000	0.000	0.000	0.000	0.000	0.000	0.000
hsa-miR-512-5p-001145	0.000	0.000	0.000	0.000	0.000	0.000	0.000	0.000	0.000	0.000	0.000	0.000
hsa-miR-513-5p-002090	0.000	0.000	0.000	0.000	0.000	0.000	0.000	0.000	0.000	0.000	0.000	0.000
hsa-miR-515-3p-002369	0.000	0.000	0.000	0.000	0.000	0.000	0.000	0.000	0.000	0.000	0.000	0.000
hsa-miR-515-5p-001112	0.000	0.000	0.000	0.000	0.000	0.000	0.000	0.000	0.000	0.000	0.000	0.000
hsa-miR-516a-5p-002416	0.000	0.000	0.000	0.000	0.000	0.000	0.000	0.000	0.000	0.000	0.000	0.000

	CCR6^{+} IL-17^{+}			CCR6^{+} IFNγ^{+} IL-17^{+}			CCR6^{+} IFNγ^{+}			CCR6^{-} IFNγ^{+}		
hsa-miR-516b-001150	0.000	0.000	0.000	0.000	0.000	0.000	0.017	0.000	0.000	0.000	0.000	0.000
hsa-miR-517a-002NA2	0.000	0.000	0.000	0.000	0.000	0.000	0.000	0.000	0.000	0.000	0.000	0.000
hsa-miR-517c-001153	0.000	0.000	0.000	0.000	0.000	0.000	0.000	0.000	0.000	0.000	0.000	0.000
hsa-miR-518a-3p-002397	0.000	0.000	0.000	0.000	0.000	0.000	0.000	0.000	0.000	0.000	0.000	0.000
hsa-miR-518a-5p-002396	0.000	0.000	0.000	0.000	0.000	0.000	0.000	0.000	0.000	0.000	0.000	0.000
hsa-miR-518b-001156	0.000	0.000	0.000	0.000	0.000	0.000	0.000	0.000	0.001	0.000	0.000	0.000
hsa-miR-518c-002NA1	0.000	0.000	0.000	0.000	0.000	0.000	0.000	0.000	0.000	0.000	0.000	0.000
hsa-miR-518d-001159	26.364	18.566	22.411	30.973	11.821	136.842	0.000	9.249	7.311	24.069	10.763	2.939
hsa-miR-518d-5p-002389	0.000	0.000	0.000	0.000	0.000	0.000	0.000	0.000	0.000	0.000	0.000	0.000
hsa-miR-518e-002395	0.000	0.000	0.000	0.000	0.000	0.000	0.000	0.000	0.000	0.000	0.000	0.000
hsa-miR-518f-002388	0.000	0.000	0.000	0.000	0.023	0.010	0.000	0.000	0.000	0.056	0.022	0.000
hsa-miR-519a-002415	0.000	0.000	0.000	0.000	0.000	0.000	0.000	0.000	0.000	0.000	0.000	0.000
hsa-miR-519d-002NA3	0.000	0.000	0.000	0.000	0.000	0.000	0.000	0.000	0.000	0.000	0.000	0.000
hsa-miR-519e-002370	0.000	0.000	0.000	0.000	0.000	0.000	0.000	0.000	0.000	0.000	0.000	0.000
hsa-miR-520a-001167	0.000	0.000	0.000	0.000	0.000	0.000	0.000	0.000	0.000	0.000	0.000	0.000
hsa-miR-520a#-001168	0.000	0.000	0.000	0.000	0.000	0.000	0.000	0.000	0.000	0.000	0.000	0.000
hsa-miR-520d-5p-002393	0.000	0.000	0.000	0.000	0.000	0.000	0.000	0.000	0.000	0.000	0.000	0.000
hsa-miR-520g-001121	0.000	0.000	0.000	0.000	0.000	0.000	0.000	0.000	0.000	0.000	0.000	0.000
hsa-miR-521-001122	0.000	0.000	0.000	0.000	0.000	0.000	0.000	0.000	0.000	0.000	0.000	0.000
hsa-miR-522-002413	0.000	0.000	0.000	0.000	0.000	0.000	0.000	0.000	0.000	0.000	0.000	0.000
hsa-miR-523-002386	0.000	0.000	0.000	0.000	0.000	0.000	0.002	0.035	0.000	0.057	0.591	0.005
hsa-miR-524-5p-001982	0.000	0.000	0.000	0.000	0.000	0.000	0.000	0.000	0.000	0.000	0.000	0.000
hsa-miR-525-3p-002385	0.000	0.000	0.000	0.000	0.000	0.000	0.000	0.000	0.000	0.000	0.000	0.000
hsa-miR-525-001174	0.000	0.000	0.000	0.000	0.000	0.000	0.000	0.000	0.000	0.000	0.000	0.000
hsa-miR-526b-002382	0.000	0.000	0.000	0.000	0.000	0.000	0.000	0.000	0.000	0.000	0.000	0.000
hsa-miR-532-3p-002355	0.000	0.000	0.000	0.000	0.000	0.000	0.000	0.000	0.000	0.000	0.119	0.004
hsa-miR-532-001518	0.000	0.000	0.000	0.000	0.000	0.000	0.000	0.000	0.000	0.000	0.000	0.000
hsa-miR-539-001286	0.000	0.000	0.000	0.000	0.000	0.000	0.000	0.000	0.000	0.000	0.000	0.000
hsa-miR-541-002201	0.000	0.000	0.000	0.000	0.000	0.000	0.000	0.000	0.000	0.000	0.000	0.000
hsa-miR-542-3p-001284	0.000	0.000	0.000	0.000	0.000	0.000	0.000	0.000	0.000	0.000	0.017	0.000
hsa-miR-542-5p-0022NA	0.000	0.000	0.000	0.000	0.000	0.000	0.000	0.000	0.000	0.000	0.000	0.000
hsa-miR-544-002265	0.000	0.000	0.000	0.000	0.000	0.000	0.000	0.000	0.000	0.000	0.000	0.000
hsa-miR-545-002267	0.000	0.000	0.000	0.000	0.000	0.000	0.000	0.576	0.131	5.108	0.000	0.000

	CCR6^{+} IL-17^{+}			CCR6^{+} IFNγ^{+} IL-17^{+}			CCR6^{+} IFNγ^{+}			CCR6^{-} IFNγ^{+}		
hsa-miR-548a-001538	0.215	0.047	0.201	0.243	0.050	0.000	0.006	0.045	0.000	0.274	0.108	0.000
hsa-miR-548a-5p-002412	0.000	0.000	0.000	0.000	0.000	0.000	0.000	0.000	0.000	0.000	0.000	0.000
hsa-miR-548b-001541	0.000	0.000	0.000	0.000	0.000	0.000	0.000	0.000	0.000	0.000	0.000	0.000
hsa-miR-548b-5p-002NA8	0.000	0.000	0.000	0.000	0.000	0.000	0.000	0.000	0.000	0.000	0.328	0.000
hsa-miR-548c-001590	0.038	0.013	0.055	0.000	0.000	0.000	0.057	0.171	0.000	0.026	0.033	0.006
hsa-miR-548c-5p-002429	0.000	0.000	0.023	0.000	0.000	0.000	0.022	0.000	0.000	0.002	0.051	0.000
hsa-miR-548d-001605	0.000	0.000	0.000	0.000	0.000	0.000	0.000	0.000	0.000	0.000	0.000	0.000
hsa-miR-548d-5p-002237	0.000	0.000	0.000	0.000	0.000	0.000	0.000	0.000	0.008	0.017	0.000	0.000
hsa-miR-551b-001535	0.000	0.000	0.000	0.000	0.000	0.017	0.000	0.000	0.000	0.000	0.000	0.000
hsa-miR-556-3p-002345	0.000	0.000	0.000	0.000	0.000	0.000	0.000	0.000	0.000	0.000	0.000	0.000
hsa-miR-556-5p-002344	0.000	0.000	0.000	0.000	0.000	0.000	0.000	0.000	0.000	0.000	0.000	0.000
hsa-miR-561-001528	0.000	0.000	0.000	0.000	0.000	0.000	0.000	0.000	0.000	0.000	0.000	0.000
hsa-miR-570-002347	0.000	0.000	0.000	0.000	0.000	0.000	0.000	0.000	0.000	0.000	0.000	0.000
hsa-miR-574-3p-002349	4.074	0.000	0.124	1.328	0.000	0.000	8.188	9.528	4.368	43.003	44.047	9.785
hsa-miR-576-3p-002351	0.000	0.000	0.000	0.000	0.000	0.000	0.000	0.000	0.000	0.000	0.000	0.000
hsa-miR-576-5p-002350	0.000	0.000	0.000	0.000	0.000	0.000	0.000	0.000	0.000	0.000	0.000	0.000
hsa-miR-579-002398	0.000	0.000	0.000	0.000	0.000	0.000	0.000	0.000	0.000	0.000	0.000	0.000
hsa-miR-582-3p-002399	0.000	0.000	0.000	0.000	0.000	0.000	0.000	0.000	0.000	0.000	0.000	0.000
hsa-miR-582-5p-001983	0.000	0.000	0.000	0.000	0.000	0.000	0.000	0.000	0.000	0.000	0.000	0.000
hsa-miR-589-002NA9	0.000	0.000	0.000	0.000	0.000	0.000	0.000	0.000	0.000	0.000	0.000	0.000
hsa-miR-590-5p-001984	0.000	0.000	0.000	0.000	0.000	0.607	0.017	0.000	0.077	0.047	0.168	0.131
hsa-miR-597-001551	0.000	0.972	2.310	1.203	1.464	9.071	0.000	0.799	0.433	2.303	1.000	0.411
hsa-miR-598-001988	0.000	0.000	0.000	0.000	0.000	0.000	0.037	0.000	0.064	0.000	0.058	0.024
mmu-miR-615-001960	0.000	0.000	0.000	0.000	0.000	0.000	0.000	0.000	0.000	0.000	0.000	0.000
hsa-miR-615-5p-002353	0.000	0.000	0.000	0.000	0.000	0.000	0.000	0.000	0.000	0.000	0.000	0.000
hsa-miR-616-002414	0.000	0.000	0.000	0.000	0.000	0.000	0.000	0.000	0.000	0.000	0.000	0.000
hsa-miR-618-001593	0.000	0.000	0.000	0.109	0.000	0.000	0.000	0.000	0.013	0.212	0.172	0.022
hsa-miR-624-002430	0.000	0.000	0.000	0.000	0.000	0.000	0.000	0.000	0.000	0.000	0.000	0.000
hsa-miR-625-002431	0.000	0.000	0.000	0.000	0.000	0.000	0.000	0.000	0.000	0.000	0.000	0.000
hsa-miR-627-001560	0.000	0.000	0.000	0.000	0.000	0.000	0.000	0.000	0.000	0.134	0.000	0.000
hsa-miR-628-5p-002433	0.000	70352.984	199379.561	51316.601	111077.724	0.000	0.000	0.000	69029.050	13455.002	51730.840	17642.532
hsa-miR-629-002436	0.000	0.000	0.000	0.000	0.000	0.000	0.000	0.000	0.000	0.000	0.000	0.000
hsa-miR-636-002088	0.000	0.000	0.000	0.000	0.000	0.000	0.000	0.000	0.000	1.132	0.000	0.138

	CCR6^{+} IL-17^{+}			CCR6^{+} IFNγ^{+} IL-17^{+}			CCR6^{+} IFNγ^{+}			CCR6^{-} IFNγ^{+}		
hsa-miR-642-001592	0.000	0.000	0.000	0.000	0.000	0.000	0.000	0.000	0.000	0.000	0.000	0.054
hsa-miR-651-001604	0.000	0.000	0.000	0.000	0.000	0.000	0.000	0.000	0.000	0.000	0.000	0.000
hsa-miR-652-002352	0.000	0.000	0.000	0.000	0.000	0.000	0.000	0.000	0.000	0.000	0.000	0.000
hsa-miR-653-002292	0.000	0.000	0.000	0.000	0.000	0.000	0.000	0.000	0.000	0.000	0.000	0.000
hsa-miR-654-3p-002239	0.000	0.000	0.000	0.000	0.000	0.000	0.000	0.000	0.000	0.000	0.050	0.000
hsa-miR-654-001611	0.000	0.000	0.000	0.000	0.000	0.000	0.000	0.000	0.000	0.000	0.000	0.000
hsa-miR-655-001612	0.000	0.000	0.000	0.000	0.000	0.000	0.000	0.000	0.000	0.000	0.000	0.000
hsa-miR-660-001515	0.000	0.000	0.000	0.000	0.000	0.000	0.000	0.000	0.000	0.000	0.000	0.000
hsa-miR-671-3p-002322	0.000	0.000	0.000	0.000	0.000	0.000	0.000	0.000	0.000	0.000	0.000	0.000
hsa-miR-672-002327	0.000	0.000	0.000	0.000	0.000	0.000	0.000	0.000	0.000	0.000	0.000	0.000
hsa-miR-674-002021	0.000	0.000	0.000	0.000	0.000	0.000	0.000	0.000	0.000	0.000	0.000	0.000
hsa-miR-708-002341	0.000	0.000	0.000	0.000	0.000	0.000	0.000	0.000	0.000	0.017	0.000	0.001
hsa-miR-744-002324	0.000	0.000	0.000	0.000	0.000	0.000	0.000	0.000	0.000	0.000	0.026	0.000
hsa-miR-758-001990	0.000	0.000	0.000	0.000	0.000	0.000	0.000	0.000	0.000	0.000	0.000	0.000
hsa-miR-871-002354	0.000	0.000	0.000	0.000	0.000	0.000	0.000	0.000	0.000	0.000	0.000	0.000
hsa-miR-872-002264	0.000	0.000	0.000	0.000	0.000	0.000	0.000	0.000	0.000	0.000	0.000	0.000
hsa-miR-873-002356	0.000	0.000	0.000	0.000	0.000	0.000	0.000	0.000	0.000	0.000	0.000	0.000
hsa-miR-874-002268	0.000	0.000	0.000	0.000	0.000	0.000	0.000	0.000	0.000	0.000	0.000	0.073
hsa-miR-875-3p-002204	0.000	0.000	0.000	0.000	0.000	0.000	0.000	0.000	0.000	0.000	0.000	0.000
hsa-miR-876-3p-002225	0.000	0.000	0.000	0.000	0.000	0.000	0.000	0.000	0.000	0.000	0.000	0.000
hsa-miR-876-5p-002205	0.000	0.000	0.000	0.000	0.000	0.000	0.000	0.000	0.000	0.000	0.000	0.000
hsa-miR-885-3p-002372	0.000	0.000	0.000	0.000	0.000	0.000	0.000	0.000	0.000	0.000	0.000	0.000
hsa-miR-885-5p-002296	0.000	0.000	0.000	0.000	0.000	0.000	0.000	0.000	0.000	0.000	0.000	0.000
hsa-miR-886-3p-002194	0.009	0.000	0.000	0.000	0.000	0.000	0.000	0.000	0.000	0.000	0.000	0.000
hsa-miR-886-5p-002193	0.000	0.000	0.000	0.000	0.000	0.000	0.000	0.000	0.000	0.000	0.000	0.000
hsa-miR-887-002374	0.000	0.000	0.000	0.000	0.000	0.000	0.000	0.000	0.000	0.000	0.000	0.000
hsa-miR-888-002212	0.000	0.000	0.000	0.000	0.000	0.000	0.000	0.000	0.000	0.000	0.000	0.000
hsa-miR-889-002202	0.000	0.000	0.000	0.000	0.000	0.000	0.000	0.000	0.000	0.000	0.000	0.000
hsa-miR-890-002209	0.000	0.000	0.000	0.000	0.000	0.000	0.000	0.000	0.000	0.000	0.000	0.000
hsa-miR-891a-002191	0.000	0.000	0.000	0.000	0.000	0.000	0.000	0.000	0.000	0.000	0.000	0.000
hsa-miR-891b-002210	0.000	0.000	0.000	0.000	0.000	0.000	0.000	0.000	0.000	0.000	0.000	0.000
hsa-miR-892a-002195	0.000	0.000	0.000	0.000	0.000	0.000	0.000	0.000	0.000	0.000	0.000	0.000
hsa-miR-147-000469	0.000	0.000	0.000	0.000	0.000	0.000	0.000	0.000	0.000	0.182	0.000	0.000

	CCR6^{+} IL-17^{+}			CCR6^{+} IFNγ^{+} IL-17^{+}			CCR6^{+} IFNγ^{+}			CCR6^{-} IFNγ^{+}		
hsa-miR-208-000511	0.000	0.000	0.000	0.000	0.000	0.000	0.000	0.000	0.000	0.000	0.000	0.000
hsa-miR-211-000514	0.000	0.000	0.000	0.000	0.000	0.000	0.000	0.000	0.000	0.000	0.000	0.000
hsa-miR-212-000515	0.000	0.000	0.143	0.000	0.000	0.000	0.000	0.000	0.000	1.000	0.000	0.000
hsa-miR-219-1-3p-002095	0.000	0.000	0.000	0.000	0.000	0.000	0.000	0.000	0.000	0.000	0.000	0.000
hsa-miR-219-2-3p-002390	0.000	0.000	0.000	0.000	0.000	0.000	0.000	0.000	0.000	0.000	0.000	0.000
hsa-miR-220-000523	0.000	0.000	0.000	0.000	0.000	0.000	0.000	0.000	0.000	0.000	0.000	0.000
hsa-miR-220b-002206	0.000	0.000	0.000	0.000	0.000	0.000	0.000	0.000	0.000	0.000	0.000	0.000
hsa-miR-220c-002211	0.000	0.000	0.000	0.000	0.000	0.000	0.000	0.000	0.000	0.000	0.000	0.000
hsa-miR-298-002190	0.000	0.000	0.000	0.000	0.000	0.000	0.000	0.000	0.000	0.000	0.000	0.000
hsa-miR-325-0005NA	0.000	0.000	0.000	0.000	0.000	0.000	0.000	0.000	0.000	0.000	0.000	0.000
hsa-miR-346-000553	0.000	0.000	0.000	0.000	0.000	0.000	0.000	0.000	0.000	0.000	0.000	0.000
hsa-miR-376c-002122	0.000	0.000	0.000	0.000	0.000	0.000	0.000	0.000	0.000	0.000	0.000	0.000
hsa-miR-384-000574	0.000	0.000	0.000	0.000	0.000	0.000	0.000	0.000	0.000	0.000	0.000	0.000
hsa-miR-412-001023	0.000	0.000	0.000	0.000	0.000	0.000	0.000	0.000	0.000	0.000	0.000	0.000
hsa-miR-448-001029	0.000	0.000	0.000	0.000	0.000	0.000	0.000	0.000	0.000	0.000	0.000	0.000
hsa-miR-492-001039	0.000	0.000	0.000	0.000	0.000	0.000	0.000	0.000	0.000	0.000	0.000	0.000
hsa-miR-506-001050	0.000	0.000	0.000	0.000	0.000	0.000	0.000	0.000	0.000	0.000	0.000	0.000
hsa-miR-509-3-5p-002155	0.000	0.000	0.000	0.000	0.000	0.000	0.000	0.000	0.000	0.000	0.000	0.000
hsa-miR-511-001111	0.000	0.000	0.000	0.000	0.000	0.000	0.000	0.000	0.000	0.000	0.000	0.000
hsa-miR-517b-001152	0.042	0.000	0.000	0.000	0.000	0.000	0.004	0.019	0.519	0.123	1.050	0.329
hsa-miR-519c-001163	0.000	0.000	0.000	0.000	0.000	0.000	0.000	0.000	0.000	0.000	0.000	0.000
hsa-miR-520b-001116	0.000	0.000	0.000	0.000	0.000	0.000	0.000	0.000	0.000	0.000	0.000	0.000
hsa-miR-520e-001119	0.000	0.000	0.000	0.000	0.000	0.000	0.000	0.000	0.000	0.000	0.000	0.000
hsa-miR-520f-001120	0.000	0.000	0.000	0.000	0.000	0.000	0.000	0.000	0.000	0.000	0.000	0.000